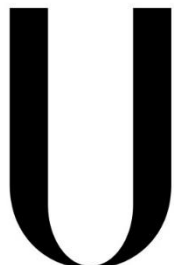


UNIVERSIDADE DE LISBOA

Faculdade de Medicina



LISBOA

UNIVERSIDADE
DE LISBOA

Bio-orthogonal site-selective labelling of carbohydrates and proteins

Annabel Katharina Kitowski

Orientador: Prof. Doutor Gonçalo Jose Lopes Bernardes

Co-orientador: Prof. Doutor Maria Manuel Dias da Mota

Tese especialmente elaborada para obtenção do grau de Doutor em Ciências Biomédicas –
Especialidade em Bioquímica Médica

2019

**The printing of this thesis was approved by the Scientific Council of the
Faculty of Medicine of the University of Lisbon on the 16th of April 2019**

UNIVERSIDADE DE LISBOA

Faculdade de Medicina



Bio-orthogonal site-selective labelling of carbohydrates and proteins

Annabel Katharina Kitowski

Orientador: Prof. Doutor Gonalo Jose Lopes Bernardes

Co-orientador: Prof. Doutor Maria Manuel Dias da Mota

Tese especialmente elaborada para obteno do grau de Doutor em Cincias Biomdicas – Especialidade em Bioqumica Mdica

Jri:

Presidente: Doutor Joo Eurico Cortez Cabral de Fonseca, Professor Catedrtico e Vice-Presidente do Conselho Cientifico da Faculdade de Medicina da Universidade de Lisboa

Vogais:

- *Doctor Fabrizio Chiodo, Senior Researcher, Amsterdam Infection and Immunity Institute Fellow, VUmc Amsterdam*
- *Doctor Francisco Corzana, Associate Professor do Centro de Investigacin en Sntesis Qumica, Universidad de La Rioja*
- Doutora Amlia Pilar Grases dos Santos Silva Rauter, Professora Catedrtica de Faculdade de Cincias da Universidade de Lisboa
- Doutor Gonalo Jos Lopes Bernardes, Investigador, *Group Leader* do Instituto de Medicina Molecular Joo Lobo Antones, Unidade de Investigacio associada  Faculdade de Medicina da Universidade de Lisboa (*Orientador*)
- Doutor Nuno Fernando Duarte Cordeiro Crrea dos Santos, Professor Associado com Agregacio da Faculdade de Medicina da Universidade de Lisboa
- Doutora Susana Constantino Rosa Santos, Professora Auxiliar da Faculdade de Medicina da Universidade de Lisboa

The opinions expressed in this thesis are from the exclusive responsibility of the autor.

As opiniões expressas nesta publicação são da exclusiva responsabilidade do seu autor.

Acknowledgements

I would like to thank Dr Gonçalo Bernardes for giving me the opportunity to conduct my doctoral research studies in his group. It was a great experience to work in both labs, Cambridge and Lisbon, and in this way to have the chance to combine chemistry with biology. I would like to thank all members of the group, present and former members in both countries, for their help and support during this time and for making these years unforgettable.

I would also like to thank Prof Dr Maria Manuel Mota for her co-supervision of this work and all her suggestions. I also would like to express my gratitude for the supply with mosquitoes from her lab, especially Ana Filipa Caetano Parreira for her constant help with this subject. I also would like to thank Dr Vanessa Alexandra Zuzarte Luís for her help and suggestions, and for being part of my thesis committee.

As part of my thesis committee, I would also like to thank Dr Pedro Cal and Dr Pedro Gois for their useful comments and critics during the meetings and for the fruitful discussions.

I would like to thank Dr Roberto Adamo and Dr Filippo Carboni, for the warm welcome in the lab of GSK and for the opportunity to increase my knowledge in the field of glycoconjugate vaccines.

Also, I would like to say thank you to all the colleague fellows of the GlyoVax ITN network, for the creation of a great atmosphere and team spirit.

I would like to thank all my friends at home, who were always there for me and despite the large distance, came for visits around Europe. I am more than lucky to have you all in my life.

Finally, my greatest gratitude is to my family. Thank you for all the support and help during the last years, for believing in me and helping me, in all situations. I could not have done this without you. Thank you, Mum and Dad, for giving me the chance to do everything I did and to be always there. Thank you my dear siblings, Amelie and Marius, for making sure that I am not getting crazy and for all the laughs we shared.

Sumário

Os hidratos de carbono e as proteínas são dois grandes grupos de macromoléculas de grande importância para os processos biológicos associados à saúde e à doença. Enquanto as proteínas são codificadas pelo genoma, as estruturas celulares glicídicas não seguem necessariamente um molde e têm de ser estudadas de forma indireta. O desenvolvimento de *metabolic oligosaccharide engineering* (“engenharia de oligossacáridos metabólicos”; MOE) deu origem a novos métodos para estudar estruturas glicídicas, no contexto de várias doenças e diferentes organismos. Embora em vários casos os derivados de manose sejam usados para estudar estruturas de ácido siálico em células cancerígenas, este trabalho apresenta resultados na incorporação metabólica de derivados de galactose em glicanos presentes em membranas de células hepáticas humanas. Foram sintetizados três derivados de galactose artificiais contendo grupos alceno terminais nas posições C2 ou C6, e as constantes de velocidade em reações Diels-Alder inversas electro-deficientes (iEDDA) foram avaliadas através de um método de triagem de alto rendimento em placas de 96 poços. Mostrou-se que nenhum dos derivados de galactose sintetizados tem efeitos citotóxicos nas linhas celulares HepG2 e Huh7. Inclusivamente, todos os monossacáridos foram incorporados com sucesso em glicanos presentes na membrana celular de ambas as linhas celulares, tendo o seu posicionamento celular sido confirmado pela observação de co-localização com um marcador de membrana celular. Depois do desenvolvimento de uma estratégia de incorporação e marcação de derivados de galactose artificiais na membrana de células hepáticas humanas, estudaram-se as alterações de incorporação de galactose durante a infeção por *Plasmodium berghei*. Com recurso a diferentes técnicas, tais como microscopia confocal, citometria de fluxo e citometria de fluxo imagiológica, foi apenas possível demonstrar um modesto aumento na marcação do derivativo de galactose artificial em células infetadas. Para explicar este resultado, determinou-se o percurso celular deste glicano artificial. A utilização de inibidores específicos e não-específicos do transportador de glucose GLUT1 demonstrou que este está envolvido no transporte de derivativos de galactose para o meio intracelular. O facto de a translocação de GLUT1 para a membrana celular estar aumentada em células hepáticas infetadas explica a tendência observada para o aumento da incorporação da galactose artificial nestas células. Como complemento dos estudos celulares, neste trabalho MOE foi aplicada pela primeira vez para elucidar uma possível

transferência de monossacáridos de galactose do mosquito para o parasita. As cascatas metabólicas de biosíntese de construção de glicídios no parasita são pouco conhecidas. A existência de evidências da implicação do mosquito em algumas destas cascatas metabólicas levou-nos a aplicar MOE neste contexto. Foi possível demonstrar que há absorção dos derivados de galactose sintetizados pelo mosquito, embora apenas se tenha observado uma reduzida transferência.

Para além do desenvolvimento de derivados monofuncionais de galactose, foi sintetizado um derivado bifuncional contendo dois grupos sinalizadores ortogonais. No entanto, até ao momento não foi possível obter incorporação metabólica ou marcação deste derivado em glicanos da membrana celular.

Depois do desenvolvimento de ferramentas para o estudo de estruturas glicídicas na célula, foi ainda desenvolvido um método para modificação seletiva de proteínas que pode ser usado na produção de potenciais vacinas conjugadas. Através da introdução seletiva de dois resíduos de dehidroalanina no local da ligação dissulfureto C186-C201 da proteína imunogénica CRM₁₉₇, foi possível obter um novo grupo químico para a conjugação de antígenos glicídicos. Mostrou-se que estes grupos químicos podem ser usados para a introdução selectiva de polissacáridos antigénicos de *Streptococcus* do grupo B (GBS) ou *Streptococcus pneumoniae*. Ambos os tipos de glicoconjugados foram sintetizados, e os ensaios preliminares para optimização do método de purificação foram iniciados. Este conceito será ainda desenvolvido para a produção futura de possíveis candidatos a vacinas conjugadas.

Finalmente, foi ainda desenvolvido um método sintético que poderá facilitar a síntese de estruturas de oligossacáridos antigénicos. O método exposto neste trabalho recorre a um promotor tiofílico *O*-mesitileno-sulfonilhidroxilamina (MSH) para a ativação de dadores de tioglicósidos. Demonstrou-se que diferentes dadores de tioglicósidos têm diferentes cinéticas de ativação, dependendo dos grupos protetores apresentados, ou do grupo anomérico de saída. Para além de se ter aplicado o método de ativação desenvolvido à síntese de vários produtos de glicosilação, demonstrou-se ainda a ativação sequencial de grupos *S*-alquilo antes de grupos anoméricos *S*-fenil na síntese de um trissacárido modelo.

Globalmente, neste trabalho desenvolveram-se e aplicaram-se métodos bio-ortogonais à investigação de estruturas glicídicas no contexto de malária, e à modificação de proteínas de forma seletiva para produção de candidatos de vacinas conjugadas.

Palavras-chave: engenharia de oligossacáridos metabólicos / Metabolic Oligosaccharide Engineering, marcação bio-ortogonal, candidatos de vacinas conjugadas, modificação seletiva de proteínas

Abstract

Carbohydrates and proteins represent two large groups of biomolecules which are tremendously important for biological processes in health and disease state. Although protein-structures are encoded in the genome, cellular glycan structures are template independent and can only be addressed in an indirect manner. The development of metabolic oligosaccharide engineering (MOE) gave rise to new methods to study carbohydrate structures in the context of different disease settings and in different organisms. While in many cases mannose derivatives are used to study the sialic acid structures in cancer cells, this work presents the results on the metabolic incorporation of galactose derivatives into cell membrane glycans of human hepatic cells. Three unnatural galactose derivatives containing terminal alkene groups in C2 or C6 position were synthesized and their reaction rates in inverse electron demand Diels Alder reactions (iEDDA) were evaluated, by using a high-throughput screening method in 96-well plates. It was shown that none of the developed galactose derivatives exhibit any cell toxic effect in HepG2 or Huh7 cell lines. Furthermore, all monosaccharides could be successfully incorporated in cell membrane glycan structures of both cell lines and the localization on the cell membrane was confirmed by co-localization with a plasma membrane dye. After developing this incorporation and labeling strategy of unnatural galactose derivatives in the cell membrane of human hepatic cells, the change in incorporation during an infection of these cells with *Plasmodium berghei* sporozoites was investigated. By using different techniques, such as confocal microscopy, flow cytometry and imaging flow cytometry, only a small trend for an increased uptake of the unnatural galactose derivative in *P. berghei* infected cells was observed. To explain this result, the pathway for the diffusion of the unnatural galactose derivative was determined. The application of specific and non-specific inhibitors for the glucose transporter GLUT1 revealed that this transporter is involved in the delivery of galactose derivatives into cultured cells. The enhanced translocation of this transporter to the surface of infected hepatic cells explains the observed tendency for an increased incorporation of the unnatural galactose derivative in these cells. Apart from cell studies, MOE was applied for the first time to study a possible transfer of galactose monosaccharides from the mosquito host to the parasite. Biosynthetic pathways for glycan assembly in the parasite are poorly understood. Suggestions on the participation of the mosquito host in some of these pathways, led to the idea to apply MOE in this situation. It was

possible to show an uptake of the presented galactose derivatives by the mosquito but only reduced transfer to the parasite seems to occur.

In addition to the development of monofunctional galactose derivatives, also a bifunctional derivative containing two orthogonal reporter groups was synthesized. However, so far it was not possible to achieve a metabolic incorporation or labeling of this derivative on cell membrane glycans.

After developing cellular tools to study carbohydrate structures, a site-selective method for protein modification was generated, to be used for the development of new glycoconjugate vaccine candidates. By introducing selectively two dehydroalanine residues in place of the disulfide bond C186-C201 of the immunogenic protein CRM₁₉₇, a new chemical moiety for the conjugation of carbohydrate antigens was obtained. It was shown that these moieties can be used for the selective introduction of polysaccharide antigens from group B *Streptococcus* (GBS) or *Streptococcus pneumoniae*. Both types of glycoconjugates could be synthesized and first trials on the purification methods were undertaken. This concept will be developed further for future vaccine candidates.

Finally, a synthetic method was developed which could facilitate the synthesis of defined antigenic oligosaccharide structures. This method uses the thiophilic promoter *O*-mesitylenesulfonylhydroxylamine (MSH) for the activation of thioglycoside donors. It was demonstrated that different thioglycoside donors are activated with different kinetics, depending on the presented protecting groups or the anomeric leaving group. Apart from applying the developed activation method for the synthesis of several glycosylation products, the sequential activation of *S*-alkyl before *S*-phenyl anomeric groups was shown during the synthesis of a model trisaccharide.

Overall, bio-orthogonal methods were developed and applied for the investigation of carbohydrate structures in the context of malaria disease, and for the site-selective modification of protein carriers during the development of glycoconjugate vaccine candidates.

Keywords: Metabolic Oligosaccharide Engineering, Bio-orthogonal labeling, Glycoconjugate Vaccine Candidates, Site-selective Protein modification

Table of Content

| | |
|--|----|
| 1. Chapter 1 – General introduction | 13 |
| 1.1. Carbohydrates – a general perspective | 13 |
| 1.1.1. <i>N</i> - and <i>O</i> -Glycosylation..... | 13 |
| 1.1.2. Carbohydrates in disease state..... | 15 |
| 1.1.3. Metabolic oligosaccharide engineering – state of the art | 18 |
| 1.1.4. Multifunctional labeling of glycan structures..... | 24 |
| 1.1.5. Inverse electron demand Diels Alder reaction for MOE..... | 26 |
| 1.1.6. Malaria and the glycobiology of <i>Plasmodium</i> | 28 |
| 1.1.7. The story of the α -Gal epitope..... | 32 |
| 1.2. Glycoconjugate vaccines | 33 |
| 1.2.1. Carbohydrates as vaccine antigens..... | 33 |
| 1.2.2. Site-selective protein modification..... | 35 |
| 1.3. Chemical synthesis of carbohydrate antigens | 41 |
| 1.3.1. The glycosylation reaction..... | 41 |
| 1.3.2. Thioglycosides as glycosyl donors | 43 |
| 1.4. The aims of this work | 45 |
| 1.4.1. Metabolic oligosaccharide engineering as a tool for malaria | 45 |
| 1.4.2. Bifunctional galactose derivatives for metabolic labeling | 46 |
| 1.4.3. The development of a site-selective glycoconjugate vaccine candidate | 46 |
| 1.4.4. Activation of thioglycoside donors using MSH | 46 |
| 2. Chapter 2 – Design and optimization of new galactopyranose-derivatives for metabolic labeling in the context of malaria | 48 |
| 2.1. Introduction..... | 48 |

| | | |
|--------|---|-----|
| 2.2. | Results and discussion | 49 |
| 2.2.1. | Chemical synthesis of artificial galactose derivatives | 49 |
| 2.2.2. | Evaluation of the kinetic properties..... | 51 |
| 2.2.3. | Metabolic incorporation into cell membrane glycans | 54 |
| 2.2.4. | Metabolic incorporation during infection with <i>Plasmodium berghei</i> | 68 |
| 2.2.5. | Transport of artificial galactose derivatives through GLUT1 | 74 |
| 2.2.6. | Transfer of artificial galactose derivatives from the mosquito host to the parasite. | 77 |
| 2.3. | Future perspective – Application of MOE in malaria..... | 80 |
| 3. | Chapter 3 – Synthesis of a bifunctional galactose derivative for metabolic labeling..... | 84 |
| 3.1. | Introduction..... | 84 |
| 3.2. | Results and Discussion | 85 |
| 3.2.1. | Chemical synthesis of a bifunctional galactose derivative | 85 |
| 3.2.2. | Studies on the metabolic incorporation | 88 |
| 3.3. | Future perspective | 90 |
| 4. | Chapter 4 – Development of a site selective glycoconjugate vaccine candidate with CRM ₁₉₇ | 94 |
| 4.1. | Introduction..... | 94 |
| 4.2. | Results and Discussion | 95 |
| 4.2.1. | Site-selective modification of CRM ₁₉₇ | 95 |
| 4.2.2. | Modification of the polysaccharide antigen | 100 |
| 4.2.3. | Synthesis and Purification of the glycoconjugate vaccine candidate | 102 |
| 4.3. | Future perspective | 107 |
| 5. | Chapter 5 – Sequential activation of thioglycoside donors using an electropositive nitrogen promoter..... | 111 |

| | | |
|--------|---|-----|
| 5.1. | Introduction..... | 111 |
| 5.2. | Results and discussion | 112 |
| 5.2.1. | Activation of thioglycosides using <i>O</i> -mesitylenesulfonyl hydroxylamine – Kinetic evaluations | 112 |
| 5.2.2. | Activation of 2-deoxy-2-fluoro-thioglycosides with MSH | 114 |
| 5.2.3. | Glycosylation reactions promoted by MSH | 115 |
| 5.2.4. | Selective activation of a <i>S</i> -alkyl thioglycoside donor | 117 |
| 5.3. | Future perspective | 118 |
| 6. | Chapter 6 – Conclusions: from synthetic chemistry to biological applications | 120 |
| 7. | Chapter 7 – Experimental section..... | 122 |
| 7.1. | General remarks..... | 122 |
| 7.2. | Materials and Methods for Chapter 2 | 123 |
| 7.2.1. | Chemical synthesis | 123 |
| 7.2.2. | Kinetic studies | 131 |
| 7.2.3. | Cell studies | 132 |
| 7.2.4. | Infection studies..... | 140 |
| 7.3. | Materials and Methods for Chapter 3 | 146 |
| 7.3.1. | Chemical synthesis | 146 |
| 7.3.2. | Cell studies | 153 |
| 7.4. | Materials and Methods for Chapter 4 | 155 |
| 7.4.1. | Site selective modification of CRM197 | 155 |
| 7.4.2. | Derivatization of Polysaccharide antigens | 159 |
| 7.4.3. | Glycoconjugation with CRM-DHA-N ₃ | 161 |
| 7.5. | Materials and Methods for Chapter 5 | 162 |
| 7.5.1. | Chemical synthesis | 162 |

| | | |
|--------|---|-----|
| 7.5.2. | General procedure of the glycosylation reaction using MSH as activating reagent | 166 |
| 7.5.3. | Procedure for the selective activation of <i>S</i> -ethyl over <i>S</i> -phenyl thioglycosides | 167 |
| 7.5.4. | Synthesis of the trisaccharide 2,3,4,6-tetrabenzylglucopyranosyl-(1,6)-2,3,4-tribenzylglucopyranosyl-(1,6)-1,2,3,4-diisopropylidengalactopyranosid (81).. | 168 |
| 7.5.5. | Computational details | 169 |
| 7.5.6. | NMR studies | 169 |
| 8. | References | 170 |

Index of Abbreviations

| | |
|------------------------|--|
| Ac ₂ O | Acetic anhydride |
| Asn | Asparagine |
| Ac ₄ GlcSEt | Ethyl-2,3,4,6-tetraacetyl-thioglucose |
| Ac ₄ GlcSPh | Phenyl-2,3,4,6-tetraacetyl-thioglucose |
| AgOTf | Silver trifluoromethanesulfonate |
| Bn ₄ GlcSEt | Ethyl-2,3,4,6-tetrabenzyl-thioglucose |
| Bn ₄ GlcSPh | Phenyl-2,3,4,6-tetrabenzyl-thioglucose |
| CDCl ₃ | Deuterated chloroform |
| CH ₃ CN | Acetonitrile |
| CSP | Circumsporozoite protein |
| Cu(OTf) ₂ | Copper(II) trifluoromethanesulfonate |
| DHA | Dehydroalanine |
| DMF | Dimethylformamide |
| DMSO | Dimethylsulfoxide |
| EDG | Electron donating group |
| ER | Endoplasmatic reticulum |
| Et ₃ N | Triethylamine |
| Et ₂ O | Diethyl ether |
| EtOAc | Ethyl acetate |
| EWG | Electron withdrawing group |
| Gal | Galactose |
| Glc | Glucose |
| GlcNAc | <i>N</i> -acetylglucosamine |
| GPI | Glycosylphosphatidylinositol |
| H ₂ O | Water |
| HOMO | Highest occupied molecular orbital |
| iEDDA | Inverse electron demand Diels Alder |

| | |
|---------------------------------|---|
| K ₂ CO ₃ | Potassium carbonate |
| LiClO ₄ | Lithium perchlorate |
| LUMO | Lowest unoccupied molecular orbital |
| Man | Mannose |
| MeOH | Methanol |
| MgSO ₄ | Magnesium sulfate |
| MHCII | Major Histone compatibility complex II |
| MOE | Metabolic Oligosaccharide Engineering |
| MSH | <i>O</i> -Mesitylsulfonyl hydroxylamine |
| MSP | Merozoites surface protein |
| NBS | <i>N</i> -bromosuccinimide |
| NaCl | Sodium chloride |
| Na ₂ CO ₃ | Sodium carbonate |
| NaH | Sodium hydride |
| NaOMe | Sodium methanoate |
| NIS | <i>N</i> -iodosuccinimide |
| NMR | Nuclear magnetic resonance |
| PFA | Paraformaldehyde |
| RNA | Ribonucleic acid |
| RT | Room temperature |
| Ser | Serine |
| TCEP | Tris-(2-carboxyethyl)-phosphine |
| TCO | Trans-cyclooctyne |
| Thr | Threonine |
| TLC | Thin-layer chromatography |
| TSR | Thrombospondin type I repeat |
| ZWI | Zwitterionic |

Index of Figures

| | |
|--|----|
| Figure 1: Schematic illustration of N- and O-linked glycosylation, displaying the initial sugar moiety connected to the corresponding amino acid. | 15 |
| Figure 2: Tn-antigen and sialyl Tn antigen, connected via O-glycosylation to serine or threonine. | 16 |
| Figure 3: Schematic overview of examples for applied unnatural monosaccharide building blocks (outer ring) and the natural substrates (inner ring 8-11). | 20 |
| Figure 4: Overview illustrating the cellular mechanisms which enable MOE. Per-acetylated monosaccharides enter the cytosol via passive diffusion or transporters, followed by the deacetylation by unspecific esterase enzymes. The generation of sugar nucleotides (NTP) allows glycan assembly by glycosyltransferases, resulting in intracellular or cell membrane protein glycosylation. | 21 |
| Figure 5: Azide derivative 15 of glucosamine for selective incorporation into O-GlcNAc-protein modifications. ³⁹ | 23 |
| Figure 6: Azide containing derivatives of rare bacterial monosaccharides bacillosamine 17 and 2,4-diacetamido-2,4,6-trideoxyhexose 18 | 24 |
| Figure 7: Chemical structures of mannosamine derivatives for click-chemistry 19 , iEDDA 20 and photoclick reaction 21 | 25 |
| Figure 8: Chemical structures of bifunctional sialic acid derivatives 22 and 23 , containing an azide group in C9 position and an alkyne or diazirine group in N-acyl position. | 25 |
| Figure 9: Schematic illustration of the orbital interaction in iEDDA. Decreasing LUMO energy of diene 24 through electron withdrawing groups, increase of HOMO energy of the dienophile by electron-donating groups. | 26 |
| Figure 10: Schematic illustration of the life cycle of the Plasmodium parasite. | 29 |
| Figure 11: Structure of the α -Gal epitope Gal α 1-3Gal β 1-4GlcNAc 26 | 31 |
| Figure 12: A. Mechanism of T-cell dependent recognition of Zwitterionic polysaccharides (ZWI-PS) via MHCII. B. Mechanism of T-cell independent recognition of Non-Zwitterionic polysaccharides (Non-ZWI-PS) by B-cells. C. Mechanism of recognition of glycoconjugates by B-cells with co-stimulation of CD4 ⁺ T-cells. ⁹⁰ | 34 |

| | |
|---|----|
| Figure 13: Classical modification methods for lysine and cysteine in native proteins. Lysine modifications I: amide formation, II: thiourea formation, III reductive amination. Cysteine modification IV: disulfide exchange, V: alkylation, VI: Maleimide addition..... | 37 |
| Figure 14: Illustration of the anomeric effect, A. Molecular orbital theory B. Dipole moment theory. ¹¹⁸ | 42 |
| Figure 15: Results of the iEDDA reaction between tetrazine 40 and galactose derivatives 37-39 . The represented data represent linear fits of at least two independent experiments. | 53 |
| Figure 16: Determination of the cell toxicity of acetylated galactose derivatives 31, 33 and 36 . A. Huh7 cells B. HepG2 cells. The cell viability was measured at the time points 48h and 72h. The data represent three independent experiments..... | 55 |
| Figure 17: Structure of 6-methyl-tetrazine-sulfo-Cy3 43 | 56 |
| Figure 18: Metabolic incorporation of galactose derivatives 31, 33 and 36 , followed by staining with 6-methyl-tetrazine-sulfo-Cy3 (43). Monosaccharide 42 was used as negative control. ... | 58 |
| Figure 19: Schematic illustration of the workflow for the metabolic incorporation of galactose derivatives 31, 33, 36 , their intracellular deprotection and the labeling strategy with 6-methyl-tetrazine-peg4-biotin (44). | 59 |
| Figure 20: A. Metabolic incorporation of galactose derivatives 31, 33 and 36 into cell membrane glycans of Huh7 cells and labeling using 6-methyl-tetrazine-peg4-biotin (44) and Alexa-Fluor-568-strep. Pentaacetyl galactose (42) was used as negative control. B. Metabolic incorporation of galactose derivative 33 into cell membrane glycans of HepG2 cells and co-staining with CellMask Deep red Plasma membrane dye. Pentaacetyl galactose (42) was used as negative control. | 62 |
| Figure 21: A. Median fluorescence intensity after incorporation of galactose derivatives 31, 33 or 36 in Huh7 cells, determined by confocal point-scanning microscopy. Pentaacetylated galactose (42) was used as negative control. Two-tailed Mann-Whitney, n = 25-30, representative example from three independent experiments. B. Ratio of the median fluorescence intensity against background signal from measurements with control sugar 42 .. | 62 |
| Figure 22: Median fluorescence intensity after incorporation of galactose derivatives 31, 33 or 36 in HepG2 cells, determined by confocal point-scanning microscopy. Pentaacetylated galactose (42) was used as negative control. Two-tailed Mann-Whitney, n = 25, representative | |

example of three experiments. **B.** Ratio of the median fluorescence intensity against background signal from measurements with control sugar **42**.63

Figure 23: **A.** Superposition of contour plots of forward-scatter detection versus PE-CF594-A fluorescence intensity, after metabolic incorporation of galactose derivative **33** (blue) in HepG2 cells. Pentaacetyl galactose (**42**) was used as negative control (red). **B.** Superposition of histograms of PE-CF594-fluorescence intensity, resulting from contour plots in **A.**64

Figure 24: Labeling of surface glycans after metabolic incorporation of alkynyl sugar analogs of **A.** fucose and **B.** N-acetyl-mannosamine. Filled histograms represent treatment with control sugars, open histograms cells treated with alkynyl sugar analogs. Figure from Hsu et al.¹³⁶ ...65

Figure 25: Metabolic incorporation of de-acetylated galactose derivative **38** into cell membrane glycans of HepG2 cells. Galactose (**45**) was used as negative control. iEDDA reaction was performed using 6-methyl-tetrazine-peg4-biotin (**44**), followed by staining with Alexa-Fluor-568-streptavidine. Nuclei were stained with Hoechst 33342. I and III, as well as II and IV represent two independent experiments.66

Figure 26: **A.** Superposition of contour plots of forward-scatter detection versus PE-CF594-A fluorescence intensity, after metabolic incorporation of de-acetylated galactose derivative **38** (blue) in HepG2 cells. Galactose (**45**) was used as negative control (red). **B.** Superposition of histograms of PE-CF594-fluorescence intensity, resulting from contour plots in **A.**67

Figure 27: **A.** Schematic illustration of the workflow for the metabolic incorporation of galactose derivative **33** into HepG2 cells after infection with sporozoites from Plasmodium berghei. **B.** Confocal images of HepG2 cells after incorporation of galactose derivative **33** and infection with sporozoites form Plasmodium berghei. Pentaacetylated galactose (**42**) was used as negative control. GFP-signal derived from the GFP-expressing parasite.69

Figure 28: Gating strategy for the acquisition and quantification of the metabolic incorporation of galactose derivative **33**, in HepG2 cells, after infection with sporozoites from Plasmodium berghei.70

Figure 29: **A.** Gating strategy for the acquisition and quantification of the metabolic incorporation of galactose derivative **33** in HepG2 cells, after infection with sporozoites from Plasmodium berghei **B.** Representative pictures from the selected populations after incorporation of galactose derivative **33**, Ch01: Brightfield picture, Ch02: GFP-channel, Ch04: Alexa-Fluor-568.71

Figure 30: Analysis of the mean fluorescence intensity after incorporation of **33** in HepG2 cells, with and without infection through Plasmodium berghei sporozoites, ratios against control **42**

A. Quantification by confocal microscopy, representative data from one out of three experiments, n = 6 pictures, each data point represents mean fluorescence intensity of 10 cells. Two-tailed Mann-Whitney. **B.** Quantification by flow cytometry, combined results of 3 independent experiments, gating of ~2000-3000 single cells (infection rate ~3%), Two-tailed Mann-Whitney. **C.** Quantification by imaging flow cytometry, combined results of 4 independent experiments, each data point corresponds to ~2000 single cell pictures (noninfected and naïve) or ~70 single infected cells (infection rate ~3%), Two-tailed Mann-Whitney.73

Figure 31: **A.** Structures of the GLUT 1 inhibitors WZB117 **46**, STF31 **47** and cytochalasine B **48**. **B.** Quantification of mean fluorescence intensity after the incorporation of galactose derivative **33** in the presence or absence of 10 µM inhibitors **46-48**. Data represented from one exemplary experiment out of two. Two-tailed Mann-Whitney. **C.** Quantification of median fluorescence intensity after incorporation of galactose derivative **33** in the presence of increasing amount of inhibitor **46**. Data represented the pool of two independent experiments.....76

Figure 32: **A.** Schematic illustration of the workflow for an administration of galactose derivative **33** to infected mosquitoes. **B.** gating strategy for acquisition and analysis of the dissected parasites and the remaining host cell debris in Amnis ImageStream Mark II. Data are represented from one feeding experiment, Two-tailed Mann-Whitney.80

Figure 33: Trial for metabolic incorporation of bifunctional galactose derivative **51** in HepG2 cell membrane glycans. Simultaneous staining with Alexa-Fluor-568-streptavidine and DIBO-alexa-fluor-488. Pentaacetyl galactose (**42**) was used as negative control.....89

Figure 34: Trial for metabolic incorporation of bifunctional galactose derivative **51** in HepG2 cell membrane glycans. Sequential staining with Alexa-Fluor-568-streptavidine and Alexa-Fluor-488-DIBO. Pentaacetyl galactose (**42**) was used as negative control.90

Figure 35: Model of CRM197 illustrating the location of the present disulfide bonds C186-C201 and C461-C471.95

Figure 36: Charge state distribution: **A.1** CRM-DHA, **B.1**, CRM-DHA-N3, **C.1** CRM₁₉₇. Comparison of the single charge state 48+ **A.2** CRM-DHA, **B.2** CRM-DHA-N3, **C.2**.CRM₁₉₇.99

| | |
|--|-----|
| Figure 37: A. 3-8% Tris-acetate gel of CRM ₁₉₇ and conjugation reactions of PN14-DBCO 65 with CRM-DHA-N3. B. 3-8% Tris-acetate gel of the conjugation reaction of GBS-Ia-DBCO 67 with CRM-DHA-N3. | 104 |
| Figure 38: A. Akta traces for the injection of the conjugation reaction CRM-DHA-N3 with GBS-Ia-DBCO 67 on a CHT type 1 resin. B. Akta traces for the injection of the conjugation reaction CRM-DHA-N3 with PN14-DBCO 65 on a CHT type 1 resin. | 105 |
| Figure 39: 3-8% Tris-acetate gel after conjugation reaction of GBS-Ia-DBCO 67 with CRM-DHA-N3 and after ammonium sulfate precipitation of the crude reaction mixture. | 106 |
| Figure 40: Possible connectivities of polysaccharide molecules to CRM-DHA-N3, A. conjugation of two polysaccharide molecules to the carrier protein. B. Conjugation of one polysaccharide molecule to the carrier protein. | 108 |
| Figure 41: Schematic illustration of the comparison of two different types of glycoconjugates with CRM ₁₉₇ | 110 |
| Figure 42: ¹ H NMR Analysis of the activation of thioglycoside donors 68-71 with MSH 28 , following the ratio of H1 (intermediate)/H1 (68-71)..... | 113 |
| Figure 43: Examples for possible derivatives of MSH for the application in glycosylation reactions. ¹⁶³ | 119 |
| Figure 44: A.1, B.1, C.1. Decrease in absorbance of tetrazine 40 at 530 nm during iEDDA reaction with galactose derivatives 37, 38 and 39 . A.2, B.2, C.2 concentration dependent determination of pseudo-first order rate constant k_{obs} for iEDDA between galactose derivatives 37, 38 and 39 and tetrazine 40 . The second order rate constant k_2 was calculated as the slope of the linear equation. | 132 |
| Figure 45: Determination of cell toxicity of galactose derivatives 31, 33 and 36 in concentrations 100 μ M and 200 μ M. The cell viability was measured using CellTiter-Blue reagent at timepoints A. 48h and B. 72h in Huh7 cells. Data are represented as % of maximum. Data from three experiments. | 134 |
| Figure 46: Determination of cell toxicity of galactose derivative 33 in concentrations 100 μ M and 200 μ M. A. The cell viability was measured using CellTiter-Blue reagent at timepoints 48h and 72h in HepG2 cells. B. Data are represented as % of maximum, Data from three experiments..... | 135 |

| | |
|---|-----|
| Figure 47: Incorporation of galactose derivative 33 in HepG2 cell membrane glycans and incorporation in the presence of the GLUT1 inhibitors WZB117 46 , STF31 47 and cytochalasine B 48 | 138 |
| Figure 48: A. Half-offset histograms of fluorescence intensity in channel PE-CF594-A, normalized mode, after metabolic incorporation of galactose derivative 33 without inhibitor (blue),with 10 μ M WZB117 46 (orange), with 20 μ M WZB117 46 (green), with 30 μ M WZB117 46 (dark green). B. Half-offset histograms of fluorescence intensity in channel PE-CF-594-A, normalized mode, after metabolic incorporation of galactose derivative 33 without inhibitor (blue) or with 10 μ M STF31 47 (orange). Pentaacetyl galactose 42 (red) was used as negative control. | 139 |
| Figure 49: Gating strategy of the analysis of the metabolic incorporation of galactose derivative 33 in HepG2 cell membrane glycans using Amnis ImageStream MarkII., non-infected samples | 142 |
| Figure 50 Gating strategy for analysis of the metabolic incorporation of galactose derivative 33 in HepG2 cell membrane glycans using Amnis ImageStream MarkII, infected with sporozoites from Plasmodium berghei. | 143 |
| Figure 51: Representative pictures acquired with Amnis ImageStream Mark II for A. HepG2 cells grown with the control sugar 42 non-infected or infected with sporozoites from Plasmodium berghei, and B. HepG2 cells grown with galactose derivative 33 , non-infected or infected with sporozoites from Plasmodium berghei. Ch01: bright field, Ch02: 488 nm/GFP, Ch04: 561 nm | 144 |
| Figure 52: Gating strategy for analysis of metabolic incorporation of galactose derivative 33 in HepG2 cell membrane glycans, A. without infection, B. after infection with sporozoites from Plasmodium berghei. | 145 |

Index of Schemes

| | |
|--|----|
| Scheme 1: Reaction scheme for the metabolic release and activation of mannosamine derivative 12 into a first precursor 13 and finally 14 . Enzymatic removal of substrate DCL by HDAC (histone deacetylase) and CTSL (cathepsin L). | 22 |
| Scheme 2: Examples for the conversion of cysteine residues into dehydroalanine. I: Selective amination and oxidative elimination using MSH 27 , II: Selective sulfenylation and base-mediated elimination, III: Bis-alkylation with methyl-2,5-dibromopentanoate (28) and elimination. ¹⁰⁸ | 39 |
| Scheme 3: Schematic illustration of examples for the activation of thioglycoside donors. | 44 |
| Scheme 4: Synthesis of the galactose derivatives 31 and 33 , from commercial starting material 29 | 50 |
| Scheme 5: Synthesis of the galactose derivative 36 , from commercial starting material 34 | 50 |
| Scheme 6: Zemplén deprotection for the derivatives 31 , 33 and 36 , resulting in the deprotected derivatives 37 , 38 and 39 | 51 |
| Scheme 7: Overview over the synthetic route for the synthesis of a bifunctional galactose derivative 50 | 85 |
| Scheme 8: Synthetic scheme for the first four steps, starting from pentaacetyl galactose (42), resulting in the intermediate 49 | 86 |
| Scheme 9: Reaction scheme for the functionalization of the primary hydroxyl group in C6 position of intermediate 56 | 86 |
| Scheme 10: Functionalization of the secondary hydroxyl group in C2 position with 5-Bromo-1-pentene. | 87 |
| Scheme 11: Deprotection of galactose derivative 56 and introduction of O-acetyl protecting groups, resulting in bifunctional galactose derivative 51 | 88 |
| Scheme 12: Example scheme for further derivatization of intermediate 49 to obtain additional bifunctional galactose derivatives 59-62 for metabolic incorporation. | 92 |
| Scheme 13: Reaction mechanism for the bisalkylation reaction of cysteine with methyl-2,5-dibromopentanoate (28) and subsequent elimination, resulting in the formation of dehydroalanine. | 96 |

| | |
|--|-----|
| Scheme 14: Site-selective introduction of DHA in CRM ₁₉₇ , followed by the introduction of an azide containing linker..... | 98 |
| Scheme 15: Reaction scheme for the introduction of the linker DBCO-NHS into the polysaccharide structures. A. PN 14 64 , B. GBS-Ia 66 | 101 |
| Scheme 16: Conjugation reaction of derivatized polysaccharides 65 and 67 to CRM-DHA-N ₃ | 103 |
| Scheme 17: Reaction scheme for the activation of thioglycosides 68-71 with MSH 60 , resulting in the final formation of hemiacetals 70a and 71a | 112 |
| Scheme 18: Reaction scheme for the activation of 2-deoxy-2-fluoro-thioglycoside donors 72a , 72b , 73a and 73b with MSH 27 | 114 |
| Scheme 19: Examples for the glycosylation reaction using thioglycoside donor 71 and an activation with MSH 27 | 116 |
| Scheme 20: Reaction scheme for the selective activation of 71 over 79 forming the disaccharide 80 . Classical activation of 80 with NBS, resulting trisaccharide 81 | 117 |

Index of Tables

| | |
|--|-----|
| Table 1: Examples of chemical reporter groups for metabolic incorporation and the corresponding bio-orthogonal labelling reactions ^{20,35} | 19 |
| Table 2: Overview of the natural amino acids and the chemical properties of the corresponding side chain. ¹⁰⁰ | 36 |
| Table 3: second order rate constants k_2 for the iEDDA reaction between tetrazine 33 and galactose derivatives 37-39 | 54 |
| Table 4: Cell growth conditions and staining procedures during the optimization of metabolic incorporation of galactose derivatives 31 , 33 and 36 | 57 |
| Table 5: Exemplary reaction conditions for the conversion of Cysteines C186-C201 into dehydroalanine. All reactions were performed in 50 mM NaPi pH = 11..... | 97 |
| Table 6: Mass results after deconvolution of the charge state distribution after 200 scans..... | 99 |
| Table 7: Reaction scope for glycosylation reactions using MSH 28 as thiophilic promotor. ^a Ratio was determined by integration of the anomeric proton signals ¹ H in the proton NMR of the products. ^b LiClO ₄ (1 equiv.) was used as additive. | 116 |
| Table 8: Different staining conditions after the metabolic incorporation of the bifunctional galactose derivative 51 | 154 |
| Table 9: All reaction conditions for the conversion of cysteins C186 and C201 into dehydroalanine..... | 156 |

Statement of Collaborations

For chapter 2, female *A. stephensi* mosquitoes infected with GFP- expressing *Plasmodium berghei* parasites, were received from Ana Filipa Caetano Parreira, Group of Maria Mota, Instituto de Medicina Molecular, Lisbon.

The work in the chapter 4 was performed in collaboration with Dr Filippo Carboni and Dr Roberto Adamo from GSK, Siena, Italy. Mass spectrometry was performed in collaboration with Prof. Carlos Cordeiro, Faculdade de Ciências da Universidade de Lisboa. The described experiments were planned and conducted by the Phd candidate.

The work in chapter 5 was performed in collaboration with Dr Ester Jiménez-Moreno, Dr Míriam Salvadó, Jordi Mestre, Prof. Sergio Castellón, Dr Gonzalo Jiménez-Osés and Dr Omar Boutureira. The experiments were conducted by the Phd candidate if not stated otherwise in the experimental section.

In this work, literature references are depicted as numbers in superscript at the end of the sentence. Chemical structures or compounds are numbered in bold letters when referred to in the text.

1. Chapter 1 – General introduction

1.1. Carbohydrates – a general perspective

Next to nucleic acids, lipids and proteins, carbohydrates belong to the main organic molecules in living systems.¹ The field of carbohydrate chemistry and glycobiology continues to evolve, due to the rising awareness of the importance of this class of biomolecules. Carbohydrates are involved in energy supply for cellular processes, structural characteristics of organisms and they are important during cell recognition, adhesion and signaling in health and disease state, just to mention some of their functions.^{1,2} The enormous complexity is remarkable, knowing that the synthesis of carbohydrate structures, in contrast to, for example, proteins or nucleic acids, is not template driven.³ Only the expression of enzymes like glycosyltransferases or glycosidases is encoded in the genome and their interplay in different cellular compartments gives rise to the large variety of glycan structures. Looking at the structure of glycans, a great number of possibilities can be found, depending on the different types of monosaccharides, the position and type of linkage, as well as the formation of linear or branched structures.¹ While all DNA or RNA structures are build out of four building blocks and the diversity of proteins is created by a certain set of alpha-amino acids, carbohydrate structures display a much larger number of varieties. This feature is a result of multiple possible configurations of the stereocenters in a single monosaccharide and the diversity of chemical modifications of the present hydroxyl groups.⁴

1.1.1. *N*- and *O*-Glycosylation

Cellular oligosaccharides can be connected to proteins with different types of linkages: most of them through the so-called *N*- or *O*-linked anomeric bond (Figure 1). For a *N*-linked oligosaccharide, the first sugar is linked to an Asparagine (Asn) residue in an amino acid sequence Asn-X-Ser(Thr). The assembly of this type of glycan starts with the synthesis of the glycan part on dolichol phosphate, from which then the entire oligosaccharide is transferred to

the Asn- residue of the final protein. All *N*-linked oligosaccharides share a common core sequence of mannose (Man) sugars. The oligosaccharide $\text{Man}\alpha 1-6(\text{Man}\alpha 1-3)\text{Man}\beta 1-4\text{GlcNAc}\beta 1-4\text{GlcNAc}\beta 1-\text{Asn}$, starts with *N*-acetylglucosamine (GlcNAc) (**1**), from which further structures can be distinguished.^{5,6} *N*-glycosylation is an important factor for protein folding in the ER, from where the proteins are then translocated to the Golgi apparatus. Here, further maturation of the *N*-glycan structures can occur, resulting in so called complex or hybrid oligosaccharides.⁶

The second type of linkage in oligosaccharide structures is represented by the *O*-linked glycosylation. Different from the *N*-linked structures, this type of glycosylation occurs by the sequential addition of single monosaccharides, starting with the covalent linkage of *N*-acetylgalactosamine (**2**) to the hydroxyl group of serine or threonine.⁷ These types of *O*-linked glycan structures are also referred to as mucins.⁷ An elongation of the initial monosaccharide can then occur with galactose, fucose, sialic acid or *N*-acetylglucosamine, which results in a complex mixture of possible oligosaccharides.¹ Also an *O*-linked glycosylation starting with β -*N*-acetylglucosamine (**3**) is known and was shown to be an important factor for protein phosphorylation, protein-protein interactions, protein localization and degradation and transcription regulation.⁸ Additional examples for *O*-linked glycosylation are modifications with α -L-fucose (**4**) on serine or threonine in fibrinolytic proteins, or β -galactose (**5**) on hydroxylysine in collagen.^{9,10}

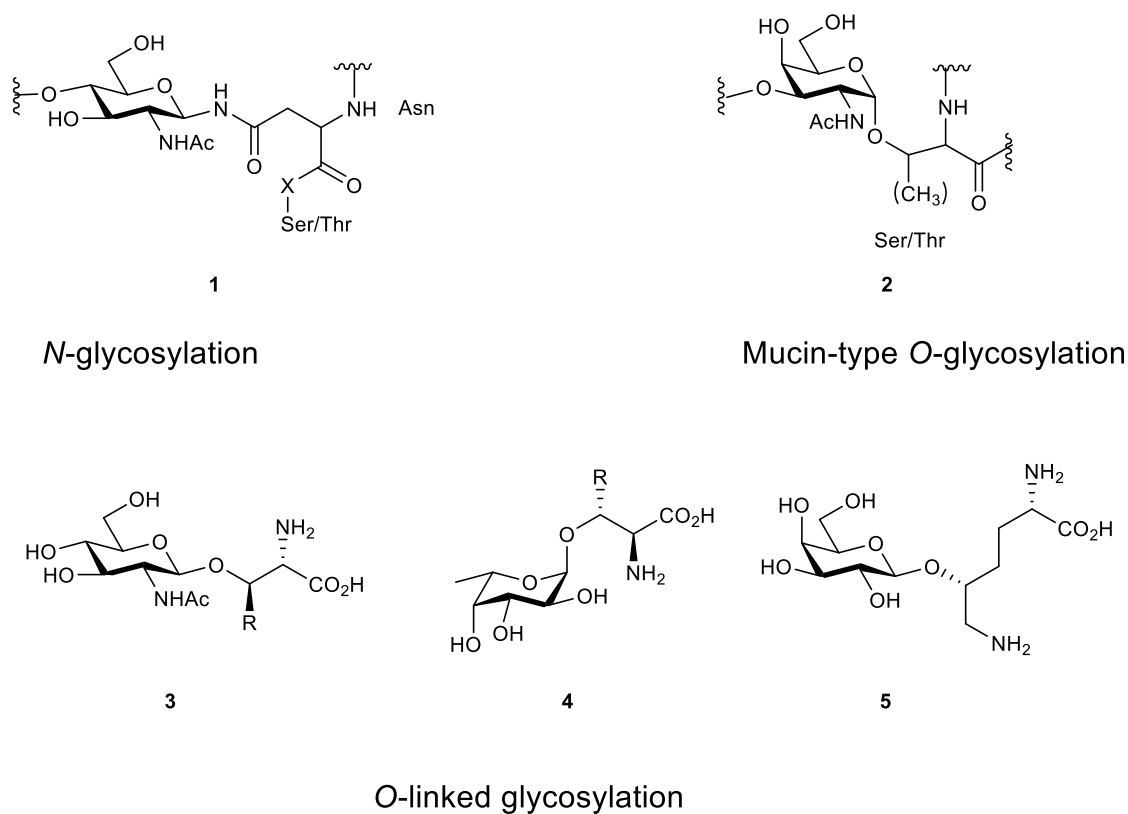


Figure 1: Schematic illustration of N- and O-linked glycosylation, displaying the initial sugar moiety connected to the corresponding amino acid.

1.1.2. Carbohydrates in disease state

All the important functions of glycosylation become even more clear when looking at disease states.¹¹ A range of alterations in the glycosylation profile of proteins during different diseases is known and only some examples will be addressed here. In the late 20th century, it was described that oligosaccharide binding lectins bind in a different way to malignant tissue than healthy tissue.¹² Today it is known that in cancer cells, a differential expression of glycosyltransferases leads to an over- or under expression of normal glycan structures.¹³ One of the most studied cases is the expression of the so called Tn- **6**, or sialyl Tn-antigen **7** on the surface of cancer cells (Figure 2). These truncated O-linked glycans result from a dysregulation of the corresponding glycosyltransferase and these glycan antigens represent important biomarkers in several types of cancers.¹³

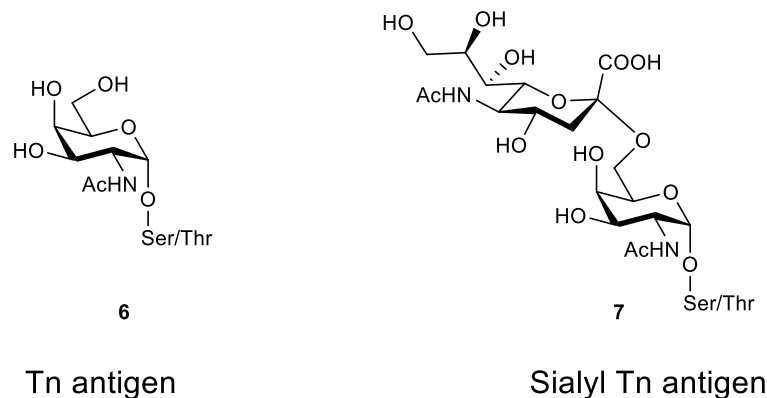


Figure 2: Tn-antigen and sialyl Tn antigen, connected via O-glycosylation to serine or threonine.

The altered glycosylation pattern of cancer cells is not only responsible for the presentation of important disease related biomarkers, but also for the modulation of cell-cell adhesion during malignancy and for the regulation of certain immunologic pathways. The glycoprotein E-cadherin represents a transmembrane protein that is strongly involved in the epithelial to mesenchymal transition process being also responsible for cell-cell adhesion in epithelial tissues.¹⁴ It has been shown that during cancer, alterations in the *N*-glycosylation pattern of this protein are related with malignant and invasive phenotypes.^{15,16} Another example for the impact of changes in cell surface glycosylation during cancer, can be found when looking at receptor tyrosine kinases (RTK). These transmembrane cell surface receptors are strongly glycosylated and are involved in the regulation of cellular signaling processes, like cell division, differentiation or migration.¹⁷ Among several possible hyper-activation mechanisms of these receptors in cancer cells, it was also reported that RTKs, which promote cell proliferation, display a higher amount of *N*-glycosylation sites, than receptors which are involved in growth-arrest.¹⁸ Furthermore, aberrant activation of sialyltransferases or fucosyltransferases can lead to increased formation of sialylated and fucosylated glycoprotein substrates, which can promote the dimerization and activation of RTKs.¹⁹

Moving from cancer to infection diseases, also here the important role of glycans is notable. The surface of bacteria and viruses is coated with specific polysaccharide structures, which are

crucial for their survival as well as for their pathogenicity.^{20,21} Bacteria display various types of glycan structures on their surface, like lipopolysaccharides, teichoic acid and glycoproteins, which contain specific bacterial monosaccharide building blocks.²⁰ An example might be the incorporation of *N*-acetylmuramic acid, which is uniquely expressed by bacteria.²²

Carbohydrates are important for the pathogenicity of the infectious organism and they are a key factor during the infection process.²³ It was shown that most bacteria interact with cell surface glycoproteins of the host cell, by adhering either to terminal or internal sugar motives.²³ Also viral pathogens were shown to invade using this strategy.²¹ Another important role of bacterial and viral glycan structures is the protection of the pathogenic organism from the host's immune system. One example is given by group A *streptococcus*, which is expressing a type of hyaluronan that is identical with a glycosaminoglycan structure in the skin. By mimicking glycan structures from the host, no immune response is activated and the pathogen can invade the organism.²⁴

The importance of carbohydrate structures during bacterial and viral infection makes them a valuable target for medicine. The probably most classical treatment method, is an interference with the cellular machinery which is producing the pathogenic glycan structures in the bacteria or virus. Antibiotics like penicillin or vancomycin interfere with the biosynthesis of bacterial peptidoglycans and new inhibitors are getting developed to target more specifically the biosynthetic pathways of rare bacterial monosaccharides.^{25,26} Also in viral infections, the inhibition of viral derived enzymes for glycoprotein maturation is an important key during treatment, as for example, shown by the mode of action of Oseltamivir (Tamiflu) against influenza virus.²⁷

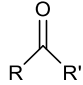
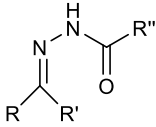
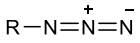
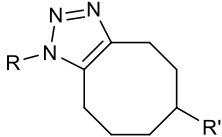
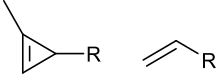
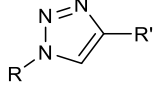
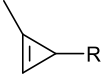
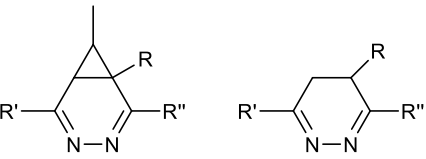
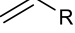
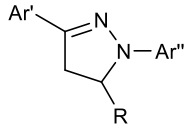
However, the use of broad-spectrum antibiotics gave also rise to increasing resistances against common treatments. Another strategy to use carbohydrates for the development of medical treatments, is the usage of antigenic glycan structure for the development of vaccines. There are already a number of vaccines available, in which specific carbohydrate antigens are used as immunogenic moiety, and the development of new candidates is ongoing.^{28,29} Not only for the fight against bacterial or viral infections, also the development of anti-cancer vaccines is ongoing.^{30,31} The usage of bacterial polysaccharide structures in vaccines was developed already in the 1940s, however it was observed that pure carbohydrate vaccines do not elicit a protective

immune response in young children. This gave rise for the development of so called glycoconjugate vaccines, in which the carbohydrate antigen is connected to an immunogenic protein carrier.²⁸

1.1.3. Metabolic oligosaccharide engineering – state of the art

The important role of carbohydrates for any organism in health or disease state became very clear during the last decades.^{11,32} As post-translational modification, the final structure of a glycan is not predefined by any template, like it is the case for proteins, which are based on their RNA-sequence. This feature can complicate investigations on the composition, structure and purpose of certain glycan structures within an organism.³³ A breakthrough was reached in 1997 when Carolyn Bertozzi and co-workers presented their work on an artificial mannosamine derivative, bearing a ketone group for condensation reactions on the cell surface after metabolic incorporation.³⁴ In the following years, several chemical reporter groups were developed and proven to be incorporated into cellular glycan structures, where they are available for selective targeting (Table 1).

Table 1: Examples of chemical reporter groups for metabolic incorporation and the corresponding bio-orthogonal labelling reactions^{20,35}

| Chemical reporter group | Bio-orthogonal labelling reaction | Product |
|---|--|---|
|  | Condensation reaction with hydrazine derivatives |  |
|  | Strain promoted click-reaction |  |
|  | Cu(I)-catalyzed cycloaddition |  |
|  | Inverse electron-demand Diels Alder reaction |  |
|  | Photo-activatable 1,3-cycloaddition |  |

Only some examples are represented by ketone groups, azides, terminal alkynes, cyclopropenes, terminal alkenes or norbornenes, which were synthetically introduced in monosaccharides, such as mannosamine (**8**) or sialic acid (**9**), glucosamine (**10**) and galactosamine (**11**) (Figure 3).³⁶

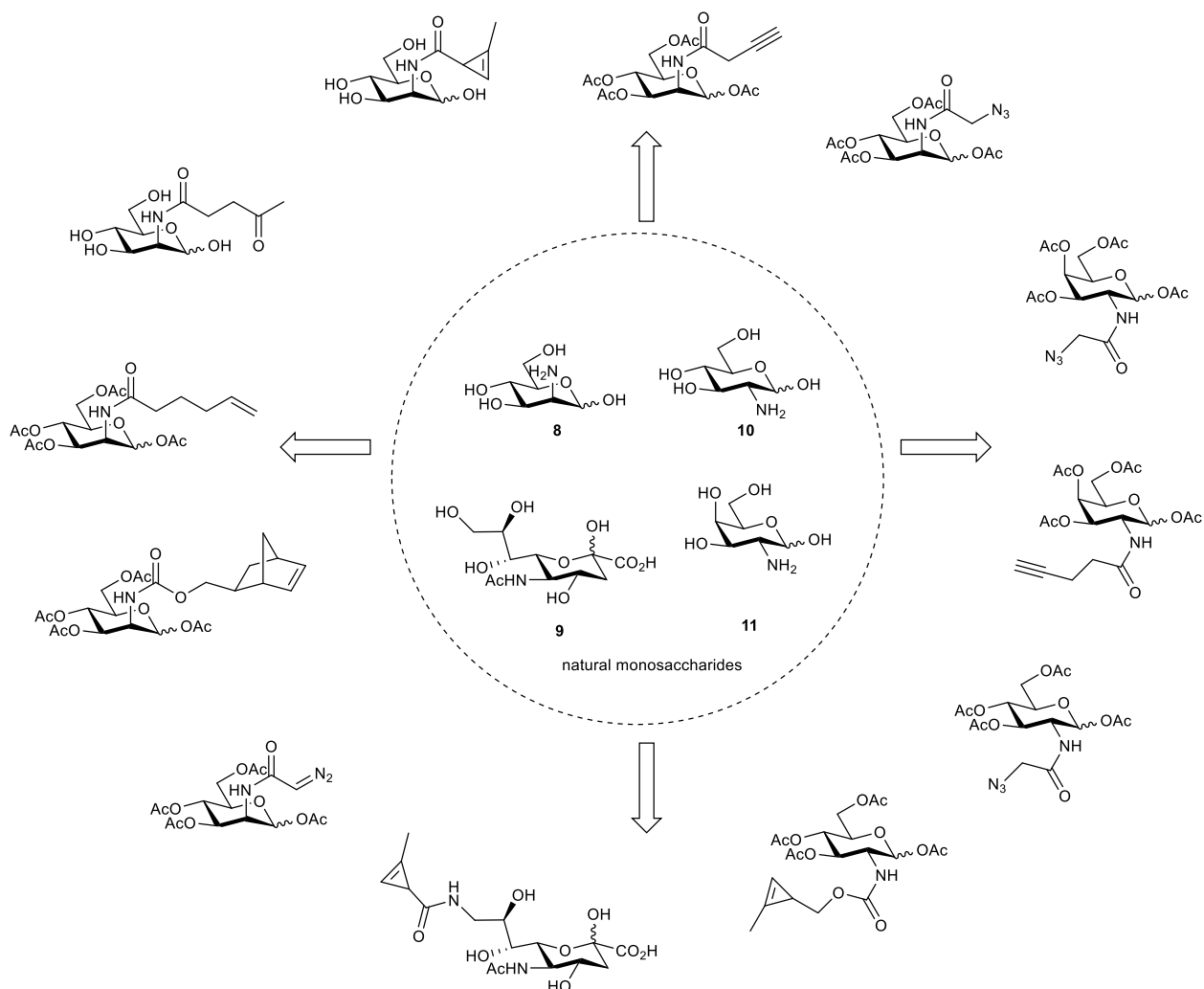


Figure 3: Schematic overview of examples for applied unnatural monosaccharide building blocks (outer ring) and the natural substrates (inner ring 8-11).

During the process of MOE, an artificial, usually acetylated monosaccharide with a chemical reporter group, is administered to a certain organism. The compound will enter the cell via diffusion or transporters and will be deacetylated by unspecific esterase enzymes, before being used in biosynthetic pathways and incorporated into cellular glycan structures (Figure 4).³⁵

It was shown that several biological systems are able to incorporate these artificial monosaccharide structures in their system and to expose the chemical reporter groups for further reactions.^{36,37} The technology of MOE is now able to provide the tools for much deeper

investigations on the biological pathways, which are responsible for glycan assembly and their structure. The obtained knowledge can be used for the development of new therapeutics based on carbohydrate entities.

Despite showing the ability of different biological systems to incorporate artificial sugar structures, increasing effort is being made to develop MOE strategies that are able to label selectively certain types of cells or proteins.

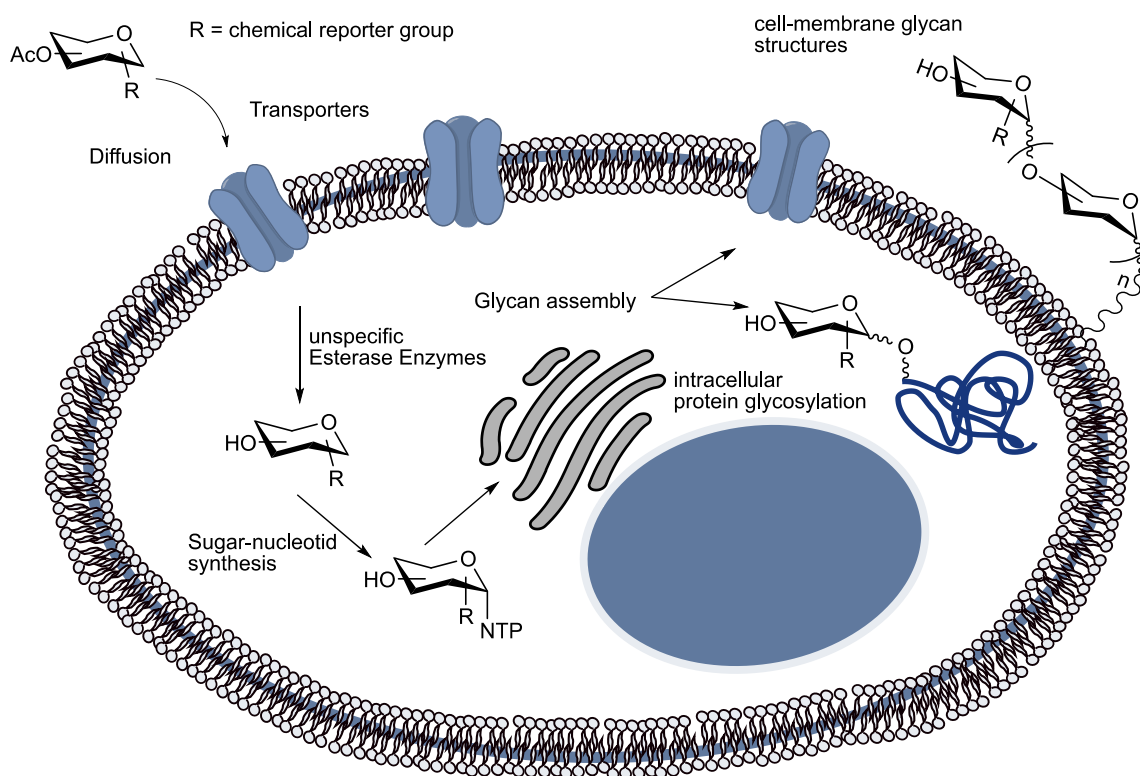
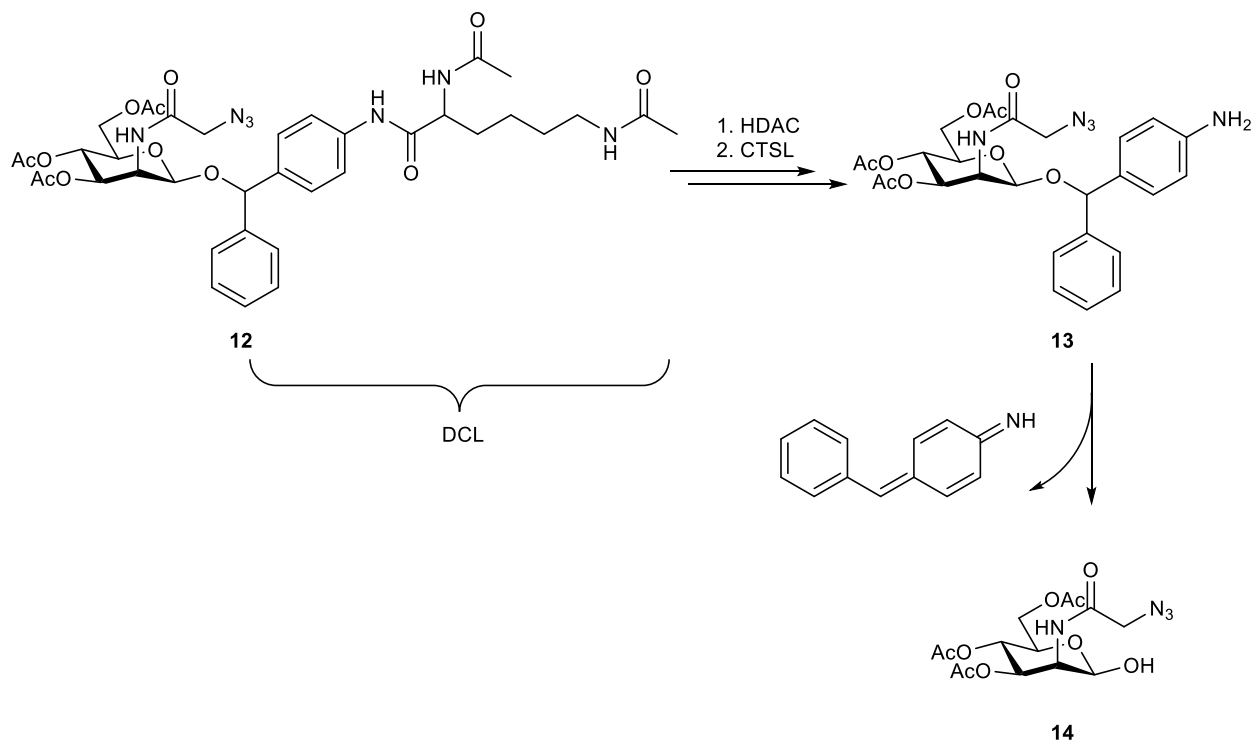


Figure 4: Overview illustrating the cellular mechanisms which enable MOE. Per-acetylated monosaccharides enter the cytosol via passive diffusion or transporters, followed by the deacetylation by unspecific esterase enzymes. The generation of sugar nucleotides (NTP) allows glycan assembly by glycosyltransferases, resulting in intracellular or cell membrane protein glycosylation.

H. Wang et al. had great success in selectively labeling cancer cells over healthy cells by using a special derivative of tetraacetyl-*N*-azidoacetylmannosamine **12**. The anomeric center in this derivative **12** was blocked through the substrate ((4-(2,6-diacetamidohexanamido)phenyl)(phenyl)methoxy (DCL), which could be removed by two

cancer-overexpressed enzymes (Scheme 1). By using this technology, their developed mannosamine derivative **12** was not metabolically processed until the anomeric position was hydrolyzed in the cancer-tissue, which then enabled its metabolic incorporation into glycan structures on the cancer cell. By using the introduced azido-group of **14**, they were able to accumulate dibenzocyclooctyne-doxorubicin selectively in cancer cells.³⁸



*Scheme 1: Reaction scheme for the metabolic release and activation of mannosamine derivative **12** into a first precursor **13** and finally **14**. Enzymatic removal of substrate DCL by HDAC (histone deacetylase) and CTSL (cathepsin L).*

A different strategy in the challenge to develop more selective monosaccharide analogues was presented by Pratt and co-workers. By altering the position of the introduced azido reporter group to the C6 position of the monosaccharide **15**, they could show selective incorporation in cytoplasmic *O*-GlcNAcylated proteins over cell surface *N*-linked or mucin *O*-linked glycan structures (Figure 5). Also, they highlight the high metabolic flexibility of biological systems which has to be taken into account while designing artificial carbohydrate structures.³⁹

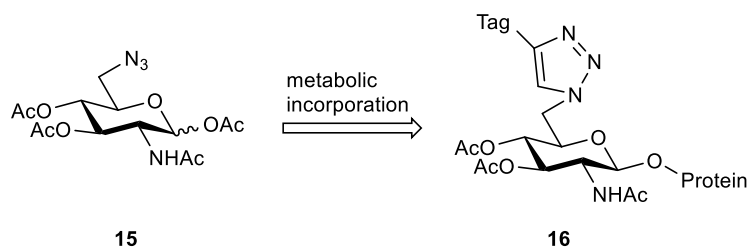


Figure 5: Azide derivative **15** of glucosamine for selective incorporation into O-GlcNAc-protein modifications.³⁹

The introduction of artificial monosaccharides into cellular glycan structures can be also used for the identification of specific glycoprotein patterns, for example in a certain disease state. Bertozzi and co-workers demonstrated the incorporation of artificial acetylated *N*-azidoacetylmannosamine in human tissue cultures from prostate cancer.⁴⁰ After an enrichment based on biotinylation, mass spectrometry could identify specific glycoproteins, which were up-regulated in prostate cancer tissue.⁴⁰ This work is one of the numerous examples in which mannosamine derivatives are used to label and study sialylated glycan structures by taking advantage of the biosynthetic conversion of mannosamine monosaccharides into sialic acid. Due to the importance of sialic acid in several biological processes as well as in disease state, a high percentage of studies in metabolic oligosaccharide engineering is focusing on this monosaccharide.^{37,41,42}

However, also examples for rare sugars can be found. Dube and co-workers could show the metabolic incorporation of azido derivatives from rare monosaccharides like bacillosamine **17** or 2,4-diacetamido-2,4,6-trideoxyhexose **18** by the *Helicobacter pylori* (Figure 6).⁴³ These results are particularly important with regard to the significance of these glycans during an infection with these bacteria.²⁰ An incorporation of artificial sugars and by using methods like described above, can lead to the identification of antigenic structures and finally to the development of efficient treatments.

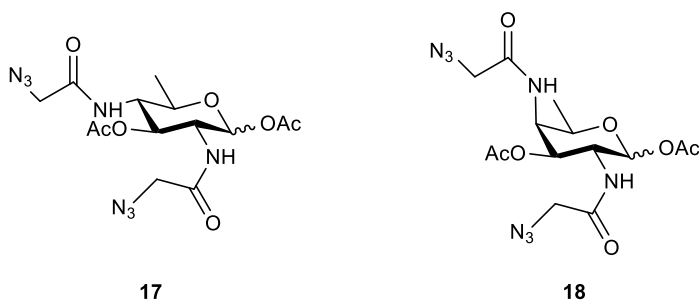


Figure 6: Azide containing derivatives of rare bacterial monosaccharides bacillosamine **17** and 2,4-diacetamido-2,4,6-trideoxyhexose **18**.

The presented examples give a brief insight in which areas MOE was already successfully applied and how artificial monosaccharides, containing a single chemical modification, were used.

1.1.4. Multifunctional labeling of glycan structures

MOE started with the introduction of single chemical reporter groups into cellular glycan structures and it was shown in different ways that cellular systems are able to incorporate single chemical reporter groups in their structures.^{36,44} Going further, instead of applying only one monosaccharide for the metabolic incorporation, also the cellular uptake of more artificial sugars simultaneously was studied. If these artificial monosaccharides contain two orthogonal chemical reporter groups, bio-orthogonal labeling reactions can be applied, which then can be used to address the co-localization of these sugars or their different metabolic routes.⁴⁵

An exemplary study, which uses a norbornene modified mannosamine derivative for a labeling via iEDDA reaction and an azide modified glucosamine derivative for click-chemistry, was presented by Wittmann and co-workers.⁴² In their experiments, they could successfully show the incorporation of both artificial sugars in cell membrane glycans during the same experiment. They went even further in a more recent publication, by combining three different labeling reactions with three different mannosamine derivatives **19** – **21** for click-chemistry, iEDDA and photoclick reaction (Figure 7).⁴⁶

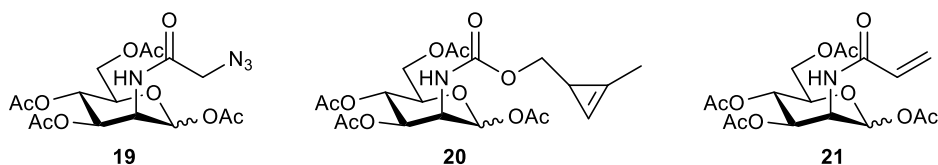


Figure 7: Chemical structures of mannosamine derivatives for click-chemistry **19**, iEDDA **20** and photoclick reaction **21**.

However, so far only one example was found in which one monosaccharide was modified with more than one chemical reporter group. Chen and co-workers demonstrated successfully the synthesis and metabolic incorporation of two sialic acid derivatives which were equipped with two orthogonal reporter groups. By introducing an azide group in C9 position and a second alkyne or diazirine group in the *N*-acyl position of the sialic acid molecule, two orthogonal reporter groups are available within one molecule (Figure 8). They could successfully show that both of derivatives **22** and **23** were incorporated into cell surface glycans of several cell lines.⁴⁷

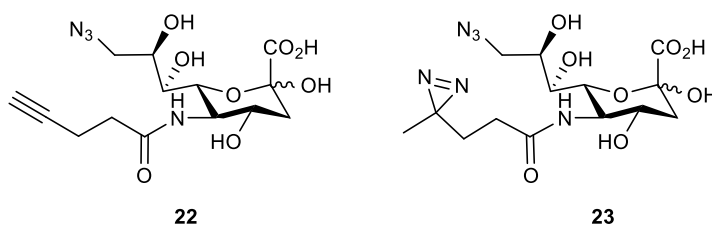


Figure 8: Chemical structures of bifunctional sialic acid derivatives **22** and **23**, containing an azide group in C9 position and an alkyne or diazirine group in *N*-acyl position.

This example demonstrates the enormous flexibility of cellular systems to use highly modified structures as substrates during biosynthetic pathways.

The diversity of MOE is not only generated by the usage of different monosaccharides, but also by the availability of a range of different chemical reporter groups. As mentioned at the beginning of this section, several bio-orthogonal labeling reactions can be applied, depending on the introduced chemical reporter group on the monosaccharide.

1.1.5. Inverse electron demand Diels Alder reaction for MOE

For this work, the choice was made to use inverse electron demand Diels Alder reactions (iEDDA), to target the incorporated sugar. The iEDDA reaction occurs between an electron-poor diene **24** and an electron-rich dienophile **25**, without the necessity of any additional metal promoters or specific pH requirements. In the applied bio-orthogonal labeling reaction, the tetrazine core represents the diene moiety, while an alkene group will react as dienophile. Both reactants of this reaction can be tuned to achieve different reaction rates, typically ranging from $1-10^6 \text{ M}^{-1}\text{s}^{-1}$.⁴⁸ While the tetrazine reactivity can be optimized by attaching electron withdrawing groups to lower the LUMO energy, the dienophile's HOMO energy can be increased by electron donating groups (Figure 9 A). Both types of modifications will lead to a decrease in the energy gap between the $\text{LUMO}_{\text{diene}}$ and the $\text{HOMO}_{\text{dienophile}}$, which finally will result in a faster reaction rate.⁴⁹

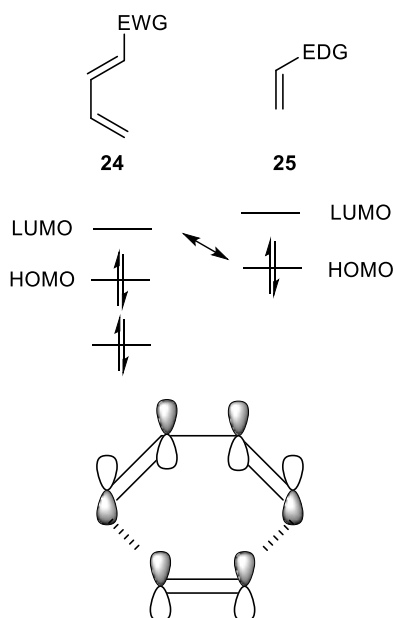


Figure 9: Schematic illustration of the orbital interaction in iEDDA. Decreasing LUMO energy of diene **24** through electron withdrawing groups, increase of HOMO energy of the dienophile by electron-donating groups.

In this context, it should be highlighted that the tuning of reactivity of the dienophile using heteroatoms, led to the discovery of a decaging reaction. During this specific reaction, a vinyl ether system was used as dienophile in an iEDDA reaction with tetrazine, which results in the release of an alcohol group and a pyridazine derivative.⁵⁰ A similar reaction was developed with this concept, using a system with TCO and vinyl protecting groups for the decaging and activation of anti-inflammatory drugs.⁵¹

Despite the interaction between the participating orbitals, several factors can influence the reaction rates of iEDDA reactions, namely the strain effect.⁴⁸ While strained dienophiles like *trans*-cyclooctene (TCO) or cyclopropenes show very fast reaction rates, they seem to be incorporated in lower levels into cellular structures. Unstrained reporter groups like terminal alkenes on the other side, show slower reaction kinetics but better incorporation rates.⁴⁶ The very fast reaction rates of strained dienophiles were explained by the pre-distorted conformation of these molecules towards the structure of the transition states, which consequently makes less energy necessary for the dienophile to enter the reaction.^{52,53}

Other factors that can strongly influence the reaction kinetics include stereochemistry and steric effects, as well as the solvent and the pH value during the reaction. Differences in the rate constants were for example found when comparing an axial isomer of functionalized TCO with its equatorial counterpart.⁵⁴ Also *exo*-norbornenes were shown to react up to three times faster than the *endo* isomere.⁵⁵ Looking at the influence of the solvent and the pH during the reaction, it has been described that protic solvents, such as water, accelerate the kinetics due to stabilizing interactions of these solvents and the activated reaction complex.⁵⁶ For the application of iEDDA in biological systems, especially the pH can be crucial, however only minor influences on the reaction rate were found here.⁵⁷

In the field of MOE, the iEDDA reaction was used to label incorporated mannosamine, glucosamine, galactosamine or sialic acid derivatives. It was shown that chemical reporter groups such as cyclopropenes, terminal alkenes or norbornenes can be incorporated in monosaccharide structures and can be addressed in cell glycan structures.^{42,58,59}

In this work, the iEDDA reaction will be used to address newly developed galactose derivatives, equipped with terminal alkene reporter groups. In the majority of reports using MOE to study

carbohydrate incorporation or glycosylation patterns, the focus is on mannosamine or sialic acid derivatives. As described in the previous section, the area of application for MOE is growing and the usage of different monosaccharides is getting investigated. The focus of this work will be on the development and utilization of galactose derivatives for MOE, with a special focus on a disease related application.

1.1.6. Malaria and the glycobiology of *Plasmodium*

The specific interest on galactose was initiated by several reports on the importance of galactose containing glycans during an immune response against the *Plasmodium* pathogen, the responsible parasite for malaria.^{60,61} Human malaria can be caused by six different *Plasmodium* parasites, namely *Plasmodium falciparum*, *P. vivax*, *P. ovale curtisi*, *P. ovale wallikeri*, *P. malariae* and *P. knowlesi*, whereby *P. falciparum* and *P. vivax* are considered to be the major causes for illness and death.⁶²

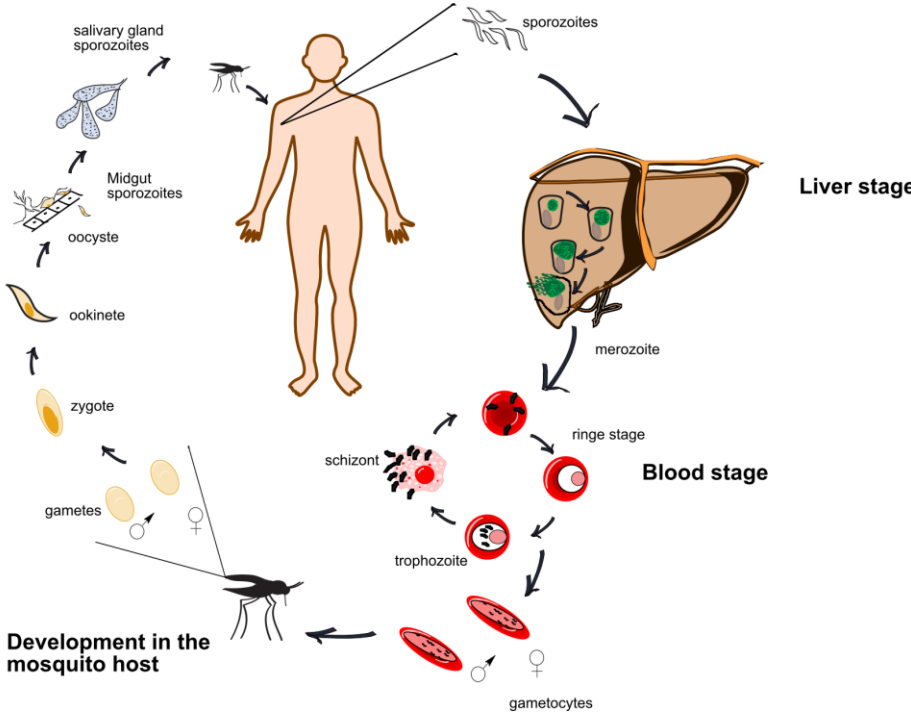


Figure 10: Schematic illustration of the life cycle of the Plasmodium parasite.

The life cycle of the *Plasmodium* parasite, which is causing the disease, alters between the mosquito and the mammalian host (Figure 10). During the mosquito bite, sporozoites are injected into the dermis of the mammalian host, which then infiltrate blood vessels to reach the liver. Here, the parasite invades very few hepatocytes, which makes this symptom less stage the bottle neck phase of the infection. The development inside the hepatocytes results in an enormous amplification of the parasite, which then are getting released from the bursting merozoites into the blood. In this stage, the typical symptoms of the disease are getting developed and the parasite develops in an asexual cycle. However, a part of the parasites will change into a sexual development which results in male and female gametocytes. In this stage, they can be taken up by mosquitoes during a blood meal and the developmental cycle will continue in the mosquito host. Here, the parasite evolves from gametes to zygotes and ookinetes, which finally progress into sporozoites in the salivary glands of the mosquito.⁶²

Even in the 21st century, malaria causes about 219 million cases and more than 435000 deaths in the year 2017, with 61% of the deaths worldwide represented by the group of children under

5 years.⁶³ It is very important to notice that between 2015 and 2017, no significant improvement in the reduction of cases was achieved.⁶³ With problems like resistances to common treatments or insecticides, the development of an efficient anti-malaria vaccine is one of the key goals in this area of research. Overall, some vaccine candidates were able to show protection in phase II clinical trials, however with moderate success.⁶⁴ A candidate for the pre-erythrocytic stage of the infection is represented by RTS,S which contains epitopes from the C-terminus and the central repeat of the circumsporozoite protein (CSP), a major surface structure of the *Plasmodium* sporozoites.⁶⁵ Despite high protection rates at the beginning, the decline in efficacy is a limitation of this vaccine candidate and has to be improved.^{66,67} A different strategy is used in the PfSPZ vaccine, in which irradiation-attenuated sporozoites are applied.^{68,69} After an invasion of the hepatocytes, these sporozoites fail in the development of a blood stage infection and it was possible to show good protection in malaria-naïve adults against homologous strains.⁷⁰ Nevertheless, this vaccine candidate did not result in efficient protection against heterologous strains.⁶⁴ There are several other examples for anti-malaria vaccine candidates, working in different stages of the infection, however the improvement of efficacy is a major challenge for present and future studies.⁶⁴

In this context, glycosylation of relevant antigenic proteins might be a possible area for further research. The glycobiology of the *Plasmodium* parasite is subject of highly controversial research during the last decades, showing both absence and presence of certain glycoconjugate structures.⁷¹⁻⁷⁴ The expression of glycosylphosphatidylinositol (GPI) anchors showed the presence of mannose, which on the contrary site could not be found in *N*-glycan structures.^{75,76} GPI anchors were found to be essential for parasite development and its pathogenicity, and several important antigens like *Pfs25*, CSP or MSP-1 and MSP2 are GPI-anchored proteins.⁷⁷ Apart from this structure, mannose was found in a *C*-mannosylation of a thrombospondin type I repeat (TSR) domain which exact function has to be evaluated.⁷⁸ Another monosaccharide, *N*-acetyl-glucosamine was found in short *N*-glycan structures of the parasite and in its de-*N*-acetylated form as component of the GPI anchor.^{76,79} For glucose, it is still unknown how an activation from glucose-1-phosphate for UDP-glucose is achieved, because no enzymes were found. However, this sugar nucleotide was found in the blood stage of the parasite.⁸⁰ It is expected that UDP-glucose is used for the synthesis of glycolipids or for *O*-glycosylation

motives. A similar situation is given for the monosaccharide fucose, which nucleotide GDP-fucose was identified in the blood stage, but no glycoconjugate structures with this sugar were described yet.^{73,80} The sugar of interest for this work, galactose, was as well identified as UDP-galactose in the blood stage.⁸⁰ However, none of the necessary enzymes with the ability to epimerize glucose or with transferase activity were identified in the parasite genome.⁸¹ Especially with regard to a special galactose containing trisaccharide, the α -Gal epitope (**26**), it is clear that more investigation is necessary on this subject (Figure 11).

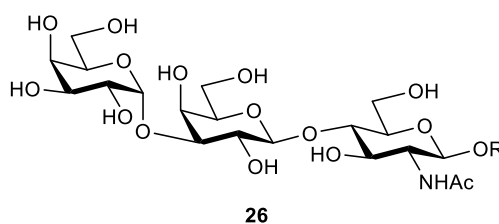


Figure 11: Structure of the α -Gal epitope Gal α 1-3Gal β 1-4GlcNAc **26**.

The α -Gal epitope **26** represents the structure Gal α 1-3Gal β 1-4GlcNAc, which is absent in humans, apes and old-world monkeys due to a loss-of-function mutation during evolution. The general exposure to this antigen, leads to the expression of 1-5% IgM and IgG antibodies against this epitope.⁸² Interestingly, it was shown that in malaria endemic areas the level of anti- α -Gal IgMs was significantly higher than in non-endemic areas and higher levels of this antibody seemed to provide some protection against an infection.⁶⁰ Yilmaz and co-workers were able to show a protective effect of anti- α -Gal IgMs against malaria transmission when using mice which were gut-colonized with a α -Gal expressing *E.coli* strain. Furthermore, they were able to show the expression of α -Gal on the surface of *Plasmodium falciparum* sporozoites.⁶⁰ More recently, the protective effect of anti- α -Gal IgMs was confirmed by Aguilar and co-workers, however several external factors like the location, the level of exposure to the *Plasmodium* parasite, the children's age or maternally-transferred antibodies, were shown to affect the anti- α -Gal IgM and IgG response.⁶¹

1.1.7. The story of the α -Gal epitope

The described α -Gal is ubiquitously expressed by basically all non-primate mammals, excluding apes, humans and old-world monkeys, as well as by many pathogenic parasites. Resulting from the constant environmental presence of this carbohydrate epitope, a natural reservoir of 1-2% anti- α -Gal IgG and 3-8% of anti- α -Gal IgM can be found as part of natural human antibodies.⁸² These antibodies are also involved in tissue rejection after xeno-transplantations.⁸³ The strong response of the human immune system towards this carbohydrate antigen led to its utilization as adjuvant in immunotherapy, during which it is increasing the uptake of presented antigens through antigen presenting cells.⁸⁴ A very recent study also describes the ability of α -Gal-antibody conjugates to recruit anti- α -Gal antibodies towards the target cell and to induce an acute immune response.⁸⁴ With regard to infection diseases like malaria, chagas disease or sleeping sickness, it is very interesting that all the responsible pathogens express the α -Gal epitope on their surface.⁸⁵ As mentioned in the previous section, anti- α -Gal IgMs were correlated with a protection against malaria transmission and similar results were reported for protection against an infection with *Trypanosoma cruzi* and leishmaniasis.^{86,87} The possibility of having one single antigenic carbohydrate structure, triggering protective effects against several different infection diseases, gave rise to the idea of a single vaccine against these threats, using the α -Gal epitope.⁸⁵

The α -Gal epitope is a good example for the importance of antigenic carbohydrate structures of potential pathogens, during the course of the development of effective vaccine candidates.

1.2. Glycoconjugate vaccines

1.2.1. Carbohydrates as vaccine antigens

The development of glycoconjugate vaccines started in the late 20th century after it was realized that vaccines containing only capsular polysaccharides from, for example, group C *Neisseria meningitides*, did not elicit protective antibodies in young children.²⁹ Looking at carbohydrate antigens, two main groups can be distinguished: zwitterionic (ZWI) and non-zwitterionic (Non-ZWI) polysaccharides. Zwitterionic polysaccharides are taken up by antigen-presenting cells (APC) and processed in endosomes. Due to their zwitterionic character, the fragments can bind to major histocompatibility complex class II (MHCII) structures and are presented on the cell surface (Figure 12 A).⁸⁸ The presented structures can then be recognized by immature CD4⁺ T-cells.⁸⁸ However, the majority of carbohydrate antigens from pathogenic bacteria belong to the group of non-zwitterionic polysaccharides. These glycan antigens are recognized by B-cells through their immunoglobulin surface receptors without prior processing. Through the antigen-recognition, these B-cells start to differentiate into plasma cells, which will produce low-affinity antibodies without the formation of memory-B cells (Figure 12 B).⁸⁹ Looking at glycoconjugate vaccines, these structures are getting processed within endosomes of B-cells by reactive oxygen species, resulting in different sized repeating units of the polysaccharide coupled to peptide fragments of the carrier protein.⁹⁰ The peptide residues of these structures can bind to MHCII which leads to a presentation of the polysaccharide fragments on the cell surface where they are recognized by CD4⁺ T-cells (Figure 12 C). A binding of the $\alpha\beta$ -T-cell receptor to the hydrophilic glycan triggers the release of several cytokines, which stimulate the B cells development to memory B-cells and towards the production of glycan specific IgGs.^{90,91}

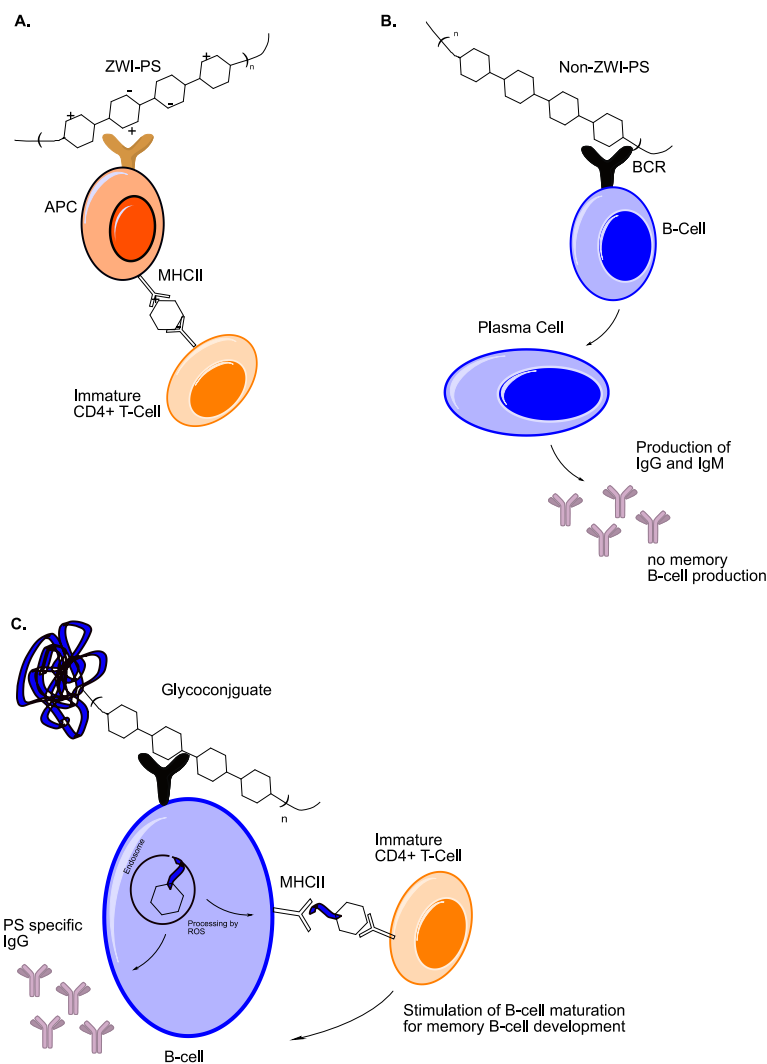


Figure 12: A. Mechanism of T-cell dependent recognition of Zwitterionic polysaccharides (ZWI-PS) via MHCII. B. Mechanism of T-cell independent recognition of Non-Zwitterionic polysaccharides (Non-ZWI-PS) by B-cells. C. Mechanism of recognition of glycoconjugates by B-cells with co-stimulation of CD4⁺ T-cells.⁹⁰

Interestingly, although a carrier protein is necessary to initiate a T cell dependent response for the presented carbohydrate antigen, it is reported that the carrier protein can be replaced by another carrier between first immunization and the booster immunization, without affecting the vaccination outcome.⁹²

Until this point, the common strategies to conjugate a carbohydrate antigen to a protein carrier are based on reductive amination, active esters, carbodiimide-mediated condensation or thioalkylation.⁹³ These methods result in a mixture of randomly conjugated carbohydrate

antigens on the carrier protein, from which each single glycoconjugate construct may have a different behavior, regarding its pharmacokinetic or immunological properties.⁹⁴ For this reason, the goal of producing defined glycoconjugate constructs with exact knowledge about the size and quantity of the conjugated antigen, as well as its selective conjugation to the carrier, is very important for a next generation of glycoconjugate vaccine candidates.

The chemical modification of the carrier protein for a site selective conjugation of the antigen moiety, represents one way of achieving this objective. It was already reported that also the chemical method with which a carbohydrate antigen is covalently bound to the carrier, can influence the immune response against this structure, as well as its position within the protein.^{90,95} All these findings suggest strongly that more selective methods for the modification of the carrier protein are needed, in order to enable selective conjugation of relevant carbohydrate antigens.

1.2.2. Site-selective protein modification

The possibility to achieve a site-selective modification of the carrier protein can be accomplished in several different ways and during the last years a large tool box for selective protein modifications has been developed.^{96,97} Various possibilities to modify natural occurring amino acids are available and the introduction of unnatural amino acids can provide additional motives for conjugation reactions.⁹⁷⁻⁹⁹

For the biosynthesis of proteins, twenty proteinogenic amino acids are available and their different chemical properties enable the formation of various proteins with different structures and functionalities in a living organism.¹⁰⁰ A main categorization can be performed based on the chemical properties of the side chains, which can be positively or negatively charged or have a polar or nonpolar character (Table 2).

Table 2: Overview of the natural amino acids and the chemical properties of the corresponding side chain.¹⁰⁰

| Amino acid | Side Chain |
|-------------------|--------------------|
| Arginine | Positively charged |
| Lysine | |
| Histidine | |
| Aspartic acid | Negatively charged |
| Glutamic acid | |
| Asparagine | Uncharged polar |
| Glutamine | |
| Serine | |
| Threonine | |
| Tyrosine | |
| Alanine | Nonpolar |
| Glycine | |
| Valine | |
| Leucine | |
| Isoleucine | |
| Proline | |
| Phenylalanine | |
| Methionine | |
| Tryptophan | |
| Cysteine | |

The modification of a natural amino acid within a native protein involves certain difficulties, which have to be overcome. The performed reaction has to be compatible with the general protein stability and should be suitable for biological systems.⁹⁸ Moreover, despite having only a limited number of different residues available, the applied modification reaction should be very selective towards a single kind of amino acid or even only one specific amino acid in the peptide chain. During the last years, especially nucleophilic amino acids like lysine or cysteine were addressed, but also methods for tryptophan or tyrosine are available.⁹⁷

Classical modification methods for lysine include amide or thiourea formation or reductive amination, while cysteine can be addressed through disulfide exchange reactions, alkylation or an addition of maleimide moieties (Figure 13).⁹⁸

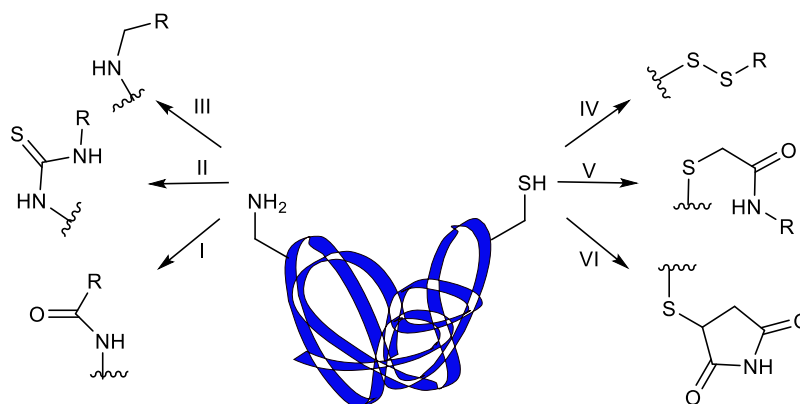


Figure 13: Classical modification methods for lysine and cysteine in native proteins. Lysine modifications I: amide formation, II: thiourea formation, III reductive amination. Cysteine modification IV: disulfide exchange, V: alkylation, VI: Maleimide addition.

More recently, a method using sulfonyl acrylate reagents, was developed for the selective modification of a single lysine residue within a native protein structure. This method takes advantage of a certain microenvironment of a specific lysine residue and enables the selective modification under mild conditions.¹⁰¹ As an alternative to maleimide chemistry on cysteine, an innovative approach was described by the utilization of carbonylacrylic reagents for the modification of this amino acid. The very efficient and selective character of this reaction results in cysteine-modified proteins which showed a high stability and retained biological function in plasma, making them ideal for *in vivo* applications.¹⁰²

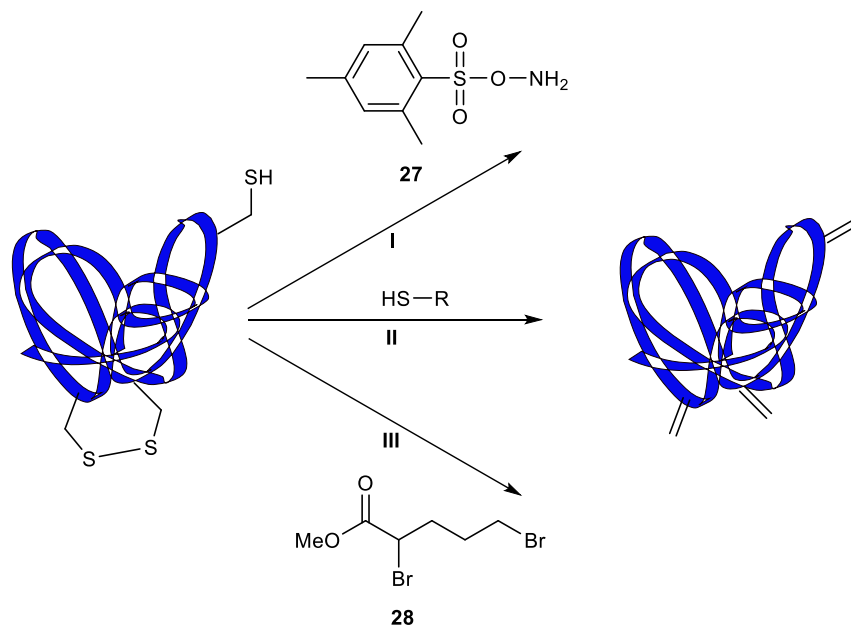
Besides the various possibilities to modify proteins based on their natural amino acid sequence, also the introduction of unnatural amino acids is commonly used to excess side selectively modified products.

The incorporation of unnatural amino acids into a protein of choice can be achieved with different methods. One possibility is to take advantage of new developments in synthetic biology and to engineer bacteria for an incorporation of unnatural amino acids into proteins. A

good example for this is the use of auxotrophic bacteria strains, which cannot produce certain amino acids and therefore are dependent on the uptake of those through nutrition. By replacing the relevant amino acid by analogues, these compounds are taken up by the bacteria and incorporated into protein structures where they are available later for selective targeting.⁹⁶ Another strategy, which uses the cellular machinery for the introduction of unnatural amino acids is the expansion of the genetic code. An orthogonal aminoacyl-tRNA synthetase is used to aminoacylate specifically related tRNAs with the applied unnatural amino acids, providing new aminoacylated tRNA molecules for the peptide synthesis in the ribosome.¹⁰³ By using this strategy, Lang and co-workers were able to incorporate an unnatural amino acid containing a norbornene group for further chemical labeling, specifically in an epidermal growth factor receptor on the cell membrane of HEK293 cells.¹⁰⁴

However, the introduction of unnatural amino acids into a protein by using the biological machinery, is often complicated and time consuming. A different approach is represented by using chemical methods to convert endogenous amino acids into unnatural derivatives. A commonly used amino acid for chemical modifications, as mentioned earlier, is cysteine. Cysteines are less abundant than other amino acids and often buried within the protein or involved in disulfide bonds.¹⁰⁵ As described above, several methods were developed for the selective modification of this amino acids by using simple chemical reactions.^{98,102,106} One type of modification is the conversion of cysteine into the unnatural amino acid dehydroalanine (DHA). This strategy was applied on several proteins and can be achieved using different reagents with different reaction mechanisms.¹⁰⁷⁻¹⁰⁹ By using *O*-mesitylensulfonyl hydroxylamine (**27**) (MSH), an oxidative elimination takes place on cysteine and results in the formation of DHA (Scheme 2, I). Although the selective formation of DHA in certain model proteins was achieved, this reagent also provokes side reactions on other amino acids like aspartic and glutamic acid, lysine, histidine or methionine. A careful assessment of the reaction conditions and the properties of each individual protein, has to be performed when using this method.¹⁰⁸ Another way for the conversion of cysteine into DHA, is the direct elimination of cysteine under basic conditions (Scheme 2, II). The Mukaiyama reagent was shown to react in an efficient manner with cysteine and displays an elimination to DHA in the presence of DBU.¹⁰⁷ However, this reaction method requires high pH values, which might be not compatible with

many types of proteins. An additional possibility to generate DHA from a cysteine residue, is the utilization of bis-alkylation reagents, followed by an elimination reaction (Scheme 2, III). The mechanism of this reaction can lead to the formation of intermediate or stapled byproducts when using too reactive alkylation reagents, however methyl 2,5-bisbromopentanoate (**28**) was shown to generate the desired DHA modified protein product.¹⁰⁹



*Scheme 2: Examples for the conversion of cysteine residues into dehydroalanine. I: Selective amination and oxidative elimination using MSH **27**, II: Selective sulfenylation and base-mediated elimination, III: Bis-alkylation with methyl-2,5-dibromopentanoate (**28**) and elimination.¹⁰⁸*

The various possibilities for the site selective modification of proteins, either through modification of natural amino acids or the introduction of unnatural building blocks and subsequent modification on these functionalities, can be used to generate a large selection of modified proteins. The introduced modifications provide the tool for the attachment of fluorophores or affinity tags, which can be used to follow and study a protein of interest in biological settings, or which can help in the purification of these proteins.⁹⁸ Furthermore, the installation of selective chemical handles allow the conjugation of the protein with drugs or

antigenic moieties. This concept is widely used for the synthesis of antibody drug conjugates or glycoconjugate vaccine candidates, just to mention two examples.^{94,98,110}

1.3. Chemical synthesis of carbohydrate antigens

Having discussed the possibilities of protein modifications through several chemical and biological methods, attention should be given as well to possible antigenic moieties that can be conjugated to a carrier protein. In the context of this work, the importance of carbohydrate structures during disease state has been already discussed and also their utilization in glycoconjugate vaccines has been described. Promoted by the high impact of carbohydrates for biological and biomedical questions, also investigations on the synthesis of these biomolecules evolved during the last decades.¹¹¹

1.3.1. The glycosylation reaction

The synthesis of defined oligosaccharides is crucial for any further application of these molecules for biological or medical approaches, such as vaccine development or other carbohydrate-based therapeutics.¹¹² However, looking at the monosaccharide building blocks, the presence of multiple reactive groups within a single molecule, makes synthetic chemistry on this structures challenging. Isolation of natural occurring carbohydrates from their sources is often difficult and less profitable, which reinforces the need for more research on the synthesis of carbohydrate structures. A successful synthesis of oligosaccharide structures depends many times on the selectivity and efficiency of the glycosylation reaction between the building blocks. A glycosylation reaction takes place between a so called glycosyl donor and a glycosyl acceptor, a nucleophilic agent, which will react with the anomeric position of the donor and will form the glycosidic bond.

This relatively simple reaction concept, however can be influenced by many factors like the solvent, counter ions or present protecting groups of the building blocks.¹¹³ A major problem during many glycosylation reactions is the lack of knowledge about the exact reaction mechanism. Depending on the type of glycosyl donor and environmental conditions, a glycosylation can occur in a S_N1 -type mechanism, forming a cationic intermediate, or in a S_N2 -type reaction which is characterized by ion pair structures or formed intermediates.^{114,115} The

knowledge about the exact reaction mechanism is crucial during the development and improvement of new glycosylation methods, and efforts have been made to understand the influence of each player on the outcome of the glycosylation reaction.^{116,117}

A main effect during glycosylation reactions is the anomeric effect on the anomeric C1 carbon of the sugar pyranose ring. The interaction of molecular orbitals of the ring oxygen with orbitals of the anomeric C1 carbon is thought to stabilize an axial conformation of an anomeric bond (Figure 14 A). This effect is supported by the dipole moment theory, which describes the repulsion of the dipole moments of the ring oxygen and the heteroatom in an equatorial anomeric position (Figure 14 B).¹¹⁸

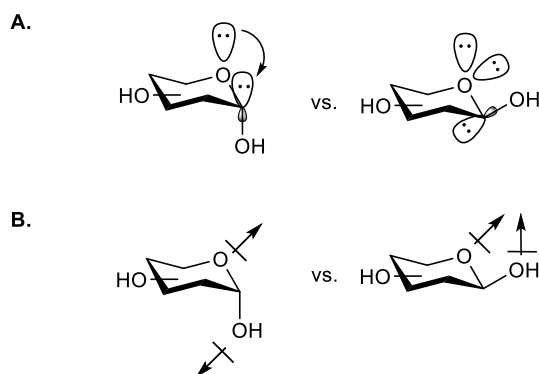


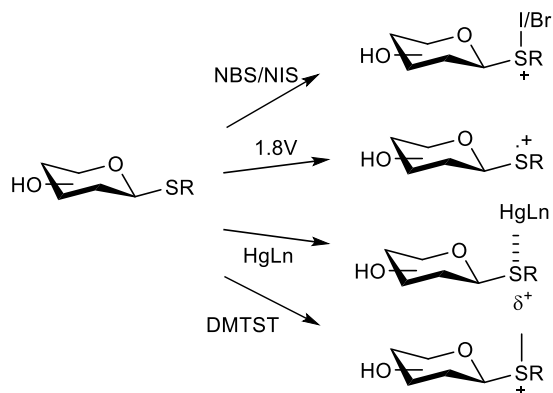
Figure 14: Illustration of the anomeric effect, A. Molecular orbital theory B. Dipole moment theory.¹¹⁸

Apart from the anomeric effect, the participation of neighboring chemical groups is probably the other main factor during glycosylation reactions. While benzyl protecting groups, for example, do not show any participating character and therefore have no influence on the anomeric stereochemistry of the glycosylation product, acetyl protecting groups can form intermediate like acyloxonium ion structures. The formation of these structures will block one side of the anomeric center, which promotes the formation of 1,2-*trans* glycoside products.¹¹⁸ This concept was further developed by using different structures with participating character, which can be used for the synthesis of several 1,2-*trans* glycosidic structures.¹¹⁸ The assessment of each glycosylation reaction regarding its underlying mechanism is crucial to improve the efficiency and selectivity of these reactions. The classification of glycosylation reactions in S_N1

or S_N2 like reactions, can give a first estimation of the possible products, however the formation of unexpected intermediate structures can change the result. A useful tool for the investigation of intermediate formation, stability and influence on the reaction outcome is nuclear magnetic resonance spectroscopy (NMR). Several studies during the last decades showed the formation of different intermediate structures and were able to explain unpredicted reaction outcomes.¹¹⁹ The enormous variety of possible glycosylation reactions to mimic and resynthesize natural carbohydrate structures, makes it still challenging to develop a method, which is able to fit all necessary requirements. During the last decades of carbohydrate research, a large selection of glycosylation strategies or possible building blocks were developed and, for example, a range of different glycosyl donors is available, just mentioning glycosyl halides, trichloroacetimidates or phosphates as examples.¹²⁰ Historically, glycosyl halides, like glycosyl bromides or chlorides, represent one of the oldest examples, which are, until today, heavily used in carbohydrate chemistry. The glycosylation reaction with halide donors and alcohol acceptors is performed in the presence of silver salts like $AgCO_3$ and was developed by Koenigs and Knorr in 1901.¹²¹ Disadvantages of this method are given by the utilization of harsh conditions and the instability of the glycosyl halide donors. Nevertheless this system can provide efficient and selective glycosylation products.¹¹⁸ Another extensively used group of glycosylation donors are glycosyl imidates, like trichloro- or trifluoroacetimidate. Developed by Schmidt and coworkers in the 1980s, this group of molecules has been actively improved over the years and a very large number of different reaction strategies is available.^{118,122}

1.3.2. Thioglycosides as glycosyl donors

Next to glycosyl halides and imidates, thioglycosides are the third big group of strongly used glycosyl donors. Thioglycosides are stable under multiple reaction conditions, which allows the modification and alteration of other present protecting groups.¹¹³ The activation of thioglycosides is usually performed with thiophilic promoters like heavy metal salts, halonium or organosulfur reagents or with single electron transfer methods (Scheme 3).^{113,118}



Scheme 3: Schematic illustration of examples for the activation of thioglycoside donors.

The broad stability of thioglycosides during several conditions makes them good candidates as glycosyl donors and acceptors during multistep or one-pot glycosylation reactions.¹²³ The development of one-pot glycosylation reactions evolved strongly over the last years, because complicated purification steps could be reduced during the assembly of large oligosaccharide structures and the overall efficiency might be improved.^{124,125} To achieve one-pot glycosylation reactions, a sequential activation of present glycosyl donors has to be possible. The reactivity of glycosyl donors can be directed by using different protecting groups or certain groups in C2 position of the sugar molecule.¹²⁶ Furthermore, also the anomeric leaving group itself can display different reactivities which can be useful for one-pot reaction systems.¹²⁷ Different systems of thioglycosides have been used for sequential or one-pot glycosylation strategies, taking advantage of different activation methods and/or different leaving groups.^{127,128} Despite all the developed methods, the enormous complexity of natural occurring glycan structures makes oligosaccharides synthesis still challenging and difficult, which promotes the development of even more new activation methods and investigations on the underlying reaction mechanism.

1.4. The aims of this work

The importance of carbohydrate structures during different diseases was intensively studied during the last decades and many treatments or analytic methods are based on this class of biomolecules. However, due to the enormous diversity of these structures, many questions concerning the identity and function of certain disease specific carbohydrate antigens, are not answered yet.

The aim of this thesis was to address different points in the identification of disease related carbohydrate antigens, the utilization of these structures in glycoconjugate vaccine candidates and possible synthetic methods, to access the necessary carbohydrate oligosaccharides.

1.4.1. Metabolic oligosaccharide engineering as a tool for malaria

During the first section of this work, the special role of galactose containing carbohydrate epitopes in Malaria disease was investigated. Following up on recent reports about the importance of α -galactose connected carbohydrate structures during the immune response against this infection disease, metabolic oligosaccharide engineering was meant to be used to address certain questions. First, if and to what extent an increase in galactose containing glycan structures can be observed on the surface of hepatic cells, after an infection with *Plasmodium* parasites. An increase of specific galactose containing carbohydrate structures on the surface of these infected cells, could lead to the identification of new carbohydrate antigens, which are specific for the liver stage infection and which could be used for the development of new glycoconjugate vaccine candidates. Furthermore, the question if metabolic oligosaccharide engineering can be used as a general tool for investigations on carbohydrate structures related to malaria, should be addressed as a proof of concept.

1.4.2. Bifunctional galactose derivatives for metabolic labeling

Besides the development of monofunctional galactose derivatives for metabolic incorporation, it was aimed to synthesize a bifunctional galactose monosaccharide with two bio-orthogonal chemical reporter groups. This compound was then meant to be tested for metabolic incorporation in hepatic cells. The introduction of a bifunctional monosaccharide structure into cellular glycan structures, could provide the opportunity for dual labeling, labeling and purification or labeling and drug delivery at the same time.

1.4.3. The development of a site-selective glycoconjugate vaccine candidate

Although the first two sections of this work were focused on new methods for the identification of potential carbohydrate antigens, this section should describe the development of a new site selective glycoconjugate vaccine candidate. For this purpose, the carrier protein CRM₁₉₇ was meant to be modified in a site selective manner, followed by the conjugation of a polysaccharide antigen moiety. The final vaccine candidate should be tested then, in comparison with the commonly used randomly conjugate vaccine, for its ability to raise a specific carbohydrate dependent immune response.

1.4.4. Activation of thioglycoside donors using MSH

Moving from the identification of new carbohydrate antigens, to the utilization of carbohydrates for glycoconjugate vaccines, the last section of this work should address the chemical synthesis of oligosaccharides. The development of a new activation method for thioglycoside donors can provide a useful tool for the synthesis of natural carbohydrate antigens. The thiophilic reagent *O*-mesitylsulfonyl hydroxylamine was meant to be used for the activation of thioglycosides and its mechanism of action should be studied.

Summarizing, this thesis will address different questions regarding antigenic carbohydrate structures related to malaria, the utilization of known carbohydrate antigens for the development of site selective glycoconjugate vaccine candidates, and a new method for the synthesis of oligosaccharide structures.

2. Chapter 2 – Design and optimization of new galactopyranose-derivatives for metabolic labeling in the context of malaria

2.1. Introduction

Carbohydrates are one of the biggest groups of biomolecules and they are involved in many crucial biological processes, both in healthy organisms as well as during disease state.^{20,129} In contrast to proteins, carbohydrate structures cannot be addressed through a genetic template, which can complicate investigations.¹¹ The introduction of metabolic oligosaccharide engineering (MOE) by Bertozzi and coworkers about 20 years ago, helped to change this situation.³⁶ The introduction of chemical reporter groups into cellular glycan structures allows selective bio-orthogonal labeling reactions on these molecules, which are further used for the identification, purification and characterization of important carbohydrate structures. As described in the first chapter of this work, different applications for MOE are described in the literature, using derivatives of mannosamine, glucosamine, sialic acid and galactosamine.^{35,130} For the envisioned project in the context of malaria, the following work presents the utilization of new galactose derivatives for MOE.

Even in the 21st century, malaria is still causing about 219 million cases of infection and 435000 deaths per year.⁶³ Recent studies report a stagnation in the reduction of infection numbers which shows the urgent need for the development of effective treatments and vaccinations.⁶³

The glycobiology of the malaria causing parasite *Plasmodium* is highly discussed and subject of several studies to identify new drug targets or vaccine antigens.^{73,131} When looking at acquired immunity against this parasite, anti- α -Gal antibodies seem to play an important role, however it is still unclear which external factors are involved and how this carbohydrate structure is formed on the parasite.^{60,61,132} An infection with malaria starts when *Plasmodium* parasites are injected in the host dermis during a mosquito bite, followed by the traversal of the sporozoites through the blood to the liver.⁶² Here, the parasite will invade few hepatic cells, which represents the first, so-called liver stage of the infection. This asymptomatic phase of the disease represents a bottle-neck phase, because up to 40000 merozoites are released from each

infected hepatocyte, initiating the blood stage of the infection.⁶² This important feature makes the liver stage a major target for the investigations on target structures for therapies and vaccines.

It is known that infected hepatic cells display certain sporozoites proteins like the circumsporozoite protein (CSP) on their surface and it was already described that these antigens contribute to the activation of CD8 T cells against the infected cells.¹³³

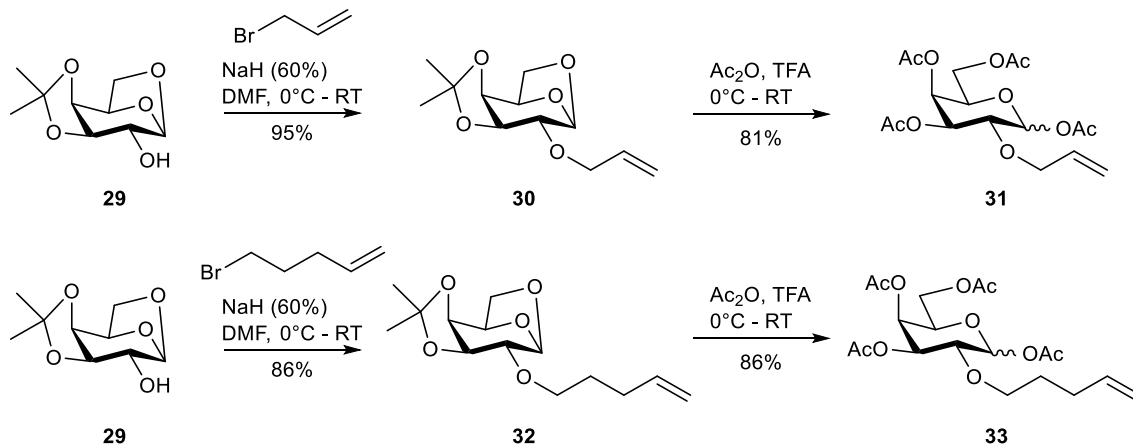
With these data in mind and the apparent importance of α -galactose containing glycan structures, the goal of this work was to use MOE in different situations related to the infection with the *Plasmodium* parasite, in order to possibly identify new carbohydrate antigens and to understand more about the general glycobiology of this protozoan parasite.

2.2. Results and discussion

2.2.1. Chemical synthesis of artificial galactose derivatives

To answer our question of whether there will be more galactose containing glycan structures on the cell membrane surface of hepatic cells after an infection with sporozoites from *Plasmodium berghei*, different galactose derivatives were synthesized containing a terminal alkene group for inverse electron demand Diels Alder reactions (iEDDA) with tetrazine compounds. It was decided to compare the properties of a shorter allyl side chain with the ones of a longer pentenyl reporter group, following studies on mannosamine derivatives by Wittmann and co-workers.¹³⁴ Despite from the different chain lengths, also the position of the chemical reporter group within the monosaccharide was altered. Although the C2 position is one of the most often altered positions in MOE for different monosaccharides, the C6 position in galactose is easily available for synthetic modifications and ELISA studies with anti- α -Gal antibodies against deoxy-derivatives of the α -Gal epitope revealed good recognition of epitopes containing modifications in this position.⁸² The derivatives 2-*O*-allyl-tetra-*O*-acetyl-galactose (**31**) and 2-*O*-pentenyl-tetra-*O*-acetyl-galactose (**33**) were synthesized from commercial available starting material 1,6-anhydro-3,4-isopropyl-galactopyranose (**29**), starting with a classical Williamson-ether synthesis to attach the terminal alkene group and followed by an opening

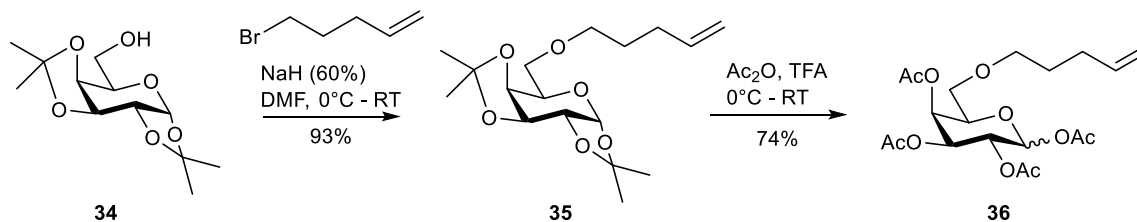
reaction of the isopropyl- and anhydro-structure and subsequent acetylation using trifluoroacetic acid and acetic anhydride (Scheme 4).



Scheme 4: Synthesis of the galactose derivatives **31** and **33**, from commercial starting material **29**.

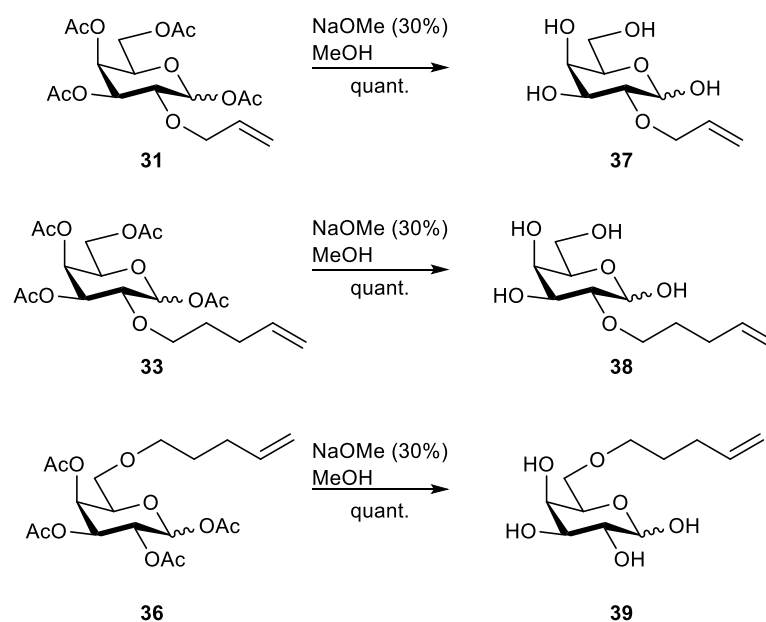
Both compounds **31** and **33** were obtained with very good yields and were fully characterized using NMR (^1H , ^{13}C , COESY, HSQC, HMBC) and mass spectrometry.

The third galactose derivative **36** with the terminal alkene in C6 position, was synthesized from the commercial available starting material 1,2,3,4-diisopropyl-galactose (**34**). Similar to the other two compounds, the terminal alkene group was introduced via a Williamson ether synthesis and the acetyl protecting groups were obtained with acetic anhydride after opening the isopropyl structures with trifluoroacetic acid (Scheme 5).



Scheme 5: Synthesis of the galactose derivative **36**, from commercial starting material **34**.

During the metabolic incorporation of the synthesized galactose derivatives, the fully acetylated monosaccharide will be taken up by the cells and cytosolic non-specific esterases will hydrolyze the acetyl protecting groups. Following this, the deprotected galactose derivatives will be processed in the glycan salvage pathway, transformed into activated nucleotide sugars for glycosyltransferases, which will incorporate these unnatural monosaccharides into various glycan structures.¹³⁵ For this reason, the synthesized acetylated galactose derivatives **31**, **33** and **36** were deprotected using a classical Zemplén deacetylation procedure, to determine the kinetic properties of these monosaccharides (Scheme 6). In this way, the conditions during the kinetic studies resemble the conditions on the cell surface.



Scheme 6: Zemplén deprotection for the derivatives **31**, **33** and **36**, resulting in the deprotected derivatives **37**, **38** and **39**.

2.2.2. Evaluation of the kinetic properties

After having successfully synthesized all three galactose derivatives and the corresponding deprotected counterparts, the kinetic properties in iEDDA were determined. For this purpose, a high-throughput method was developed, by using 96-well plates and a microplate reader to

perform the reactions and to follow the decline in tetrazine-specific absorbance at 530 nm. The reactions were performed under pseudo-first order reaction conditions, providing a 4- to 26-fold excess of the terminal alkene group over the tetrazine reaction partner. The tetrazine compound 6-methyl—tetrazine-amine (**40**) was used for the kinetic evaluations, representing the tetrazine core of future fluorophore-tetrazine or biotin-tetrazine constructs. The optimal concentration of 6-methyl-tetrazine-amine (**40**) per well was determined by a concentration screen at 530 nm and 0.6 mM were chosen for all further measurements. From a stock solution of 20 mM, further dilutions of 16, 12, 8 and 4 mM were prepared for every de-acetylated galactose derivative **37-39** and were mixed with 6-methyl-tetrazine-amine (**40**) in 96-well plates. The decline in absorption at 530 nm was followed for 16 h in the microplate reader at 37 °C. With this method, the pseudo-first order rate constant k_{obs} was calculated for every concentration as the slope of the exponential decay in the absorption of 530 nm. To determine the final second order rate constant k_2 , the obtained values for k_{obs} were plotted against the corresponding concentration and the resulting linear relation gave the value for k_2 as the slope of the function (Figure 15).

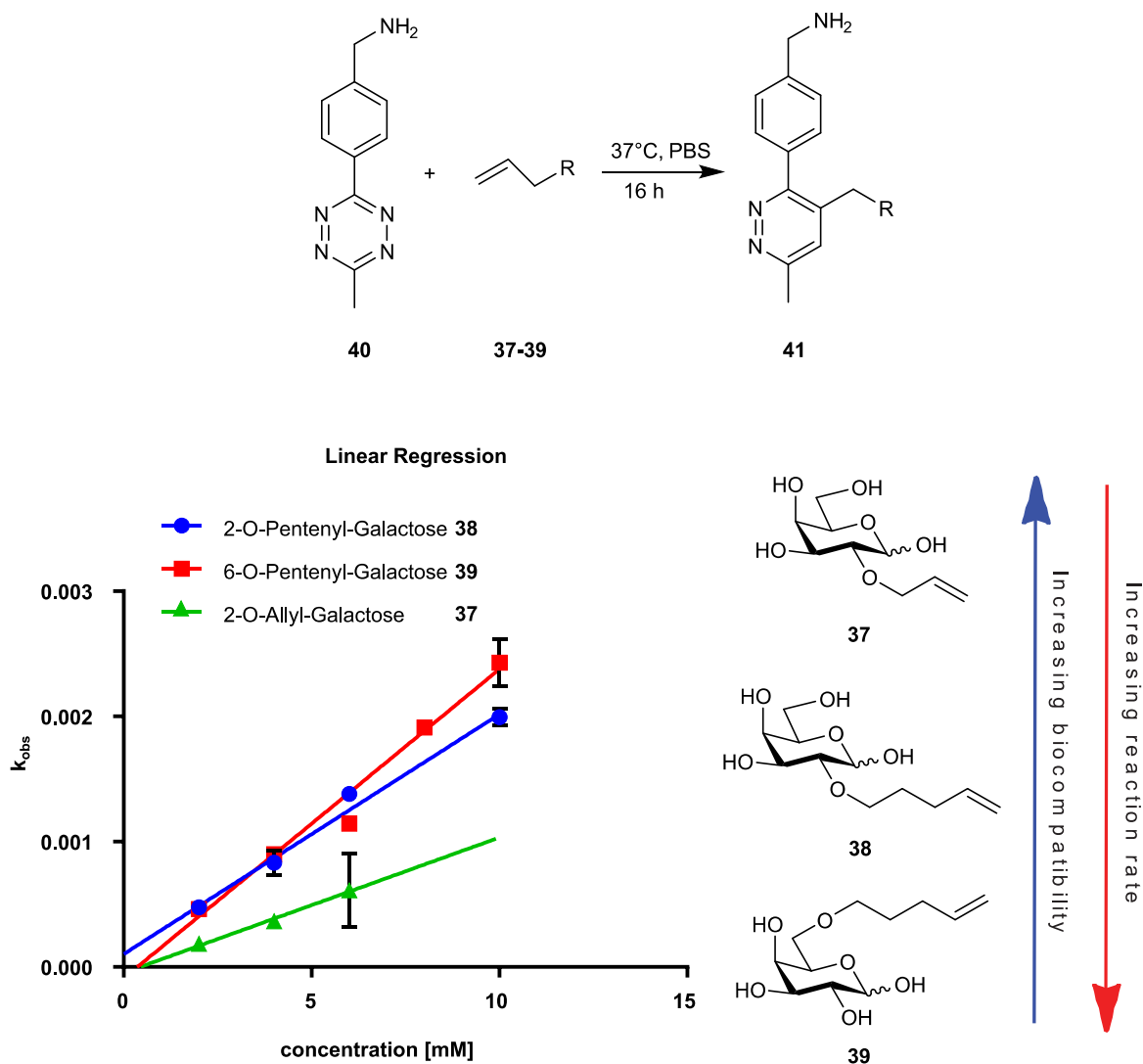


Figure 15: Results of the iEDDA reaction between tetrazine **40** and galactose derivatives **37-39**. The represented data represent linear fits of at least two independent experiments.

As expected from literature reviews concerning mannosamine derivatives in iEDDA reactions, the galactose derivatives **38** and **39**, bearing the longer pentenyl reporter group, gave a higher rate constant k_2 than the derivative **37**, which contains the shorter allyl side chain.¹³⁴ According to the measurements, the installation of the pentenyl reporter group in C6 position of derivative **39** increases the rate constant k_2 slightly in comparison with k_2 from the derivative **38**, which is modified in C2 position.

Table 3: second order rate constants k_2 for the iEDDA reaction between tetrazine **33** and galactose derivatives **37-39**.

| k_2 of iEDDA of tetrazine 40 | k_2 [$M^{-1} s^{-1}$] |
|---|--|
| 5-Norbornene-2-methanol | 180.3×10^{-4} |
| 6- <i>O</i> -Pentenyl-Galactose 39 | 2.44×10^{-4} |
| 2- <i>O</i> -Pentenyl-Galactose 38 | 2.10×10^{-4} |
| 2- <i>O</i> -Allyl-Galactose 37 | 0.17×10^{-4} |

A possible explanation in this case might be the higher flexibility of the side chain in C6 position, facilitating the iEDDA reaction and increasing the rate constant k_2 .

It was successfully shown that all synthesized galactose derivatives undergo iEDDA reaction with 6-methyl-tetrazine-amine **33**, so the next step in this project was initiated, testing the possibility of using these compounds for metabolic incorporation in cellular glycan structures.

2.2.3. Metabolic incorporation into cell membrane glycans

In the first step, it was confirmed in different cell lines that all three galactose derivatives **31**, **33** and **36** do not cause any cell toxic effect (Figure 16). Until concentrations of 200 μM sugar for a time period of 3 days, no toxic effect was observed when using a CellTiter-Blue[®] Cell viability assay. The presented data result from three independent experiments. For the following experiments, the liver derived cell lines Huh7 and HepG2 were used.

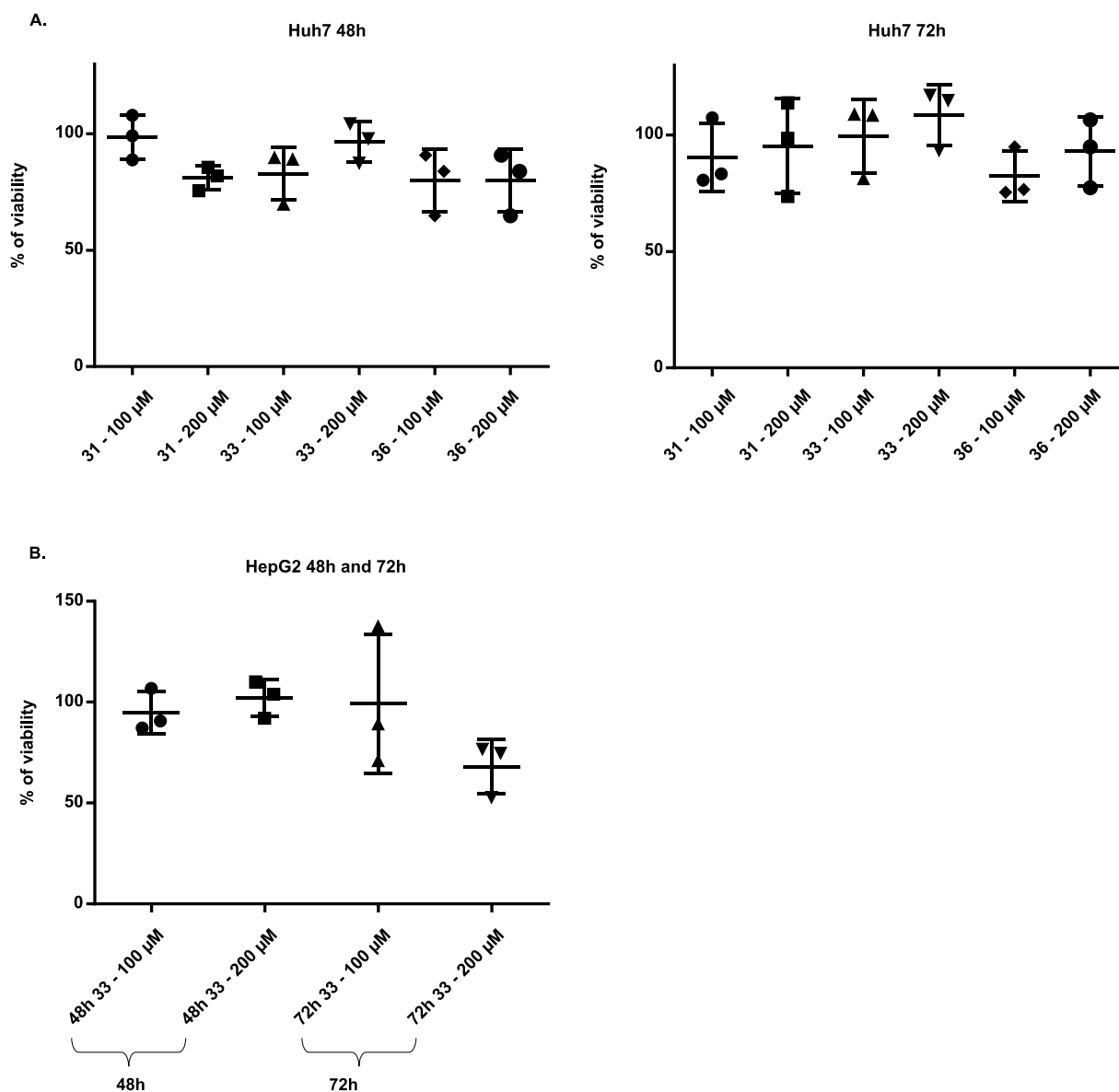


Figure 16: Determination of the cell toxicity of acetylated galactose derivatives **31**, **33** and **36**. **A.** Huh7 cells **B.** HepG2 cells. The cell viability was measured at the time points 48h and 72h. The data represent three independent experiments.

Knowing that the developed galactose derivatives are not causing cell toxic effects, prior to the planned infection studies, the metabolic incorporation and the staining procedure *in vitro* was optimized. For this, starting with Huh7 cells, these cells were grown for 72 h in the presence of 100 μM of the galactose derivatives or the control sugar pentaacetyl-galactose (**42**), followed by a staining with the tetrazine-fluorophore construct 6-methyl-tetrazine-sulfo-cy3 (**43**).

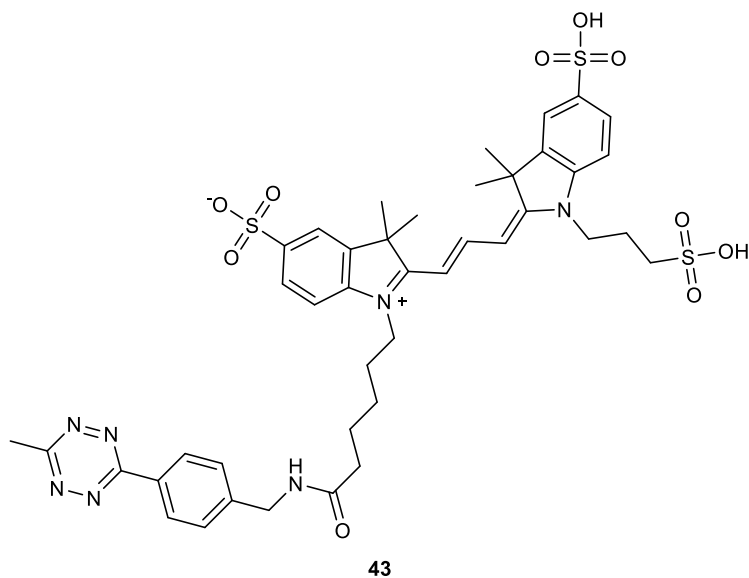


Figure 17: Structure of 6-methyl-tetrazine-sufo-Cy3 **43**.

Although some more signal was observed with the unnatural galactose derivatives **31**, **33** or **36**, a lot of unspecific signal was observed as well in the cells treated with the control sugar **42**. Also, the signal seemed to be dislocated over the whole cell body, although only cell membrane labeling was aimed for. Several experiments were conducted, including permeabilization steps to wash out any unbound dye, however no improvement was observed (Table 4).

Table 4: Cell growth conditions and staining procedures during the optimization of metabolic incorporation of galactose derivatives 31, 33 and 36.

| Entry | Cell growth conditions | Staining conditions |
|-------|--|---|
| 1 | 24h, 100 μ M galactose derivative | <ol style="list-style-type: none"> 1. 15 μM 6-Methyl-tetrazine-Cy3 for 3h @ 37°C 2. Hoechst 1:1000, 8 min, RT 3. Fixation with 4% PFA |
| 2 | 72h, 100 μ M galactose derivative | <ol style="list-style-type: none"> 1. 20 μM 6-Methyl-tetrazine-Cy3 for 6h @ 37°C 2. Hoechst 1:1000, 8 min, RT 3. Fixation with 4% PFA |
| 3 | 72h, 100 μ M galactose derivative | <ol style="list-style-type: none"> 1. 20 μM 6-Methyl-tetrazine-Cy3 for 45 min @ 37°C 2. Hoechst 1:1000, 8 min, RT 3. Fixation with 4% PFA |
| 4 | 72h, 200 μ M galactose derivatives | <ol style="list-style-type: none"> 1. 20 μM 6-Methyl-tetrazine-Cy3 for 6h @ 37°C 2. Fixation with 4% PFA 3. Permeabilization and washing 4. Hoechst 1:1000, 8 min RT |

The best results during these experiments was obtained with the conditions from Table 4, entry 2 and representative pictures are presented below.

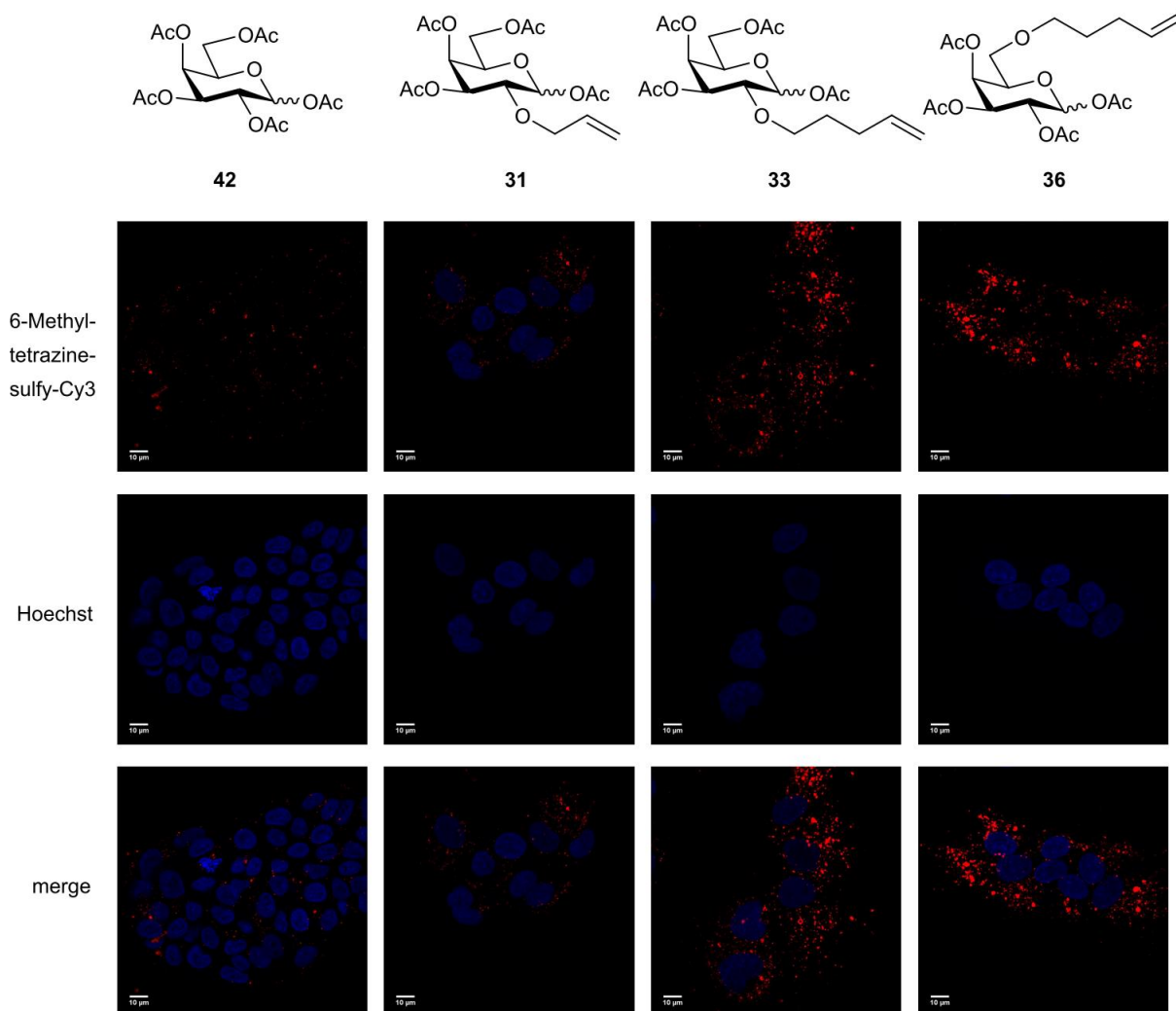


Figure 18: Metabolic incorporation of galactose derivatives **31**, **33** and **36**, followed by staining with 6-methyl-tetrazine-sulfo-Cy3 (**43**). Monosaccharide **42** was used as negative control.

The observed problematic when using a tetrazine-fluorophore construct for direct staining of the incorporated galactose derivatives, led on to rethink the planned staining procedure.

Going back to literature, instead of the envisioned one-step staining procedure, usually a two-step approach with a tetrazine-biotin probe and a streptavidin-fluorophore compound is used.¹³⁴ Repeating the metabolic incorporation of the galactose derivatives in Huh7 cells for 72 h, now the introduced terminal alkene group was targeted with 6-methyl-tetrazine-peg4-biotin (**44**) to undergo the iEDDA reaction (Figure 19).

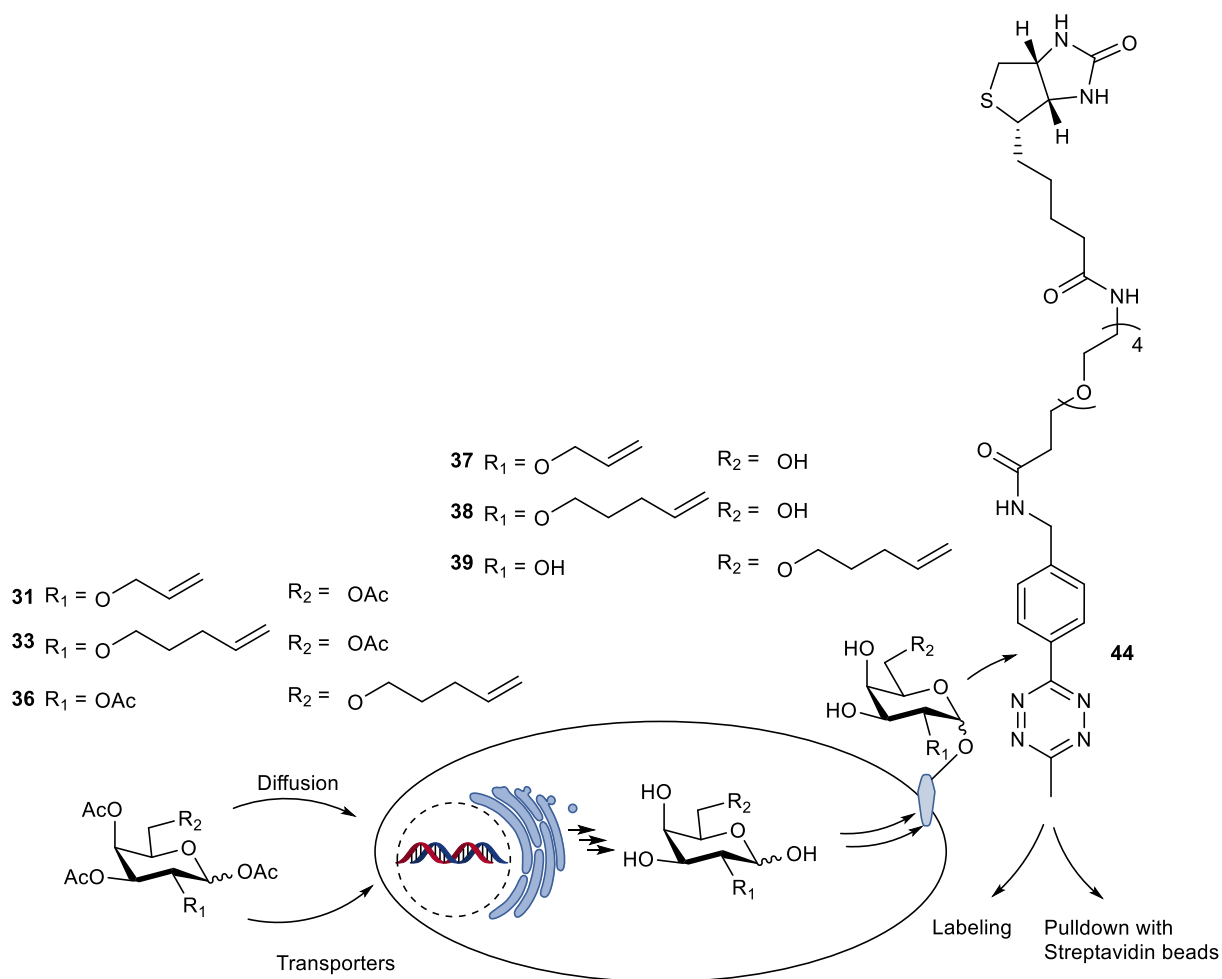
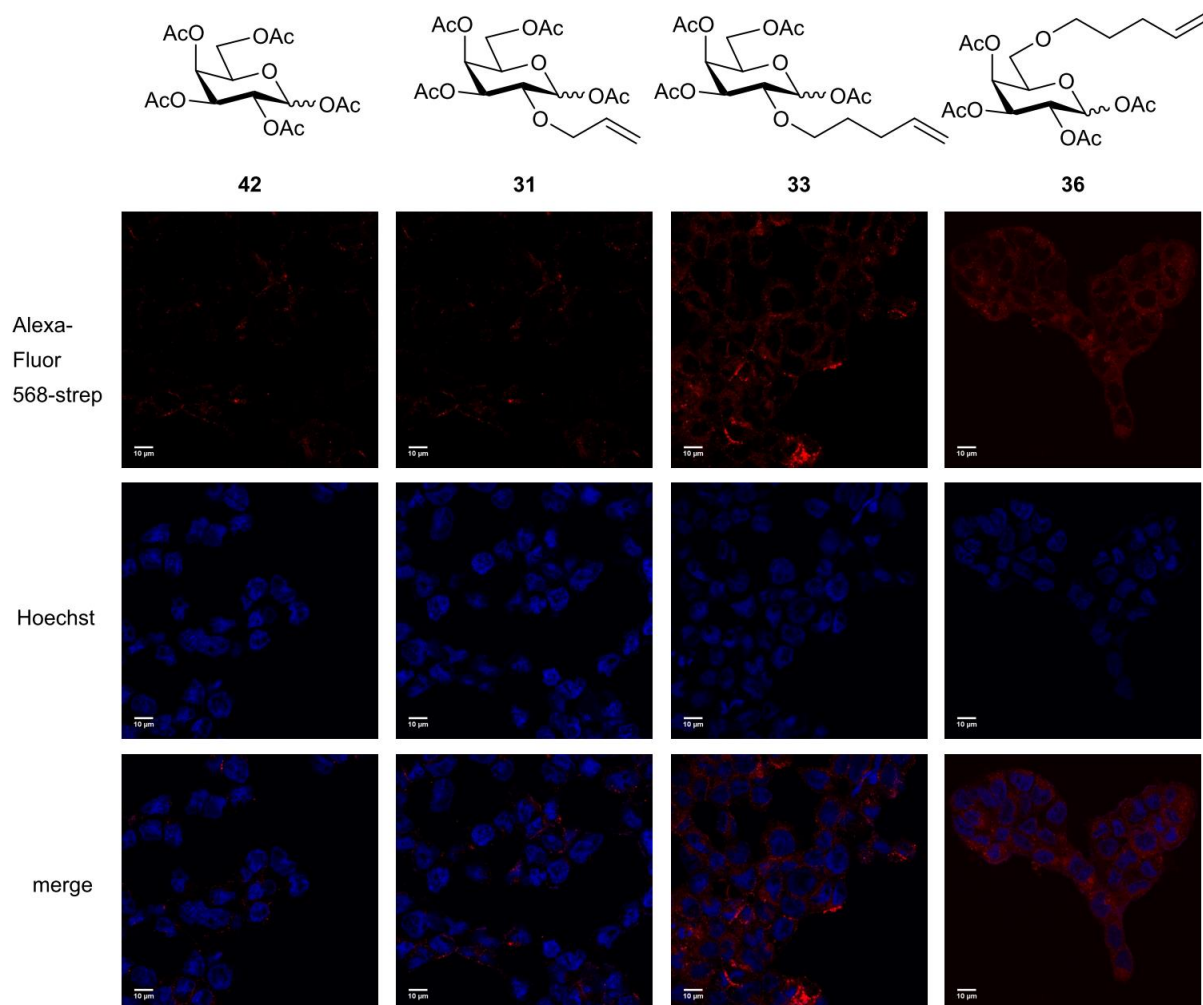


Figure 19: Schematic illustration of the workflow for the metabolic incorporation of galactose derivatives **31**, **33**, **36**, their intracellular deprotection and the labeling strategy with 6-methyl-tetrazine-peg4-biotin (**44**).

In a second step, the free biotin-tag was labeled with alexa-fluor-568-streptavidin (Alexa-fluor-568-strep) for further analysis. Here it was possible to detect specific labeling on the cell membrane. An improvement was further achieved with blocking the endogenous biotin of the cells with 25 µg/mL streptavidin for 40 min prior to the staining procedure (Figure 20 A). With this strategy, it could be shown that all three galactose derivatives were successfully incorporated into cell membrane glycan structures. To proof the incorporation of the unnatural galactose derivative in cell membrane glycan structures, a co-staining with CellMask[®] Deep

Red Plasma Membrane dye was performed and could successfully show the expected co-localization of the two stainings (Figure 20 B).

A.



B.

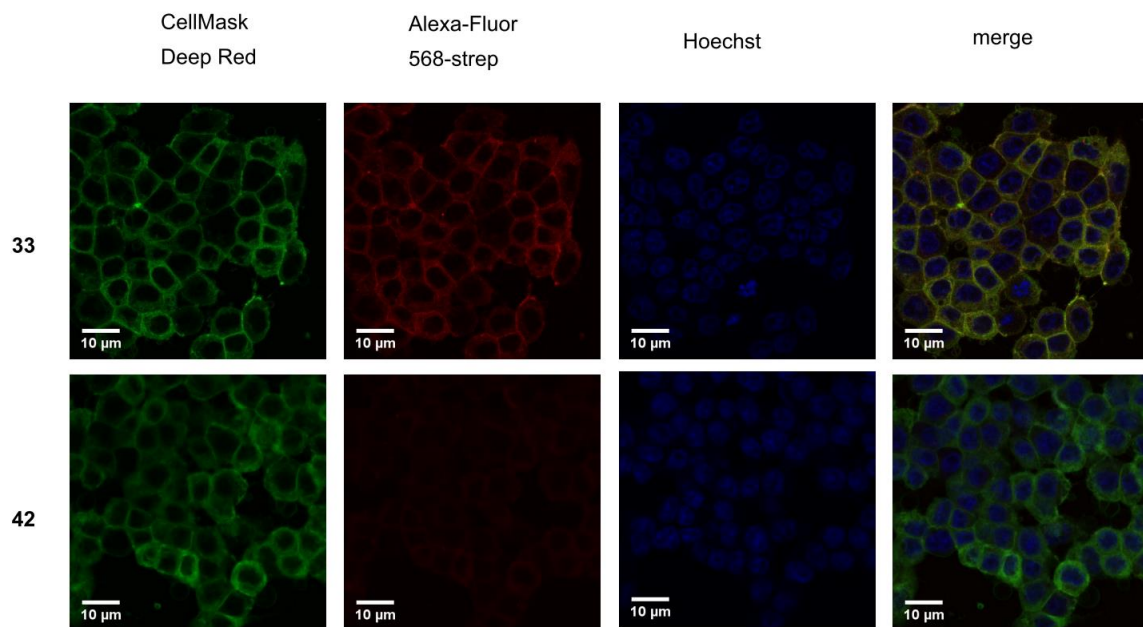


Figure 20: **A.** Metabolic incorporation of galactose derivatives **31**, **33** and **36** into cell membrane glycans of Huh7 cells and labeling using 6-methyl-tetrazine-peg4-biotin (**44**) and Alexa-Fluor-568-strep. Pentaacetyl galactose (**42**) was used as negative control. **B.** Metabolic incorporation of galactose derivative **33** into cell membrane glycans of HepG2 cells and co-staining with CellMask Deep red Plasma membrane dye. Pentaacetyl galactose (**42**) was used as negative control.

To compare the efficiency of labeling *in vitro*, the pixel intensity of single cells was measured using ImageJ software package (Figure 21). Having the data from the kinetic studies in hand, it was expected that with the same time for the iEDDA reaction on the cell surface, a higher fluorescence signal should be obtained from samples incubated with the longer pentenyl chain substituted galactose derivatives **33** and **36**. Consistent with this, the quantification gave higher values for the fluorescence intensity in cell samples grown with these derivatives than cells, which incorporated the sugar **31** with the shorter allyl side chain. For the statistics analysis, d'Agostino and Pearson omnibus normality test was performed and a two-tailed Mann-Whitney test was chosen. Three independent experiments were conducted with at least 25-30 data samples.

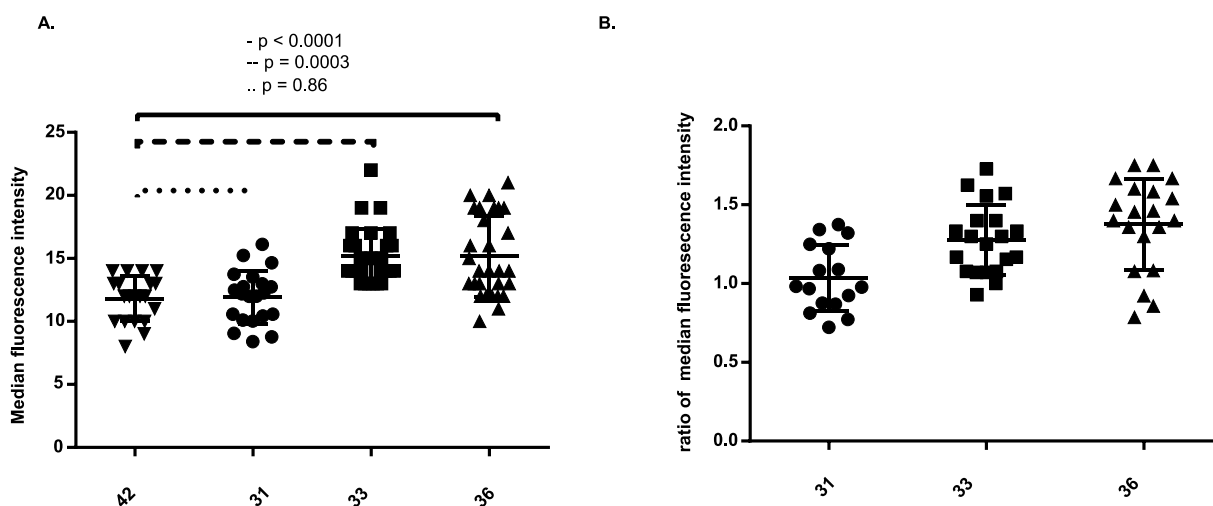


Figure 21: **A.** Median fluorescence intensity after incorporation of galactose derivatives **31**, **33** or **36** in Huh7 cells, determined by confocal point-scanning microscopy. Pentaacetylated galactose (**42**) was used as negative control. Two-tailed Mann-Whitney, $n = 25-30$, representative example from three independent experiments. **B.** Ratio of the median fluorescence intensity against background signal from measurements with control sugar **42**.

The slight increase going from the derivative **33** with the pentenyl substituted in C2 position, to the C6 modified counterpart **36** can be explained with regard to how these two sugars can be incorporated. The unnatural derivative **33** bearing the pentenyl group in C2 position cannot be modified into galactosamine structures while the modification in C6 position of derivative **36**, still allows this transformation. In this way, the compound with C6 reporter group can be introduced in more glycan structures than its counterpart **33**. For the further experiments, the galactose derivative **33** with the pentenyl reporter group in C2 position was used, because specifically the incorporation of galactose and not derivatives like galactosamine, were the center of interest. Apart from Huh7 cells, also the incorporation of this sugar into HepG2 cells was tested, giving a similar result for the incorporation efficiency (Figure 22). At least three independent experiments were conducted. For the statistics analysis, d'Agostino and Pearson omnibus normality test was performed and a two-tailed Mann-Whitney test was chosen to analyze the data.

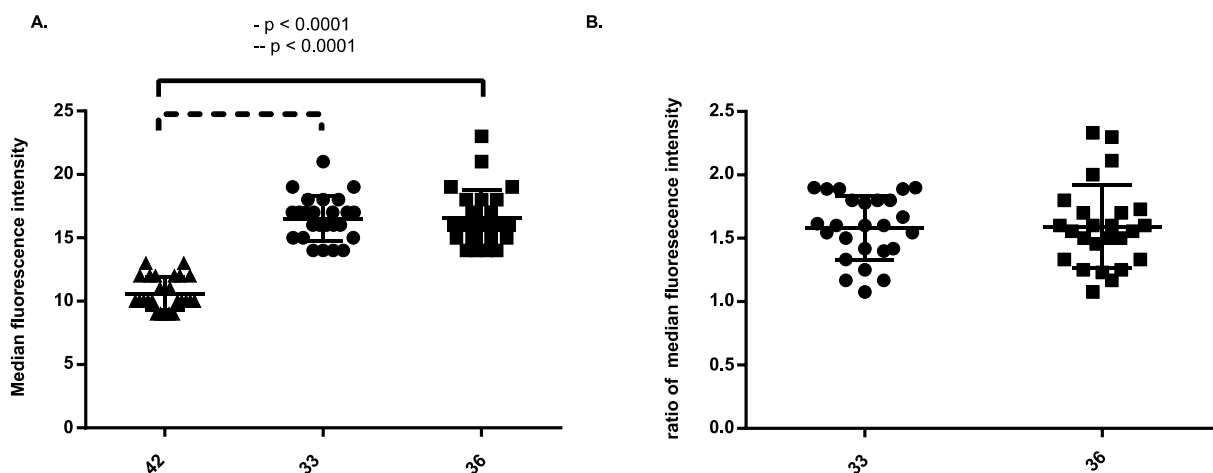


Figure 22: Median fluorescence intensity after incorporation of galactose derivatives **31**, **33** or **36** in HepG2 cells, determined by confocal point-scanning microscopy. Pentaacetylated galactose (**42**) was used as negative control. Two-tailed Mann-Whitney, $n = 25$, representative example of three experiments. **B.** Ratio of the median fluorescence intensity against background signal from measurements with control sugar **42**.

With regard to the planned infection studies later in this work, also an analysis by flow cytometry was developed. In this setting, cells were grown in the same manner with 100 μM of the unnatural galactose derivative for 72 h before a reaction with 6-methyl-tetrazine-peg4-biotin

(44) and detachment with EDTA solution. It is important to emphasize in this part that the detachment of the cells should be done with EDTA solution, rather than using trypsin based reagents. The application of trypsin can lead to a loss of cell membrane glycoproteins due to the digestive mechanism and like this disturb the detection of incorporated galactose derivatives in cell membrane glycoproteins. The staining was performed in the same way than for the microscopy analysis with an alexa-fluor-568-streptavidin construct.

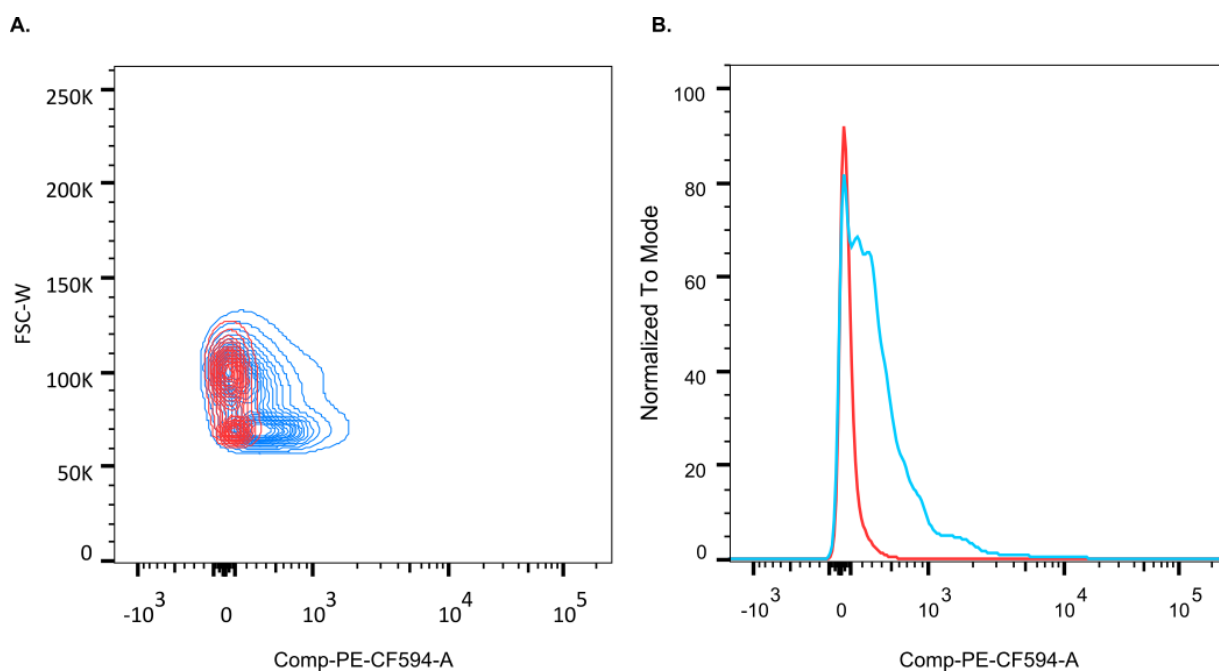


Figure 23: **A.** Superposition of contour plots of forward-scatter detection versus PE-CF594-A fluorescence intensity, after metabolic incorporation of galactose derivative **33** (blue) in HepG2 cells. Pentaacetyl galactose (**42**) was used as negative control (red). **B.** Superposition of histograms of PE-CF594-fluorescence intensity, resulting from contour plots in A..

Also with this method, it could be shown that the unnatural galactose derivative **33** is incorporated by the cells and a shift in the fluorescence intensity can be observed (Figure 23). Unfortunately, despite several optimizations, the observed shift of the positive samples over the negative control could not be improved for a better separation. This fact might be due to the lower abundance of galactose in contrast with other sugars like galactosamine or mannose in glycan structures. A work from Hsu et al. showed a similar observation comparing fucose and mannosamine derivatives (Figure 24).¹³⁶ The obtained shift of labeled cells after an

incorporation of a fucose derivative, was considerably smaller than the shift which was observed in cells treated with the corresponding *N*-acetyl-mannosamine derivative. The observed small shift in the presented experiments with galactose derivative **33** can be explained with this observations. However, the presented strategy can distinguish the different set of treated cells.

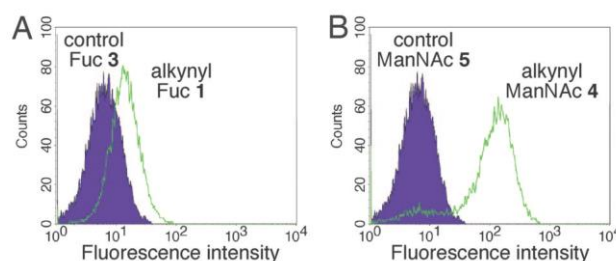
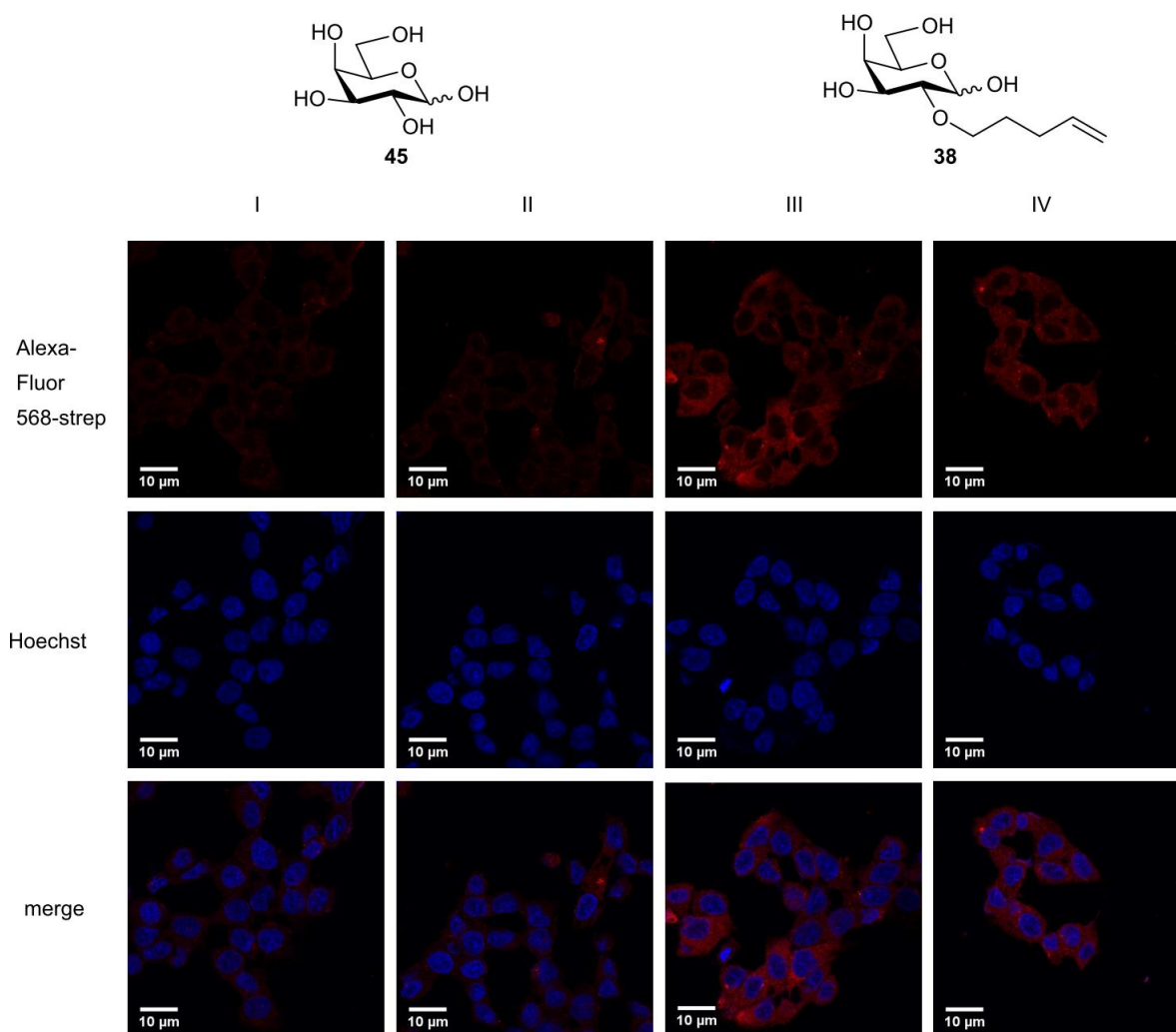


Figure 24: Labeling of surface glycans after metabolic incorporation of alkynyl sugar analogs of **A.** fucose and **B.** *N*-acetyl-mannosamine. Filled histograms represent treatment with control sugars, open histograms cells treated with alkynyl sugar analogs. Figure from Hsu et al.¹³⁶

Following typically applied procedures in MOE, so far only the metabolic incorporation of fully acetylated galactose derivatives **31**, **33** and **36** was shown. Usually, peracetylated monosaccharides are used during incorporation studies, because they are considered to be less hydrophilic and to show a better membrane permeability. Inside the cell, the acetyl protecting groups are expected to be removed by unspecific esterase enzymes.¹³⁷ However, Chen and co-workers showed recently that acetylated versions of unnatural monosaccharides can lead to artificial *S*-glycosylation of cellular proteins.¹³⁸ This observed modification would not describe the envisioned metabolic processing of the applied unnatural monosaccharides, but an unspecific side reaction. In order to verify a selective labeling of the synthesized galactose derivatives, a further experiment was conducted with the de-acetylated derivative **38**. Using the same procedures then previously presented for the incorporation of acetylated galactose derivatives, HepG2 cells were grown for 72h with the de-acetylated galactose derivative **38** before the staining procedure by iEDDA reaction was applied. Commercial galactose (**45**) was used as negative control. Also with the deprotected derivative **38**, a successful labeling was achieved (Figure 25).



*Figure 25: Metabolic incorporation of de-acetylated galactose derivative **38** into cell membrane glycans of HepG2 cells. Galactose (**45**) was used as negative control. iEDDA reaction was performed using 6-methyl-tetrazine-peg4-biotin (**44**), followed by staining with Alexa-Fluor-568-streptavidine. Nuclei were stained with Hoechst 33342. I and III, as well as II and IV represent two independent experiments.*

Next to the analysis by confocal point-scanning microscopy, the incorporation of the de-acetylated galactose derivative **38** in cell membrane glycans of HepG2 cells, was also confirmed by flow cytometry (Figure 26).

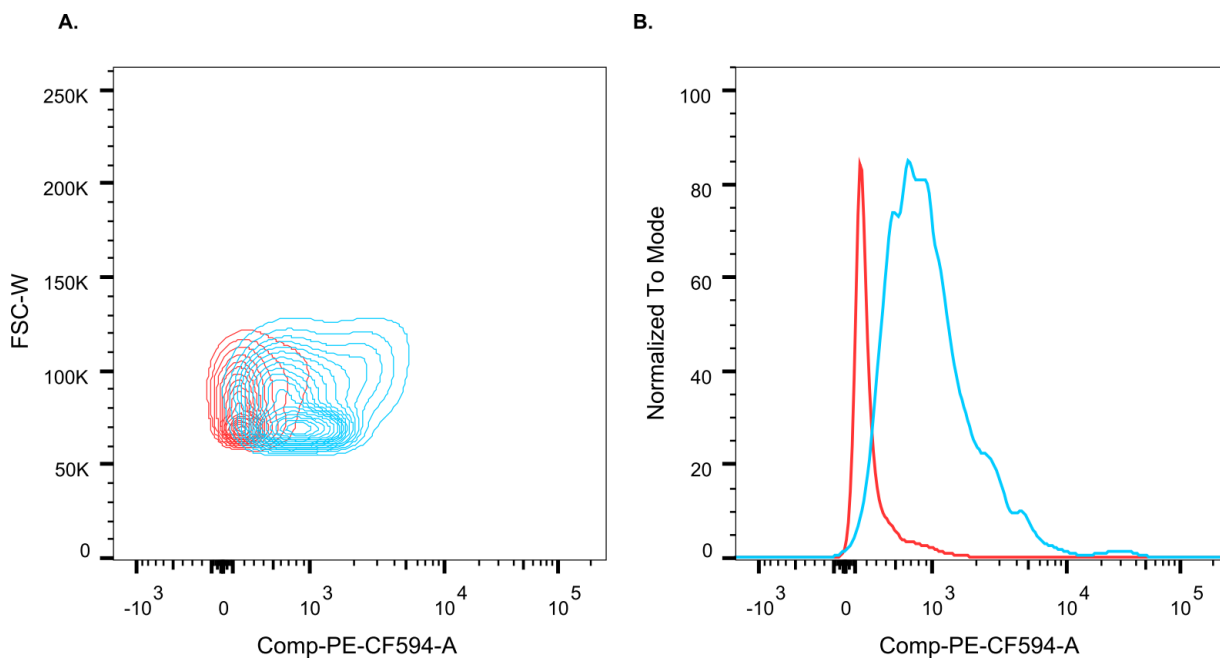


Figure 26: **A.** Superposition of contour plots of forward-scatter detection versus PE-CF594-A fluorescence intensity, after metabolic incorporation of de-acetylated galactose derivative **38** (blue) in HepG2 cells. Galactose (**45**) was used as negative control (red). **B.** Superposition of histograms of PE-CF594-fluorescence intensity, resulting from contour plots in **A.**

The labeling of cell membrane glycan structures was achieved with both, acetylated and de-acetylated galactose derivatives. To be consistent with experiments from the literature and to exclude issues related to the more polar character of the de-acetylated galactose derivative **38**, the following experiments were conducted with the acetylated version **33**.

Until this point, it was successfully shown that unnatural galactose derivatives can be metabolized by human hepatic cells and are incorporated into cell membrane glycan structures. The final goal of this work was to investigate a possible increase of galactose containing structures in hepatic cells after an infection with sporozoites from *Plasmodium berghei*. An identification of certain expressed glycan structures in this stage of the disease could lead to the development of anti-malaria vaccine candidates based on these antigenic structures.

2.2.4. Metabolic incorporation during infection with *Plasmodium berghei*

To study the impact of an infection on the uptake and incorporation of galactose in the glycan structures of infected cells, a new protocol was developed and different techniques were used for analysis.

All experiments of the infection studies were done in HepG2 cells, by using the unnatural galactose derivative 2-*O*-pentenyl-1,3,4,6-tetraacetyl-galactose (**33**) and pentaacetyl galactose (**42**) as negative control. GFP-expressing sporozoites from *Plasmodium berghei* were dissected from salivary glands of infected female *A. stephensi* mosquitoes and used for the infection of HepG2 cells. The cells were grown in the presence of 100 μ M of the galactose derivative **33** or the negative control **42** until 48 hpi to reach the maximum stage of parasite development. In the following, the cells were stained with the same method, which was developed and described in the previous part, using 6-methyl-tetrazine-peg4-biotin (**44**) and alexa-fluor-568-streptavidin (Figure 27). Staining results were improved by changing the cell media 2 hpi to remove possible debris from the mosquito host which resulted in strong background signal. For the analysis, confocal point scanning microscopy, flow cytometry and imaging flow cytometry were used and negative controls were used for non-infected cells, as well as for the cells infected with sporozoites. It was decided to analyze these experiments with different techniques to overcome certain limitations and to compare the different outcomes.

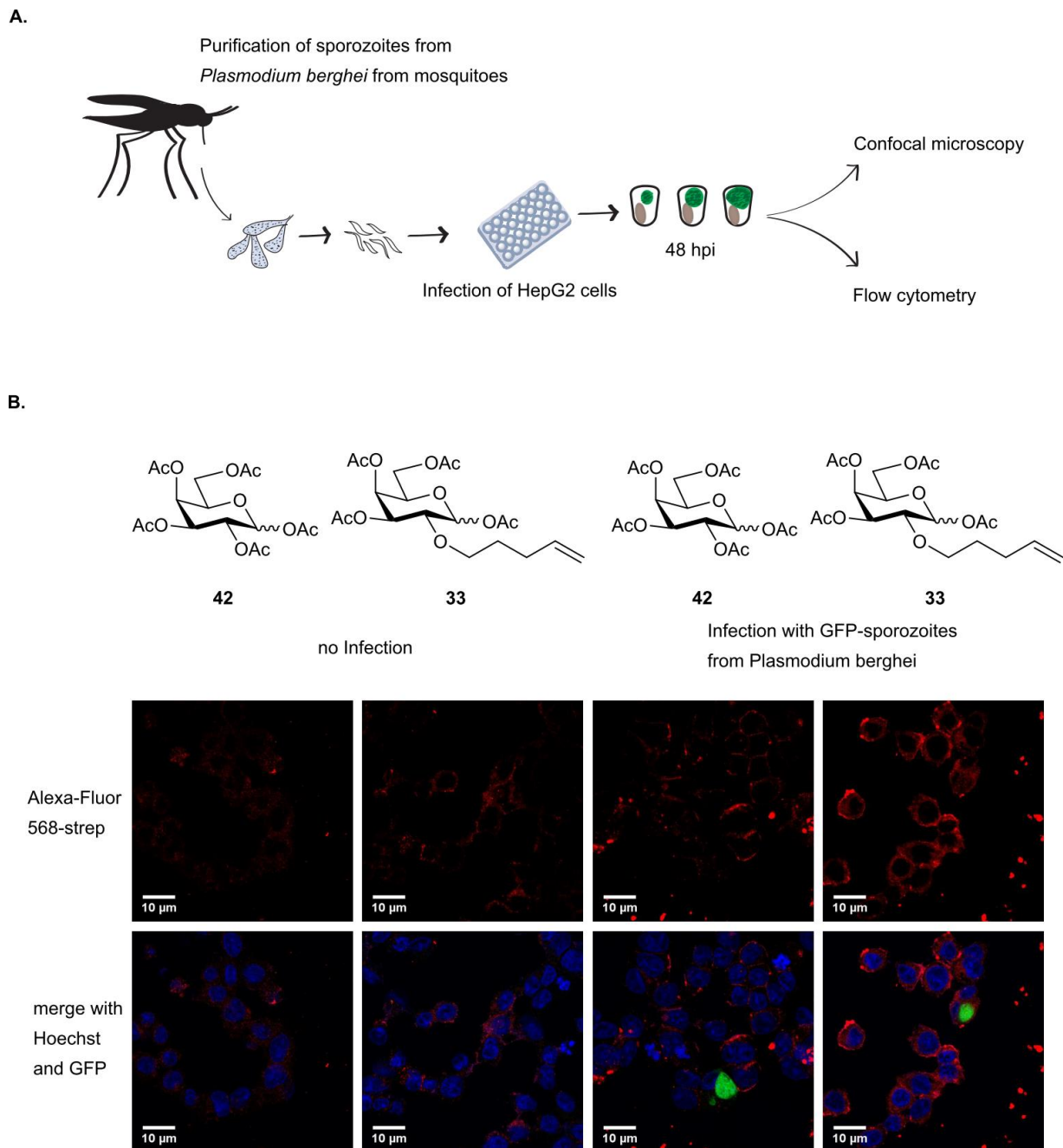


Figure 27: **A.** Schematic illustration of the workflow for the metabolic incorporation of galactose derivative **33** into HepG2 cells after infection with sporozoites from *Plasmodium berghei*. **B.** Confocal images of HepG2 cells after incorporation of galactose derivative **33** and infection with sporozoites from *Plasmodium berghei*. Pentaacetylated galactose (**42**) was used as negative control. GFP-signal derived from the GFP-expressing parasite.

Confocal point-scanning microscopy provides the possibility to compare infected cells and direct neighboring cells in terms of their fluorescence intensity, however large-scale

quantification is time consuming and has to be carefully planned to provide an unbiased set of data. Flow cytometry allows fast acquisition of many cells and the quantification of their fluorescence intensity resulting from the incorporated galactose derivative. In this setting the gating was done based on the intensity of the GFP signal to distinguish between non-infected and infected cells, however debris from the mosquito host could interfere in some cases due to its auto-fluorescence (Figure 28). Three independent experiments were conducted with an infection rate between 3-5 % and at least 3000 live, single cells were gated for analysis.

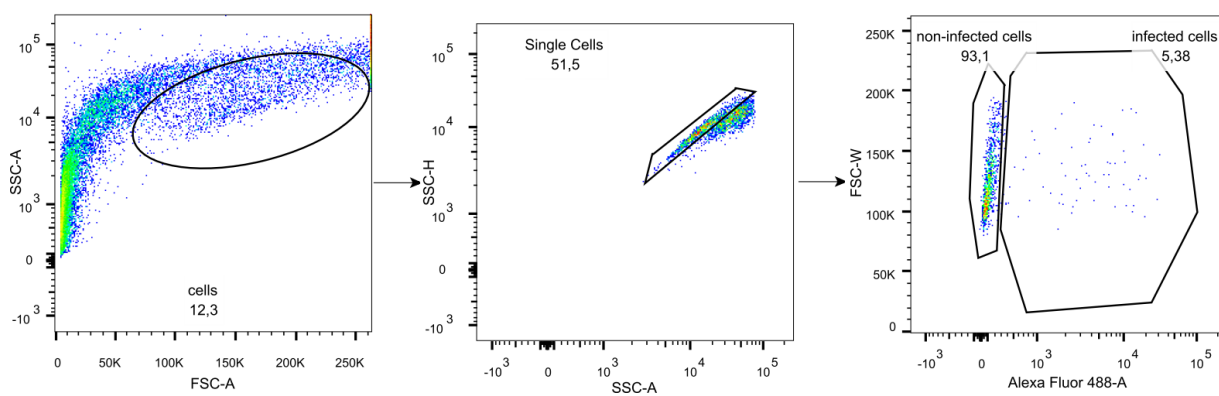


Figure 28: Gating strategy for the acquisition and quantification of the metabolic incorporation of galactose derivative **33**, in HepG2 cells, after infection with sporozoites from *Plasmodium berghei*.

The third technique used for this work was an imaging flow cytometer Amnis ImageStreamX MarkII. This instrument provides the possibility to acquire single cell pictures of selected cell populations, which can be gated based on various factors. The big advantage over conventional flow cytometry in this special context was given by the fact that gated populations could be examined with the help of the acquired pictures, which made it easier to exclude particles coming from mosquito cell debris. At the same time, the fluorescence intensity from the labeling reaction of derivative **33** could be determined of the selected populations. The gating strategy relies on the selection of focused single cells, which were then divided in infected and non-infected cells, based on the intensity of the GFP signal (Figure 29 A). Four independent experiments were conducted, with an acquisition of each 5000 single cell picture. The infection rate was calculated to be around 3% during each experiment. The identity of the selected populations was verified by the acquired single cell pictures in the brightfield channel (Ch01),

in the GFP channel (Ch02) and in the channel, which corresponds to the incorporated galactose derivative (Ch04) (Figure 29 B).

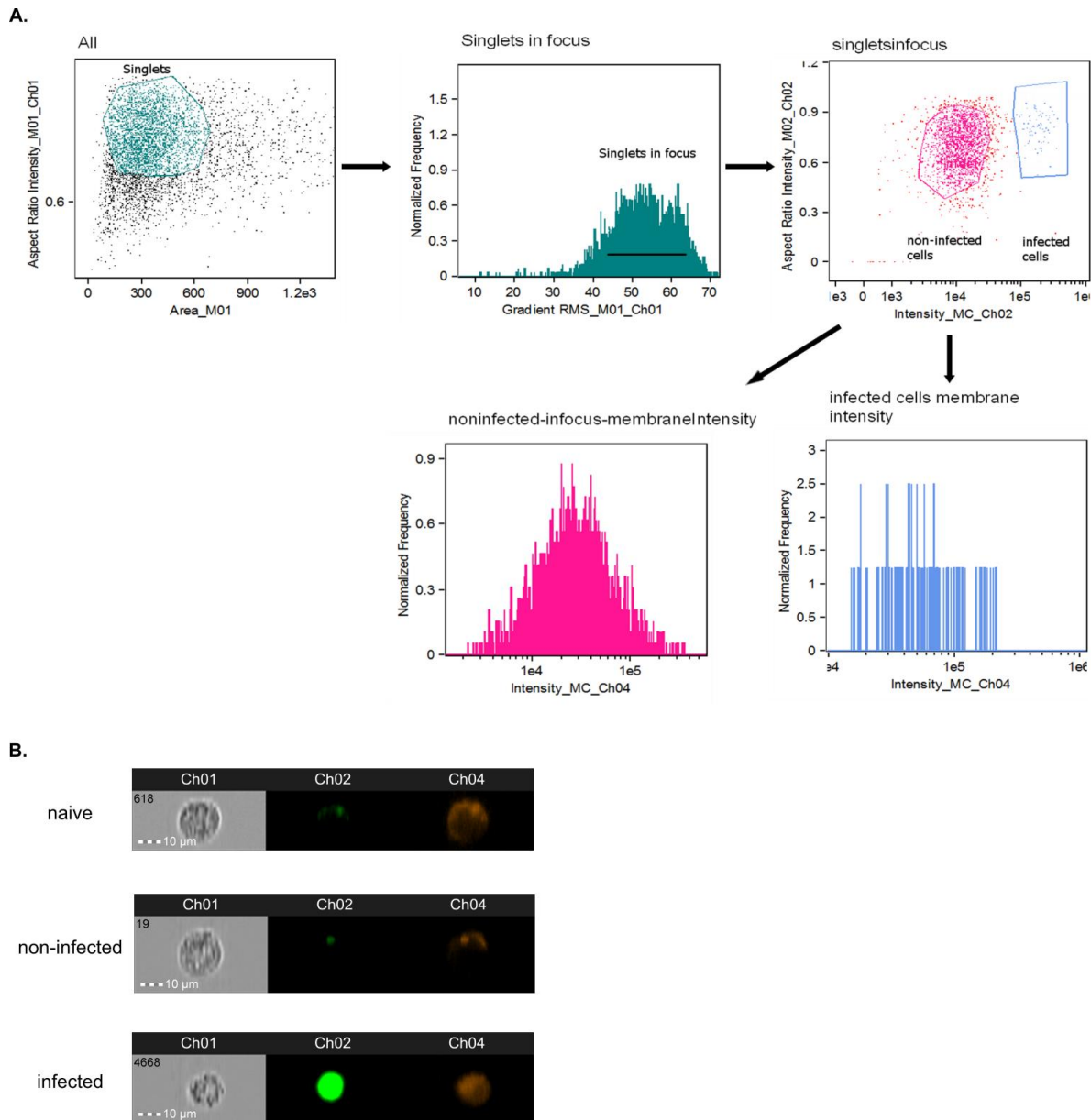


Figure 29: **A.** Gating strategy for the acquisition and quantification of the metabolic incorporation of galactose derivative **33** in HepG2 cells, after infection with sporozoites from *Plasmodium berghei* **B.** Representative pictures from the selected populations after incorporation of galactose derivative **33**, Ch01: Brightfield picture, Ch02: GFP-channel, Ch04: Alexa-Fluor-568.

A combination of all these three methods could ensure the acquisition and analysis of the data sets in an unbiased manner. The quantification of pictures acquired through confocal

point-scanning microscopy was performed using ImageJ software package. From three independent experiments, about 6-10 pictures were acquired for each condition and about 6-10 cells per picture were analyzed. The mean fluorescence intensity of the staining with Alexa-Fluor-568-streptavidine (Figure 27 B), which corresponds to the incorporated galactose derivative **33**, was measured based on the pixel intensity. Each condition was calculated as ratio to the corresponding control with pentaacetyl galactose (**42**). Two-tailed Mann-Whitney t-test was performed for nonparametric, unpaired data (Figure 30 A). The analysis of the results from confocal microscopy showed a tendency for an increased fluorescence intensity in infected cells. Very similar results were obtained when analyzing the incorporation of derivative **33** by flow cytometry (Figure 30 B). Again, three independent experiments were conducted, during which 2000-3000 live, single cells were gated. The rate of infected cells was between 3-5% and for each condition, the ratio of median fluorescence intensity against the corresponding control was calculated. A two-tailed Mann-Whitney t-test was performed for nonparametric, unpaired data. Consistent with the results from confocal microscopy and flow cytometry, also the analysis by imaging flow cytometry gave a tendency for a higher fluorescence intensity in infected cells (Figure 30 C). Four independent experiments were conducted, during which 5000 single cell pictures were acquired and the ratio of median fluorescence intensity was calculated against the corresponding control. The infection rate was similar to the conventional flow cytometry around 3%.

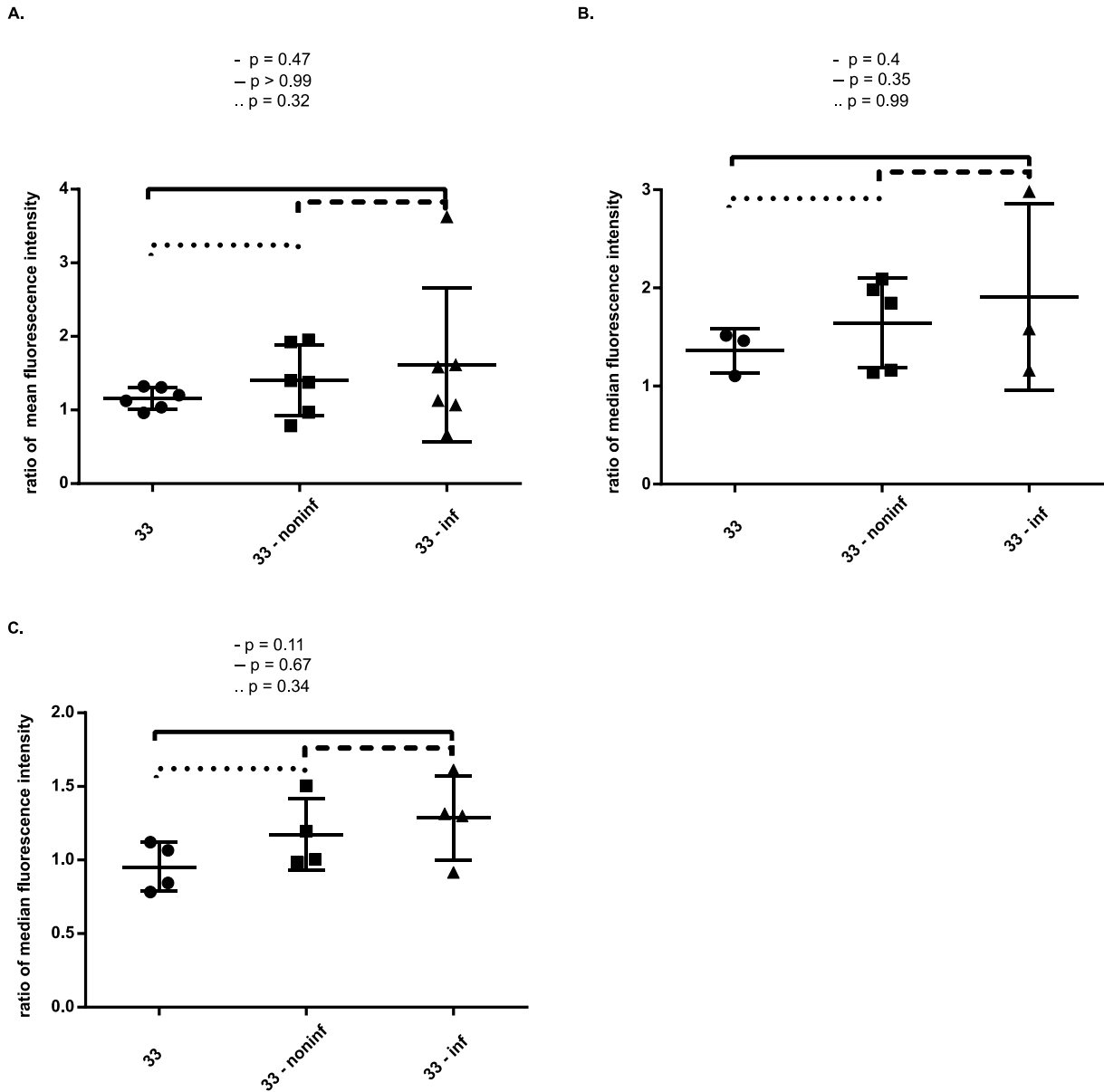


Figure 30: Analysis of the mean fluorescence intensity after incorporation of 33 in HepG2 cells, with and without infection through *Plasmodium berghei* sporozoites, ratios against control 42 **A.** Quantification by confocal microscopy, representative data from one out of three experiments, $n = 6$ pictures, each data point represents mean fluorescence intensity of 10 cells. Two-tailed Mann-Whitney. **B.** Quantification by flow cytometry, combined results of 3 independent experiments, gating of ~2000-3000 single cells (infection rate ~3%), Two-tailed Mann-Whitney. **C.** Quantification by imaging flow cytometry, combined results of 4 independent experiments, each data point corresponds to ~2000 single cell pictures (noninfected and naïve) or ~70 single infected cells (infection rate ~3%), Two-tailed Mann-Whitney.

With all three methods, it was possible to show that the ratio of fluorescence intensity against the corresponding control tends to increase from naïve cells to non-infected cells and infected cell containing the parasite. The observed pattern in the increase in fluorescence intensity,

coming from the unnatural galactose derivative **33**, was very small and attempts to improve the uptake by starving the cells before incubation did not result in any further increase. However, because the observed trend was consistent in all settings, a reasonable explanation for this finding was meant to be found.

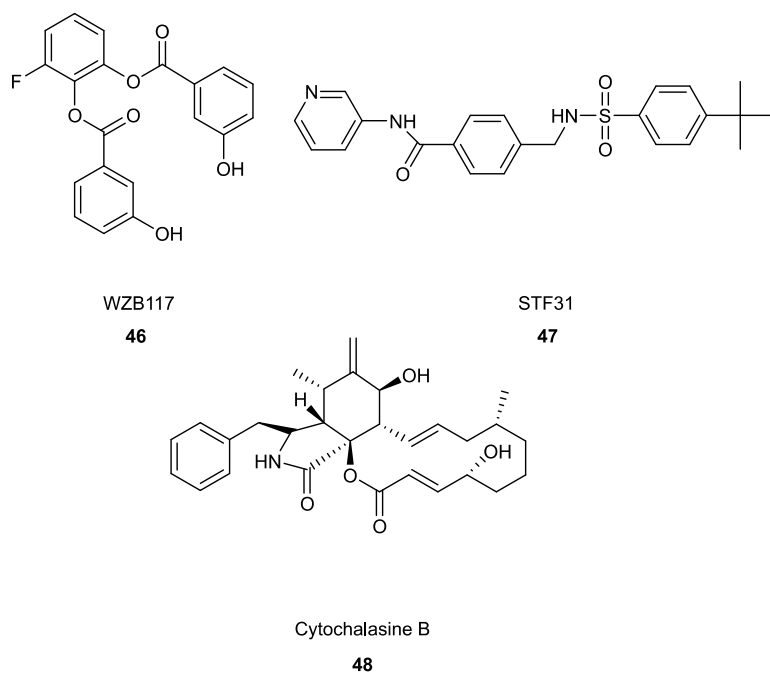
2.2.5. Transport of artificial galactose derivatives through GLUT1

An increase in the taken-up galactose derivatives, based on a metabolic signal of the developing parasite was expected to result in a higher increase compared to the non-infected samples. Having this in mind, literature research was undertaken, with regard to known metabolic events during this stage of the infection. An important point, which came out very quickly, was the energy supply for the developing parasite in this stage. It was known earlier that during the blood stage, the *Plasmodium* parasite is depending on glycolysis to produce the necessary adenosine tri-phosphate (ATP). In this stage, glucose is imported from the blood plasma via a facilitative hexose transporter (PfHT).^{139,140} Recently, Prudêncio and co-workers could show that during the liver stage, the GLUT1 transporter provides the necessary glucose for the parasite development. Furthermore it was shown in this work that especially in infected cells, an increase in GLUT1 transporter translocation to the cell membrane during later stages of the infection occurs.¹⁴¹ A closer look at the transporter GLUT1 revealed that besides glucose, also galactose and ascorbic acid can be transported by this structure.^{142,143} The common procedure during MOE uses fully acetylated monosaccharides in order to increase their hydrophobic properties and to enable passive diffusion through the cell membrane.⁴⁴ However, with regard to the literature concerning facilitative transporters and the involvement of GLUT1 in the energy supply during the liver stage of an infection with *Plasmodium*, a simple experiment was designed to test a possible transport of the unnatural galactose compounds through GLUT1. Different inhibitors were chosen in order to block GLUT1 during the culturing time with the unnatural galactose compound to test if a block of this transporter will lead to a reduced uptake of the monosaccharides. The inhibitors WZB117 **46**, STF 31 **46** and cytochalasine B **48** were used at a concentration of 10 μ M during the whole culturing time of 72 h (Figure 31 A).^{144,145} An analysis by confocal point-scanning microscopy revealed a significant decrease of the

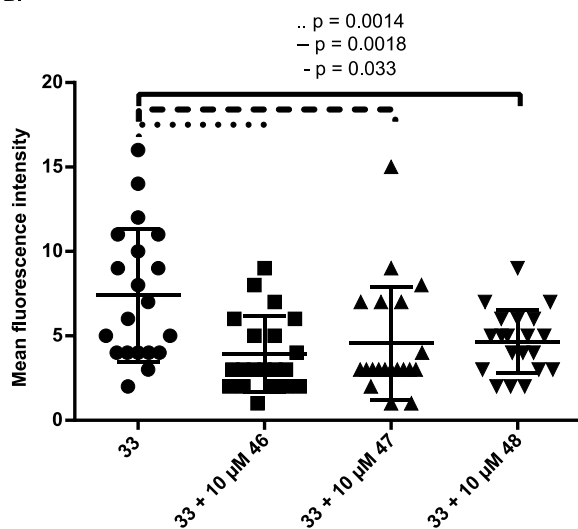
fluorescence intensity derived from the incorporated monosaccharide, in samples grown in the presence of one of the inhibitors (Figure 31 B). For each condition 5-8 pictures from different positions in the well were analyzed and the mean fluorescence intensity of 5-7 single cells per picture was measured, using ImageJ software package. Two-tailed Mann-Whitney was performed for unpaired, non-parametric data sets.

Encouraged by these results, a further experiment was conducted, applying increasing concentrations of the inhibitor WZB117 **46** during the 72 h of culturing time. It was very pleasant to see a concentration dependent decrease in fluorescence intensity when analyzing samples from two independent experiments by flow cytometry (Figure 31 C).

A.



B.



C.

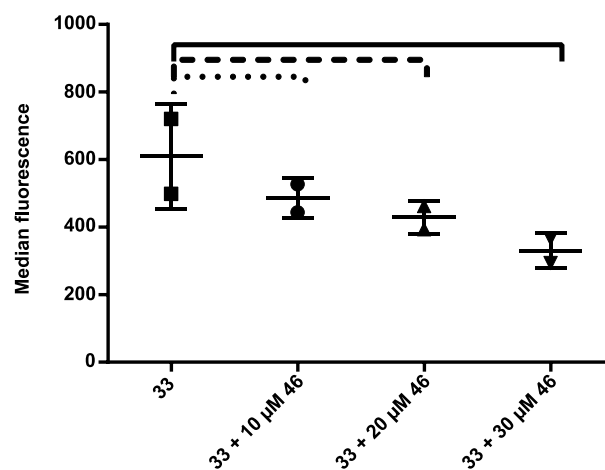


Figure 31: A. Structures of the GLUT 1 inhibitors WZB117 46, STF31 47 and cytochalasin B 48. B. Quantification of mean fluorescence intensity after the incorporation of galactose derivative 33 in the presence or absence of 10 μ M inhibitors 46-48. Data represented from one exemplary experiment out of two. Two-tailed Mann-Whitney. C. Quantification of median fluorescence intensity after incorporation of galactose derivative 33 in the presence of increasing amount of inhibitor 46. Data represented the pool of two independent experiments.

Data represented from one exemplary experiment out of two. Two-tailed Mann-Whitney. C. Quantification of median fluorescence intensity after incorporation of galactose derivative 33 in the presence of increasing amount of inhibitor 46. Data represented the pool of two independent experiments.

The described experiments of inhibiting the facilitative transporter GLUT1 lead to a review of the previously obtained results during the infection studies. Knowing about the importance of

GLUT1 for the developing parasite during the liver stage of the infection, a possible explanation for the observed small increase in fluorescence labeling, is an increased transport of the artificial galactose derivative **33** through the present GLUT1 transporters in this stage. By inhibiting this transporter, the resulting decrease in galactose derivative derived fluorescence intensity, proves that this unnatural sugar is also transported via this facilitative hexose transporter. The in the literature described enhanced translocation of GLUT1 to the cell membrane of infected cells, will enable an increased uptake of the present galactose derivative and consequently provide more of this sugar for metabolic incorporation.¹⁴¹ The observed and described increase in metabolic labeling due to incorporated galactose derivative is not due to the presentation of certain glycan antigens on the surface of infected hepatocytes, but a side effect of the elevated energy demand of infected cells due to the developing parasite.

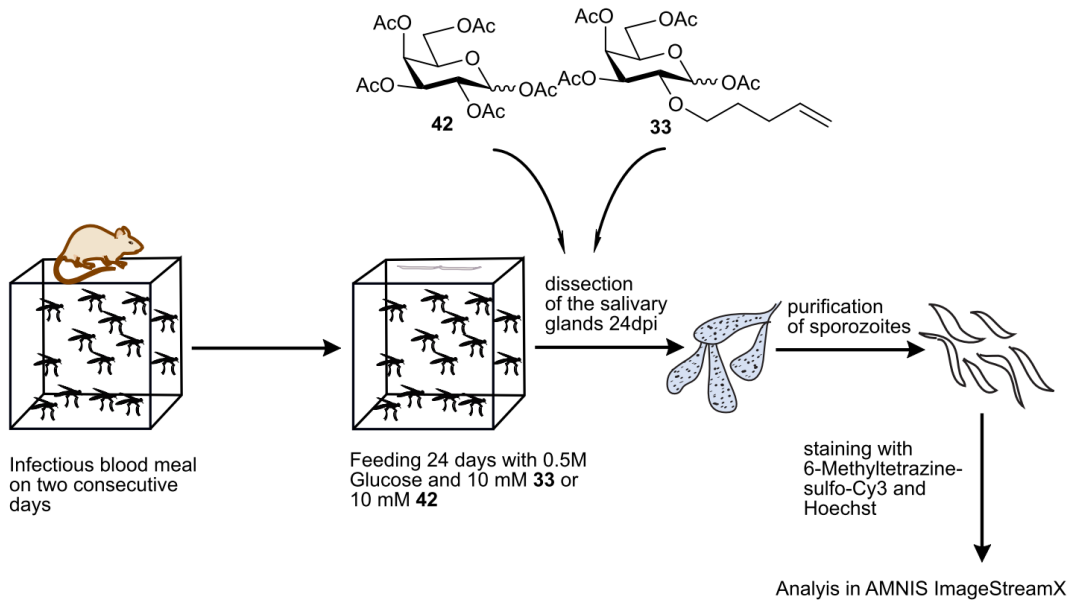
2.2.6. Transfer of artificial galactose derivatives from the mosquito host to the parasite

Until this point, the application of a modified galactose monosaccharide for metabolic labeling in cells was established. However, during these experiments, the consideration came up if the strategy of MOE could be used as well to study a possible connection between the mosquito host and the *Plasmodium berghei* parasite. Regarding galactose containing structures, it is still poorly understood how the parasite is able to synthesize these glycans, because neither enzymes for the epimerization of glucose, nor enzymes for the activation of galactose were identified in the parasite genome so far.¹⁴⁶ However, the presence of UDP-galactose was identified in the blood stage form of *Plasmodium falciparum* and the trisaccharide α -Gal was confirmed by anti- α -Gal antibody binding on sporozoites from *Plasmodium falciparum*.^{60,80,147} A possible hypothesis might be a transfer of components from the mosquito vector to the parasite.¹⁴⁷ To test this idea, female *A. stephensi* mosquitoes were fed with a sugar solution containing 10 mM of the unnatural galactose derivative **33** or the control sugar **42** for the 21 days after the infectious blood meal. During this time, the parasite develops from the ingested gametocytes into sporozoites, which then traverse into the salivary gland of the mosquito.¹⁴⁸ The expectations were that if a transfer of galactose monosaccharides or of its activated forms galactose-1-

phosphate or UDP-galactose occurs, the unnatural galactose derivative should be transferred to the parasite and the introduced terminal alkene reporter group should be available on the sporozoites for detection via iEDDA reaction. After 24 days, the mosquitoes were dissected and the sporozoites were obtained from the salivary glands (Figure 32 A). For the analysis, staining with 6-methyl-tetrazine-sulfo-cy3 (**43**) and Hoechst was performed and the parasites were analyzed using the imaging flow cytometer Amnis ImageStream MarkII. With this instrument it was possible to acquire single pictures of a number of parasites and to separate them from mosquito host cells. In the first step, the brightfield pictures were analyzed using their areas and aspect ratio. This allowed to determine a certain ratio of these values which defined an area in the plot in which the single parasite could be found. The remaining area represented host cell debris from the mosquito. For the analysis of the parasite, an additional refinement step was undertaken, to isolate pictures from clean parasites. In the last step, the fluorescence intensity of these parasites in channel Ch04, which represents the fluorescence intensity resulting from incorporated galactose derivative **33**, was analyzed. Also the selection representing the host cell debris was analyzed for the fluorescence intensity in channel Ch04 (Figure 32 B). In total, 20000 pictures were acquired, from which around 500 were gated as clean parasites and around 15000 as mosquito host cell debris.

By comparing the two different groups, it was interesting to see that for the parasite populations, only a non-significant difference was observed. However, the analysis of the structures coming from the mosquito host, showed a highly significant difference between the mosquitoes fed with unnatural galactose derivative **33** and the ones which received the normal food with the natural galactose sugar. With this result, it can be shown that the unnatural galactose derivative **33** is successfully taken up by the mosquito, however the transfer to the sporozoites still has to be evaluated further. An explanation of the only minor increase of galactose derived fluorescence intensity on the sporozoites, might be for example a very low expression of galactose containing structures on the parasite surface or only a limited transfer of metabolites from the mosquito to the parasite.

A.



B.

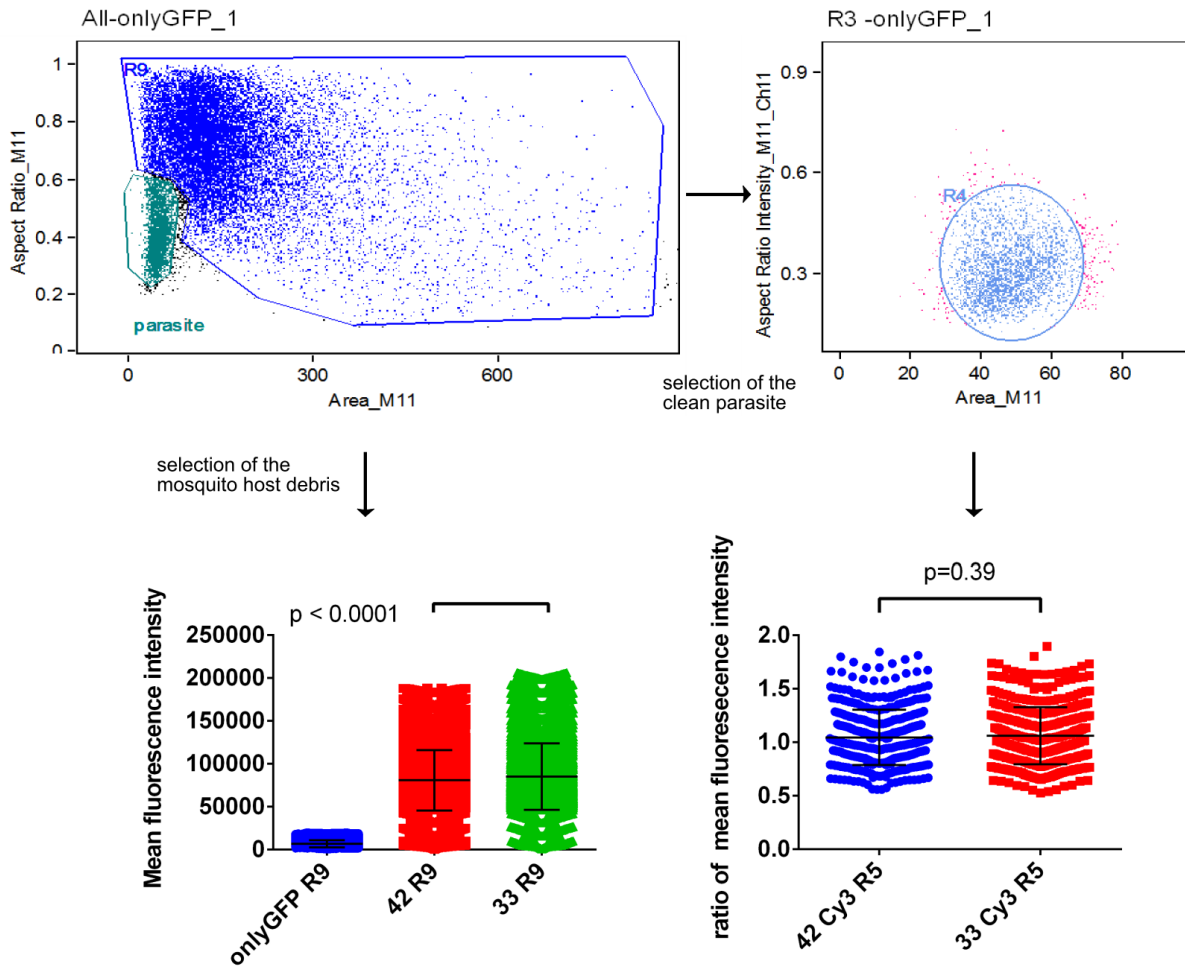


Figure 32: A. Schematic illustration of the workflow for an administration of galactose derivative 33 to infected mosquitoes. B. gating strategy for acquisition and analysis of the dissected parasites and the remaining host cell debris in Amnis ImageStream Mark II. Data are represented from one feeding experiment, Two-tailed Mann-Whitney.

In this experiment, the fully acetylated galactose derivative **33** was used during the feeding process, in order to maintain a similar protocol as for the cell studies. However, increased mortality was observed in the mosquitoes fed with this sugar after the first two weeks which also lead to the question if the surviving individual mosquitos represent the ones which absorbed less of the unnatural sugar solution. It is not clear whether the mosquitos possess similar unspecific esterase enzymes to remove the acetyl protecting groups, it might be a possibility to use the deprotected galactose derivative **38** during the feeding process. Also, it might be an option to start the feeding process after the infections blood meal with the usual glucose solution and only provide the substituted food after 5 to 7 days. During this first period, the parasites development in de mosquito host is still at the beginning of the sporogonic cycle and less contribution to the incorporation of **33** in sporozoite glycans could be expected during this time. However, the survival of the mosquito host could be increased by feeding the normal food for a certain time after the infectious blood meal.

2.3. Future perspective – Application of MOE in malaria

In this work, the synthesis of three unnatural galactose monosaccharides with terminal alkene groups for iEDDA reaction was shown. All compounds were characterized for their kinetic properties in iEDDA reactions with 6-methyl-tetrazine derivatives and the metabolic incorporation in cell glycan structures of different cell lines was successfully achieved. The alteration of the chemical reporter group from C2 to C6 position seemed not to interfere with the incorporation process, which could be useful for further metabolic labeling approaches. Furthermore, for the first time, an unnatural galactose structure was used for investigations on the liver stage of a malaria infection. Here, it was possible to show that this monosaccharide did not had any influence on the parasite development or on cell growth. In combination with a short study on the sugar transporter GLUT1, this work could show the tendency of infected

hepatic cells to have a slightly higher uptake of the unnatural galactose compound due to its facilitated diffusion via GLUT1. In addition, the uptake of the artificial galactose by the mosquito host during the feeding process was shown, representing an example how these sugars could be used to explore the glycobiology of the *Plasmodium* parasite.

In possible future improvement for the application of galactose derivatives for MOE could be a change to different chemical reporter groups. During trial experiments to study the cellular location of the presented galactose derivatives **31**, **33** and **36** on the endoplasmic reticulum or Golgi apparatus, it was observed that the applied tetrazine derivatives for iEDDA reaction, seems to bind in unspecific manner to previously fixed cell samples. Since successful membrane staining of the incorporated galactose derivatives was achieved, for the goal of this work, the labeling reaction by iEDDA reaction using tetrazine was acceptable. However, in order to look have a deeper look on the biosynthetic pathways these unnatural sugars may be involved in, a different strategy should be developed.

The introduction of different chemical reporter groups like norbornenes might be considered, to enable a faster reaction kinetic. Also the choice of tetrazine derivative can be optimized. A possibility for better detection results could be the utilization of so-called turn on probes. These tetrazine probes were developed to provide a fluorescence turn-on of up to 10000 fold after iEDDA reaction, which resulted from through-bond energy transfer.¹⁴⁹ A highly efficient iEDDA reaction using a very fast chemical reporter group like norbornene, combined with a highly fluorogenic tetrazine probe, could provide a better setting for the detection of incorporated galactose derivatives.

The initial intention of this project was to investigate the possible presentation or modulation of galactose containing glycan antigens on the surface of with *Plasmodium berghei* sporozoites infected hepatocytes, however the results presented in this work do not suggest a significant increase in such structures. A possibility to use the observed changes for medical purposes might be to evaluate a strategy to use unnatural galactose structures as delivering agent for liver stage specific drugs. Since it was shown in this work that an unnatural galactose compound is tolerated and metabolized by hepatic cells without impeding the parasites' development, these compounds could be used in conjugation with a drug like Primaquine, to deliver these agents more selective to infected hepatic cells than healthy ones.

Furthermore, the method of metabolic oligosaccharide engineering could be developed further in the context of an infection with *Plasmodium*. The glycobiology of *Plasmodium* is still not completely understood, however the importance of certain carbohydrate structures and sugars becomes more and more clear. The introduction of modified monosaccharides might provide the necessary tool to explore the function of glycans for example in the context of antigenic structures during the liver stage infection.

An antigen of great interest is the so called circumsporozoite protein (CSP), a surface protein on the sporozoites with high importance for their motility, on the invasion of the salivary gland and on hepatocyte infection.¹⁵⁰ During the liver stage, the CSP is presented on the surface of infected hepatocytes, which are also known to trigger a CD8⁺-dependent immune response.¹³³ In a recombinant protein, the CSP is part of the anti-malaria vaccine candidate RTS,S/AS01, which was shown to cause protection against clinical malaria during a Phase III clinical trial.⁶⁴ The recent review of E.D. Goddard-Borger and J.A. Boddey is discussing the possible influence of glycosylation on an improvement of vaccine efficacy, as well as the still unknown function of *N*- and *O*-glycosylation in the parasites lifecycle.¹⁵¹ The CSP would provide multiple options in which metabolic oligosaccharide engineering could be applied. During the sporozoites stage, this protein is anchored to the plasma membrane by GPI anchors, which are composed of mannose units that start from a glucosamine unit.¹⁴⁸ It might be an option, to test if unnatural mannose monosaccharides could be incorporated by the parasite and how an artificial structure might influence the function of the GPI anchors.

Looking at other monosaccharides, CSP was shown to be fucosylated in its TSR (thrombospondin type I repeat) domain, when expressed in HEK293T cells and it was also shown to expose posttranslational modifications on the surface of sporozoites.^{152,153} It would be very interesting to test, if modified fucose derivatives can be introduced in this glycan structure during for example recombinant expression. In this way, this special glycan structure could be purified and characterized with regard to its function during an immune response during the liver stage. A possibility would be to test the recognition of this artificial glycan structure by anti-CSP antibodies and if a modified glycan in this position increases or weakens the interaction. By using MOE in these experiments can provide the opportunity to localize, track

and purify relevant glycan structures which can result in more knowledge about the importance of these molecules for vaccine development.

An additional possibility to work with unnatural galactose derivatives in the context of malaria, would be to address the blood stage of the infection. The sugar nucleotide UDP-Gal was identified in the blood stage parasite using liquid chromatography-tandem mass spectrometry, however enzymes for the biosynthetic pathway of this molecule have not been identified yet.¹⁵⁴ So far, it has not been possible to identify terminal galactosylation in proteins or glycolipids in the blood stage, which also raised the question for what purpose UDP-Gal might be used by the parasite. The application of MOE with unnatural galactose derivatives might provide an opportunity to develop selective enrichment methods of galactose containing glycan structures in this stage of the parasite, which could lead to the identification and characterization of important galactosylated structures in this stage of the infection.

3. Chapter 3 – Synthesis of a bifunctional galactose derivative for metabolic labeling

3.1. Introduction

The great success of MOE for investigations on cellular carbohydrate structures and the necessary biosynthetic pathways, proves the wide range of possible applications of this strategy. As described in the first chapter, several different chemical reporter groups were shown to be suitable for the metabolic incorporation into cellular glycan structures and several different organisms were already tested.

Despite using only one unnatural sugar derivative, some examples show the simultaneous incorporation of up to three different monosaccharides and Chen and coworkers described the successful incorporation of bifunctional sialic acid derivatives.^{46,47} This study demonstrates the enormous flexibility of cellular systems and the combination of several bio-orthogonal labeling reactions within the same molecule.

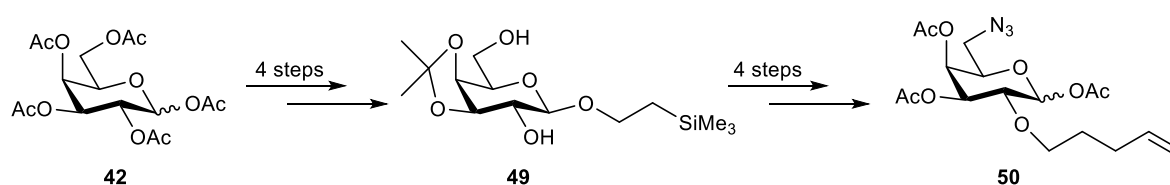
The previous chapter reported the synthesis and metabolic incorporation of monofunctional galactose derivatives in hepatic cells. Following up on this idea, a bifunctional galactose compound was meant to be developed, to test the possibility of its metabolic incorporation. An incorporation of an unnatural sugar with two bio-orthogonal chemical reporter groups can provide additional tools for investigations on carbohydrate structures. Apart from labeling, it could be possible to enrich the carbohydrate structure of interest via the second reporter group, or the second reporter groups could be used for the attachment of drugs.

Overall, I aimed to develop a bifunctional galactose derivative which is easy to synthesize and, if necessary, easy to modify with regard to the introduced chemical reporter groups.

3.2. Results and Discussion

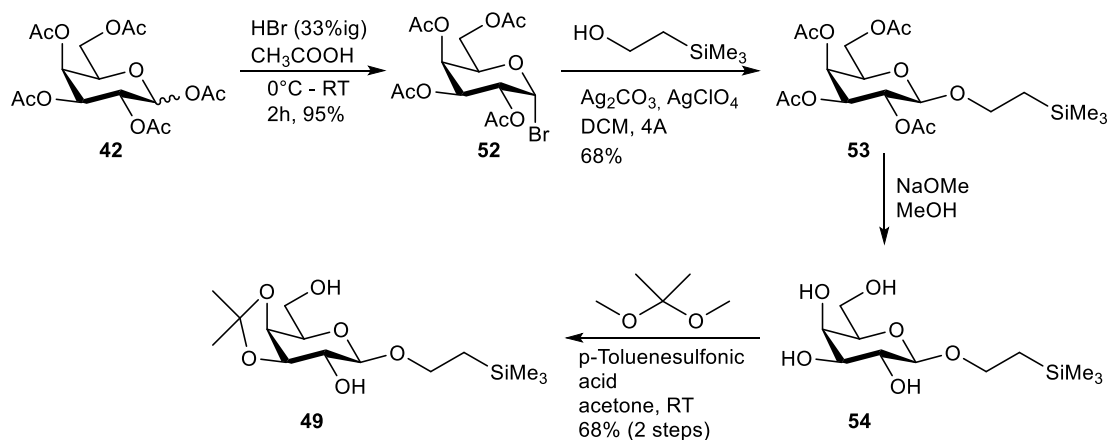
3.2.1. Chemical synthesis of a bifunctional galactose derivative

With the goal to obtain a bifunctional galactose derivative, a synthetic route was designed with a special focus on an easy variability of the final compound. The final route consisted of eight steps, including a flexible intermediate which could allow further modifications of the galactose derivative (Scheme 7).



Scheme 7: Overview over the synthetic route for the synthesis of a bifunctional galactose derivative **50**.

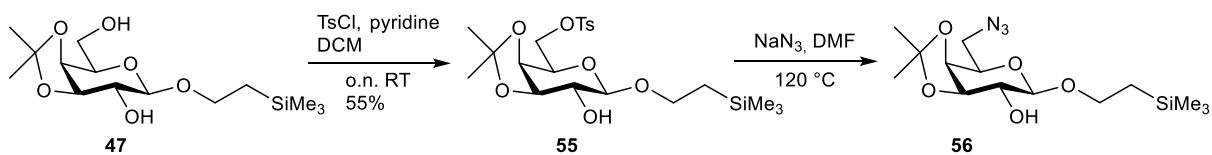
Starting from commercial 1,2,3,4,6-penta-*O*-acetyl-galactose (**42**), the anomeric position was activated in the first step using hydrobromic acid, giving α -tetra-*O*-acetyl-galactosyl bromide (**50**) with a high yield of 95%. The galactosyl bromide **50** was used for the following *Koenigs-Knorr* glycosylation reaction with 2-(Trimethyl-silyl)ethyl. Due to the participating protecting group in C2 position, the pure β -product **53** was obtained with a yield of 68%. In preparation for the intermediate with only two unprotected hydroxyl groups, the acetyl protecting groups were removed using the classical *Zémpfen* method and an isopropyl protecting group was introduced, blocking C3 and C4 position simultaneously. Intermediate **49** was obtained with an overall yield of 44% after four steps (Scheme 8).



Scheme 8: Synthetic scheme for the first four steps, starting from pentaacetyl galactose (**42**), resulting in the intermediate **49**.

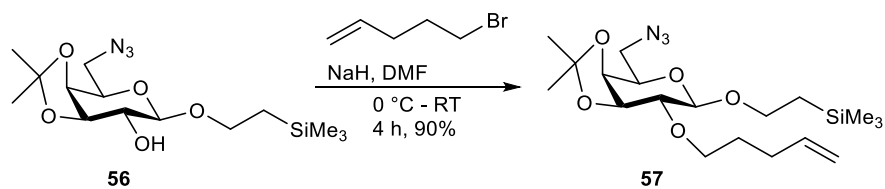
The advantage of this intermediate compound **49**, is given by the fact that the two free hydroxyl groups in C2 and C6 position show different reactivities and it was assumed that the C6 position can be modified selectively when the correct reagents were chosen. As chemical reporter groups for the final galactose derivative, the decision was made to introduce an azide group in C6 position and a terminal alkene in C2 position. In this way, two orthogonal reactions, click-chemistry and iEDDA, can be applied to the cells after the incorporation of the bifunctional derivative.

Since the primary hydroxyl group in C6 position should show a higher reactivity than the secondary one in C2 position, it was decided to pursue this part of the synthesis first. The alcohol group was activated using tosyl group and it was nice to see a selective introduction of the aromatic entity in C6 position. For the following substitution of the tosyl group with the azide functionality, sodium azide was chosen. It was possible to obtain the substitution product **56** with a yield of 55%, however high temperatures were required (Scheme 9).



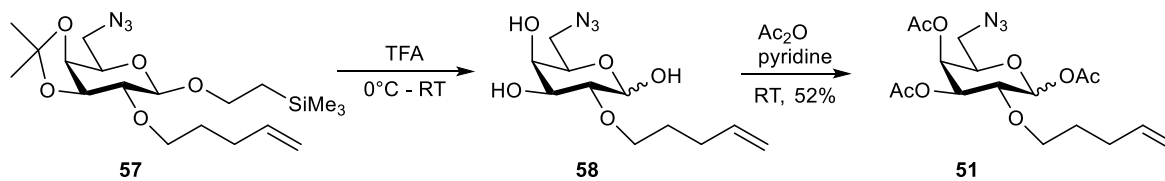
Scheme 9: Reaction scheme for the functionalization of the primary hydroxyl group in C6 position of intermediate **56**.

In this stage of the synthesis, also different routes were explored, in order to facilitate the conditions of the substitution reaction. On one hand, the replacement of the tosyl group by a smaller mesyl group was explored, however under these conditions both hydroxyl groups in C2 and C6 were observed to react, which was not desired. Also, *N*-phenyl-bis(trifluoromethyl)sulfonamide was used for this reaction, however, no activation of the hydroxyl group was observed. Despite the harsh reaction conditions to obtain the azide modified galactose derivative, enough material could be synthesized to continue further. After having modified the C6 part of the molecule, the C2 hydroxyl group was substituted with the same method than the monofunctional derivatives described in the previous chapter, using a Williamson ether synthesis procedure. This reaction gave the protected, bifunctional galactose derivative **57** with a yield of 90% (Scheme 10).



Scheme 10: Functionalization of the secondary hydroxyl group in C2 position with 5-Bromo-1-pentene.

In the final step of this synthesis, the isopropyl protecting group and the anomeric (trimethylsilyl) ethyl group were removed using trifluoroacetic acid (TFA) and acetyl groups were introduced using acetic anhydride and pyridine. As a byproduct, (trimethylsilyl)ethyl-2-*O*-pentenyl-3,4-isopropyl-6-azido galactose was obtained, however the desired product 2-*O*-pentenyl-1,3,4-tri-*O*-acetyl-6-azido-galactose (**51**) was obtained with 52% yield (Scheme 11).



*Scheme 11: Deprotection of galactose derivative **56** and introduction of *O*-acetyl protecting groups, resulting in bifunctional galactose derivative **51**.*

Having this bifunctional galactose derivative **51** in hand, experiments were conducted to test an incorporation of this sugar into cell membrane structures of HepG2 cells.

3.2.2. Studies on the metabolic incorporation

In several trial experiments, HepG2 cells were grown for 72h with either the bifunctional galactose derivative **51** or the control sugar pentaacetyl galactose (**42**). To address the two chemical reporter groups, simple click-chemistry between the azide group of the sugar and Alexa-Fluor-488 DIBO alkyne was performed and the terminal alkene handle was reacted, like in the previous section described, with 6-methyl-tetrazine-peg4-biotin (**44**) and Alexa-Fluor-568-streptavidin. Different times and sequences for the application of the two fluorophores were tested, including a simultaneous staining with Alexy-Fluor-568-streptavidin and Alexa-Fluor-488-DIBO alkyne for 15 min (Figure 33) and a sequential strategy in which the two dyes were applied separately from each other (Figure 34).

Despite all these attempts it was not possible to achieve a selective labeling in cell samples treated with the bifunctional sugar when comparing it to the negative control.

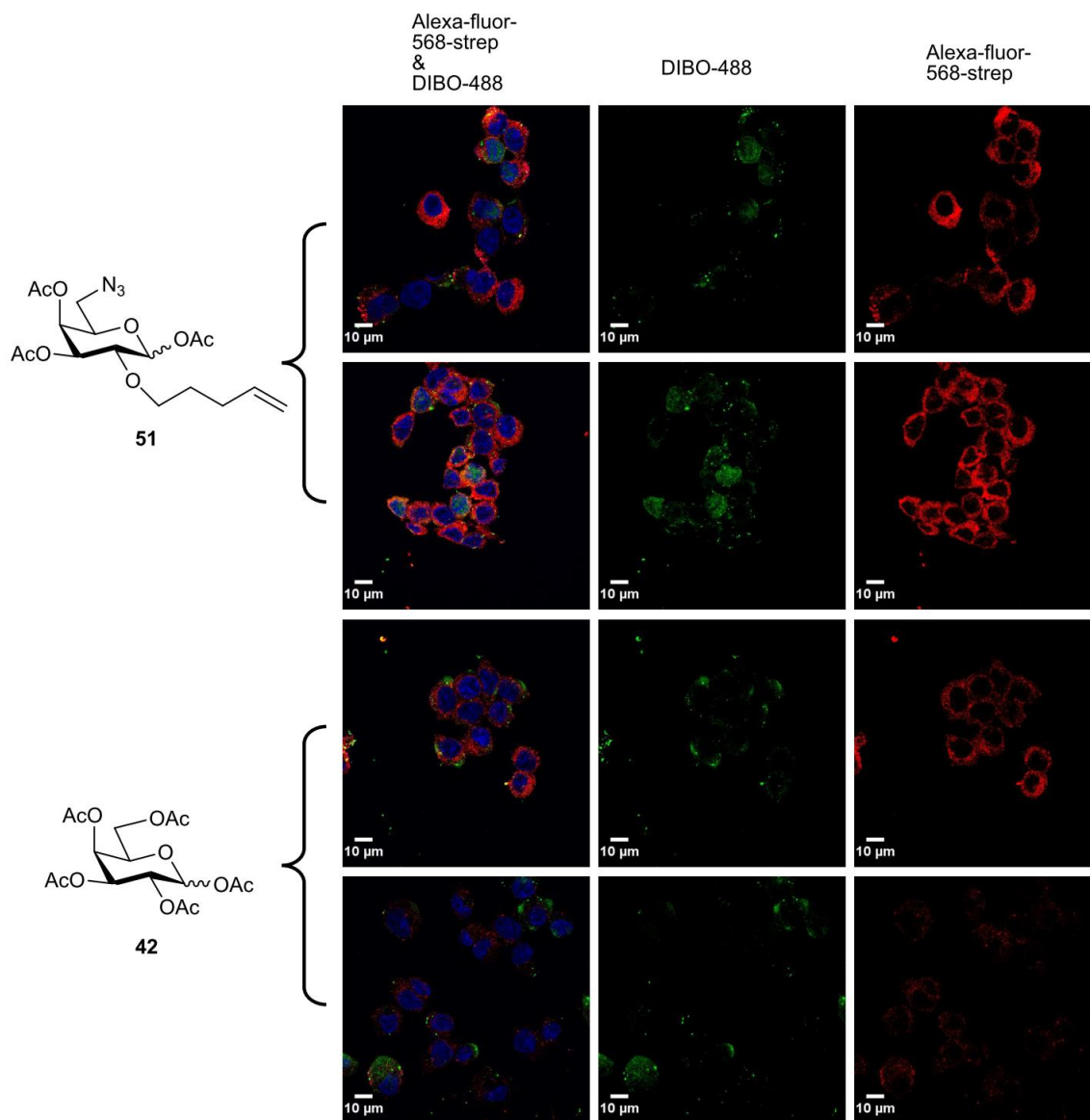


Figure 33: Trial for metabolic incorporation of bifunctional galactose derivative **51** in HepG2 cell membrane glycans. Simultaneous staining with Alexa-Fluor-568-streptavidine and DIBO-alexa-fluor-488. Pentaacetyl galactose (**42**) was used as negative control.

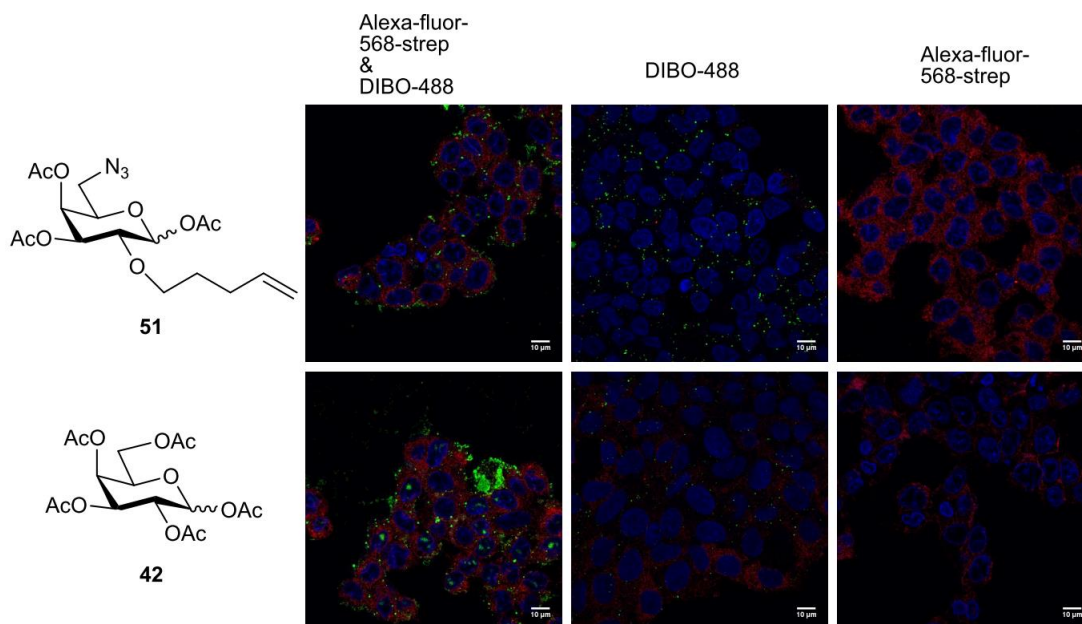


Figure 34: Trial for metabolic incorporation of bifunctional galactose derivative **51** in HepG2 cell membrane glycans. Sequential staining with Alexa-Fluor-568-streptavidine and Alexa-Fluor-488-DIBO. Pentaacetyl galactose (**42**) was used as negative control.

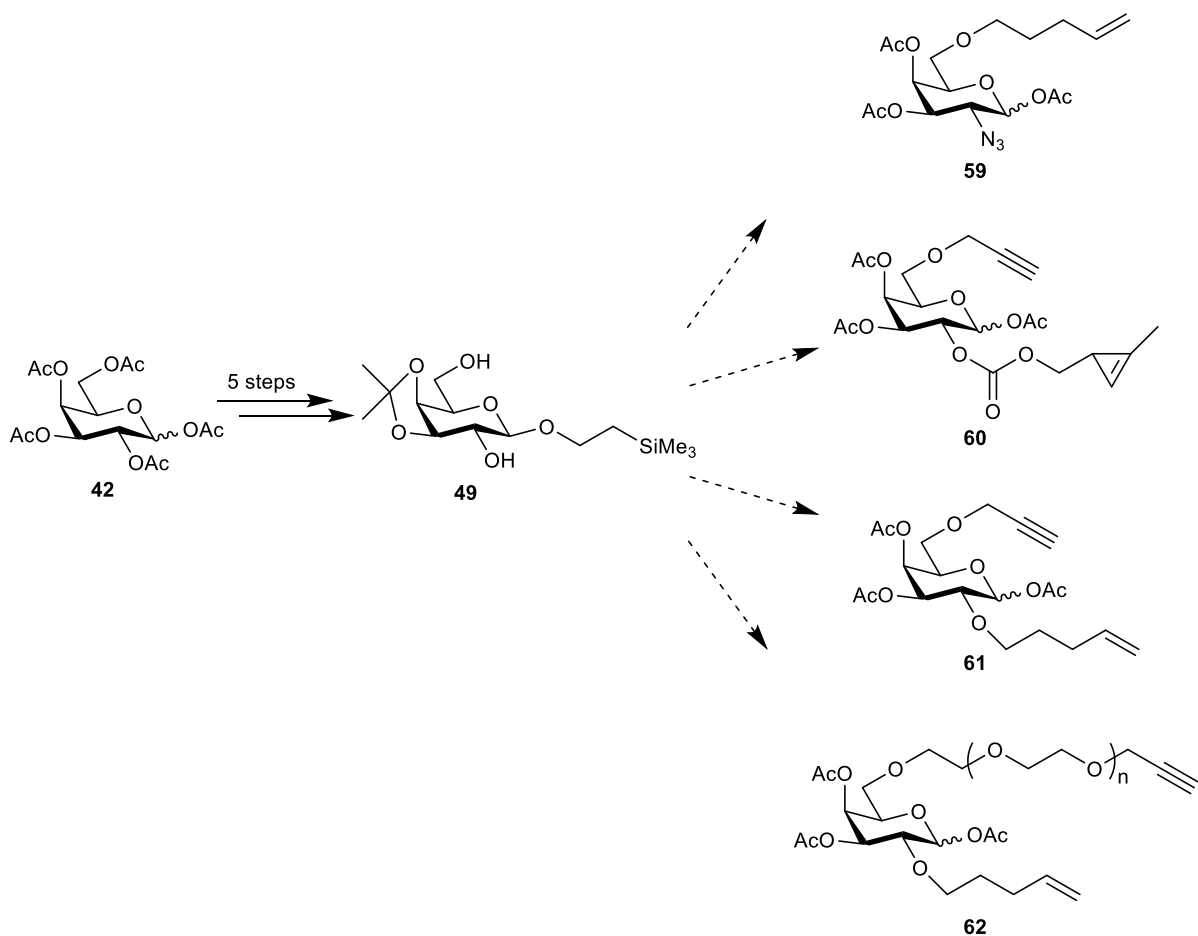
3.3. Future perspective

A new synthetic route for a bifunctional galactose derivative was successfully developed and the unnatural monosaccharide was obtained. Unfortunately, it was not possible to observe any selective labeling in HepG2 cells, despite several different approaches. Due to the present acetyl protecting groups, passive diffusion of the sugars into the cytoplasm can be assumed however the presented results do not show any further metabolic incorporation.

During the staining procedure, different sequences for the staining were tested without resulting in a labeling of the bifunctional galactose derivative **51** within cell membrane glycans. Following recent reports from Pratt and co-workers, in which they demonstrated the incorporation of 6-azido-6-deoxy-glucose into intracellular protein modifications, there might be the possibility also for the presented galactose derivative to be incorporated in such structures.¹⁵⁵ However, trials for intracellular staining did not show specific staining but high unspecific labeling in samples treated with the negative control sugar **42**.

For development of a project like this, it could be a solution to modify the present protecting groups and test the double labeling strategy in a test tube as well as on cells. The synthetic route for this bifunctional galactose derivative includes the intermediate **49**, which can be easily modified to obtain additional functionalized monosaccharides. The most obvious change could be an alteration of the position of the azide and alkene group, resulting in a bifunctional derivative **59** with an azide modification in C2 and a terminal alkene in C6 position (Scheme 12).

A different strategy might also be, to include new chemical reporter groups, like alkynes, cyclopropenes or norbornenes. Also more flexible groups including linker moieties like PEG could be tested for metabolic incorporation (Scheme 12). Alternatively, also different linkages of the already used terminal alkene groups could be explored, like it was shown from Wittmann and co-workers for mannosamine derivatives.⁴¹ All these changes could lead to a successful incorporation of the new galactose derivative.



Scheme 12: Example scheme for further derivatization of intermediate **49** to obtain additional bifunctional galactose derivatives **59-62** for metabolic incorporation.

Having two chemical reporter groups present in the same monosaccharide could also lead to steric hindrance when performing the staining procedures. It could be a possibility to develop an experiment to test the successful conjugation of two different fluorophore molecules to the monosaccharide in a test tube, before conducting *in vitro* experiments. An option might be the utilization of a HPLC based method to see an overlap of the absorption spectra when both fluorophores are bound to the sugar.

As already mentioned in the introduction to this chapter, it was shown with two sialic acid derivatives that cells can be able to incorporate monosaccharides with two functionalities. A successful transfer of this technology to other monosaccharides could open several opportunities. In case of an effective incorporation of a bifunctional galactose derivative, it

could be applied for example for the delivery and labeling of liver specific drugs in the context of an infection with *Plasmodium*. In the previous chapter, the slight increase in galactose uptake by *Plasmodium* infected cells was shown. By using a bifunctional galactose derivative, it could be a chance to deliver a liver stage specific drug towards infected cells and study the uptake or intra-cellular processing by labeling the galactose compound.

During the last years, the strategy of MOE was developed in a great way, opening many possibilities for the research on carbohydrate biology and their structures. It was shown by many groups how the flexibility of cellular systems can be used to manipulate natural structures and to use these strategies for biomedical research. However, the recent developments also show the limitations of the existing strategies, making more research necessary to develop more selective incorporation of monosaccharide building blocks in different cell types or organisms.

4. Chapter 4 – Development of a site selective glycoconjugate vaccine candidate with CRM₁₉₇

4.1. Introduction

The previous chapters describe in different ways the great importance of carbohydrate structures in disease state and as targets during biomedical research. However, as described in the introduction on carbohydrate vaccines, there are also limitations in the utilization of these structures. Pure carbohydrate vaccines were shown to be not effective in small children, which led to the development of glycoconjugate constructs as vaccine candidates.²⁹ By coupling the carbohydrate antigen to an immunogenic protein carrier, the conjugate is getting processed in a different way and peptide-carbohydrate moieties are presented through MHCII, which finally results in the activation of B-cells and memory B-cell production.⁸⁹ For the conjugation of carbohydrate antigens to protein carriers, amino acid side chains of the protein are addressed through chemical reactions. So far, reactions like reductive amination, active ester formation or carbodiimide-mediated condensation are used for the conjugation reaction. Successful examples for these glycoconjugate vaccines are PRP-TT against *Haemophilus influenzae* type b, MenC-CRM197 against *Neisseria meningitidis* serotype C or a 13-valent-CRM197 against *Streptococcus pneumoniae*.⁹³ In all these glycoconjugate vaccines, the carbohydrate antigen was conjugated in a random manner to the protein carrier. This means that it was not possible until this point, to selectively modify only specific amino acids of the protein carrier. Since it was already shown that the site in which the carbohydrate moiety is getting conjugated, can have an influence on the immunogenic properties of the final vaccine candidate, it is crucial for the future development to find ways for site-selective conjugation.⁹⁵

As it was explained in the introduction, selective modification of proteins can be achieved in different ways and a toolbox of reactions is available.

In this project, a new site-selective modification of the protein carrier CRM197 was developed and used for the generation of glycoconjugate vaccine candidates against *Streptococcus pneumoniae* and group B *Streptococcus*. These new types of conjugates can be compared with

the approved randomly conjugated vaccine and can help to understand the impact of a certain type of protein modification on antigen presentation and its immunogenic properties.

4.2. Results and Discussion

4.2.1. Site-selective modification of CRM197

The objective of the presented work was to develop a new strategy for the development of chemically defined glycoconjugate vaccine candidates. Starting with the carrier protein, a selective chemical modification was meant to be introduced, which should then allow site selective conjugation of glycan antigens.

The carrier protein CRM₁₉₇ comprises two disulfide bonds C186-C201 and C461-C471, from which the one between C186 and C201 can be targeted in a selective way (Figure 35).⁹⁵

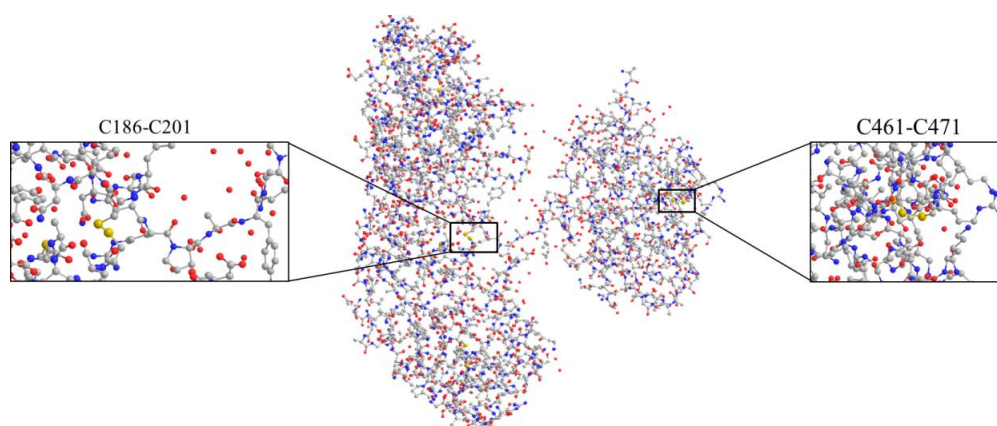
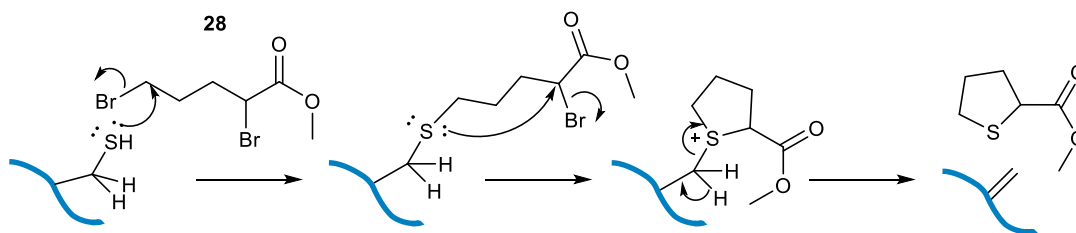


Figure 35: Model of CRM197 illustrating the location of the present disulfide bonds C186-C201 and C461-C471.

For the introduction of the modification dehydroalanine (DHA), this disulfide bond was reduced by using tris-(2-carboxyethyl)-phosphine (TCEP) at RT for 3h. Following the opening of this bond, methyl-2,5-dibromopentanoate (**28**) was used to initiate a bisalkylation reaction and subsequent elimination at pH = 11, resulting in the formation of two dehydroalanine (DHA) residues (Scheme 13). Experiments using lower pH values, did not result in any elimination

reaction or did only show the addition of the reagent. Also higher temperatures did not promote the necessary elimination reaction (Table 5).



Scheme 13: Reaction mechanism for the bisalkylation reaction of cysteine with methyl-2,5-dibromopentanoate (28) and subsequent elimination, resulting in the formation of dehydroalanine.

The best results for a complete conversion of the starting material were achieved after a reaction time of 5 h at pH = 11 (Table 5, entry 3). The modified protein CRM-DHA was purified in 100 mM NaPi pH = 6.3, either using a G25 column (130 mL) or Zeba spin desalting columns (7 kDa MWCO).

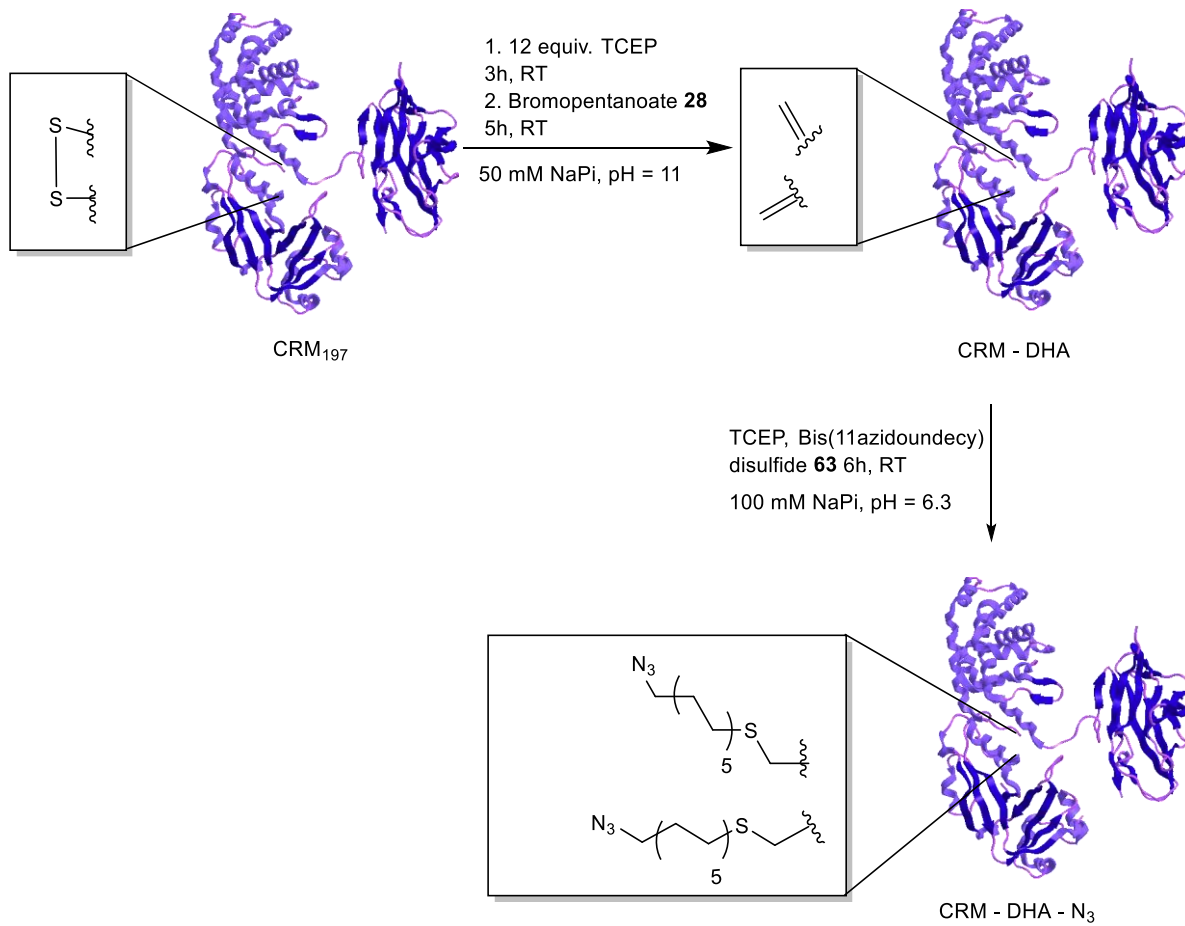
Table 5: Exemplary reaction conditions for the conversion of Cysteines C186-C201 into dehydroalanine. All reactions were performed in 50 mM NaPi pH = 11.

| Entry | c [mg/mL] | equiv. TCEP | h _{red} | T [°C] | equiv. Methyl-2,5- dibromopentanoate | h _{reac.} | T [°C] | Result |
|----------|--------------|----------------|------------------|-----------|---|--------------------|-----------|--|
| 1 | 20 | 12 | 3 | 21 | 500 | 3 | 21 | Precipitation, only traces of Dha |
| 2 | 2 | 12 | 3 | 21 | 500 | 3 | 21 | Main peak for Dha, smaller for side product |
| 3 | 5 | 12 | 3 | 21 | 500 | 5 | 21 | DHA |
| 4 | 10 | 12 | 3 | 21 | 500 | 5 | 21 | Precipitation |
| 5 | 2 | 12 | 3 | 21 | 500 | 5 | 21 | - |
| 6 | 2 | 12 | 3 | 21 | 500 | 18 | 21 | - |
| 7 | 2 | 12 | 3 | 21 | 500 | 3 | 37 | - |
| 8 | 2 | 12 | 3 | 21 | 500 | 5 | 37 | - |

It should be noticed in this section that CRM-DHA shows a high tendency for aggregation when prepared in too high concentrations (>2 mg/mL). However, since a high protein concentration was observed to be necessary to reach an efficient yield during later glycoconjugation reactions, CRM-DHA should be prepared fresh prior to its usage. The introduction of two DHA groups in the carrier protein was confirmed by high resolution mass spectrometry (Figure 36 A.1, Table 6).

For the further conjugation, an additional linker bis-(11-azidoundecyl) disulfide (**63**) was introduced. In this reaction, the reduced thiol moiety was planned to undergo a Thiol-Michael addition on the double bond of DHA, giving the desired selective modification. About 100 equiv. of the linker were reduced with TCEP for 2 h at room temperature, before the protein CRM-DHA in 100 mM NaPi pH = 6.3 was added. After additional 4 h reaction time, the excess

of linker and TCEP were removed using Zeba Spin desalting columns (7 kDa MWCO) and the buffer was exchanged to 12 mM NaPi pH = 7.2 (Scheme 14).



Scheme 14: Site-selective introduction of DHA in CRM₁₉₇, followed by the introduction of an azide containing linker.

Using high resolution mass spectrometry, it was shown that two linker molecules were successfully introduced in the main fraction of the protein, while only a minor part was shown to contain only one linker molecule (Figure 36 B.1, Table 6). Comparing one exemplary charge state distribution, the different species could be identified. The formation of CRM-DHA can be assumed as a complete conversion, since the initial peak of CRM₁₉₇ (Figure 36 C.2, 5) did disappear. For CRM-DHA-N₃ the main species (Figure 36 B.2, 2) represents the protein with two linker molecules attached, the mentioned side product is visible in a smaller peak (Figure

36 B.2, 3). An impurity could be detected in CRM-DHA (Figure 36 A.2, 4) as well as in CRM-DHA-N₃ (Figure 36 B.2, 4), however mass deconvolution did not show another dominant protein species.

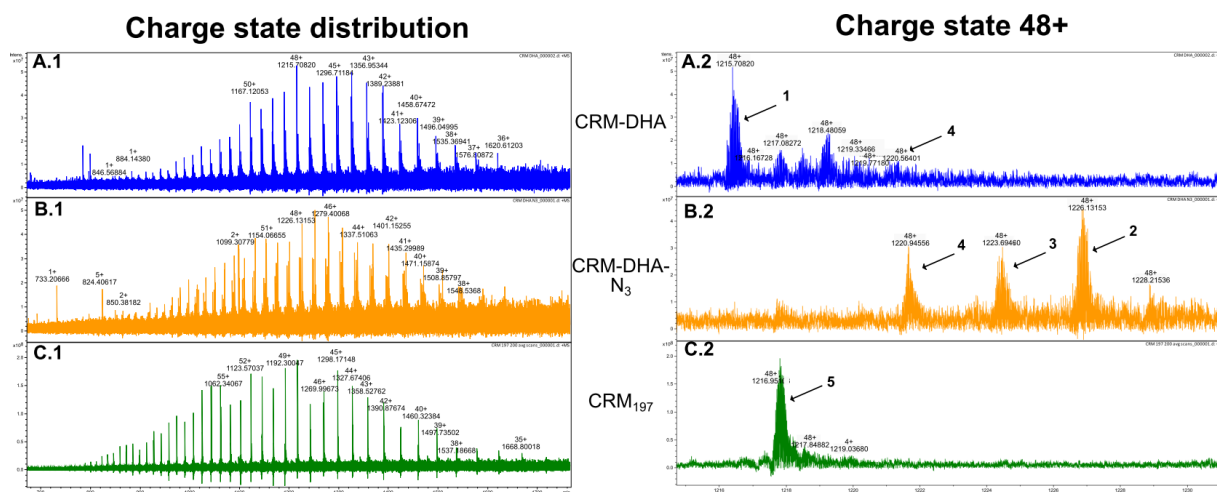


Figure 36: Charge state distribution: A.1 CRM-DHA, B.1, CRM-DHA-N₃, C.1 CRM₁₉₇. Comparison of the single charge state 48+ A.2 CRM-DHA, B.2 CRM-DHA-N₃, C.2. CRM₁₉₇.

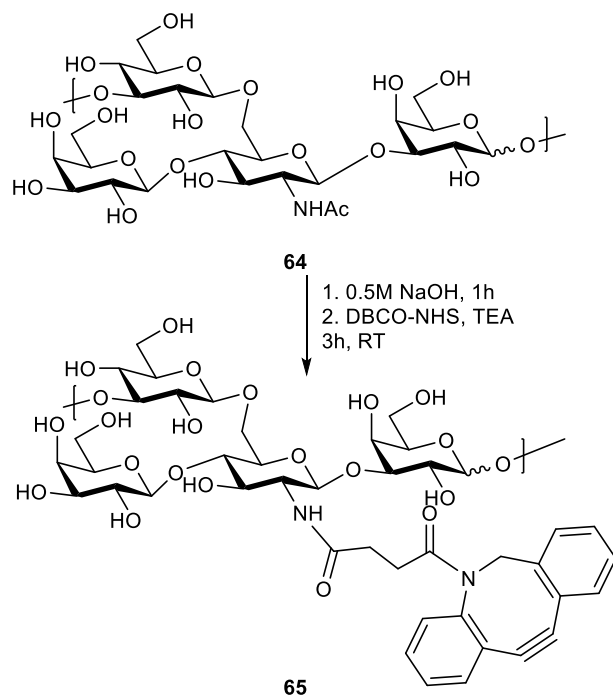
Table 6: Mass results after deconvolution of the charge state distribution after 200 scans.

| Sample | Mass found | Abundance [%] | Mass calculated | Calculated difference | Error [%] |
|------------------------|------------|---------------|-------------------------------|-----------------------|-----------|
| CRM ₁₉₇ | 58374.1311 | 100 | 58376.4102 | 2.2791 | 0.004 |
| CRM-DHA | 58306.7085 | 100 | 58308.1713 | 1.4628 | 0.003 |
| CRM-DHA-N ₃ | 58807.0504 | 100 | 58764.4781 | 1.5458 | 0.003 |
| | | | For [M+ CH ₃ CN] = | | |
| | | | 58805.5046 | | |
| CRM-DHA-N ₃ | 58557.9713 | 41.25 | 58536.3247 | 1.3426 | 0.002 |
| | | | For [M + Na ⁺] = | | |
| | | | 58559.3139 | | |

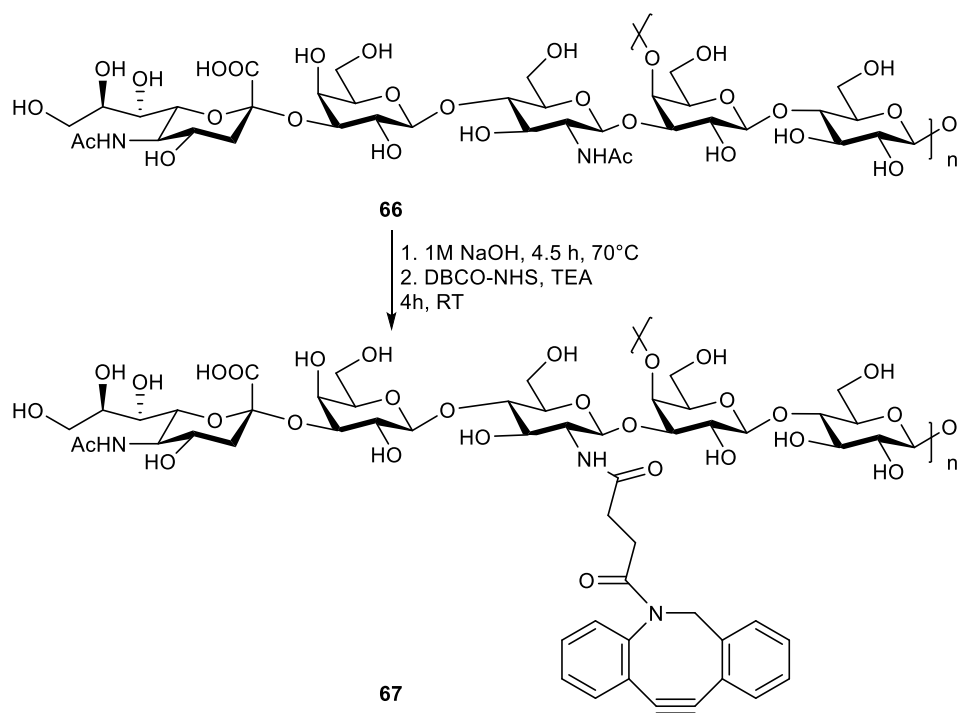
4.2.2. Modification of the polysaccharide antigen

Having the carrier protein CRM-DHA-N₃ readily synthesized, the carbohydrate antigen had to be prepared. In this context, polysaccharide antigens from group B streptococcus serotype Ia, **66** (GBS-Ia) and pneumococcal type 14 capsular polysaccharide **64** (PN14) were derivatized with a Dibenzocyclooctyne-N-hydroxysuccinimidyl ester (DBCO-NHS) in the position of their *N*-acetyl-glucosamine (GlcNAc) units. In the case of PN14, the best results for this derivatization were achieved by de-*N*-acetylation of the polysaccharide for 1.5 h at 70 °C in 0.5 M NaOH, followed by a substitution reaction of the free amine on the DBCO-NHS compound (Scheme 15 A). For GBS-Ia, slightly stronger conditions with 1 M NaOH at 70 °C and for 4.5 h were necessary (Scheme 15 B). The attachment of the DBCO-linker was performed with the same method than for PN14 polysaccharide.

A.



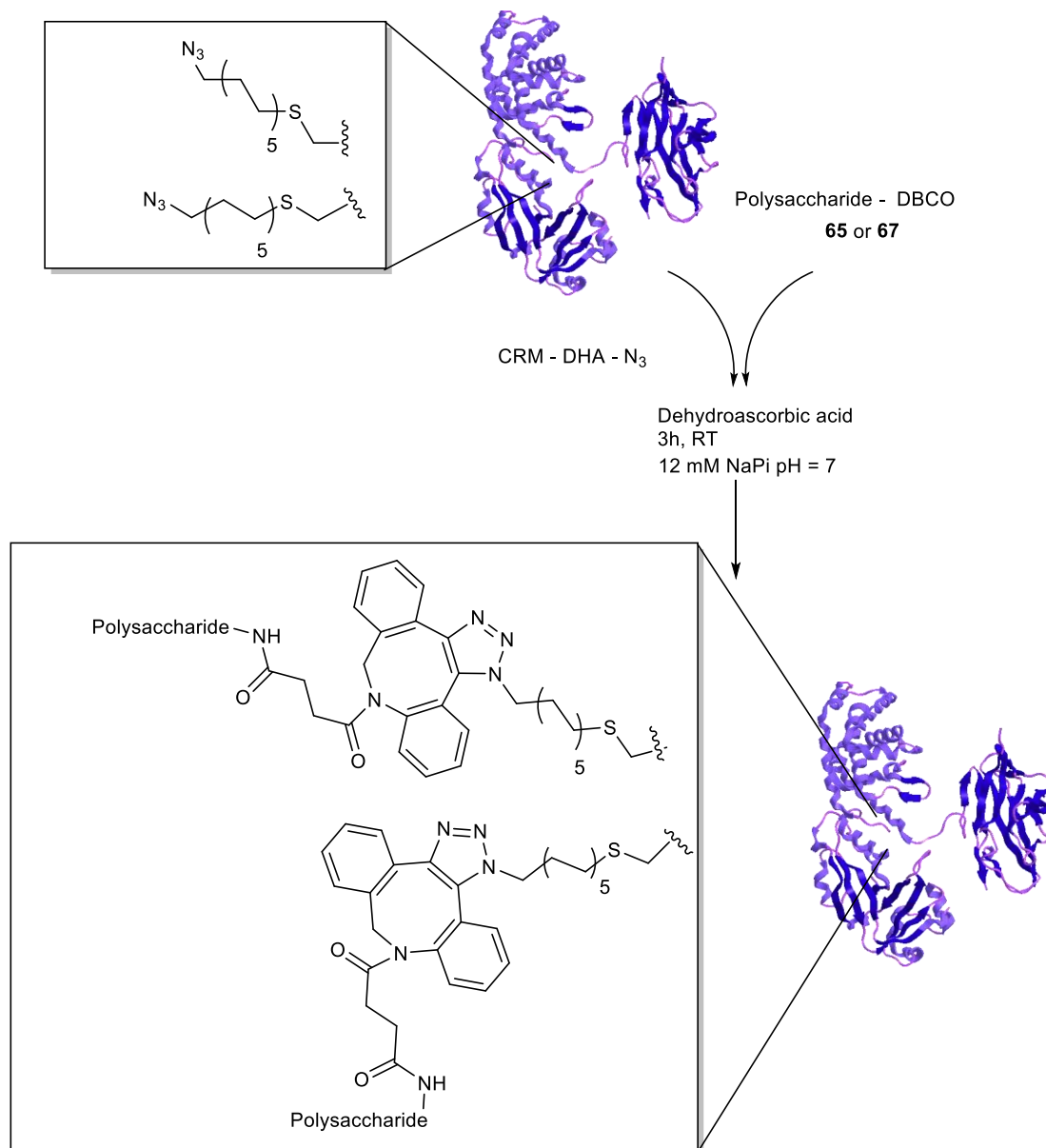
B.



Scheme 15: Reaction scheme for the introduction of the linker DBCO-NHS into the polysaccharide structures. **A.** PN 14 **64**, **B.** GBS-Ia **66**.

4.2.3. Synthesis and Purification of the glycoconjugate vaccine candidate

During the final conjugation reaction between the carrier protein CRM-DHA-N₃ and the corresponding polysaccharide **65** or **67** (Scheme 16), different ratios protein/polysaccharide were tested in order to maximize the conjugation yield. The best results were obtained with a ratio of 1:4 protein /polysaccharide for conjugations using PN14-DBCO **65** (Figure 37 A), however for conjugations with GSB-Ia-DBCO **67** a ratio of 1:2 protein/polysaccharide was sufficient since no further improvement of the conjugation yield was observed with higher amounts of polysaccharide (Figure 37 B).



Scheme 16: Conjugation reaction of derivatized polysaccharides **65** and **67** to CRM-DHA-N₃.

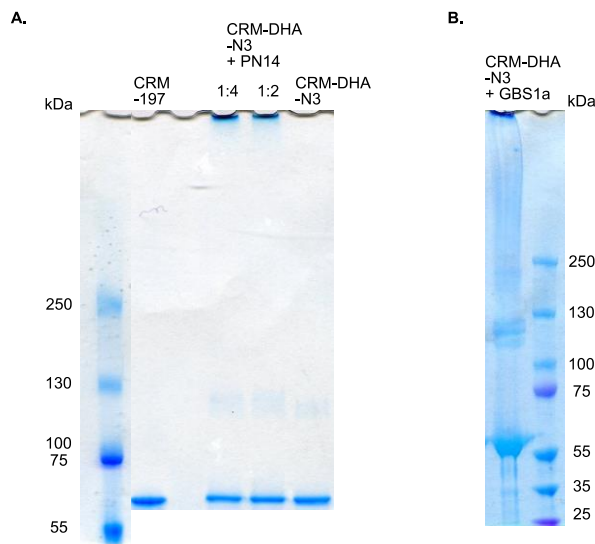
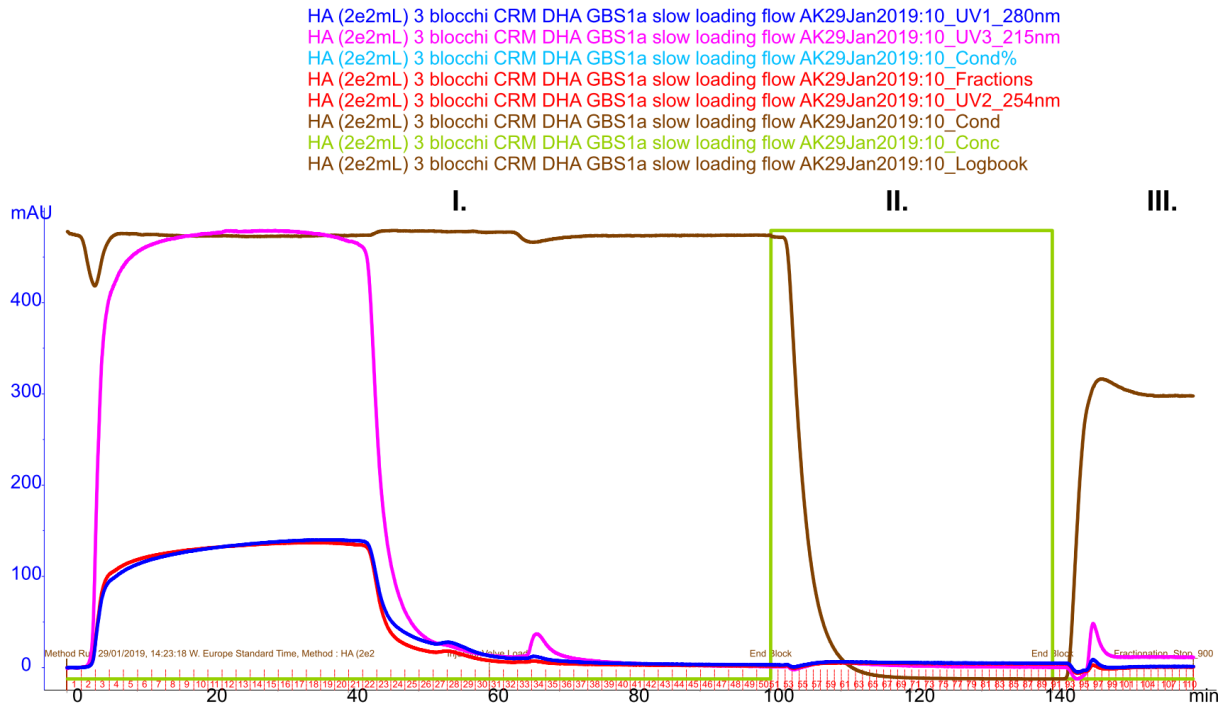


Figure 37: **A.** 3-8% Tris-acetate gel of CRM₁₉₇ and conjugation reactions of PN14-DBCO 65 with CRM-DHA-N3. **B.** 3-8% Tris-acetate gel of the conjugation reaction of GBS-1a-DBCO 67 with CRM-DHA-N3.

To purify the obtained glycoconjugates from unconjugated polysaccharides and remaining free carrier protein, the first strategy of choice was to use a ceramic hydroxyapatite type I resin (CHT) which should enable, based on the applied buffer systems, to separate all three components due to their different interactions with resin. However, despite several attempts with different conditions, it was not possible to observe a separation of the three components. It was expected that a equilibration and loading of the columns with a buffer containing 2 mM NaPi and 500 mM NaCl at pH = 7.2, would result in binding of the glycoconjugate and the free protein, but not in the polysaccharide (Figure 38, blocks I). In the next step, the buffer was changed to 35 mM NaPi, pH = 7.2, which was anticipated to elute the glycoconjugate (Figure 38, blocks II) before the free protein would have been obtained with the third buffer of 400 mM NaPi, pH = 7.2 (Figure 38, blocks III).

A.



B.

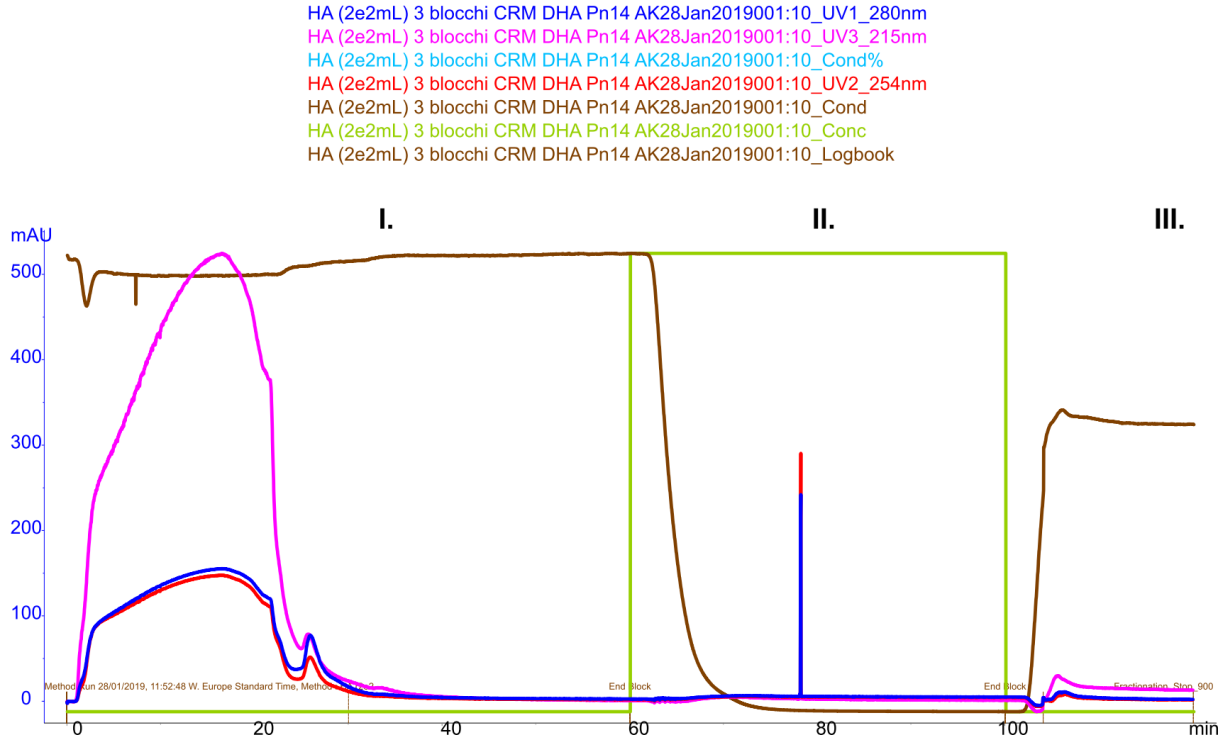


Figure 38: A. Aktas traces for the injection of the conjugation reaction CRM-DHA-N3 with GBS1a-DBCO 67 on a CHT type 1 resin. B. Aktas traces for the injection of the conjugation reaction CRM-DHA-N3 with Pn14-DBCO 65 on a CHT type 1 resin.

Unfortunately, for both types of conjugates, with polysaccharide from PN14 **64** or GBS-Ia **66**, no separation could be observed. A trial precipitation with ammonium sulfate showed both, glycoconjugate and free carrier protein in the very first fraction of the elution which suggested that none of the reaction components bound to the CHT resin. Since size-exclusion chromatography cannot be applied directly to the crude reaction mixture, due to the similar sizes of unbound polysaccharide and glycoconjugate, it was decided to change the purification procedure to an initial ammonium sulfate precipitation.

Focusing on a glycoconjugate with GBS-Ia-DBCO **67**, the ammonium sulfate precipitation was directly applied to the crude reaction mixture and it was possible to recover a mixture of glycoconjugate and free protein carrier with a yield of 40% after six rounds of precipitation. In general 500 mg/mL ammonium sulfate were used and the reaction solution was incubated on ice for 15 min before the precipitate was obtained after centrifugation (4500 g, 10 min). The obtained precipitate was dissolved in 10 mM NaPi, pH = 7 and a gel-analysis showed a similar ratio of glycoconjugate and free protein then in the initial crude reaction mixture (Figure 39).

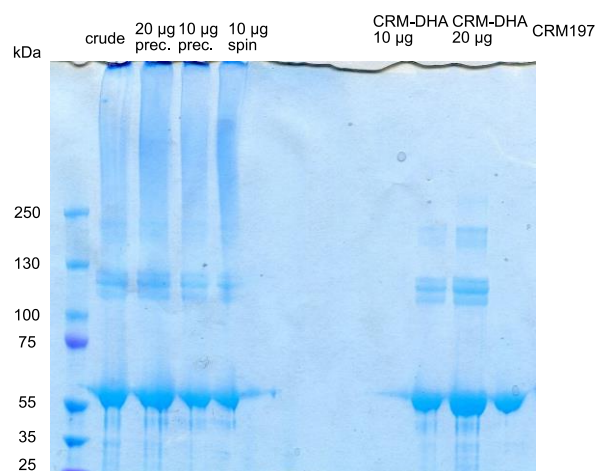


Figure 39: 3-8% Tris-acetate gel after conjugation reaction of GBS-Ia-DBCO **67** with CRM-DHA-N3 and after ammonium sulfate precipitation of the crude reaction mixture.

4.3. Future perspective

Until this point, it was possible to show the development of a new site-selective chemical modification on the carrier protein CRM₁₉₇, which could be used for the synthesis of defined glycoconjugate vaccine candidates. In an exemplary approach, polysaccharides from PN14 **64** and GBS-Ia **66** were modified with a linker moiety containing a DBCO group for further click reaction to the azide modified protein CRM-DHA-N₃. It was possible to show the formation of both types of glycoconjugates in reproducible manner. However, so far it was not possible to purify these conjugates due to their unexpected interaction behavior with the CHT type I resin. It can be speculated if this behavior is a result of the present polysaccharide, which could inhibit an interaction of the protein with the column. In case of the glycoconjugate, there are also several options in the stoichiometry of attached polysaccharide to one protein carrier, which could be an additional factor for the problematic interaction with the resin. Despite having a defined number of azide containing linkers attached to the introduced DHA residues on the carrier protein CRM, it remains unknown if only one polysaccharide molecule is attached through two repeating units (Figure 40, A), or if two different polysaccharide molecules are attached though each one repeating unit (Figure 40, B).

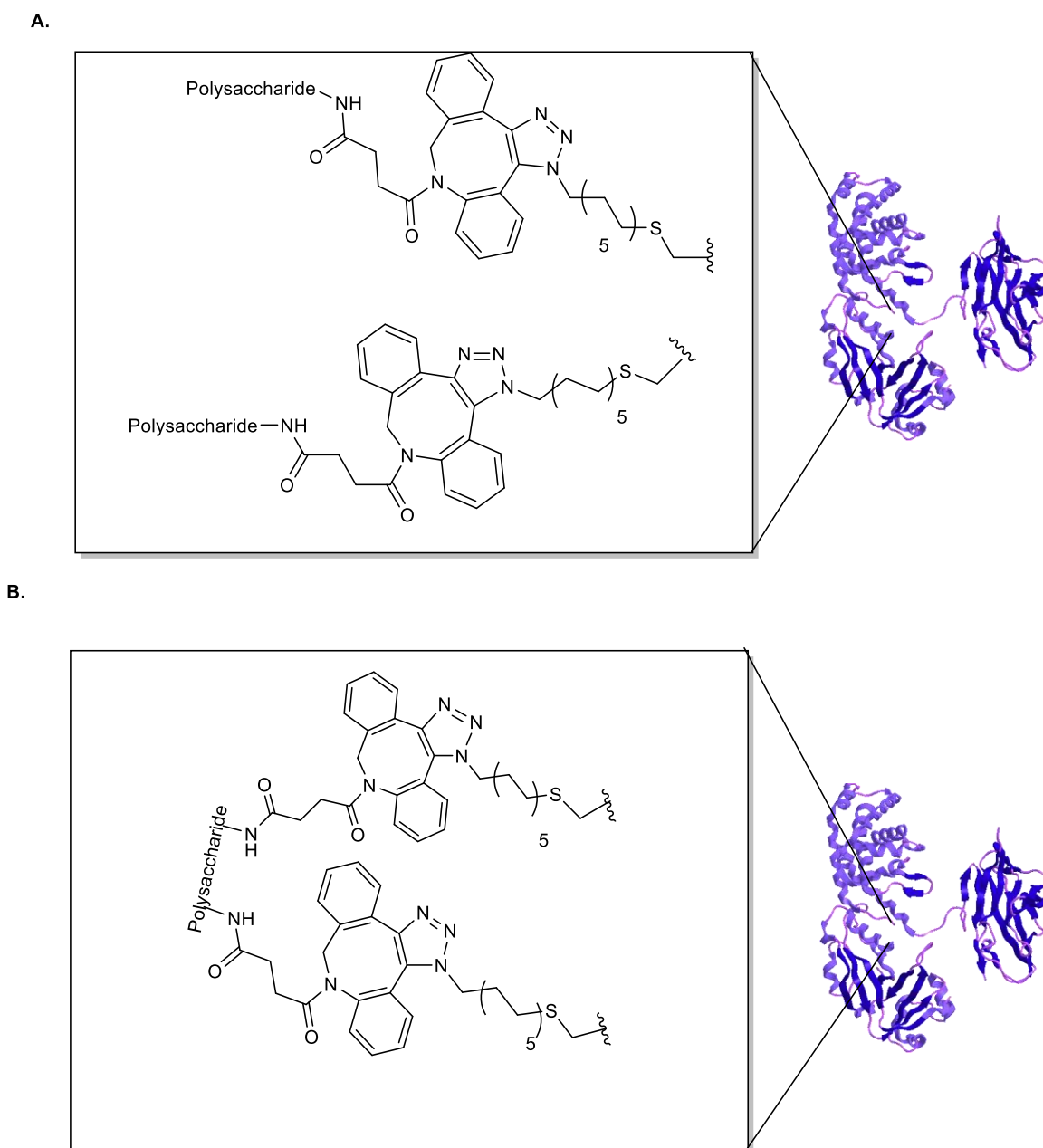


Figure 40: Possible connectivities of polysaccharide molecules to CRM-DHA-N3, **A.** conjugation of two polysaccharide molecules to the carrier protein. **B.** Conjugation of one polysaccharide molecule to the carrier protein.

In these cases, the final structure of the glycoconjugate might be different, resulting in different ways of interaction with the applied resin. For this reason, a purification protocol starting with an ammonium sulfate precipitation, seems to be a more promising choice. With the ammonium

sulfate precipitation, the free polysaccharide can be separated from the glycoconjugates and the free protein, which can then be purified by size-exclusion chromatography.

To validate the final glycoconjugate, made based on the new modification strategy of the carrier protein, another type of conjugate was produced previously, in which the carrier protein CRM₁₉₇ has been stapled with di-chloroacetone in the disulfide bond C186-C201.⁹⁵ Also with this method, a defined chemical attachment of the carbohydrate antigen is achieved, however, in contrast with the presented DHA modification, the disulfide bond C186-C201 was not opened permanently, but had been reconnected by the stapling reagent.

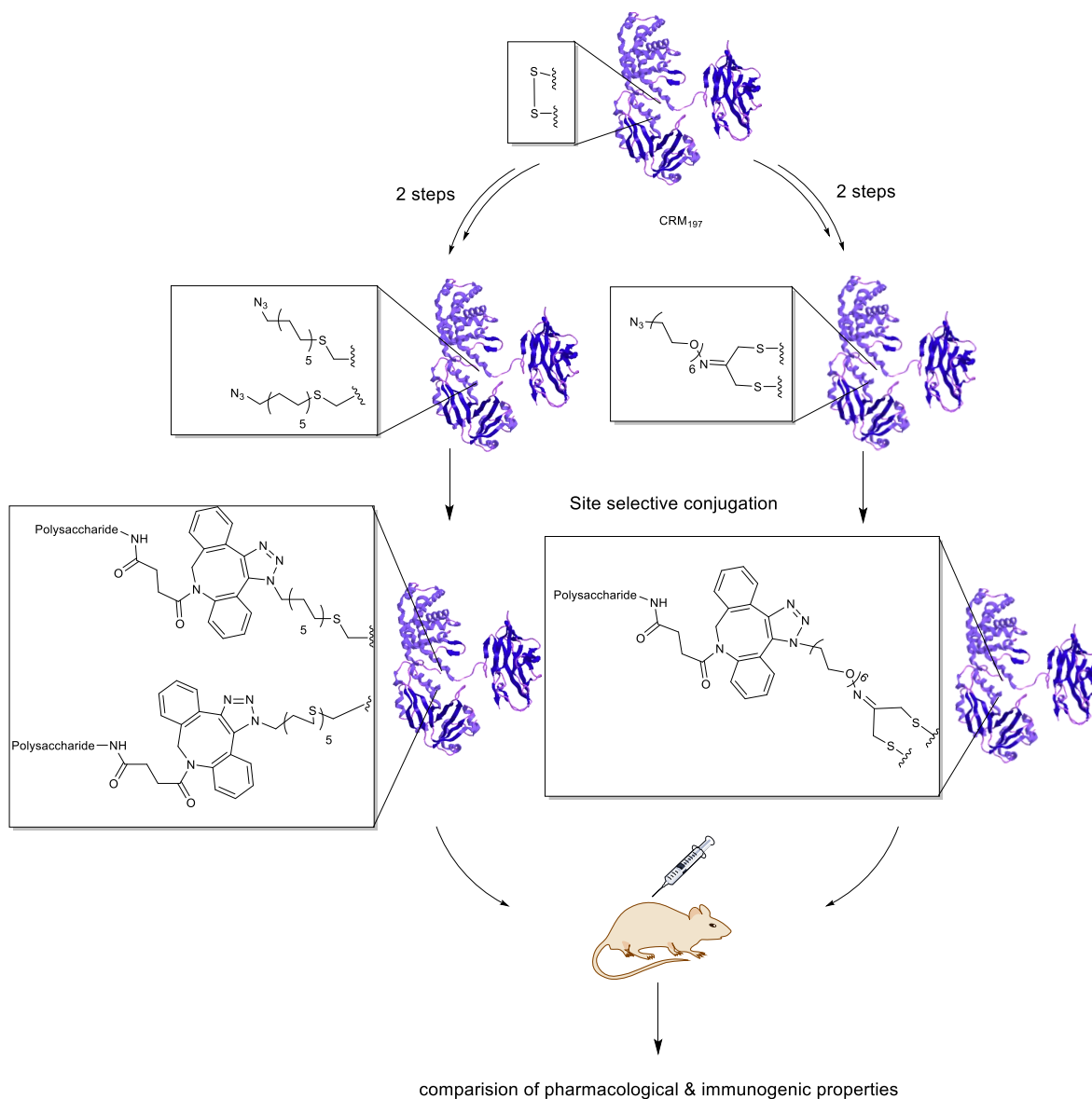


Figure 41: Schematic illustration of the comparison of two different types of glycoconjugates with CRM₁₉₇.

The final goal of this work will be to evaluate the properties of both types of glycoconjugates in *in vivo* settings, to determine and compare the elicited immune response of these vaccine candidates (Figure 41). Both presented site-selective constructs should be compared with a glycoconjugate vaccine candidate in which the carbohydrate moiety is conjugated in a random manner to the carrier protein.

5. Chapter 5 – Sequential activation of thioglycoside donors using an electropositive nitrogen promoter

5.1. Introduction

In the previous chapters of this work, two main aspects of glycobiological research were addressed. On one hand, the strategy of MOE was used for research on the identification of new carbohydrate antigens during Malaria disease and on the other hand, the development of a glycoconjugate vaccine candidate was pursued, which represents an example for the further utilization of carbohydrate epitopes in the development of effective treatments.

However, even with the knowledge about structure and function of a carbohydrate epitope, it has to be available in large quantities and in a pure state for further application. In many cases, it is difficult and less efficient to purify the carbohydrate structure of interest from its natural source. For this reason, chemical synthesis of oligosaccharide structures also developed strongly during the last decades.

Although very large numbers of different reactions have been developed, the enormous variety of natural carbohydrate structures, still shows the need for different selective reactions.¹¹⁸

As discussed in the introduction, the glycosylation reaction between a glycosyl donor and a glycosyl acceptor molecule can be influenced by many different factors and has to be optimized for different reaction situations.

Thioglycoside donors are commonly used during oligosaccharide synthesis, due to their stability in many different reaction conditions. Over the years, many strategies have been developed for the activation of these glycosyl donors, however the possibility to sequentially activate different thioglycoside donors within one reaction was still missing.¹²³ A sequential activation can be a useful tool for one-pot synthesis reactions or during the utilization of automated systems.

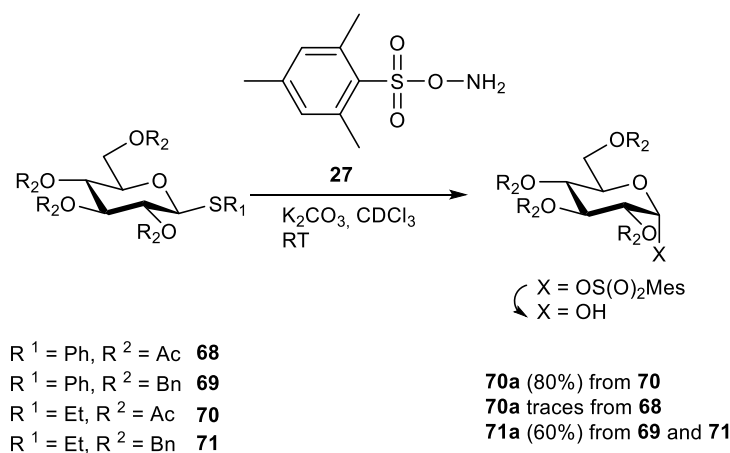
The following chapter will explain and present the development of a new activation strategy for thioglycosides, using the reagent *O*-mesitylsulfonyl hydroxylamine (MSH).

5.2. Results and discussion

5.2.1. Activation of thioglycosides using *O*-mesitylenesulfonyl hydroxylamine – Kinetic evaluations

Reports in the literature show the reaction of thiols with MSH **27** via a nucleophilic attack of the thiol on the electron positive nitrogen of MSH, forming sulfilimine or sulfoximines species. On proteins, MSH was shown to promote the conversion of cysteine into dehydroalanine via an oxidative elimination mechanism and *S*-alkyl thioglycosides were shown to be activated by this thiophilic reagent.^{107,156}

During the first part of this study, a set of four different thioglycoside donors was studied with regard to their reactive behavior towards MSH (Scheme 17). With regard to the influence of different protecting groups on the reactivity of glycosyl donors, the benzylated and acetylated versions of each *S*-ethyl and *S*-phenyl thioglucose were investigated.



Scheme 17: Reaction scheme for the activation of thioglycosides **68-71** with MSH **60**, resulting in the final formation of hemiacetals **70a** and **71a**.

To monitor the reactivity of each of the selected monosaccharides during a reaction with MSH, the reactions were performed in deuterated chloroform (CDCl_3) and the behavior of the anomeric proton signal *H1* was studied. The signal of the anomeric proton *H1* for thioglycosides **68-71** can be found around 4.5 ppm with a coupling constant of typically $J_{1,2} \sim 10$ Hz, when

starting from β -thioglycosides. During the reaction with MSH, it was possible to observe a disappearance of this anomeric peak and the formation of a downfield shifted signal around ~ 5.9 ppm ($J_{1,2} \sim 4$ Hz). This shift resembles the formation of a α -1-*O*-sulfonylmesitylene intermediate which was observed to be hydrolyzed from residual water, giving the corresponding hemiacetals **69a** and **70a** of the starting material. The formation of similar intermediates during glycosylation reactions was described by Bennett et al and Taylor.^{157,158} Interestingly, the expected *syn*-elimination of the thioglycosides to their glycal structures was not observed during the reaction with MSH. The reaction kinetics were visualized by following the ratio of the anomeric protons ^1H (intermediate)/(^1H **68** – **71**) (Figure 42)

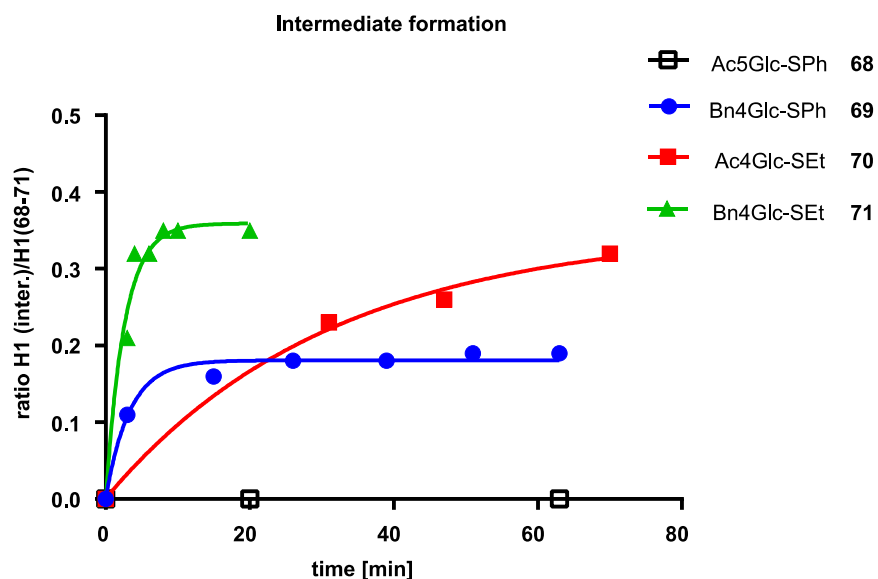
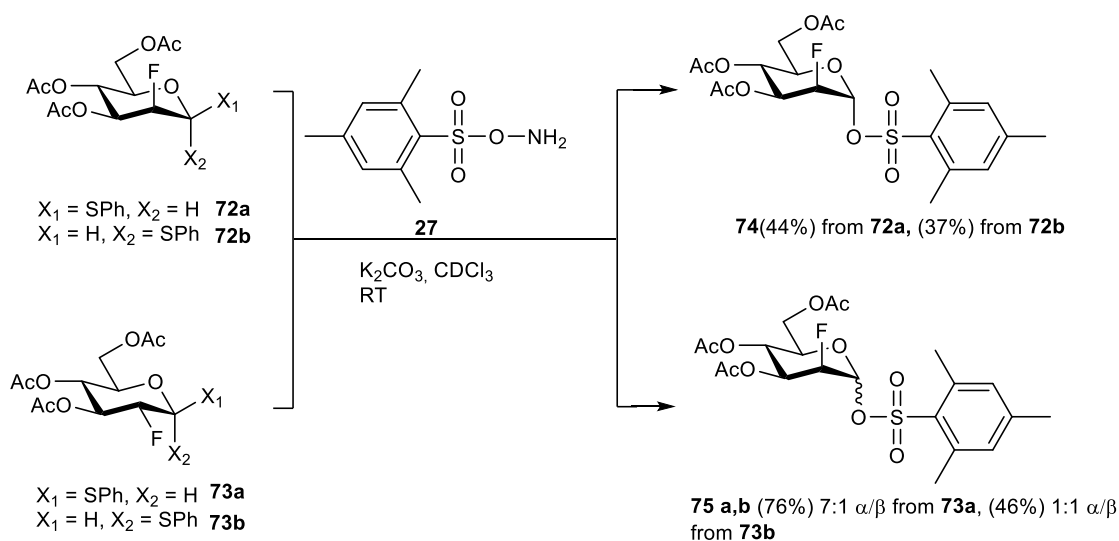


Figure 42: ^1H NMR Analysis of the activation of thioglycoside donors **68-71** with MSH **28**, following the ratio of H1 (intermediate)/H1 (**68-71**)

The four applied monosaccharides Bn₄GlcSEt **71**, Ac₄GlcSEt **70**, Bn₄GlcSPh **69** and Ac₄GlcSPh **68** could be arranged according to their reactivity by following the armed-disarmed effect of the protecting groups and the properties of their anomeric groups to react as a leaving group.¹⁵⁹

5.2.2. Activation of 2-deoxy-2-fluoro-thioglycosides with MSH

For a better understanding of the formed intermediate species during the reaction of the thioglycoside donors with MSH, an additional series of 2-deoxy-2-fluoro thioglycosides **72a**, **72b**, **73a** and **73b** was used to perform the same reaction.¹⁶⁰ The strong impact of different chemical entities in C2 position of a monosaccharide on the outcome of a glycosylation reaction is known in the literature, which is why the following fluoro-substituted monosaccharides were chosen.¹¹⁹ It was very interesting to observe that an activation of these glycosyl donors with MSH, under the same conditions then used before, resulted in the formation of stable 1-*O*-sufonylmesitylen intermediates **74**, **75a** or **75b**, which were purified and fully characterized (Scheme 18). While pure α -substituted products were obtained from mannose configured starting material, a mixture of α - and β -products was obtained starting from glucose configured sugars.



Scheme 18: Reaction scheme for the activation of 2-deoxy-2-fluoro-thioglycoside donors **72a**, **72b**, **73a** and **73b** with MSH **27**.

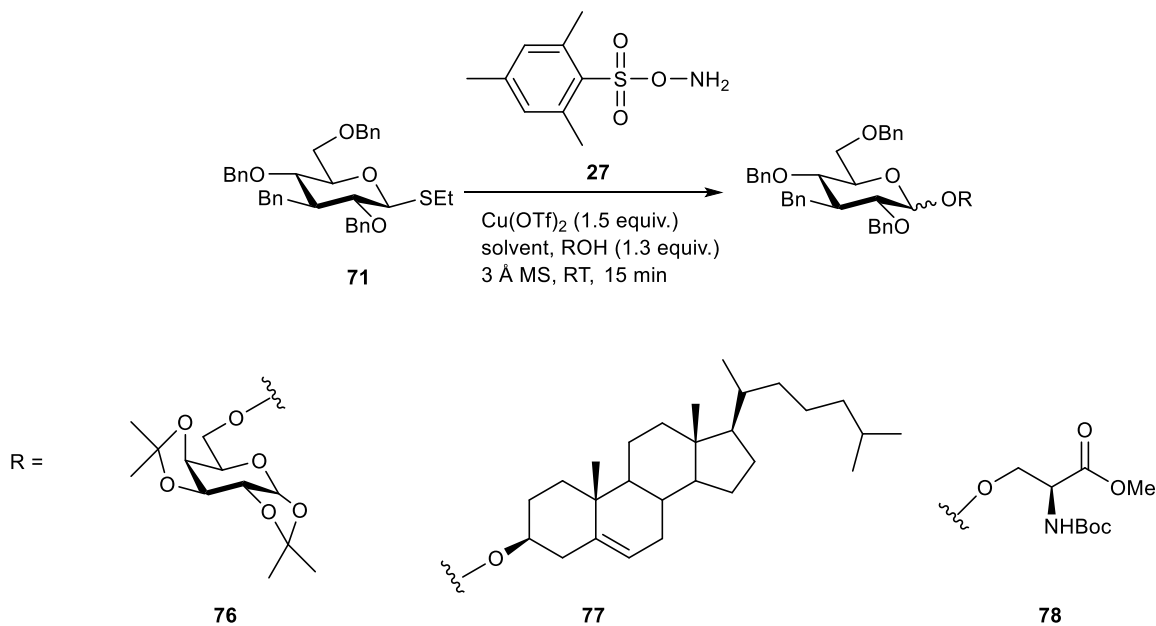
To show that these purified intermediates can be used during glycosylation reactions, the purified 1-*O*-sulfomesitylen intermediates **74a** and **74b** from the glucose series, were activated using $\text{Cu}(\text{OTf})_2$ in the presence of MeOH as glycosyl acceptor. As expected, a complete

conversion of the starting material into a mixture (1:1) of the β -methyl glycoside and a 6-OH byproduct was observed. Since it was possible to purify and characterize the 1-*O*-sulfomesitylen molecules in the 2-deoxy-2-fluoro series from glucose and mannose, it strongly suggested the formation of similar structures when using the non-fluoro substituted thioglycosides **68** - **71**. From the described $^1\text{H-NMR}$ studies with these compounds, it was assumed that a decreased stability of these intermediates leads to immediate hydrolysis. To confirm this theory, transition state calculations were performed. These calculations should reveal the reactivity of the described intermediates from fluoro-substituted and non-fluoro-substituted thioglycosides towards hydrolysis. It was pleasant to see that these calculations revealed a difference of $\sim 4 \text{ kcal mol}^{-1}$ between the transition states of the non-fluorinated compounds and their fluorinated counterparts. This energy difference corresponds to a ~ 850 times faster hydrolysis reaction for the 1-*O*-sulfomesitylen intermediates which do not display a fluorine atom in C2 position.

5.2.3. Glycosylation reactions promoted by MSH

After these investigation on the activation mechanism when reacting thioglycoside donors with MSH, this method was extended for glycosylation reactions. Under the described conditions, no glycosylation could be observed which is probably due to a lack in reactivity of the described intermediates when attacked by less nucleophilic acceptors. To achieve a successful glycosylation reaction, several strategies were tested. A strong activation of the acceptor molecules using NaH only resulted in a very low yield of the glycosylation product. With regard to the presence of the 1-*O*-sulfomesitylen intermediates, typical additives such as AgOTf or $\text{Cu}(\text{OTf})_2$ and stereo directing solvents like CH_2Cl_2 , Et_2O or CH_3CN were explored.¹⁶¹ The best results were obtained when using stoichiometric amounts of $\text{Cu}(\text{OTf})_2$ at room temperature and gave the glycosylation product with a good yield and α/β -selectivity (Table 7). The developed glycosylation reaction was observed to be complete after a short period of 15 min and a control experiment showed the absolute necessity of MSH for the activation of the thioglycoside donor in presence of $\text{Cu}(\text{OTf})_2$. Looking at the stereoselectivity of the product, it was interesting to see that the addition of LiClO_4 in stoichiometric amounts resulted in the exact conversion of the

anomeric selectivity, promoting the formation of the α -product (Table 7, entry 2). A strong coordination of the ClO_4^- anion in β -position during an exchange of the 1-*O*-sulfomesitylen group, would promote the formation of a α -connected glycosylation product. As examples for this new glycosylation method, different acceptor molecules were screened, including amino acids, natural products and monosaccharides (Scheme 19).



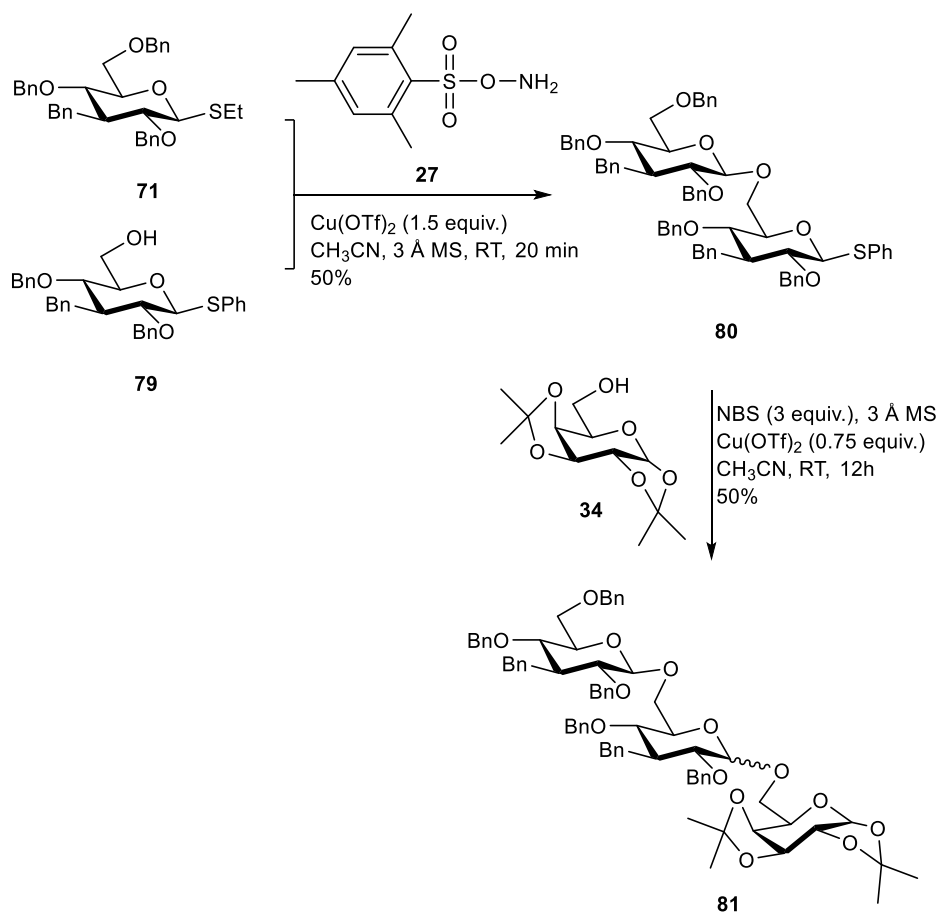
Scheme 19: Examples for the glycosylation reaction using thioglycoside donor **71** and an activation with MSH **27**.

Table 7: Reaction scope for glycosylation reactions using MSH **28** as thiophilic promotor. ^a Ratio was determined by integration of the anomeric proton signals ¹H in the proton NMR of the products. ^b LiClO₄ (1 equiv.) was used as additive.

| Entry | Donor | Product | Solvent | yield | α/β ratio ^a |
|----------------|-----------|-----------|---------------------------------|-------|-----------------------------------|
| 1 | 71 | 76 | CH ₂ Cl ₂ | 26 | 1.3:1 |
| 2 ^b | 71 | 76 | Et ₂ O | 54 | 5:1 |
| 3 | 71 | 76 | CH ₃ CN | 71 | 1:5 |
| 4 | 71 | 77 | CH ₃ CN | 35 | 1:3.7 |
| 5 | 71 | 78 | CH ₃ CN | 50 | 1:2.2 |

5.2.4. Selective activation of a *S*-alkyl thioglycoside donor

Having the different reactivities of the studied thioglycosyl donors in mind, an experiment was designed to show the possibility of a sequential activation of *S*-alkyl over *S*-aryl donors. The more reactive *S*-ethyl thioglycosyl donor **71** was activated in the presence of the *S*-phenyl acceptor molecule **79** and the disaccharide **80** with intact anomeric *S*-phenyl group could be purified. In the following step, the thiogroup of disaccharide **80** was activated with classical conditions using NBS/Cu(OTf)₂ for the synthesis of a Glc(1→6)Glc(1→6)Gal model trisaccharide **81** (Scheme 20).



Scheme 20: Reaction scheme for the selective activation of **71** over **79** forming the disaccharide **80**. Classical activation of **80** with NBS, resulting trisaccharide **81**.

With this experiment, it was possible to successfully address the different reactivities of the single thioglycoside donors and to use these specific properties during oligosaccharide synthesis.

5.3. Future perspective

In summary, it was possible to show the utilization of a N^+ -thiophilic reagent like MSH as a promotor for the activation of thioglycosides. This study is a great example for how important intermediate structures can be and how they can influence the outcome of the planned reactions. As mentioned in the introduction for this chapter, the access to defined oligosaccharides is essential for further developments in biomedicine or vaccine development. To achieve this goal, exact knowledge about the mechanisms during a glycosylation reaction is crucial, in order to maximize the potential of each reaction. The comparative study of fluoro-substituted thioglycosides **72a**, **72b**, **73a**, **73b** and their non-fluorinated counterparts **68** - **71**, also shows once more the high impact of neighboring chemical moieties on the properties of the anomeric center. Stabilizing or destabilizing effects can be used to direct glycosylation reactions towards specific results, by for example favoring one stereoisomer over the other or making the formation of unwanted side-products impossible.¹⁶²

For a further work on the activation of thioglycosides with N^+ -thiophilic reagents, it might be an option to investigate different derivatives of the here presented MSH reagent. The activation of the anomeric thio-group should still occur through a nucleophilic attack of the sulfur on the amino group but the formation of intermediate structures could probably be controlled in a better way. By using derivatives of MSH, it could be investigated if the formation of intermediate structures can be avoided or stabilized.¹⁶³

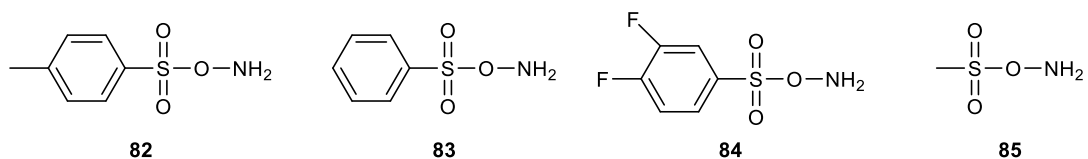


Figure 43: Examples for possible derivatives of MSH for the application in glycosylation reactions.¹⁶³

By avoiding the manifestation of an intermediate, the introduction of a glycosyl acceptor could be facilitated and the reaction conditions could be optimized with just focusing on one direct reaction pathway. On the other hand, the formation of a fully stable intermediate might also give rise to new methods. Like in the described reactions with 2-deoxy-2-fluoro thioglycosides, an intermediate which can be purified and characterized, can be also used for clean glycosylation reactions because it represents a new kind of glycosyl donor.

There are multiple possibilities for an optimization of this strategy, however the fact that MSH can be used to distinguish between different types of thioglycoside donors, opens new possibilities for this field of glycosylation chemistry.

These new strategies can be used for the synthesis of defined oligosaccharide structures which can be then further investigated and used, for example for the development of glycoconjugate vaccine candidates or carbohydrate-based drugs.

6. Chapter 6 – Conclusions: from synthetic chemistry to biological applications

In the presented work, several different topics were addressed and discussed. In the first chapter, synthetic modifications of natural occurring molecules, in this scenario galactose monosaccharides, were used to study the metabolic incorporation of such molecules into cellular glycan structures. In addition, the synthesized unnatural galactose molecules were used to study a possible transfer of these sugar structures from the mosquito host to the *Plasmodium berghei* parasite. The ability of biological systems to tolerate modified substrates was extended further, by testing the possibility of an incorporation of a bifunctional galactose derivative in the following chapter. Although it was not possible to successfully incorporate this specific bifunctional galactose molecule in cell glycan structures, this project can be pursued further. An incorporation of two orthogonal chemical reporter groups within the same monosaccharide could provide new possibilities for the identification and targeting of important glycan structures. By moving from carbohydrate to protein structures, a chemical method was developed to achieve a site-selective modification of the immunogenic carrier protein CRM₁₉₇. By using defined chemical reactions, the site-selective introduction of an immunogenic carbohydrate moiety on a carrier protein can be achieved. As mentioned earlier, the possibility of synthesizing defined glycoconjugate constructs is crucial for the development of future glycoconjugate vaccine candidates. Finally, the last chapter presents a new approach for sequential activation of different thioglycoside donors. This new method can be applied during the chemical assembly of necessary oligosaccharide structures and could provide an additional tool for a facile and efficient one-pot synthesis.

Due to new emerging technologies, the access to large platforms and the easy interaction between different fields of research, a rapid development in biomedical research can be expected. It is crucial for future developments to strongly crosslink the different areas of research to take advantage of the different expertise and to optimize possible results.

This work gave a brief overview of the interconnections between different areas of carbohydrate research, including synthetic chemistry, cell studies and vaccine development. The developed

strategies, which were presented in this work, can be used for further projects and could enable new insights in the important role of carbohydrates in infection disease and as part of glycoconjugate vaccines.

7. Chapter 7 – Experimental section

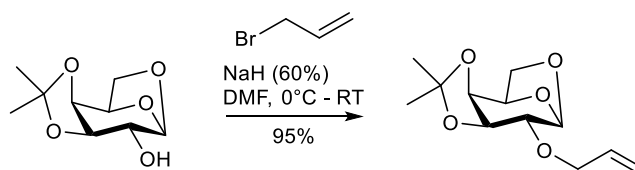
7.1. General remarks

All reagents were purchased from Alfa Aesar, Carbosynth Limited, Fisher Scientific and Sigma Aldrich and were used without further purification. Dry solvents were obtained after distillation with common procedures. The purification of the synthesized compounds was performed by chromatography by using Silica Gel 60 (mesh 230-240) from Material Harvest. Silica gel coated glass or aluminium plates (60 F₂₅₄, Merck) were used for thin layer chromatography (TLC) and a 5% sulfuric acid solution in ethanol was used for visualization. NMR-spectra (¹H for proton and ¹³C for carbon) were measured with a Bruker 500 MHz DCM Cryoprobe or a 400 MHz DPX-400 Dual spectrometer. Fluorine (¹⁹F) NMR spectra were recorded with a Bruker 400 MHz Avance III HD Smart Probe spectrometer. All compounds were fully assigned by using COESY, HSQC, HMBC, ¹H and ¹³C spectra. The chemical shifts were quoted relative to the solvent peak (CDCl₃: ¹H = 7.26 ppm, ¹³C = 77.16 ppm) as internal standard. During the analysis, the coupling constants *J* were reported in Hz and the following splitting abbreviations were used: s = singlet, d = duplet, t = triplet, dd = duplet from duplet, m = multiplet. A Thermo Finnigan Orbitrap Classic or a Waters' Xevo G2-S bench top QTOF were used for high resolution mass spectrometry for essential compounds. When anhydrous conditions were reported, the reactions were performed in flame dried flasks under argon atmosphere and using molecular sieve of 3 or 4 Å.

7.2. Materials and Methods for Chapter 2

7.2.1. Chemical synthesis

7.2.1.1. Synthesis of 2-*O*-allyl-1,3,4,6-tetra-*O*-acetyl-galactose (31)

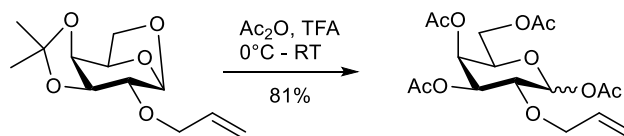


1,6-Anhydro-3,4-isopropylgalactopyranose (300 mg, 1.48 mmol) was dissolved in 6 mL anhydrous DMF and cooled to 0 °C. NaH (60% suspension in mineral oil, 149 mg, 4.45 mmol) was added and the reaction was stirred for 30 min. Allylbromid (0.387 mL, 4.45 mmol) was added slowly and the reaction was stirred over night from 0 °C – RT. Water was added carefully. The reaction mixture was extracted with CH₂Cl₂, the organic layer was washed three times with 5 mL of saturated solution of NaCl, dried with MgSO₄, filtrated through a cotton patch and concentrated. The product 1,6-anhydro-2-allyl-3,4-isopropylgalactose was obtained after column chromatography (petrol/EtOAc 3:1) with a yield of 95% (339.8 mg, 1.4 mmol).

¹H-NMR (300 MHz, CDCl₃): δ = 5.88 (ddt, *J* = 17.2 Hz, *J* = 10.4 Hz, *J* = 5.6 Hz, 1H, CH=CH₂), 5.38 (s, 1H, **H1**), 5.28 (dq, *J* = 17.2, *J* = 1.5 Hz, 1H, CH=CH₂), 5.19 (ddd, *J* = 10.4 Hz, *J* = 2.7 Hz, *J* = 1.2 Hz, 1H, CH=CH₂), 4.46 (t, *J* = 5.6 Hz, 1H, **H3**), 4.40 (t, *J* = 6.4 Hz, 1H, **H5**), 4.14 (dd, *J* = 5.9, *J* = 4.9 Hz, 1H, **H4**), 4.12 – 4.06 (m, 2H, **H6**), 4.06 – 4.00 (m, 1H, CH₂-CH), 3.53 (dt, *J* = 10.2, *J* = 4.2 Hz, 1H, CH₂-CH), 3.48 (s, 1H, **H2**), 1.49 (s, 3H, CH₃), 1.32 (s, 3H, CH₃) ppm.

¹³C-NMR (75 MHz, CDCl₃): δ = 133.81 (CH=CH₂), 117.79 (CH=CH₂), 108.36 (C(CH₃)₂), 99.60 (C1), 76.56 (C2), 74.05 (C4), 71.92 (C3), 71.06 (C6), 69.21 (C5), 62.89 (OCH₂-CH=CH₂), 25.66 (CH₃), 24.17 (CH₃) ppm.

HRMS-ESI+ (m/z): calculated [M + H⁺] = 243.1227, found [M + H⁺] = 243.1240

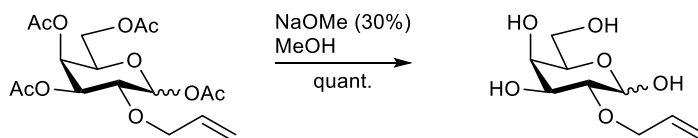


The obtained material (339.8 mg, 1.4 mmol) was dissolved in Ac₂O (7.5 mL/ mmol) and cooled to 0 °C. Trifluoroacetic acid (TFA, 1.26 mL/mmol) was added dropwise and the reaction was stirred overnight from 0 °C – RT. The reaction was diluted with EtOAc (10 mL) and washed with saturated solution of Na₂CO₃ (3 x 10 mL) and saturated solution of NaCl (2 x 10 mL). The organic layer was dried with MgSO₄, filtrated through a cotton patch and concentrated. The crude mixture was purified by column chromatography (petrol/ EtOAc 3:1 -> 1:1) and the product 2-allyl-1,3,4,6-*O*-acetyl-galactopyranose was obtained with a yield of 81% (444.3 mg, 1.14 mmol).

¹H-NMR (400 MHz, CDCl₃): δ = 6.39 (d, *J* = 3.6 Hz, 1H, **H**1α), 5.82 (ddd, *J* = 22.8 Hz, *J* = 10.8 Hz, *J* = 5.6 Hz, 1H, **CH=CH**₂), 5.61 (d, *J* = 8.2 Hz, 1H, **H**1β), 5.46 (d, *J* = 2.2 Hz, 1H, **H**4α), 5.39 (d, *J* = 2.7 Hz, 1H, **H**4β), 5.26 (dd, *J* = 13.5 Hz, *J* = 2.4 Hz, 1H, **CH=CH**₂), 5.22 (dd, *J* = 6.6 Hz, *J* = 3.3 Hz, 1H, **H**3α), 5.19 (dd, *J* = 10.5 Hz, *J* = 1.2 Hz, 1H, **CH=CH**₂), 4.99 (dd, *J* = 10.1 Hz, *J* = 3.4 Hz, 1H, **H**3β), 4.28 (t, *J* = 6.7 Hz, 1H, **H**5), 4.10 – 4.04 (m, 4H, **H**6a/b, **OCH**₂), 3.87 (dd, *J* = 10.6 Hz, *J* = 3.6 Hz, 1H, **H**2α), 3.68 (dd, *J* = 10.1 Hz, *J* = 8.2 Hz, 1H, **H**2β), 2.15, 2.14, 2.03, 2.02 (4 × s, 4 × 3H, **CH**₃CO) ppm.

¹³C-NMR (100 MHz, CDCl₃): δ = 170.6, 170.3, 170.2, 169.4 (4 × **CH**₃CO), 134.2 (**CH=CH**₂), 117.9 (**CH=CH**₂), 90.2 (**C**1), 72.3 (**C**2), 72.2 (**OCH**₂), 69.5 (**C**3), 68.7 (**C**5), 67.9 (**C**4), 61.5 (**C**6), 21.1, 20.9, 20.8, 20.7 (4 × **CH**₃CO) ppm.

HRMS-ESI+ (*m/z*): calculated [**M** + **H**⁺] = 389.1442, found [**M** + **H**⁺] = 389.1440

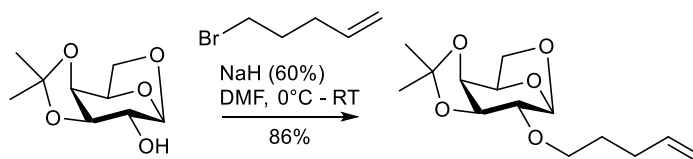
7.2.1.2. Synthesis of 2-*O*-allyl-galactose (37)

The fully acetylated sugar 2-allyl-1,3,4,6-tetra-*O*-acetyl-galactopyranose (100 mg, 0.257 mmol) was dissolved in 2 mL MeOH and 30% NaOMe solution (0.142 mL) was added. The reaction was stirred at RT until TLC showed complete consumption of the starting material. The mixture was neutralized with Dowex 50W (H⁺ from), filtrated and concentrated. The final, unprotected monosaccharide was purified by chromatography (EtOAc/MeOH 3:1) and obtained in quantitative yield as mix of both anomers.

¹H-NMR (400 MHz, D₂O): δ = 6.06 – 5.92 (m, 2H, CH=CH₂, CH'=CH₂), 5.44 (d, *J* = 3.7 Hz, 1H, **H1** α), 5.41 – 5.25 (m, 4H, CH=CH₂, CH=CH'₂), 4.64 (d, *J* = 7.9 Hz, 1H, **H1** β), 4.34 (ddd, *J* = 39.2 Hz, *J* = 12.1 Hz, *J* = 6.2 Hz, 2H, **H6'**), 4.23 – 4.15 (m, 2H, OCH₂), 4.07 (dd, *J* = 11.8 Hz, *J* = 5.5 Hz, 1H, **H3'**), 4.00 (d, *J* = 2.9 Hz, 1H, **H3'**), 3.97 – 3.88 (m, 1H, **H4**), 3.79 – 3.71 (m, 2H, **H6**), 3.71 – 3.64 (m, 2H, **H3**, **H2'**), 3.39 (dd, *J* = 9.9 Hz, *J* = 8.4 Hz, 1H, **H2**) ppm.

¹³C NMR (101 MHz, D₂O): δ = 134.1 (CH=CH₂), 118.5 (CH=CH₂), 96.4 (C1), 90.3 (C1'), 79.9 (C2), 75.6 (C2'), 73.9 (C6'), 72.4 (C3), 71.5 (OCH₂), 70.2 (C3'), 69.3 (C5), 68.8 (C4), 61.1 (C6, C6'), 60.9 (C6, C6') ppm.

Signals assigned with ' represent the alpha-conformer.

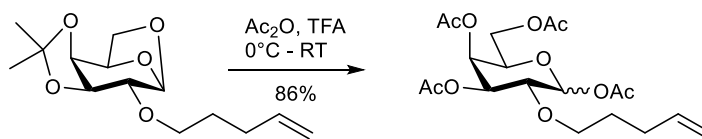
7.2.1.3. Synthesis of 2-*O*-pentenyl-1,3,4,6-tetra-*O*-acetyl-galactose (33)

1,6-Anhydro-3,4-isopropylgalactopranose (300 mg, 1.48 mmol) was dissolved in 6 mL anhydrous DMF and cooled to 0 °C. NaH (60% suspension in mineral oil, 149 mg, 4.45 mmol) was added and the reaction was stirred for 30 min. 5-Bromo-1-pentene (0.387 mL, 4.45 mmol) was added slowly and the reaction was stirred over night from 0 °C – RT. Water was added carefully. The reaction mixture was extracted with CH₂Cl₂, the organic layer was washed three times with 5 mL of saturated solution of NaCl, dried with MgSO₄, filtrated through a cotton patch and concentrated. The product 1,6-anhydro-2-pentenyl-3,4-isopropylgalactose was obtained after column chromatography (petrol/EtOAc 3:1) with a yield of 86% (343.8 mg, 1.27 mmol).

¹H-NMR (500 MHz, CDCl₃): δ = 5.80 (ddt, $J_{\text{CH}/\text{CH}_2=\text{CH}} = 16.9$ Hz, $J_{\text{CH}/\text{CH}_2=\text{CH}} = 10.2$ Hz, $J_{\text{CH}/\text{CH}_2} = 6.7$ Hz, 1H, **CH=CH₂**), 5.41 (d, $J_{\text{H}_1/\text{H}_2} = 1.3$ Hz, 1H, **H1**), 5.03 (dq, $J_{\text{CH}_2=\text{CH}/\text{CH}} = 17.1$ Hz, $J_{\text{CH}_2=\text{CH}/\text{CH}_2=\text{CH}} = 1.7$ Hz, 1H, **CH=CH₂**), 4.97 (m, 1H, **CH=CH₂**), 4.50 (t, $J_{\text{H}_6/\text{H}_{6,5}} = 5.7$ Hz, 1H, **H6**), 4.46 – 4.41 (m, 1H, **H4**), 4.16 (dt, $J_{\text{H}_3/\text{H}_4} = 7.2$ Hz, $J_{\text{H}_3/\text{H}_1} = 1.1$ Hz, 1H, **H3**), 4.08 (d, $J_{\text{H}_6/\text{H}_5} = 7.5$ Hz, 1H, **H6**), 3.64 – 3.60 (m, 1H, **H5**), 3.60 – 3.55 (m, 2H, **O-CH₂**), 3.43 (d, $J_{\text{H}_2/\text{H}_1} = 0.9$ Hz, 1H, **H2**), 2.13 (m, 2H, **CH₂-CH=CH₂**), 1.70 (m, 2H, **CH₂-CH₂-O**), 1.53 (s, 3H, **CH₃**), 1.36 (s, 3H, **CH₃**) ppm.

¹³C NMR (120 MHz, CDCl₃): δ = 138.1 (**CH=CH₂**), 115.2 (**CH=CH₂**), 99.9 (**C1**), 78.3 (**C2**), 74.3 (**C3**), 72.2 (**C6**), 69.5 (**C6**), 63.2 (**CH₂O**), 31.1, 30.3 (**CH₂-CH=CH₂**), 28.9 (**CH₂-CH₂O**), 25.9 (**CH₃**), 24.5 (**CH₃**) ppm.

HRMS-ESI+ (m/z): calculated [M + H⁺] = 271.1540, found [M + H⁺] = 271.1546



The obtained material (343.8 mg, 1.27 mmol) was dissolved in Ac₂O (7.5 mL/ mmol) and cooled to 0 °C. Trifluoroacetic acid (TFA, 1.26 mL/mmol) was added dropwise and the reaction was stirred overnight from 0 °C – RT. The reaction was diluted with EtOAc (10 mL) and washed

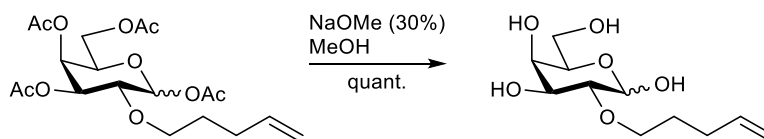
with saturated solution of Na_2CO_3 (3 x 10 mL) and saturated solution of NaCl (2 x 10 mL). The organic layer was dried with MgSO_4 , filtrated through a cotton patch and concentrated. The crude mixture was purified by column chromatography (petrol/ EtOAc 3:1 \rightarrow 1:1) and the product 2-pentenyl-1,3,4,6-*O*-acetyl-galactopyranose was obtained with a yield of 86% (455.6 mg, 1.09 mmol).

$^1\text{H-NMR}$ (400 MHz, CDCl_3): δ = 6.41 (d, J = 3.6 Hz, 1H, $\mathbf{H1\alpha}$), 5.77 (ddt, J = 16.9 Hz, J = 10.1 Hz, J = 6.7 Hz, 1H, $\mathbf{CH=CH_2}$), 5.59 (d, J = 8.1 Hz, 1H, $\mathbf{H1\beta}$), 5.46 (d, J = 2.4 Hz, 1H, $\mathbf{H4\alpha}$), 5.38 (d, J = 3.1 Hz, 1H, $\mathbf{H4\beta}$), 5.20 (dd, J = 10.5 Hz, J = 3.2 Hz, 1H, $\mathbf{H3\alpha}$), 5.04 – 4.92 (m, 3H, $\mathbf{H3\beta}$, $\mathbf{CH=CH_2}$), 4.28 (t, J = 6.6 Hz, 1H, $\mathbf{H5\alpha}$), 4.07 (dd, J = 6.7 Hz, J = 2.0 Hz, 2H, $\mathbf{H6a/b}$), 3.78 (dd, J = 10.5 Hz, J = 3.6 Hz, 1H, $\mathbf{H2\alpha}$), 3.63 (ddd, J = 15.2 Hz, J = 11.1 Hz, J = 4.6 Hz, 2H, $\mathbf{H2\beta}$, $\mathbf{OCH_2}$), 3.48 (dt, J = 9.1 Hz, J = 6.5 Hz, 1H, $\mathbf{OCH_2}$), 2.15 (2 \times s, 6H, $\mathbf{CH_3}$), 2.06 (d, J = 5.3 Hz, 2H, $\mathbf{OCH_2CH_2CH_2}$), 2.03, 2.02 (2 \times s, 6H, $\mathbf{CH_3}$), 1.63 – 1.55 (m, 2H, $\mathbf{OCH_2CH_2}$) ppm.

$^{13}\text{C-NMR}$ (100 MHz, CDCl_3): δ = 170.7, 170.4, 170.3, 169.4 (4 \times $\mathbf{CH_3CO}$), 138.1 ($\mathbf{CH=CH_2}$), 115.1 ($\mathbf{CH=CH_2}$), 94.1 ($\mathbf{C1\beta}$), 90.1 ($\mathbf{C1}$), 73.2 ($\mathbf{C2}$), 70.9 ($\mathbf{OCH_2}$), 69.4 ($\mathbf{C3}$), 68.7 ($\mathbf{C5}$), 67.9 ($\mathbf{C3}$), 61.5 ($\mathbf{C6}$), 29.9 ($\mathbf{OCH_2CH_2CH_2}$), 29.1 ($\mathbf{OCH_2CH_2}$), 21.1, 20.9, 20.8, 20.7 (4 \times $\mathbf{CH_3CO}$) ppm.

HRMS-ESI+ (m/z): calculated $[\text{M} + \text{Na}^+] = 439.1575$, found $[\text{M} + \text{Na}^+] = 439.1571$

7.2.1.4. Synthesis of 2-*O*-pentenyl-galactopyranose (38)



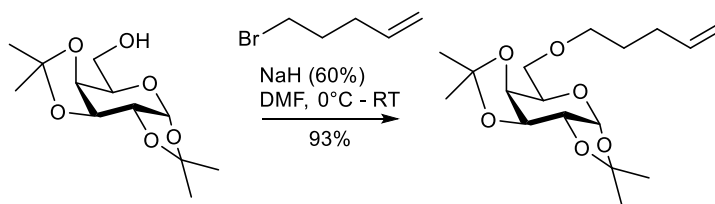
2-*O*-pentenyl-1,3,4,6-*O*-acetyl-galactopyranose (100 mg, 0.24 mmol) was dissolved in 2 mL MeOH and 30% NaOMe solution (0.136 mL) was added. The reaction was stirred at RT until TLC showed complete consumption of the starting material. The mixture was neutralized with

Dowex 50W (H⁺ form), filtrated and concentrated. The final, unprotected monosaccharide was purified by chromatography (EtOAc/MeOH 3:1) and was obtained in quantitative yield.

¹H NMR (400 MHz, D₂O) δ = 6.00 – 5.85 (m, 2H, CH=CH₂, CH'=CH₂), 5.44 (d, *J* = 3.5 Hz, 1H, H1 α), 5.10 (d, *J* = 17.3 Hz, 2H, CH=CH₂, CH=CH'₂), 5.03 (d, *J* = 10.2 Hz, 2H, CH=CH₂, CH=CH'₂), 4.62 (d, *J* = 7.9 Hz, 1H, H1 β), 4.08 (dd, *J* = 11.5 Hz, *J* = 5.3 Hz, 1H, H5'), 3.96 (dd, *J* = 25.6 Hz, *J* = 2.7 Hz, 2H, H4, H5), 3.92 – 3.84 (m, 2H, H3 α , OCH₂), 3.82 – 3.63 (m, 10H, OCH₂, OCH'₂, H3', H4', H6a,b, H6'a,b), 3.60 (dd, *J* = 10.3 Hz, *J* = 3.9 Hz, 1H, H2'), 3.35 – 3.27 (m, 1H, H2), 2.15 (q, *J* = 7.0 Hz, 4H, CH₂CH=CH₂, CH'₂CH=CH₂), 1.76 – 1.67 (m, 4H, OCH₂CH₂, OCH₂CH'₂) ppm.

¹³C NMR (101 MHz, D₂O) δ = 139.0, 138.9 (CH=CH₂, C'H=CH₂), 114.7 (CH=CH₂), 96.3 (C1 β), 90.2 (C1 α), 80.3 (C2), 76.3 (C2'), 75.0 (C3), 72.6 (OCH₂), 72.4 (C3/C4'), 70.2 (C5'), 70.0 (OCH₂), 69.3 (C5), 68.8 (C4), 68.4 (C3'), 61.14, 60.89 (C6, C6') 29.4 (CH₂CH=CH₂), 28.2 (OCH₂CH₂) ppm.

7.2.1.5. Synthesis of 6-*O*-pentenyl-1,2,3,4-tetra-*O*-acetyl-galactopyranose (36)

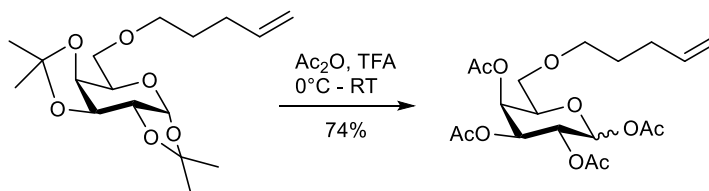


The monosaccharide 1,2,3,4-diisopropyl-galactopyranose (300 mg, 1.15 mmol) was dissolved in 5 mL anhydrous DMF and cooled to 0 °C. NaH (60% suspension in mineral oil, 116 mg, 3.46 mmol) was added and the mixture was stirred for 30 min. 5-Bromo-1-pentene (0.409 mL, 3.46 mmol) was added slowly to the reaction and the mixture was stirred overnight from 0 °C to RT. 2 mL of water were added carefully to the reaction and the mixture was extracted with CH₂Cl₂ (3 x 5 mL). The organic layer was washed with saturated solution of NaCl (3 x 5 mL),

dried with MgSO_4 , filtrated through a cotton patch and concentrated. The crude mixture was purified by chromatography (petrol/EtOAc 3:1 \rightarrow 1:1) and the product 6-*O*-pentenyl-1,2,3,4-diisopropyl-galactopyranose was obtained with a yield of 93% (350 mg, 1.07 mmol)

$^1\text{H-NMR}$ (400 MHz, CDCl_3): δ = 5.87 – 5.74 (m, 1H, $\text{CH}=\text{CH}_2$), 5.53 (d, J = 5.0 Hz, 1H, **H1**), 5.05-4.97 (m, 1H, $\text{CH}=\text{CH}_2$), 4.97-4.91 (m, 1H, $\text{CH}=\text{CH}_2$), 4.59 (dd, J = 7.9 Hz, J = 2.3 Hz, 1H, **H3**), 4.29 (dd, J = 5.0 Hz, J = 2.4 Hz, 1H, **H2**), 4.25 (dd, J = 7.9 Hz, J = 1.8 Hz, 1H, **H4**), 3.95 (td, J = 6.3 Hz, J = 1.8 Hz, 1H, **H5**), 3.66 – 3.53 (m, 2H, **H6**), 3.53 – 3.44 (m, 2H, OCH_2CH_2), 2.15-2.06 (m, 2H, $\text{CH}_2\text{CH}=\text{CH}_2$), 1.67 (dt, J = 13.7 Hz, J = 6.7 Hz, 2H, OCH_2CH_2), 1.53, 1.44, 1.33, 1.32 ($4 \times$ s, $4 \times$ 3H CH_3) ppm.

$^{13}\text{C-NMR}$ (100 MHz, CDCl_3): δ = 138.5 ($\text{CH}=\text{CH}_2$), 114.8 ($\text{CH}=\text{CH}_2$), 109.3, 108.6 ($2 \times$ $\text{C}(\text{CH}_3)_2$), 96.5 (**C1**), 71.3 (**C4**), 70.9, 70.8 (**C2**, **C3**, OCH_2CH_2), 69.4 (**C6**), 66.8 (**C5**), 30.4 ($\text{CH}_2\text{CH}=\text{CH}_2$), 28.9 (OCH_2CH_2), 26.2, 26.1, 25.1, 24.6 ($4 \times$ CH_3) ppm.



The sugar 6-*O*-pentenyl-1,2,3,4-diisopropyl-galactopyranose (350 mg, 1.07 mmol) was dissolved in Ac_2O (8.33 mL, 7.5 mL/mmol) and cooled to 0 °C. TFA (1.39 mL, 1.26 mL/mmol) was added dropwise and the reaction was stirred from 0 °C-RT overnight. The reaction was diluted with EtOAc and the organic layer was washed with saturated solution of Na_2CO_3 (3 x 5 mL), saturated solution of NaCl (2 x 5 mL), dried with MgSO_4 , filtrated and concentrated. The crude mixture was purified by chromatography (petrol/EtOAc 4:1 \rightarrow 2:1) and the product was obtained with a yield of 74% (0.79 mmol, 329 mg).

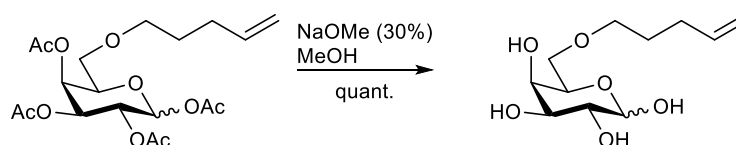
$^1\text{H-NMR}$ (500 MHz, CDCl_3): δ = 6.35 (d, J = 2.7 Hz, 1H, **H1**), 6.08 (d, J = 1.5 Hz, 1H, **H1'**), 5.82-5.70 (m, 1H, $\text{CH}=\text{CH}_2$), 5.53 (s, 1H, **H3**), 5.32 (t, J = 2.8 Hz, 1H, **H2**), 4.99 (dd, J = 17.1 Hz, J = 1.4 Hz, 1H, $\text{CH}=\text{CH}_2$), 4.93 (d, J = 10.2 Hz, 1H, $\text{CH}=\text{CH}_2$), 4.24 (dd,

$J = 13.3$ Hz, $J = 6.8$ Hz, 1H, **H4**), 3.49 – 3.29 (m, 5H, **H5**, **H6a/b**, OCH_2CH_2), 2.13 (s, 6H, $2 \times \text{CH}_3\text{CO}$), 2.07 (dd, $J = 5.2$ Hz, $J = 2.6$ Hz, 2H, $\text{CH}_2\text{CH}=\text{CH}_2$), 2.00, 1.98 ($2 \times$ s, 6H, $2 \times \text{CH}_3\text{CO}$), 1.63 – 1.56 (m, 2H $\text{CH}_2\text{CH}_2\text{CH}_2$) ppm.

^{13}C -NMR (126 MHz, CDCl_3): $\delta = 170.3, 170.2, 170.1, 169.2$ ($4 \times \text{CH}_3\text{CO}$), 138.2 ($\text{CH}=\text{CH}_2$), 114.9 ($\text{CH}=\text{CH}_2$), 89.9 (**C1**), 71.2 (OCH_2CH_2), 70.1 (**C4**), 68.4 (**C6**), 68.1 (**C3**), 67.7, 66.8 (**C2**), 30.1 ($\text{CH}_2\text{CH}=\text{CH}_2$), 28.7 ($\text{CH}_2\text{CH}_2\text{CH}_2$), 20.8, 20.7, 20.6, 20.5 ($4 \times \text{CH}_3\text{CO}$) ppm.

HRMS-ESI+ (m/z): calculated $[\text{M} + \text{Na}^+] = 439.1575$, found $[\text{M} + \text{Na}^+] = 439.1571$

7.2.1.6. Synthesis of 6-*O*-pentenyl-galactose (**39**)



6-*O*-pentenyl-1,2,3,4-tetra-*O*-acetyl-galactopyranose (100 mg, 0.24 mmol) was dissolved in 2 mL MeOH and 30% NaOMe solution (0.136 mL) was added. The reaction was stirred at RT until TLC showed complete consumption of the starting material. The mixture was neutralized with Dowex 50W (H^+ form), filtrated and concentrated. The final, deprotected monosaccharide 6-*O*-pentenyl-galactopyranose was obtained after chromatography (EtOAc/MeOH 3:1) in quantitative yield.

^1H -NMR (400 MHz, D_2O): $\delta = 5.92$ (ddt, $J = 16.9$ Hz, $J = 10.4$ Hz, $J = 6.6$ Hz, 2H, $\text{CH}=\text{CH}_2$, $\text{CH}'=\text{CH}_2$), 5.26 (d, $J = 3.5$ Hz, 1H, **H1 α**), 5.09 (t, $J = 12.3$ Hz, 2H, $\text{CH}=\text{CH}_2$, $\text{CH}=\text{CH}'_2$), 5.03 (d, $J = 10.2$ Hz, 2H, $\text{CH}=\text{CH}_2$, $\text{CH}=\text{CH}'_2$), 4.58 (d, $J = 7.8$ Hz, 1H, **H1 β**), 4.24 – 4.18 (m, 1H, **H5'**), 3.97 (s, 1H, **H5**), 3.92 (d, $J = 3.1$ Hz, 1H, **H4**), 3.86 (dd, $J = 10.6$ Hz, $J = 3.1$ Hz, 1H, **H3'**), 3.81 (dd, $J = 9.5$ Hz, $J = 4.3$ Hz, 1H, **H2'**), 3.69 (t, $J = 5.5$ Hz, 2H, **H6a,b**), 3.67 – 3.62 (m, 1H, **H3**), 3.62 – 3.54 (m, 2H, OCH_2), 3.53 – 3.46 (m, 1H, **H2**), 2.13 (dd, $J = 13.9$ Hz, $J = 6.9$ Hz, 4H, $\text{CH}_2\text{CH}=\text{CH}_2$, $\text{CH}'_2\text{CH}=\text{CH}_2$), 1.76 – 1.65 (m, 4H, OCH_2CH_2 , $\text{OCH}_2\text{CH}'_2$) ppm.

^{13}C -NMR (101 MHz, D_2O): $\delta = 138.8$ ($\text{CH}=\text{CH}_2$), 114.7 ($\text{CH}=\text{CH}_2$), 96.4 ($\text{C1}\beta$), 92.3 ($\text{C1}\alpha$), 73.3 ($\text{C2}'$), 72.7 (C3), 71.8 (C2), 70.8 (OCH_2), 69.7 (C6), 69.6 (C5), 69.1 ($\text{C3}'$), 69.0 (C4), 68.6 (C5), 29.5 ($\text{CH}_2\text{CH}=\text{CH}_2$), 27.7 (OCH_2CH_2) ppm.

7.2.2. Kinetic studies

To determine the second order rate constant k_2 of the synthesized galactose derivatives in iEDDA reactions with 6-methyl-tetrazine-amine, a high-throughput method that used a microplate reader was developed. The reactions were performed in PBS buffer at $\text{pH} = 7.4$ at a temperature of $37\text{ }^\circ\text{C}$ in a flat bottom 96-well plate. To follow the reaction, the decrease in tetrazine absorption at 530 nm was recorded. A concentration of 0.6 mM 6-methyl-tetrazine-amine was found as optimal concentration per well. The deacetylated galactose derivatives were prepared in 20 mM stock solutions, from which further dilutions of 16, 12, 8 and 4 mM were prepared. A final volume of 100 μM per well was obtained by mixing the solutions containing tetrazine and galactose derivative. Each set of reactions was recorded for 16 h at $37\text{ }^\circ\text{C}$. Using GraphPad Prism 6.01 and an exponential decay function, the pseudo-first order rate constant k_{obs} was calculated for every concentration (Figure 44, A1, B1, C1). By plotting the obtained values for k_{obs} against the corresponding concentration, the second order rate constant k_2 was obtained as slope of the linear function (Figure 44, A2, B2, C2).

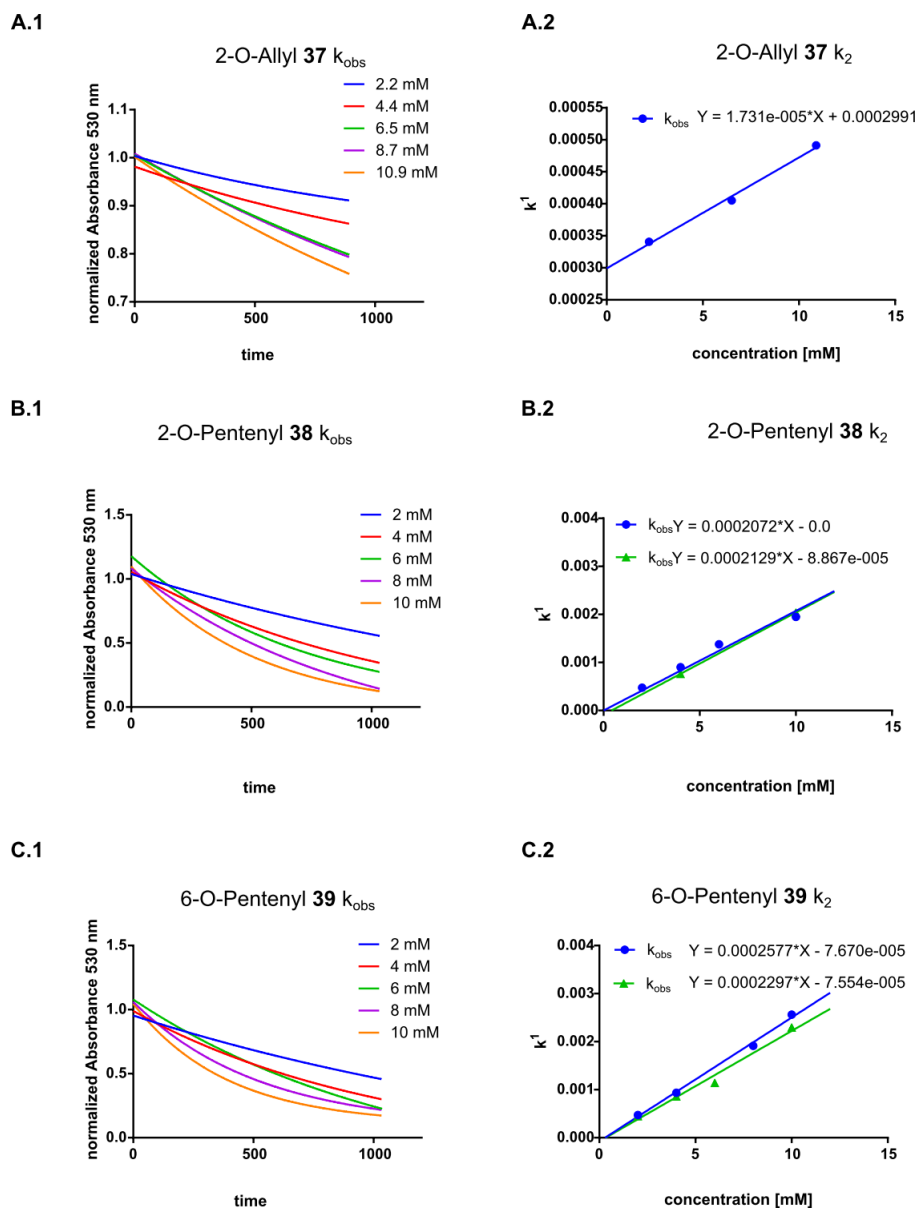


Figure 44: A.1, B.1, C.1. Decrease in absorbance of tetrazine **40** at 530 nm during iEDDA reaction with galactose derivatives **37**, **38** and **39**. A.2, B.2, C.2 concentration dependent determination of pseudo-first order rate constant k_{obs} for iEDDA between galactose derivatives **37**, **38** and **39** and tetrazine **40**. The second order rate constant k_2 was calculated as the slope of the linear equation.

7.2.3. Cell studies

The cell lines Huh7 and HepG2 were maintained at 37 °C in a humidified incubator under 5% CO₂ in DMEM medium (high glucose) which was supplemented with 10% heat-inactivated

FBS, 2mM GlutaMAX™, 10 mM HEPES, 1% Non-essential amino acids, 100 units/mL penicillin and 100 µg/mL streptomycin. The fully supplemented media will be further referred as complete medium (cDMEM). The cells were grown until 80% confluence before being split using TrypLE™ Express. All reagents were bought from Gibco, Life Technologies (USA).

7.2.3.1. Determination of cell toxicity

To determine the toxicity of the synthesized galactose derivatives, a CellTiter-Blue^R Cell Viability Assay (Promega, USA) was used. Cells were seeded in flat bottom 96-well plates at a concentration of 10000 cells/well for a 48 h time point and with 5000 cells/well for 72 h. The cells were allowed to adhere to the plates for 24 h before the medium was exchanged to cDMEM containing either 100 µM or 200 µM of the corresponding galactose derivative **31**, **33** or **36**. Negative controls were performed using plain cDMEM or an equal amount of DMSO as represented in the different concentrations. Technical triplicates were performed for each concentration. To determine the cell viability in the defined time points, the cell culture medium was exchanged to a 1:20 dilution of CellTiter-Blue reagent in cDMEM and the plates were incubated for another 1.5 h at 37 °C in the cell incubator. Finally, the fluorescence intensity ($\lambda_{\text{ex}} = 530 \text{ nm}$, $\lambda_{\text{em}} = 590 \text{ nm}$) was analyzed in an Infinite M200 (Tecan, USA) plate reader (Figure 45 A, Figure 46 A). Normalization of the relative fluorescence units to the corresponding vehicle controls allowed the presentation of the cell viability as percentage of the control (Figure 45 B, Figure 46 B).

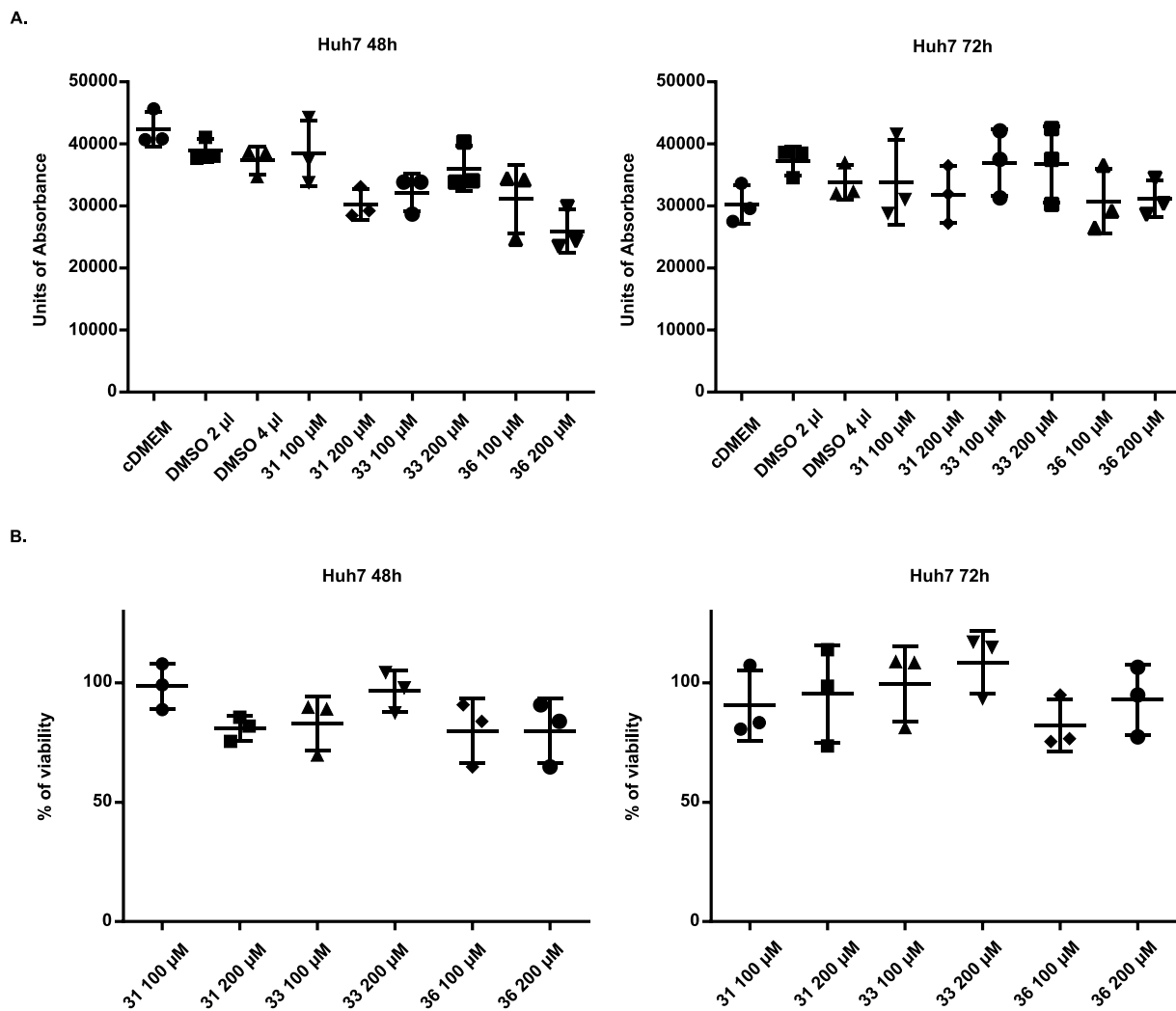


Figure 45: Determination of cell toxicity of galactose derivatives **31**, **33** and **36** in concentrations 100 μM and 200 μM . The cell viability was measured using CellTiter-Blue reagent at timepoints **A**, 48h and **B**, 72h in Huh7 cells. Data are represented as % of maximum. Data from three experiments.

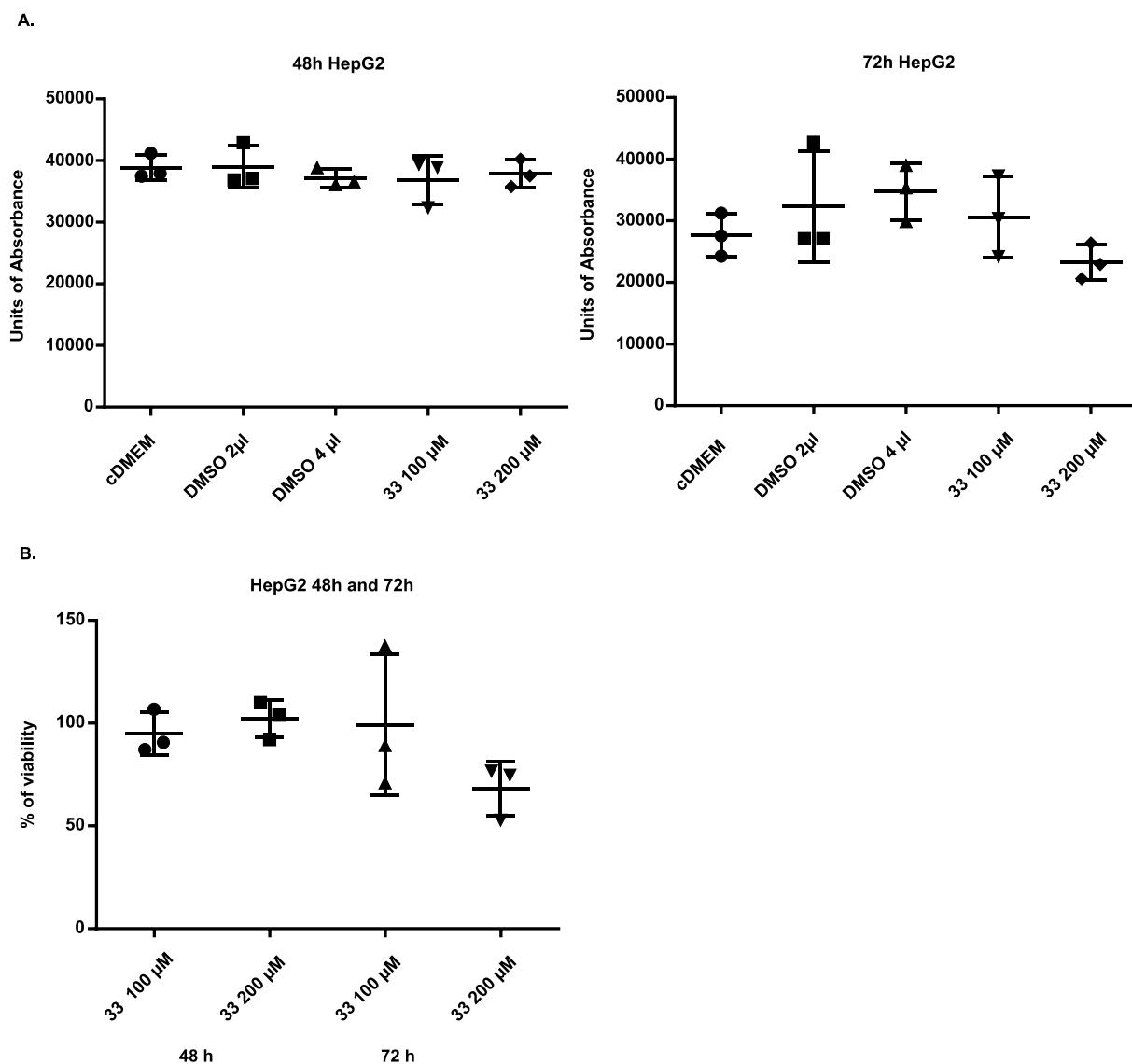


Figure 46: Determination of cell toxicity of galactose derivative **33** in concentrations 100 μM and 200 μM . **A.** The cell viability was measured using CellTiter-Blue reagent at timepoints 48h and 72h in HepG2 cells. **B.** Data are represented as % of maximum, Data from three experiments.

7.2.3.2. Metabolic labeling in Huh7 and HepG2 cells

For the analysis of the metabolic incorporation of the galactose derivatives by confocal point-scanning microscopy, cells were seeded with a density of 15000 cells/well on glass cover slips in 24-well plates. After 24 h, the cell culture medium was exchanged to cDMEM containing 100 μM of galactose derivatives **31**, **33** or **36** and the cells were grown for 72 h. For

the staining process, endogenous biotin was blocked using cDMEM supplemented with 25 $\mu\text{g}/\text{mL}$ streptavidin (from 1 mg/mL stock solution in water) for 40 min. After this, a 200 μM solution of 6-methyl-tetrazine-peg4-biotin in cDMEM was added for 5 h, to allow the iEDDA reaction to take place on the cell surface. The cells were rinsed with PBS (3 x 200 $\mu\text{L}/\text{well}$), before stained with 6.6 $\mu\text{g}/\text{mL}$ Alexa-Fluor-568-streptavidine (in PBS + 5% FBS, 20 min, RT) and Hoechst 33342 (1:1000 in PBS + 5% FBS, 5 min, RT). During experiments including a co-staining of the cell membrane, in this point CellMaskTM Deep Red Plasma membrane stain (1:1000, 2 min, 37 °C, PBS + 5%FBS) was applied. The cells were fixed with a 4% PFA solution (8 min, RT) and the coverslips were mounted on glass objective slides with Fluoromount GTM. A LSM880 confocal point-scanning microscope (Zeiss, Germany) with a Diode 405-30 nm, a DPSS 561-20 nm and a HeNe594-2 nm laser unit was used for the analysis, in which the pictures were acquired with a 63x Plan-Apochromat Oil objective. The pictures were processed using ImageJ 1.49 software to remove background noise and representative pictures were chosen from 5 different experiments. The quantification of the fluorescence intensity in channel 561 nm, resulting from the iEDDA reaction after sugar incorporation, was done using ImageJ 1.49 software by selecting the individual cells per picture as region of interest and comparing their intensities. The intensities were represented as ratio to the intensities measured in the corresponding controls.

The here described procedure was performed in the same way for acetylated and de-acetylated monosaccharides.

7.2.3.3. Metabolic labeling and inhibition of GLUT1 in HepG2 cells

For an analysis by confocal point-scanning microscopy, HepG2 cells were seeded with a density of 15000 cells/well on glass coverslips in 24-well plates, for an analysis by flow cytometry 50000 cells/well were seeded in 24-well plates one day prior to the experiment. The cell culture medium was exchanged to cDMEM supplemented with 100 μM of the sugar derivative and different concentrations of the inhibitor (10 μM of STF31 **47** and cytochalasine B **48**, 10-30 μM WZB117 **46**). The inhibitors were prepared with a concentration of 2 mM (cytochalasine B) or

20 mM (STF31, WZB117) in DMSO. The cells were grown for 72 h under these conditions, before being analyzed.

For the analysis by confocal point-scanning microscopy, the protocol was exactly the same as in the section described above (Figure 47).

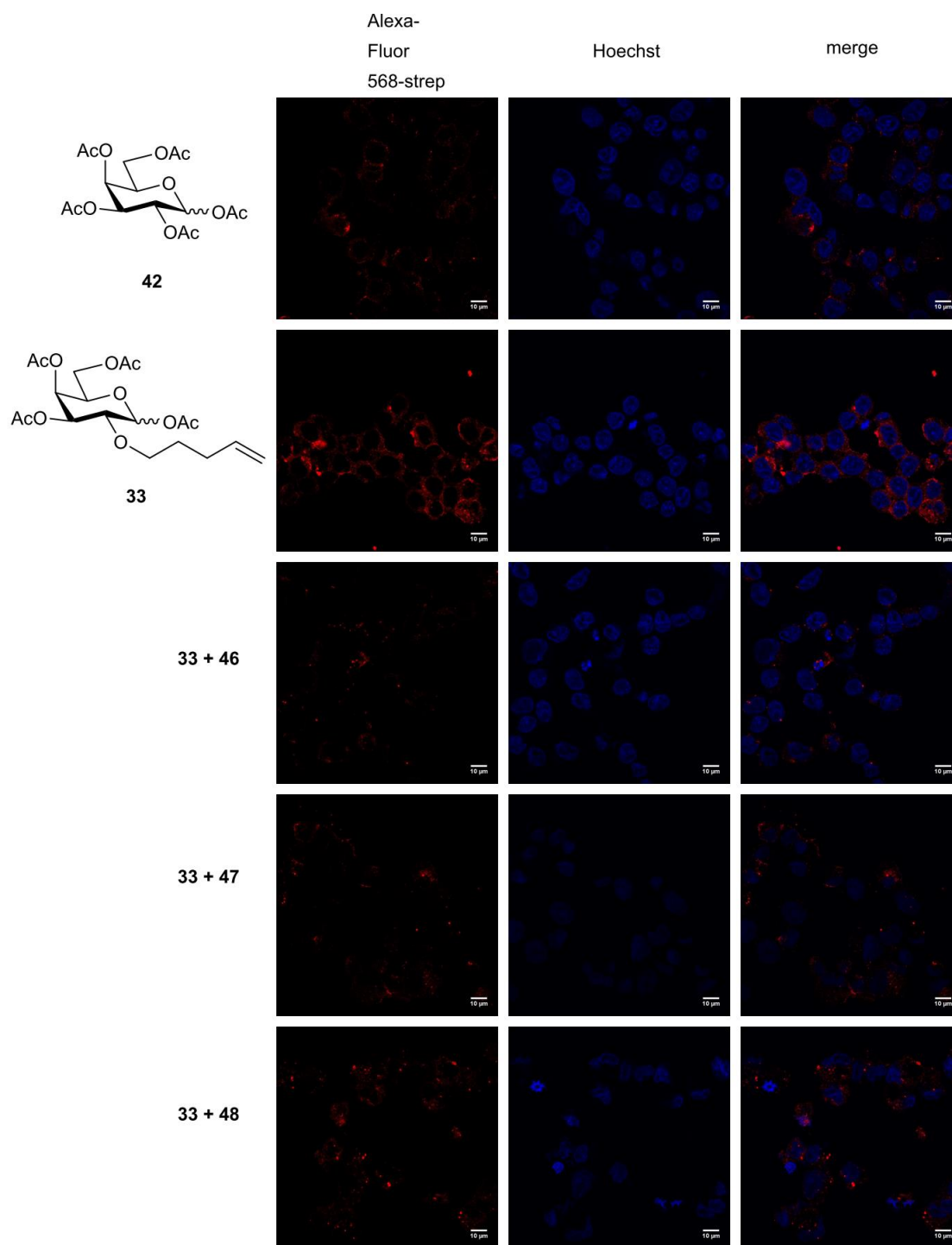


Figure 47: Incorporation of galactose derivative 33 in HepG2 cell membrane glycans and incorporation in the presence of the GLUT1 inhibitors WZB117 46, STF31 47 and cytochalasin B 48.

For analysis by flow cytometry, endogenous biotin was blocked with 25 $\mu\text{g}/\text{mL}$ streptavidine in cDMEM for 40 min, before a 200 μM solution of 6-methyl-tetrazine-peg4-biotin in cDMEM was added for 5 h at 37 $^{\circ}\text{C}$. The culture medium was removed and the cells were detached with 20 mM EDTA solution (5 min, 37 $^{\circ}\text{C}$) and collected by centrifugation (2000 g, 5 min). After washing the cells (PBS + 5% fbs), 6.6 $\mu\text{g}/\text{mL}$ Alexa-Fluor-568-streptavidin (20 min, RT, PBS + 5% FBS) were added for the staining. The cells were repeatedly washed (PBS + 5% FBS) and fixed with 4% PFA solution (8 min, RT). For the analysis in a BD LSRFortessa X-20 cell analyzer, the cells were resuspended in 300 μL PBS + 5% FBS and acquired using a 561 nm laser. The results were analyzed using FACSDiva, FLOWJOW and GraphPad Prism software (Figure 48).

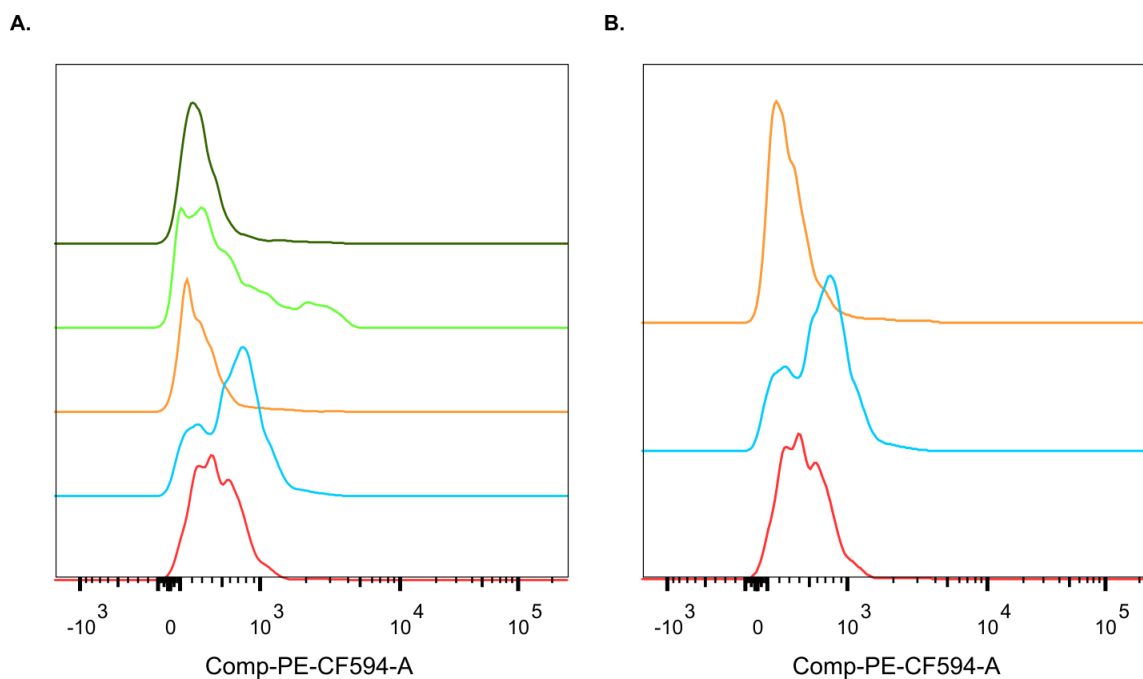


Figure 48: **A.** Half-offset histograms of fluorescence intensity in channel PE-CF594-A, normalized mode, after metabolic incorporation of galactose derivative **33** without inhibitor (blue), with 10 μM WZB117 **46** (orange), with 20 μM WZB117 **46** (green), with 30 μM WZB117 **46** (dark green). **B.** Half-offset histograms of fluorescence intensity in channel PE-CF-594-A, normalized mode, after metabolic incorporation of galactose derivative **33** without inhibitor (blue) or with 10 μM STF31 **47** (orange). Pentaacetyl galactose **42** (red) was used as negative control.

7.2.4. Infection studies

For all experiments, GFP-expressing sporozoites from *Plasmodium berghei* were dissected in DMEM from the salivary glands of infected female *A. stephensi* mosquitoes and HepG2 cells were seeded one day prior to infection.

7.2.4.1. Experiments analyzed by confocal point scanning microscopy

One day prior to infection, HepG2 cells were seeded with a density of 15000 cells/well on glass coverslips in 24-well plates. For the infection, the cell medium was changed to cDMEM containing 100 μ M of the galactose derivative **33** or the control sugar **42** and Fungizone (1:200). The freshly dissected GFP-expressing sporozoites were added with a concentration of 60000 sporozoites/well and the cell culture plate was centrifuged (4 min, 200 g) to allow a simultaneous settling of all parasites. After 2 h, assuming a complete invasion took place, the medium was removed and the cells were rinsed with PBS (3x200 μ L) to remove mosquito host debris. With fresh cDMEM including 100 μ M galactose derivative or control sugar as well as fungizone, the cells were incubated for 48 h in the cell culture incubator. At 48 hpi, the same staining procedure as described above (section 3) was applied and the experiment was analyzed using a LSM880 confocal point-scanning microscope (Zeiss, Germany). The pictures were acquired with a 63x Plan-Apochromat Oil objective and processed with ImageJ 1.49 software to remove background noise and to perform the quantification of the galactose derived fluorescence intensity. Representative images were chosen from 5 different experiments. The fluorescence intensities were presented as ratios to the corresponding negative control.

7.2.4.2. Experiments analyzed by flow cytometry and imaging flow cytometry

The cells were seeded with a concentration of 50000 cells/well in 24-well plates one day prior to the experiment. The cell culture medium was removed and replaced with cDMEM containing 100 μ M of the galactose derivative **33** or the control sugar **42**, as well as fungizone (1:200). The freshly dissected GFP-expressing sporozoites were added directly to the cells (60000 sporozoites/well) and the cell culture plate was centrifuged (4 min, 200 g) to allow simultaneous settling of the parasites. The medium was changed 2 hpi, including rinsing the cells with PBS, to remove mosquito host debris, and the cells were grown until 48 hpi. For the analysis, endogenous biotin was blocked as previously described and the iEDDA reaction was performed with a solution of 200 μ M 6-methyl-tetrazine-peg4-biotin in cDMEM for 5 h. The cells were detached with 20 mM EDTA solution (5 min, 37 °C) and collected by centrifugation (2000 g, 5 min). After washing them with PBS + 5%FBS, staining was achieved with 6.6 μ g/ml Alexa-Fluor-568-streptavidin (100 μ l per well, 20 min, RT) in PBS + 5% FBS. After washing the cells with PBS + 5% FBS, they were fixed with 4% PFA solution (8 min, RT) and the cells were resuspended in 300 μ l PBS + 5% FBS for analysis in a BD LSRFortessa X-20 or in 100 μ l PBS + 5% FBS for analysis in the imaging flow cytometer Amnis ImageStreamX Mark II. With both machines, the fluorescence intensity resulting from incorporated galactose derivative was presented as ratio to the corresponding control and naïve cells were compared with non-infected and infected cells.

Gating in Amnis ImageStream MarkII started from the bright field images to select single cells and in a next step single cells in focus of the camera. Infected and non-infected cells were differentiated on the basis of their fluorescence intensities in channel Ch02, representing the GFP-signal (Figure 49). Channel Ch04 was used for to detect the fluorescence intensity resulting from incorporated galactose derivative **33**. Unstained controls were used to adjust laser powers.

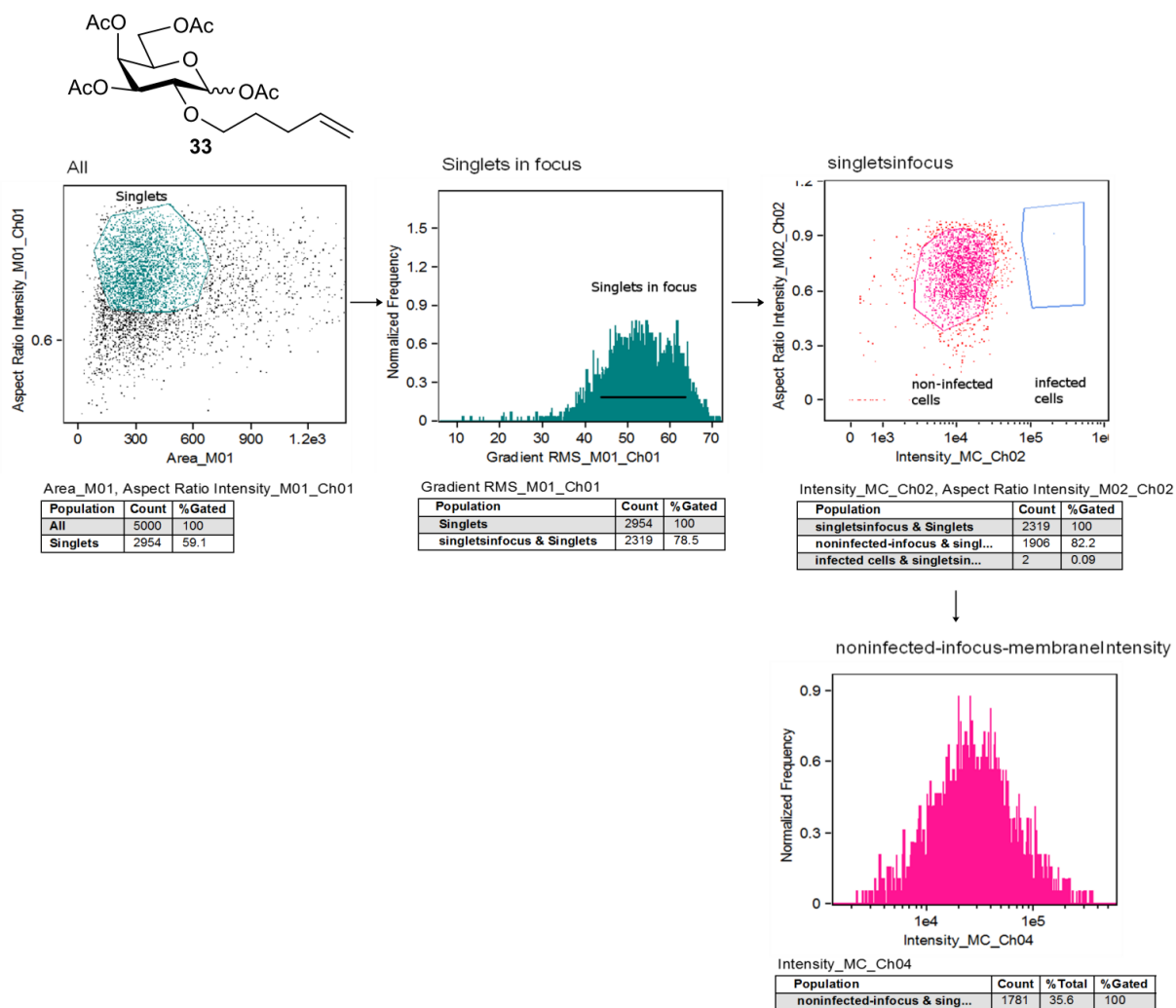


Figure 49: Gating strategy of the analysis of the metabolic incorporation of galactose derivative **33** in HepG2 cell membrane glycans using Amnis ImageStream MarkII, non-infected samples

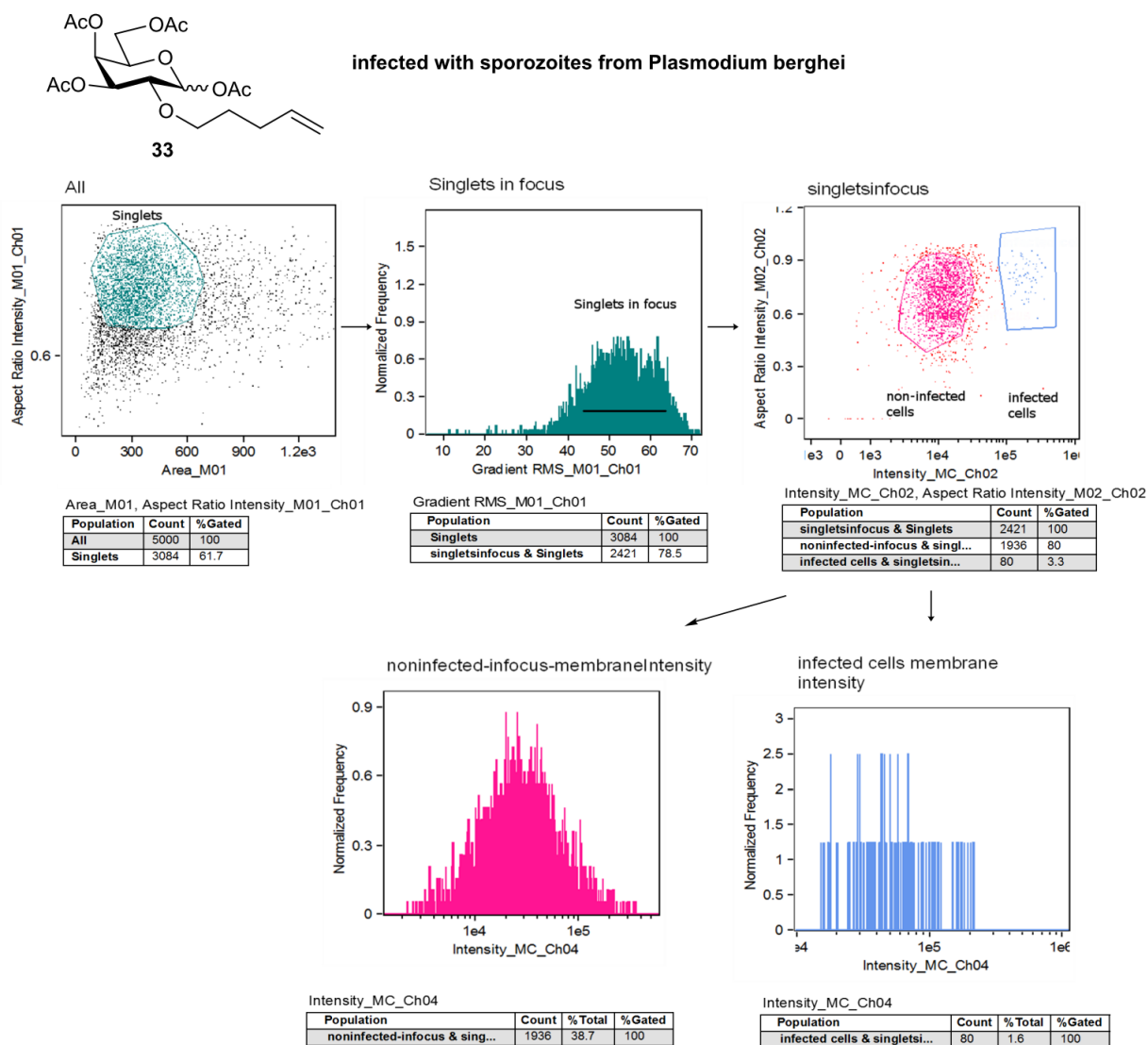
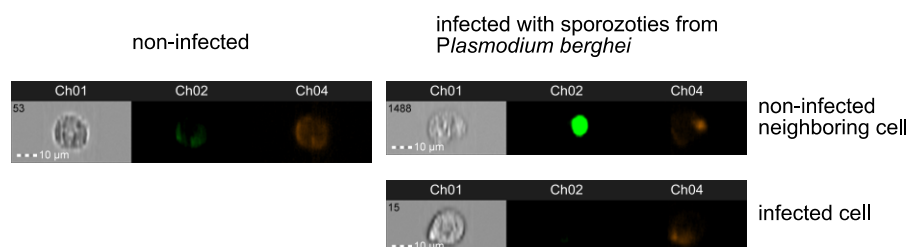
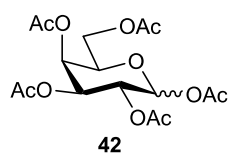


Figure 50 Gating strategy for analysis of the metabolic incorporation of galactose derivative 33 in HepG2 cell membrane glycans using Amnis ImageStream MarkII, infected with sporozoites from *Plasmodium berghei*.

Representative pictures acquired with Amnis ImageStream Mark II are represented below (Figure 51).

A.



B.

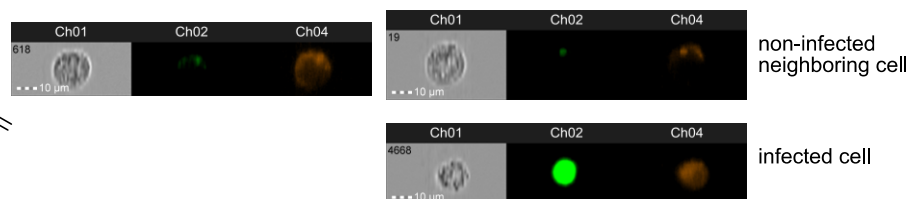
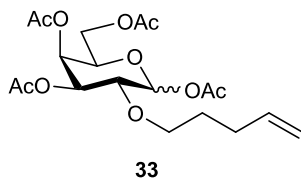


Figure 51: Representative pictures acquired with Amnis ImageStream Mark II for **A.** HepG2 cells grown with the control sugar **42** non-infected or infected with sporozoites from *Plasmodium berghei*, and **B.** HepG2 cells grown with galactose derivative **33**, non-infected or infected with sporozoites from *Plasmodium berghei*. Ch01: bright field, Ch02: 488 nm/GFP, Ch04: 561 nm

The gating during an analysis by flow cytometry is represented below, as example from one of three experiments. Infected and non-infected cells were distinguished on the basis of their fluorescence intensity in the GFP channel Alexa-Fluor-488 (Figure 52).

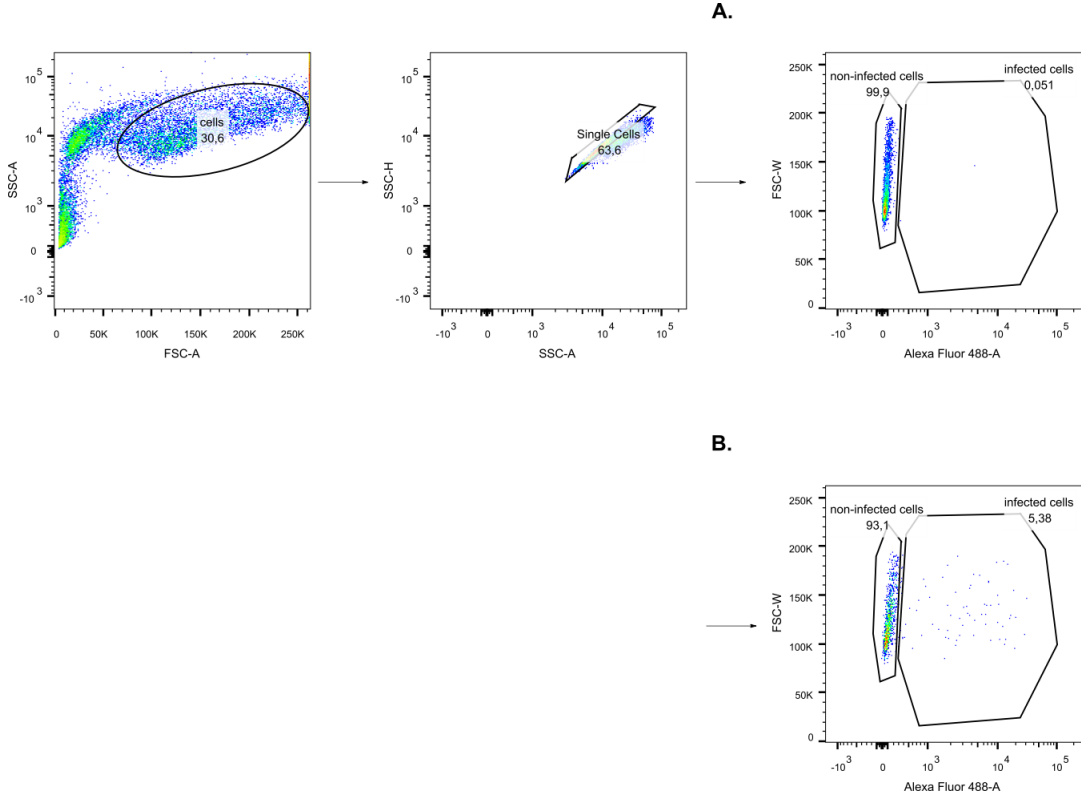


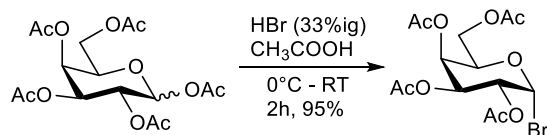
Figure 52: Gating strategy for analysis of metabolic incorporation of galactose derivative **33** in HepG2 cell membrane glycans, **A.** without infection, **B.** after infection with sporozoites from *Plasmodium berghei*.

7.3. Materials and Methods for Chapter 3

7.3.1. Chemical synthesis

The assigned literature citations in this section represent guidelines for the adapted procedures which were used during the synthesis

7.3.1.1. Synthesis of 2,3,4,6-tetra-*O*-acetylgalactosylbromide¹⁶⁴ (52)



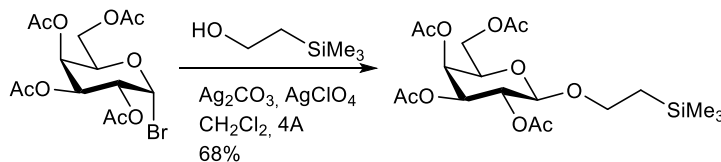
Acetic anhydride (2.5 mL) and HBr (33% in acetic acid, 10 mL) were cooled to 0°C. Pentaacetylgalactopyranose (5 g, 12.8 mmol) was added in small portions and the mixture was stirred 1h at 0°C and 1h at RT.

The reaction mixture was diluted with CH₂Cl₂ (30 mL) and washed with ice cold water (2x). The organic layer was washed with NaHCO₃ solution (3x) and NaCl solution (2x). All aqueous layers were extracted with CH₂Cl₂ and the combined organic layers were dried with MgSO₄, filtrated and concentrated. The desired product (5.01 g, 12.2 mmol) was obtained with a yield of 95%.

¹H-NMR (400 MHz, CDCl₃): δ = 6.69 (d, *J* = 3.9 Hz, 1H, **H1**), 5.51 (dd, *J* = 3.2 Hz, *J* = 1.0 Hz, 1H, **H4**), 5.39 (dd, *J* = 10.6 Hz, *J* = 3.3 Hz, 1H, **H3**), 5.04 (dd, *J* = 10.6 Hz, *J* = 4.0 Hz, 1H, **H2**), 4.48 (t, *J* = 6.6 Hz, 1H, **H5**), 4.22 – 4.06 (m, 2H, **H6a/b**), 2.14, 2.10, 2.05, 2.00 (4 × s, 12H, CH₃CO) ppm.

¹³C-NMR (100 MHz, CDCl₃): δ = 170.4, 170.2, 170.0, 169.8 (4 × CH₃CO), 88.3 (**C1**), 71.2 (**C5**), 68.1 (**C3**), 67.9 (**C2**), 67.1 (**C4**), 60.9 (**C6**), 20.9, 20.8, 20.7, 20.6 (4 × CH₃CO) ppm.

7.3.1.2. Synthesis of 2-(trimethylsilyl)ethyl-2,3,4,6-tetra-*O*-acetyl-galactopyranose¹⁶⁵ (**53**)



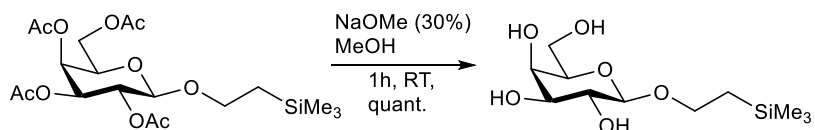
Tetraacetyl-galactosyl bromide **52** (1g, 2.43 mmol) and 2-(Trimethyl)silylethanol (523 μ L, 3.65 mmol) were dissolved in dry CH₂Cl₂ (10 mL) and stirred over molecular sieve 4 \AA for 2h at room temperature and Ar-atmosphere. Ag₂CO₃ (1.01 g, 3.65 mmol) and AgClO₄ (120 mg, 0.58 mmol) were added (start 16:00 h) and the reaction was stirred under the same conditions and at darkness overnight. After a reaction time of 18h, the mixture was filtrated through Celite and the solvent was removed. The glycosylation product (747 mg, 1.66 mmol) was obtained by chromatography (petrol/EtOAc 4:1 -> 3:1 -> EtOAc) with a yield of 68%.

¹H-NMR (500 MHz, CDCl₃): δ = 5.38 (dd, J = 3.4 Hz, J = 1.0 Hz, 1H, **H4**), 5.18 (dt, J = 16.8 Hz, J = 8.4 Hz, 1H, **H2**), 5.01 (dd, J = 10.4 Hz, J = 3.4 Hz, 1H, **H3**), 4.48 (d, J = 8.0 Hz, 1H, **H1**), 4.23 – 4.09 (m, 3H, **H6a/b**), 3.98 (ddd, J = 10.8 Hz, J = 9.6 Hz, J = 5.3 Hz, 1H, **OCH₂**), 3.92 – 3.87 (m, 1H, **H5**), 3.59 – 3.52 (m, 1H, **OCH₂**), 2.14, 2.04, 2.04, 1.98 (4 \times s, 12H, 4 \times **CH₃CO**), 1.03 – 0.85 (m, 2H, **CH₂CH₂Si**), 0.00 (s, 9H, 3 \times **CH₃Si**) ppm.

¹³C-NMR (126 MHz, CDCl₃): δ = 170.6, 170.5, 170.4, 169.5 (4 \times **CH₃CO**), 100.9 (**C1**), 71.3 (**C3**), 70.7 (**C5**), 69.1 (**C2**), 67.8 (**OCH₂**), 67.2 (**C4**), 61.4 (**C6**), 20.9, 20.8, 20.7 (4 \times **CH₃CO**), -1.3 (**Si(CH₃)₃**) ppm.

HRMS-ESI⁺ (m/z): calculated [M + Na⁺] = 471.1657, found 471.1642

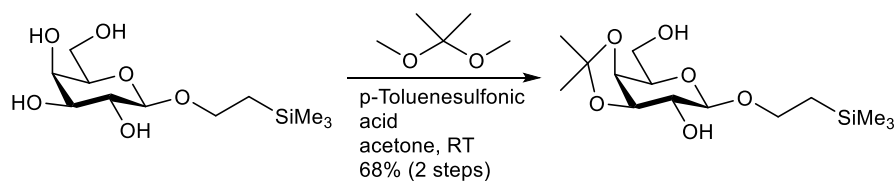
7.3.1.3. Synthesis of 2-(trimethylsilyl)ethyl-galactopyranose (54)



2-(Trimethylsilyl)ethanyl-2,3,4,6-tetraacetyl-galactopyranose (200 mg, 0.446 mmol) was dissolved in 2 mL MeOH. NaOMe (30% solution, 0.284 mL) was added and the reaction was stirred at RT for 1h. The solution was neutralized with Dowex 50W (H⁺ form), filtrated and concentrated. The crude product was verified by mass analysis and used without further purification for the next reaction.

HRMS-ESI⁺ (m/z): calculated [M + Na⁺] = 303.1234, found [M + Na⁺] = 303.1226

7.3.1.4. Synthesis of 2-(trimethylsilyl)ethyl-3,4-isopropylgalactopyranose¹⁶⁶ (49)



Trimethylsilylethanyl-galactopyranose **54** (125 mg, 0.446 mmol) was dissolved in 2 mL acetone. 2,2-Dimethoxypropane (66.9 μ L, 0.544 mmol) and p-toluenesulfonic acid monohydrate (1.7 mg, 0.02 mmol) were added and the reaction was stirred at RT. After a reaction time of 12 h, Et₃N (0.085 mL) was added and the solvent was removed. The product (61.4 mg,

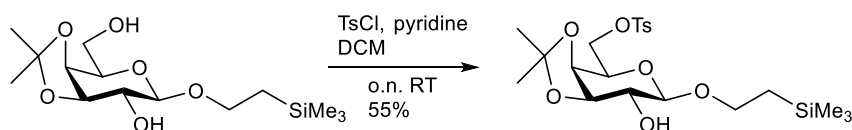
0.192 mmol) was purified by chromatography (petrol/EtOAc 3:1 → EtOAc) with a yield of 43%.

$^1\text{H-NMR}$ (400 MHz, CDCl_3): δ = 4.18 (t, J = 8.3 Hz, 1H, **H1**), 4.14 (dd, J = 5.6 Hz, J = 1.9 Hz, 1H, **H4**), 4.11 – 4.04 (m, 1H, **H3**), 4.04 – 3.92 (m, 2H, **H6a**, **OCH₂**), 3.84 (dt, J = 12.3 Hz, J = 5.1 Hz, 1H), **H5**, 3.61 – 3.47 (m, 2H, **H6b**, **OCH₂**), 1.49, 1.32 (2 × s, 2 × 3H, **CH₃**), 1.06 – 0.88 (m, 2H, **CH₂Si**), 0.02 – -0.12 (m, 9H, **Si(CH₃)₃**) ppm.

$^{13}\text{C-NMR}$ (100 MHz, CDCl_3): δ = 110.5 (**C(CH₃)₂**), 101.9 (**C1**), 78.9 (**C3**), 74.0 (**C4**), 73.7 (**C2**), 73.5 (**C5**), 67.6 (**OCH₂**), 62.5 (**C6**), 28.2, 26.5 (**C(CH₃)₂**), 18.38 (**CH₂Si**), -1.33 (**Si(CH₃)₃**) ppm.

HRMS-ESI⁺ (m/z): calculated [$\text{M} + \text{Na}^+$] = 323.1547, found 343.1544.

7.3.1.5. Synthesis of 2-(trimethylsilyl)ethyl-3,4-isopropyl-6-tosyl-galactose¹⁶⁷ (55)



2-(Trimethylsilyl)ethyl-3,4-isopropyl-galactose (60 mg, 0.187 mmol) was dissolved in 1 mL CH_2Cl_2 and tosylchloride (107 mg, 0.562 mmol) and pyridine (90.7 μL , 1.122 mmol) were added. The reaction was stirred at RT overnight before being concentrated. After chromatography (petrol/EtOAc 2:1 → 1:1 → EtOAc) the tosylated product was obtained with a yield of 57% (51 mg, 0.107 mmol).

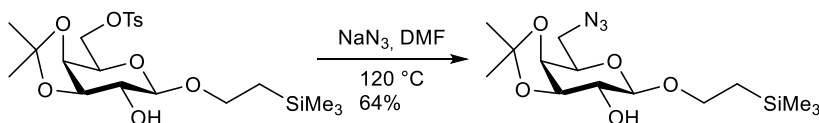
$^1\text{H-NMR}$ (400 MHz, CDCl_3): δ = 7.79 (d, J = 8.3 Hz, 2H, **H-Aryl**), 7.34 (d, J = 8.0 Hz, 2H, **H-Aryl**), 4.26 (qd, J = 10.5 Hz, J = 6.1 Hz, 2H, **H6a/b**), 4.13 (d, J = 8.3 Hz, 1H, **H1**), 4.11 – 4.08 (m, 1H, **H4/5**), 4.05 (d, J = 6.4 Hz, 1H, **H3**), 4.03 (d, J = 5.1 Hz, 1H, **H4/5**), 4.00 – 3.91 (m, 1H, **OCH₂**), 3.54 (ddd, J = 11.0 Hz, J = 9.7 Hz, J = 6.3 Hz, 1H, **OCH₂**), 3.46 (dd, J = 8.1 Hz,

$J = 7.4$ Hz, 1H, **H2**), 2.44 (s, 3H, **CH**₃-Aryl), 1.43, 1.27 ($2 \times$ s, 6H, $2 \times$ **CH**₃), 1.05 – 0.88 (m, 2H, **CH**₂SiMe₃), 0.02 (s, 9H, Si(**CH**₃)₃) ppm.

¹³C-NMR (101 MHz, CDCl₃): $\delta = 145.1$, 132.8 (**C**^{4°}-Aryl), 130.0, 128.1 (**CH**-Aryl), 110.6 (**C**(**CH**₃)₂), 101.7 (**C**1), 78.7 (**C**3), 73.6 (**C**2), 73.1 (**C**4/5), 71.1 (**C**4/5), 68.7 (**C**6), 67.6 (**OCH**₂), 28.1, 26.4 (**C**(**CH**₃)₂), 21.8 (**CH**₃-Aryl), 18.3 (**CH**₂SiMe₃), -1.3 (Si(**CH**₃)₃) ppm.

HRMS-ESI⁺ (m/z): calculated [M + H⁺] = 474.1744, found [M + H⁺] = 474.1700

7.3.1.6. Synthesis of 2-(trimethylsilyl)ethyl-3,4-isopropyl-6-azido-galactose (56)



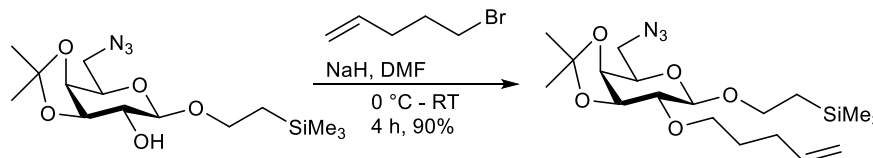
The monosaccharide 2-(trimethylsilyl)ethyl-3,4-isopropyl-6-tosyl-galactose (51 mg, 0.107 mmol) was dissolved in 4 mL anhydrous DMF and NaN₃ (42 mg, 0.645 mmol) was added. The reaction was stirred at 115-120 °C for 12 h, before being diluted with EtOAc. The organic layer was washed with saturated solution of NaCl (3x5 mL), dried with MgSO₄, filtrated and concentrated. The desired product was obtained after chromatography (hexane/EtOAc 2:1 → 1:1) with a yield of 64% (24 mg, 0.069 mmol).

¹H-NMR (400 MHz, CDCl₃): $\delta = 4.21$ (d, $J = 8.3$ Hz, 1H, **H**1), 4.09 (dd, $J = 5.0$ Hz, $J = 3.2$ Hz, 2H, **H**3, **H**4), 4.05 (ddd, $J = 10.9$ Hz, $J = 9.6$ Hz, $J = 6.1$ Hz, 1H, **OCH**₂), 3.93 (ddd, $J = 8.2$ Hz, $J = 4.2$ Hz, $J = 1.7$ Hz, 1H, **H**5), 3.73 (dd, $J = 13.1$ Hz, $J = 8.3$ Hz, 1H, **H**6a), 3.62 – 3.52 (m, 2H, **H**2, **OCH**₂), 3.32 (dd, $J = 13.1$ Hz, $J = 4.3$ Hz, 1H, **H**6b), 1.53, 1.35 ($2 \times$ s, $2 \times$ 3H, **C**(**CH**₃)₂), 1.01 (tdd, $J = 13.7$ Hz, $J = 9.4$ Hz, $J = 5.5$ Hz, 2H, **CH**₂Si(**CH**₃)₃), 0.02 (s, 9H, Si(**CH**₃)₃) ppm.

¹³C-NMR (100 MHz, CDCl₃): $\delta = 110.7$ **C**(**CH**₃)₂, 101.7 (**H**1), 78.7 (**C**3), 73.9 (**C**4), 73.8 (**C**2), 73.2 (**C**5), 67.6 (**OCH**₂), 51.2 (**C**6), 28.2, 26.5 (**C**(**CH**₃)₂), 18.3 (**CH**₂Si(**CH**₃)₃), -1.3 (Si(**CH**₃)₃) ppm.

HRMS-ESI⁺ (m/z): calculated [M + Na⁺] = 368.1612, found [M + Na⁺] = 368.1640

7.3.1.7. Synthesis of 2-(trimethylsilyl)ethyl-2-O-pentenyl-3,4-isopropyl-6-azido-galactose¹⁶⁸ (57)



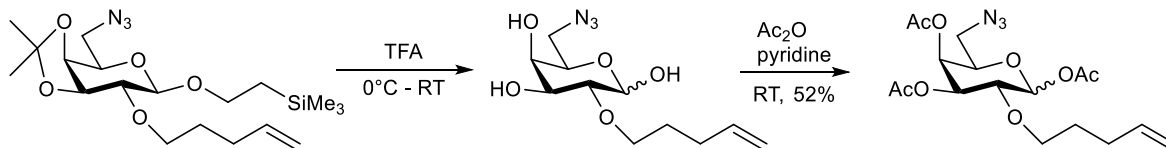
The sugar 2-(trimethylsilyl)ethyl-3,4-isopropyl-6-azido-galactose (24 mg, 0.069 mmol) was dissolved in 1 mL anhydrous DMF and cooled to 0 °C. Sodium hydride (60% in mineral oil, 13.9mg, 0.417 mmol) was added and after 15 min, 5-Bromo-1-pentene (32.6 μ L, 0.276 mmol) was added. The reaction was stirred from 0 °C to RT for 8 h. The reaction was quenched with water (1 mL) and diluted with EtOAc. The organic layer was washed with saturated solution of NaCl (3x2 mL), dried with MgSO₄, filtrated and concentrated. The crude mixture was purified by chromatography (hexane/EtOAc 2:1) and the product was obtained with a yield of 97% (27.8 mg, 0.067 mmol).

¹H-NMR (300 MHz, CDCl₃): δ = 5.82 (ddt, J = 16.9 Hz, J = 10.2 Hz, J = 6.6 Hz, 1H, CH=CH₂), 5.02 (ddd, J = 17.1 Hz, J = 3.6 Hz, J = 1.6 Hz, 1H, CH=CH₂), 4.95 (ddt, J = 10.2 Hz, J = 2.2 Hz, J = 1.2 Hz, 1H, CH=CH₂), 4.26 (d, J = 7.9 Hz, 1H, **H1**), 4.12 – 4.04 (m, 2H, **H3**, **H4**), 4.05 – 3.94 (m, 1H, OCH₂), 3.89 – 3.81 (m, 1H, **H5**), 3.80 – 3.71 (m, 1H), 3.71 – 3.63 (m, 1H), 3.61 – 3.51 (m, 1H), 3.30 (d, J = 4.2 Hz, 1H, **H6**), 3.28 – 3.22 (m, 1H), 2.19 – 2.08 (m, 2H, OCH₂CH₂CH₂), 1.74 – 1.61 (m, 2H, OCH₂CH₂), 1.52 (s, 3H, CH₃), 1.33 (s, 3H, CH₃), 1.00 (ddt, J = 12.3 Hz, J = 8.3 Hz, J = 4.2 Hz, 2H, CH₂Si(CH₃)₃), 0.85 (dd, J = 11.4 Hz, J = 4.5 Hz, 2H), 0.01 (s, 9H, Si(CH₃)₃).

¹³C-NMR (75 MHz, CDCl₃): δ = 138.6 (CH=CH₂), 114.7 (CH=CH₂), 110.3 (C(CH₃)₂), 102.4 (C1), 80.7 (C3), 79.2 (C2), 74.0 (C4), 72.8 (C5), 71.7 (OCH₂), 67.4 (OCH₂), 51.3 (C6), 30.3 (OCH₂CH₂), 29.3 (OCH₂CH₂CH₂), 27.8 (CH₃), 18.8 (CH₂Si(CH₃)₃), -1.32 (Si(CH₃)₃) ppm.

HRMS-ESI⁺ (m/z): calculated [M + Na⁺] = 436.2238, found [M + Na⁺] = 436.2200

7.3.1.8. Synthesis of 2-*O*-pentenyl-1,3,4-tri-*O*-acetyl-6-azido-galactopyranose (51)



The monosaccharide 2-(trimethylsilyl)ethyl-2-*O*-pentenyl-3,4-isopropyl-6-azido-galactose (27 mg, 0.065 mmol) was dissolved in 1 mL CH₂Cl₂ and cooled to 0 °C. Trifluoroacetic acid (29.9 μL, 0.392 mmol) was added and the reaction was stirred overnight from 0 °C to RT. The solvent was evaporated and co-evaporated with CH₂Cl₂ (3x5 mL). The crude residue was dissolved in 1 mL CH₂Cl₂ and pyridine (500 μL) as well as acetic anhydride (82 μL, 0.876 mmol) were added. The reaction was stirred for 12h at RT before being further diluted with CH₂Cl₂. The organic layer was washed with 1M HCl (2x3 mL) and saturated solution of NaCl (1x3 mL), dried with MgSO₄, filtrated and concentrated. The final product was obtained after chromatography (hexane/EtOAc 4:1 →2:1 → EtOAc) with a yield of 52% (13.7 mg, 0.034 mmol).

¹H-NMR (300 MHz, CDCl₃): δ = 6.43 (d, *J* = 3.7 Hz, 1H, **H1**), 6.27 (d, *J* = 4.4 Hz, 1H, **H1'**), 5.87-5.69 (m, 2H, **CH=CH₂**), 5.47 – 5.33 (m, 3H, **H4**), 5.20 (dd, *J* = 10.6 Hz, *J* = 3.4 Hz, 1H, **H3**), 5.05 – 4.93 (m, 5H, **CH=CH₂**), 4.34 (t, *J* = 4.1 Hz, 1H, **H5'**), 4.18 (t, *J* = 6.9 Hz, 1H), 4.14 – 4.06 (m, 1H), 3.95 – 3.85 (m, 2H, **H5**), 3.79 (dd, *J* = 10.5, *J* = 3.7 Hz, 1H, **H2**), 3.71 – 3.35 (m, 12H, **OCH₂**, **H6**), 2.16 (s, 3H, **CH₃**), 2.12 (s, 2H, **CH₃**), 2.02 (s, 2H, **CH₃**), 1.73 – 1.53 (m, 5H, **OCH₂CH₂**) ppm.

¹³C-NMR (75 MHz, CDCl₃): δ = 170.3, 170.2, 170.1 (**COCH₃**), 138.1 (**CH=CH₂**), 138.08 (**C'H=CH₂**), 115.28 (**CH=CH₂**), 115.09 (**CH=C'H₂**), 100.2 (**C1'**)_c, 94.11, 90.0 (**C1**), 87.3 (**C5**) 83.3, 77.36, 75.69, 73.19, 73.1 (**C2**), 72.69, 72.58, 70.8 (**C3**), 70.0 (**C6**)_c, 69.42, 68.7 (**C4**),

68.14, 50.6 (OCH₂), 50.3 (OC'H₂), 29.3, (CH₂CH=CH₂), 29.1 (C'H₂CH=CH₂), 21.4, 21.1, 21.0, 20.9, 20.8, 20.7 (CH₃ and C'H₃) ppm.

HRMS-ESI⁺ (m/z): calculated [M + Na⁺] = 422.1534, found [M + Na⁺] = 422.1600

7.3.2. Cell studies

The incorporation of the bifunctional galactose derivative was tested in HepG2 cells by confocal point-scanning microscopy. For this experiment, the cells were seeded on glass coverslips with a density of 15000 cells/well in 24-well plates (300 μL volume). The cells were allowed to attach to the coverslips for 24 h before the cell media was removed and replaced by cDMEM containing 100 μM or 200 μM of the bifunctional galactose derivative **51**. Pentaacetylated galactose (**42**) was used as negative control. The cells were grown in the presence of the unnatural sugar for 72 h, after which different staining procedures were applied.

The initial part of each staining procedure was the same during all conditions and represents the iEDDA of the terminal alkene of the sugar with 6-methyl-tetrazine-peg4-biotin. The cell culture medium was aspirated and endogenous biotin was blocked with 25 μg/mL streptavidin (from 1 mg/mL stock in water) in cDMEM for 40 min at 37 °C. The solution was removed and the cells were rinsed with PBS (2 x 200 μL). 200 μL of a 200 μM solution of 6-methyl-tetrazine-peg4-biotin in cDMEM was applied for 5 h at 37 °C. After this step, the cells were again rinsed with PBS (2x200 μL).

Different staining conditions were applied (Table 8):

Table 8: Different staining conditions after the metabolic incorporation of the bifunctional galactose derivative 51.

| Entry | 1 st staining step | 2 nd staining step |
|--------------|---|---|
| Condition 1: | 1h, RT 10 μ M DIBO-Alexa-Fluor-488 | 6.6 μ g/mL Alexa-Fluor-568-streptavidin, 20 min, RT |
| Condition 2: | 20 min 6.6 μ g/mL Alexa-Fluor-568-streptavidin, 20 min, RT | 1h, RT 10 μ M DIBO-Alexa-Fluor-488 |
| Condition 3: | 1h, RT 20 μ M DIBO-Alexa-Fluor-488 | 6.6 μ g/mL Alexa-Fluor-568-streptavidin, 20 min, RT |
| Condition 4: | 6.6 μ g/mL Alexa-Fluor-568-streptavidin, 15 min, RT | 15 min, RT 20 μ M DIBO-Alexa-Fluor-488 |
| Condition 5: | 6.6 μ g/mL Alexa-Fluor-568-streptavidin + 10 μ M DIBO-Alexa-Fluor-488, 30 min, RT | |

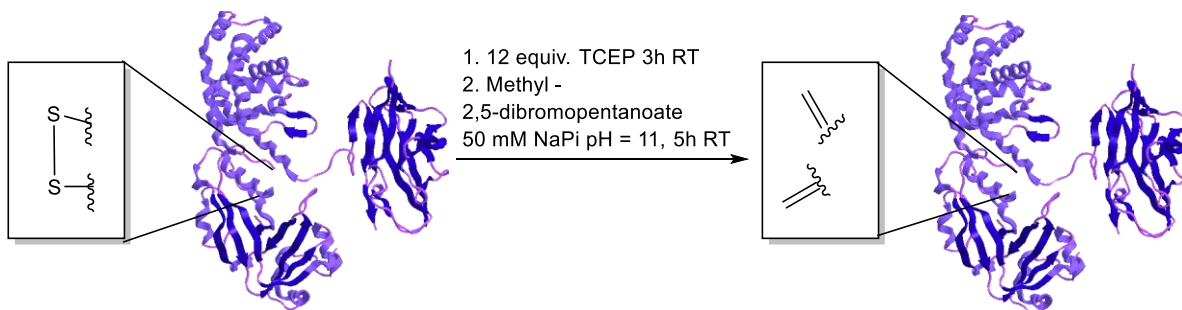
After the staining for the sugar moiety, the cell nuclei were stained with Hoechst33342 (1:1000) for 5 min in PBS + 5% FBS at RT. The cell samples were fixed with 4% PFA solution for 8 min at RT before being mounted on glass objectives, using Fluoromount GTM.

The samples were analyzed in a LSM880 confocal point-scanning microscope (Zeiss, Germany) with a Diode 405-30 nm, a Argon 488, a DPSS 561-20 nm and a HeNe594-2 nm laser unit. The pictures were acquired with a 63x Plan-Apochromat Oil objective and processed with ImageJ software package to remove background signal.

7.4. Materials and Methods for Chapter 4

7.4.1. Site selective modification of CRM197

7.4.1.1. Synthesis of CRM-DHA



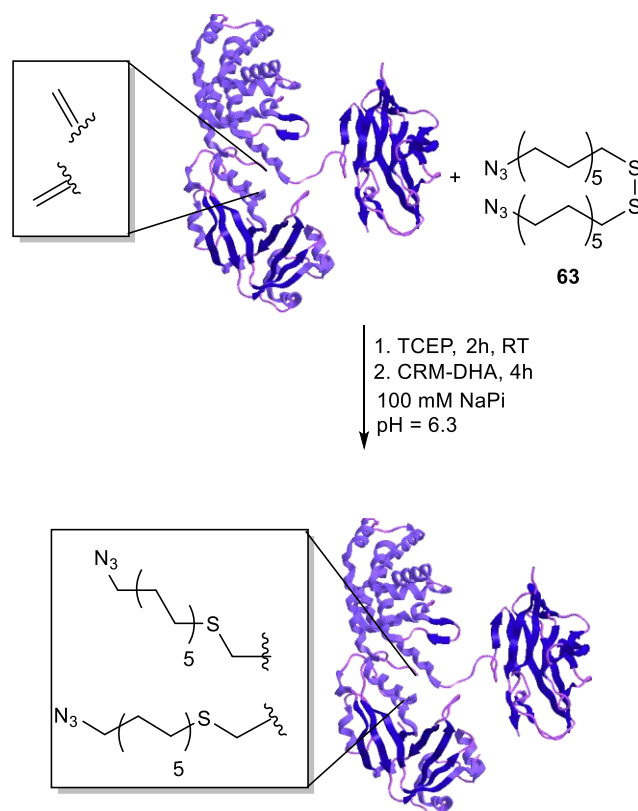
5 mg of CRM₁₉₇ (105.5 μ l of stock with $c=47.4$ mg/mL) were diluted to a final concentration of 5 mg/mL with 50 mM NaPi pH=11. A solution of TCEP (12 equiv. from 0.05M stock in 50 mM NaPi, pH=11) was added and the reaction mixture was kept in the dark gently moving at room temperature for 3 hours. Methyl-2,5-dibromopentanoate (**28**) (500 equiv., from 2 M stock in DMSO) was added, the mixture was vortex for 10 seconds and the reaction was completed after 3 hours at room temperature. CRM-DHA was purified in a Zeba Spin desalting column (7 kDa, MWCO) previously equilibrated with 100 mM NaPi, pH = 6.3. The concentration was determined by BCA assay and the protein aliquots were either stored at 4 °C or directly used.

Table 9: All reaction conditions for the conversion of cysteins C186 and C201 into dehydroalanine.

| Entry | TCEP (equiv.) | Time [h] | T [°C] | pH | 28 (equiv.) | Time [h] | T [°C] | Result |
|-----------|------------------|-------------|-----------|-----------|----------------|-------------|-----------|--|
| 1 | 6 | 1.5 | 37 | 8-9.5 | 50 | 2 | 21 | - |
| 2 | 6 | 1 | 37 | 9 | 50 | 4 | 21 | - |
| 3 | 6 | 1 | 37 | 9 | 50 | 7 | 21 | - |
| 4 | 6 | 1 | 37 | 9 | 50 | 8 | 21 | - |
| 5 | 6 | 1 | 37 | 9 | 50 | 15 | 21 | - |
| 6 | 12 | 2.5 | 37 | 9 | 50 | 24 | 21 | - |
| 7 | 6 | 2.5 | 37 | 9 | 50 | 24 | 21 | - |
| 8 | 12 | 3 | 21 | 9 | 50 | 48 | 21 | - |
| 9 | 12 | 3 | 21 | 9 | 100 | 48 | 21 | adduct |
| 10 | 12 | 3 | 21 | 9-10 | 100 | 24 | 21 | - |
| 11 | 12 | 3 | 21 | 9-10 | 100 | 3 | 21 | - |
| 12 | 12 | 3 | 21 | 10 | 100 | 3 | 21 | Partial elimination |
| 13 | 12 | 3 | 21 | 9-10 | 100 | 24 | 21 | - |
| 14 | 12 | 3 | 21 | 10 | 100 | 24 | 21 | Partial elimination |
| 15 | 20 | 12 | 3 | 21 | 500 | 3 | 21 | Precipitation, only traces of Dha |
| 16 | 2 | 12 | 3 | 21 | 500 | 3 | 21 | Main peak for Dha, smaller for side product |
| 17 | 5 | 12 | 3 | 21 | 500 | 5 | 21 | Dha |
| 18 | 10 | 12 | 3 | 21 | 500 | 5 | 21 | Precipitation |
| 19 | 2 | 12 | 3 | 21 | 500 | 5 | 21 | - |
| 20 | 2 | 12 | 3 | 21 | 500 | 18 | 21 | - |

| | | | | | | | | |
|----|---|----|---|----|-----|---|----|---|
| 21 | 2 | 12 | 3 | 21 | 500 | 3 | 37 | - |
| 22 | 2 | 12 | 3 | 21 | 500 | 5 | 37 | - |

7.4.1.2. Synthesis of CRM-DHA-N₃



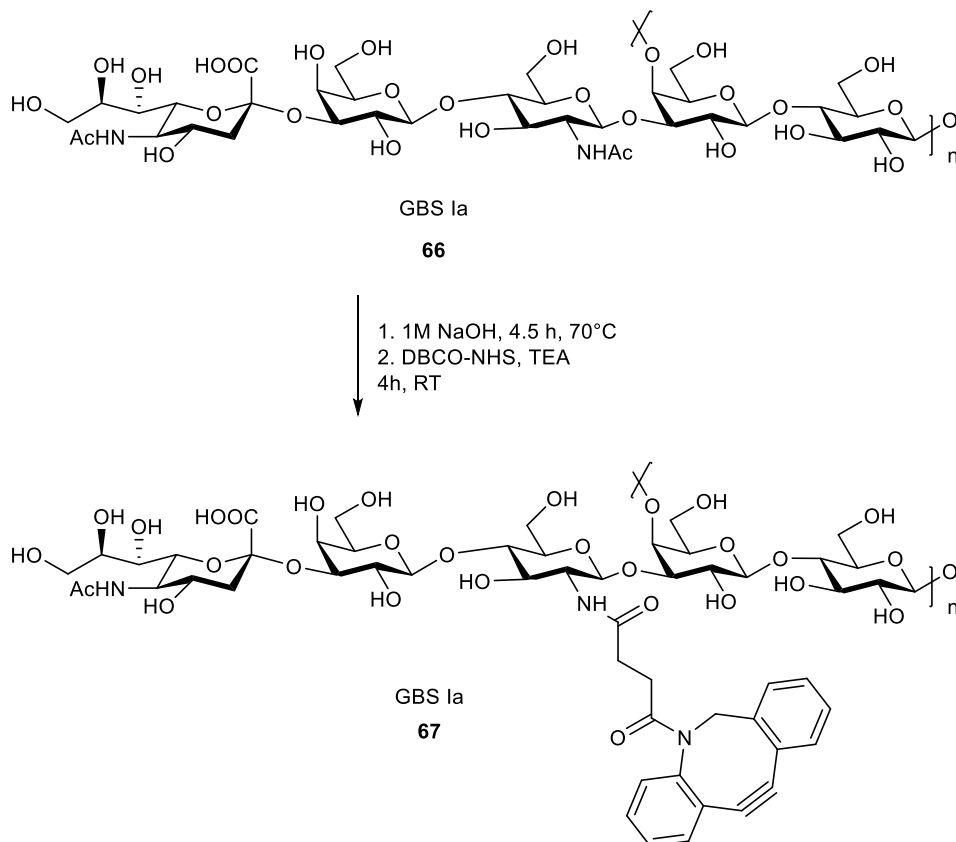
A sample of bis(11-azidoundecyl)disulfide **63** (100 equiv., from stock 43.8 mM in DMSO) was mixed with a freshly prepared solution of TCEP (100 equiv. from stock 0.05 M in H₂O) and kept gently moving in the dark at room temperature for 2h. An aliquot of CRM-DHA (in 100 mM NaPi pH=6.3, c~2 mg/mL) was added directly and the reaction was kept gently moving at room temperature for 4 h. The modified protein was purified using Zeba Spin desalting columns (7 kDa MWCO) which were previously equilibrated with 12 mM NaPi, pH = 7.2. The purified protein CRM-DHA-N₃ was used directly for the following conjugation step.

7.4.1.3. Preparation of the protein samples for High Resolution Mass Spectrometry

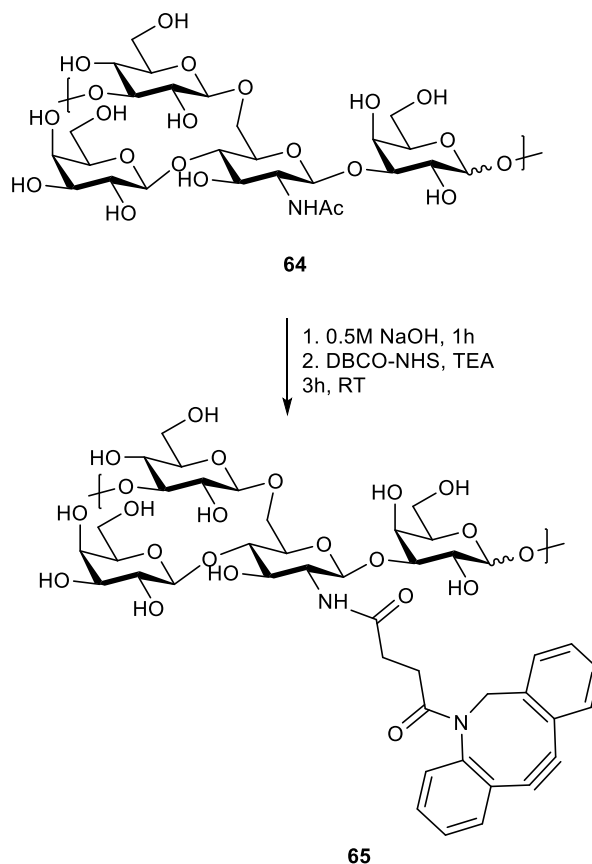
Around 150 μg of each protein sample were prepared for analysis by high resolution mass spectrometry. The samples were loaded on an amicon centrifugal filter (10 kDa MWCO), which were previously washed with water (2 x 500 μL), and desalted with 400 μl water (13000 g, 10 min). To ensure a buffer exchange to ammonium acetate, the protein solution was washed 3x with a 5 mM solution of ammonium acetate (3 x 400 μL , 13000 g, 10 min). The final concentration was obtained by a centrifugation with 400 μL 5 mM ammonium acetate at 13000 g for 15 min. The protein samples were recovered from the centrifugal filters using the spin protocol at 1000 g for 2 min. For the analysis, 10 μl of each sample were diluted with 90 μL water and 100 μL acetonitrile and were acidified by adding 0.5 μL formic acid. The samples were analyzed in a Bruker Solarix FT-ICR-MS machine, equipped with a 7 Tesla magnet.

7.4.2. Derivatization of Polysaccharide antigens

7.4.2.1. Derivatization of polysaccharide from group B streptococcus serotype Ia 67



The polysaccharide GBS1a **66** was diluted to a final concentration of 2 mg/mL in 1.25 M NaOH and heated to 70 °C for 4.5 h. After neutralization with acetic acid, the polysaccharide was purified in PD10 G25 columns, equilibrated with water. The evaporated residue was resolved in 80 μ l DMSO and 80 μ l water, followed by the addition of 10 μ l DBCO-NHS solution (1 mg DBCO-NHS in 50 μ l DMSO) and 2 μ l triethylamine solution (2 μ l triethylamine in 18 μ l water). The reaction was purified on PD 10 G25 columns after 4 h at room temperature and the solvent was evaporated. The polysaccharide was used in a concentration of 10 mg/mL in deuterated water.

7.4.2.2. Derivatization of pneumococcal type 14 capsular polysaccharide **64**

A sample of 10 mg of pneumococcal type 14 polysaccharide **64** was dissolved in Milli Q water to reach a final concentration of 20 mg/mL. The solution was diluted with 0.55 M NaOH to a concentration of 2 mg/mL polysaccharide and 0.5 M final concentration of NaOH. The reaction was incubated at 70 °C for 1 h, before being neutralized with concentrated acetic acid. The mixture was purified in PD 10 G25 columns, previously equilibrated with water. After evaporation of the solvent, the residue was resolved in 25 μ L water and 175 μ L DMSO. 50 μ L of the linker DBCO-NHS (1 mg per 50 μ L) were added, together with 2 μ L of TEA solution (2 μ L triethylamine in 18 μ L water). The reaction was performed at room temperature for 3 h, before being purified on a PD 10 G25 column, equilibrated with water. The solvent was evaporated. The polysaccharide was used in a concentration of 10 mg/mL in deuterated water.

7.4.3. Glycoconjugation with CRM-DHA-N₃

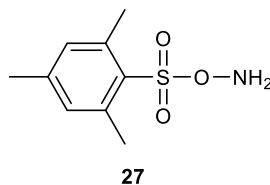
The conjugation reactions between CRM-DHA-N₃ and the polysaccharides GBS-Ia-dbcO **67** or PN14-dbcO **65** were performed in the same manner, however for GBS-Ia-dbcO **67** a ratio of 1:2 protein/polysaccharide was used, in contrast to conjugations with PN1-dbcO **65** in which a ratio of 1:4 was applied.

For the conjugation reaction, the protein CRM-DHA-N₃ in 12 mM NaPi, pH = 7, was mixed with the aqueous solution of the corresponding polysaccharide. A suspension of dehydroascorbic acid (36 mg/mL) in water was added with a concentration of 2.5 µg per µg protein. The reaction was performed at room temperature for at least 5 h, however in this stage, the reaction can be also performed overnight. The crude mixture was used directly for the purification method of choice.

7.5. Materials and Methods for Chapter 5

7.5.1. Chemical synthesis

7.5.1.1. Synthesis of *O*-mesitylsulfonylhydroxylamine (**27**) (MSH)¹⁰⁷



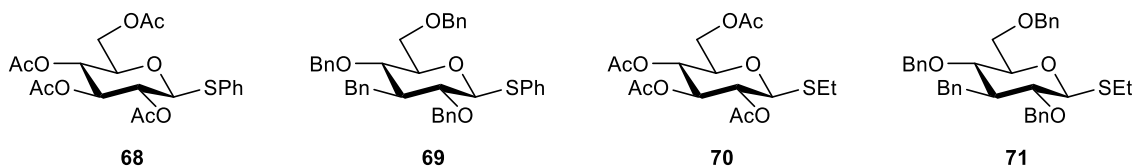
The starting material ethyl *N*-hydroxyacetamidate (1.18 mg, 11.4 mmol) was dissolved in 6 mL DMF and triethylamine (1.5 mL) was added. The solution was cooled to 0 °C and 2-mesitylsulfonylchlorid (2.5 g, 11.4 mmol) was added in small portions while the mixture was stirred vigorously. After 30 min, the reaction was diluted with Et₂O (100 mL) and washed repeatedly with H₂O (4x50 mL). The aqueous layers were extracted with Et₂O and the combined organic layers were dried with MgSO₄ and concentrated. The intermediate compound ethyl-*O*-(mesitylsulfonyl)acetohydroxamate (2.39 mg, 8.39 mmol, 74%) was obtained as white solid and was directly used for the next step.

The obtained residue (2.39 g, 8.39 mmol) was dissolved in 3 mL dioxane and cooled to 0 °C. Perchloric acid (70%, 1 mL) was added dropwise and the reaction was stirred for 10 min. When the mixture solidified, it was transferred into 100 mL of ice cold H₂O and the flask was rinsed with H₂O and Et₂O. After extraction of the aqueous layer with Et₂O (3x30 mL), the combined organic layers were washed with saturated solution of NaCl (2x50 mL) and dried/neutralized with K₂CO₃. The solution was filtrated and carefully concentrated to a volume less than 50 mL before poured into 50 mL of ice cold petrol. The desired product MSH was obtained after crystallization with a yield of 49% (885 mg, 4.11 mmol).

¹H-NMR (400 MHz, CDCl₃): δ = 7.00 (s, 2H, **H3**, **H5**), 2.59 (s, 6H, 2 × o/p-**CH**₃), 2.34 (s, 3H, m-**CH**₃) ppm.

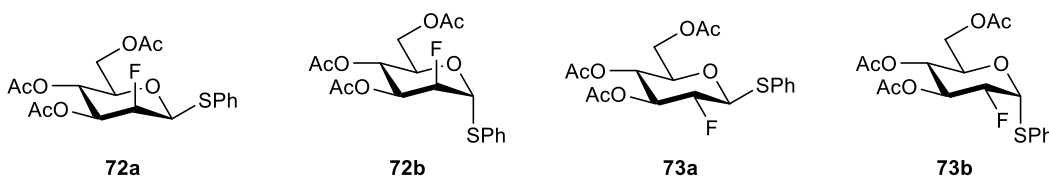
¹³C-NMR (100 MHz, CDCl₃): δ = 141.0, 131.7 (C-Ar), 22.7 (2 × **CH**₃), 21.1 (**CH**₃) ppm.

7.5.1.2. Synthesis of the thioglycoside donors 68-71



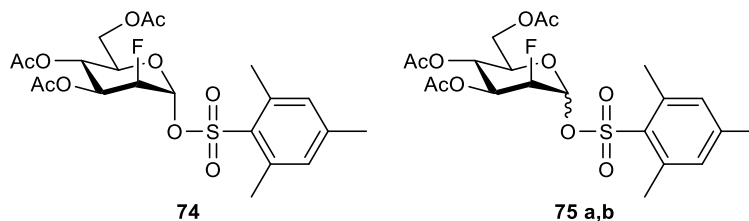
The four thioglycoside donors phenyl-2,3,4,6-tetra-*O*-acetyl-1-thio- β -glucopyranose (**68**), phenyl-2,3,4,6-tetra-*O*-benzyl-1-thio- β -glucopyranose (**69**), ethyl-2,3,4,6-tetra-*O*-acetyl-1-thio- β -glucopyranose (**70**) and ethyl-2,3,4,6-tetra-*O*-benzyl-1-thio- β -glucopyranose (**71**) were synthesized based on reported procedures in the literature.¹⁶⁹ The fully characterized spectra were conform with the ones published earlier.

7.5.1.3. Synthesis of the 2-deoxy-2-fluoro-thioglycoside donors 72a, b, 73a, b



The 2-deoxy-2-fluoro substituted thioglycoside donors phenyl-3,4,6-tri-*O*-acetyl-2-deoxy-2-fluoro-1-thio- α -D-mannopyranose (**72b**), phenyl-3,4,6-tri-*O*-acetyl-2-deoxy-2-fluoro-1-thio- β -D-mannopyranose (**72a**), phenyl-3,4,6-tri-*O*-acetyl-2-deoxy-2-fluoro-1-thio- α -D-glucopyranose (**73b**) and phenyl-3,4,6-tri-*O*-acetyl-2-deoxy-2-fluoro-1-thio- β -D-glucopyranose (**73a**) were synthesized according to literature procedure by Míriam Salvadó (Department de Química Analítica I Química Orgànica, Universitat Rovira I Virgili, C/Marcellí Domingo 1, 43007 Tarragona, Spain).^{160,170,171}

7.5.1.4. Synthesis of the 1-*O*-sulfofmesitylen intermediates from 2-deoxy-2-fluoro-glycosides **74**, **75a,b**



The same procedure was applied for all 2-deoxy-2-fluoro-thioglycosides.

A sample of the corresponding 2-deoxy-2-fluoro-thioglycoside **72a**, **72b**, **73a** or **73b** was dissolved in dry CH_2Cl_2 , followed by the addition of MSH (5 equiv.) and K_2CO_3 (2 equiv.). The reaction was stirred at room temperature for 16 h, before being diluted with DCM and washed with saturated Na_2CO_3 and saturated NaCl solution. The 1-*O*-sulfofmesitylen products were obtained after chromatography.

^1H - and ^{13}C -NMR of 2-fluoro-3,4,6-triacetyl-sulfonylmesitylmannopyranose (**74**)

^1H -NMR (500 MHz, CDCl_3): δ = 7.01 (s, 2H, **H**-Mes), 5.91 (dd, J = 6.3 Hz, J = 1.9 Hz, 1H, **H**1), 5.35 (t, J = 10.1 Hz, 1H, **H**4), 5.27 – 5.13 (m, 1H, **H**3), 4.88 – 4.72 (m, 1H, **H**2), 4.07 (dd, J = 12.6 Hz, J = 3.9 Hz, 1H, **H**6), 3.79 – 3.69 (m, 1H, **H**5), 3.64 (dd, J = 12.6 Hz, J = 2.3 Hz, 1H, **H**6), 2.65 (s, 6H, **CH**₃-Mes), 2.33 (s, 3H, **CH**₃-Mes), 2.10, 2.06 – 2.03, 2.03 (3 × s, 9H **CH**₃CO) ppm.

^{13}C -NMR (126 MHz, CDCl_3): δ = 170.6, 169.9, 169.4 (3 × **CH**₃CO), 144.4, 140.1 (2 × **C**4°-Mes), 132.1, 131.3 (**CH**-Mes), 95.9 (**C**1), 86.92, 85.39 (**C**2, **C**2'), 71.3 (**C**5), 69.4, 69.2 (**C**3, **C**3'), 64.8 (**C**4), 60.8 (**C**6), 22.8, 21.3 (**CH**₃-Mes), 20.77, 20.71 (**CH**₃CO) ppm.

^{19}F NMR (376 MHz, CDCl_3) δ -202.59 (s) ppm.

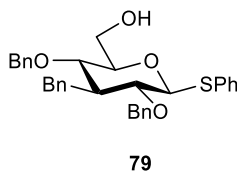
^1H - and ^{13}C -NMR of 2-fluoro-3,4,6-triacetyl-sulfonylmesitylglucopyranose (**75a, b**)

$^1\text{H-NMR}$ (400 MHz, CDCl_3): $\delta = 6.98$ (d, $J = 12.5$ Hz, 2H, **H-Aryl**), 5.99 (d, $J = 3.9$ Hz, 1H, **H1**), 5.54 – 5.41 (m, 1H, **H3**), 5.04 (dd, $J = 19.9$ Hz, $J = 9.9$ Hz, 1H, **H4**), 4.67 – 4.47 (m, 2H, **H2**, **H2'**), 4.18 (dt, $J = 12.3$ Hz, $J = 6.2$ Hz, 1H, **H6**), 4.04 (ddd, $J = 10.4$ Hz, $J = 3.8$ Hz, $J = 2.1$ Hz, 1H, **H5**), 3.79 (ddd, $J = 8.7$ Hz, $J = 7.3$ Hz, $J = 2.3$ Hz, 1H, **H6**), 2.65 (s, 6H, $2 \times \text{CH}_3\text{-Mes}$), 2.31 (s, 3H, $\text{CH}_3\text{-Mes}$), 2.05 (s, 6H, $2 \times \text{CH}_3\text{O}$), 2.03 (s, 3H, CH_3O) ppm.

$^{13}\text{C-NMR}$ (100 MHz, CDCl_3): $\delta = 170.6$, 169.9, 169.6 ($3 \times \text{CH}_3\text{CO}$), 144.2 (*p*-**C-Mes**), 140.3 (**C1-Mes**), 132.0, 131.1 ($\text{C4}^\circ\text{-CH}_3\text{Mes}$), 94.9, 94.7 (**C1**, **C1'**), 87.0, 85.0 (**C2**, **C2'**), 70.3 (**C3**), 69.9 (**C5**), 67.1 (**C4**) 60.7 (**C6**), 22.8 ($2 \times \text{CH}_3\text{-Mes}$), 21.2 ($\text{CH}_3\text{-Mes}$), 20.7, 20.6 ($3 \times \text{CH}_3\text{O}$) ppm.

$^{19}\text{F NMR}$ (376 MHz, CDCl_3) δ -199.38 (ddd, $J = 50.3$, 14.7, 3.2 Hz), -201.26 (dd, $J = 48.3$, 11.8 Hz).

7.5.1.5. Synthesis of phenyl-2,3,4-tri-*O*-benzyl-1-thio- β -*D*-glucose (**79**)¹⁷²



Phenyl-tetra-*O*-acetyl-1-thio- β -*D*-glucopyranosid (170 mg, 0.389 mmol) was dissolved in MeOH and 0.23 mL of 30% NaOMe solution in MeOH was added. The reaction was stirred at RT until reaction control by TLC (Petrol/EtOAc 2:1) showed complete consumption of the starting material. The mixture was neutralized with Dowex 50W (H^+ form), filtrated and concentrated. Phenyl-thioglucofuranose was obtained with 100%. Phenyl-thioglucofuranosid (106 mg, 0.389 mmol) and trityl chloride (109 mg, 0.389 mmol) were dissolved in pyridine (1 mL) and stirred at RT. The reaction was controlled by TLC (EtOAc). After 16h another 70 mg trityl chloride were added. After 22 h, the reaction mixture was poured into H_2O and extracted with DCM, the organic layers were washed with H_2O , dried over MgSO_4 , filtrated and

concentrated. The crude phenyl-6-*O*-trityl-thioglucofuranose was dissolved in 2 mL anhydrous DMF and cooled to 0°C. NaH (60% in mineral oil, 62.6 mg, 1.87 mmol) was added and the mixture was stirred for 30 min. Benzyl bromide (0.22 mL, 1.87 mmol) was added and the reaction was stirred overnight at 0° - RT. The reaction mixture was cooled again and 2 mL H₂O were added carefully. The reaction was extracted with CH₂Cl₂ (3 x 10 mL), the combined organic layers were washed with NaCl (saturated solution 3 x 10 mL) and dried over MgSO₄. After filtration and concentration, the crude product was directly used for the next reaction. Phenyl-tribenzyl-6-*O*-trityl-1-thio-β-D-glucofuranose was dissolved in MeOH/DCM (4:1) and *p*-TsOH (37.1 mg, 0.195 mmol) was added. After a reaction time of 24 h, TLC showed complete consumption of the starting material. The mixture was neutralized with Et₃N and the solvent was removed. The final compound was purified by chromatography (from petrol/ EtOAc 6:1 to EtOAc), resulting in **79** (51%, 63.1 mg, 0.2 mmol) as a white solid.

HRMS-ESI⁺ (m/z) C₃₃H₃₄O₅S: calculated [M + Na⁺] = 565.2019, found [M + Na⁺] = 565.2019.

¹H-NMR (400 MHz, CDCl₃): δ = 7.51 (dt, *J* = 4.4 Hz, *J* = 2.4 Hz, 2H, Bn/SPh), 7.42 – 7.27 (m, 18H, Bn/SPh), 4.96 – 4.81 (m, 4H, 2 × CH₂Ph), 4.77 (d, *J* = 10.3 Hz, 1H, CH₂Ph), 4.72 (d, *J* = 9.8 Hz, 1H, **H1**), 4.65 (d, *J* = 11.0 Hz, 1H, CH₂P), 3.88 (dd, *J* = 12.0 Hz, *J* = 2.6 Hz, 1H, **H6**), 3.78 – 3.64 (m, 2H, **H6**, **H3**), 3.58 (t, *J* = 9.4 Hz, 1H, **H4**), 3.53 – 3.45 (m, 1H, **H2**), 3.39 (ddd, *J* = 9.6 Hz, *J* = 4.9 Hz, *J* = 2.7 Hz, 1H, **H5**) ppm.

¹³C-NMR (100 MHz, CDCl₃) δ = 139.2, 138.4, 138.0, 137.9 (4 × C^{4°} in Ph), 132.0, 129.2, 128.7, 128.6, 128.5, 128.4, 128.2, 128.1, 128.0, 127.9 (CH in Ph), 87.4 (**C1**), 86.7 (**C3**), 81.2 (**C2**), 79.4 (**C5**), 77.8 (**C4**), 75.9, 75.7, 75.2 (4 × PhCH₂), 62.5 (**C6**).

7.5.2. General procedure of the glycosylation reaction using MSH as activating reagent

The indicated glycosyl acceptor (1.3 equiv.) was dissolved in the indicated dry solvent and stirred over molecular sieve 3 Å for 30 min. Cu(OTf)₂ (1.5 equiv.) was added for 10 min, followed by the addition of the assigned thio-glycosyl donor (1 equiv.) MSH (5 equiv.) was

added and the reaction was stirred at room temperature until monitoring by TLC indicated the completion of the reaction. The reaction mixture was filtered through Celite and the organic layer was washed with saturated solutions of Na₂CO₃ and NaCl. The final products were obtained after purification by chromatography. The yields and stereoselectivity were indicated in the corresponding table. All compounds were fully characterized and correspond to spectra published in the literature.

7.5.3. Procedure for the selective activation of *S*-ethyl over *S*-phenyl thioglycosides

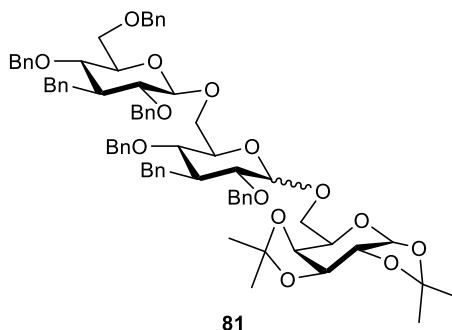
The glycosyl acceptor 6-*O*-tripbenzylthiophenyl-glucofuranose **78** (23.8 mg, 0.044 mmol) was dissolved in 2 mL dry CH₃CN and stirred over molecular sieve 3 Å for 30 min. Cu(OTf)₂ (18.4 mg 0.051 mmol) was added for 10 min, followed by the addition of the donor ethyl-2,3,4,6-tetrabenzylthioglucose **71** (20 mg, 0.034 mmol). MSH (36.6 mg, 0.17 mmol) was added and the reaction was stirred at RT for 15 min. The mixture was filtered through Celite and the organic layer was washed with saturated solutions of Na₂CO₃ and NaCl. The disaccharide was obtained after chromatography (petrol/EtOAc 3:1) with a yield of 50% (18.1 mg, 0.017 mmol)

¹H-NMR (500 MHz, CDCl₃): δ = 7.54 (d, *J* = 7.5 Hz, 2H), 7.42-7.15 (m, 38H, *H*-Phenyl), 5.02 (s, 1H, *H*1), 5.01 – 4.42 (m, 19H), 4.40 (d, *J* = 7.7 Hz, 1H, *H*1'), 4.17 (d, *J* = 11.1 Hz, 1H), 3.76 – 3.55 (m, 8H), 3.52 – 3.39 (m, 4H) ppm.

¹³C-NMR (126 MHz, CDCl₃): δ = 139.1, 138.9, 138.8, 138.7, 138.6, 138.6, 138.4, 138.3, 138.2, 135.4, 134.2, 132.3, 131.6, 129.1, 128.7, 128.6, 128.5, 128.4, 128.4, 128.3, 128.2, 128.1, 128.0, 127.9, 127.8, 127.8, 127.6, 127.6, 127.5, 127.4, 104.1 (*C*1'), 97.6 (*C*1), 88.3, 87.5, 86.9, 84.9, 82.5, 81.9, 81.3, 81.0, 80.3, 79.1, 78.2, 75.9, 75.6, 75.2, 75.1, 74.9, 73.7, 69.1, 68.8 ppm.

LRMS-ESI⁺ (m/z) C₆₇H₆₈O₁₀S: calculated [M + Na⁺] = 1087.4425, found [M + Na⁺] = 1087.4386.

7.5.4. Synthesis of the trisaccharide 2,3,4,6-tetrabenzylglucopyranosyl-(1,6)-2,3,4-tribenzylglucopyranosyl-(1,6)-1,2,3,4-diisopropylidengalactopyranosid (81)



Diisopropylgalactose (4.7 mg, 0.014 mmol) and the disaccharide phenyl-6-*O*-(2,3,4,6-tetra-*O*-benzylglucopyranose)-2,3,4-tri-*O*-benzyl- β -thioglucopyranose (6.4 mg, 0.006 mmol) were dissolved in dry CH₃CN (2 mL) and stirred over molecular sieve 3 Å for 10 min. NBS (3.2 mg, 0.018 mmol) was added, followed by the addition of Cu(OTf)₂ (1.63 mg, 0.0045 mmol) after 5 min. The reaction was stirred at RT for 16 h, before being filtered through Celite. The concentrated mixture was purified by chromatography (petrol/EtOAc 3:1 → EtOAc). The trisaccharide was obtained with a yield of 50% (4 mg, 0.003 mmol, α/β 1:1).

¹H-NMR (500 MHz, CDCl₃): δ = 7.36 – 7.17, 5.54 (d, J = 4.8 Hz, 1H, **H1_c**), 5.52 (d, J = 5.0 Hz, 1H, **H1_c**), 5.12, 5.05, 4.94, 4.82 – 4.68, 4.63 – 4.48, 4.42 (d, J = 7.8 Hz, 1H, **H1_b**), 4.40 (d, J = 7.8 Hz, 1H, **H1_a**), 4.35 – 4.34, 4.33 – 4.32, 4.32 – 4.26, 4.24, 4.00 – 3.95, 3.94 – 3.90, 3.79 – 3.58, 3.45 – 3.39, 1.53, 1.37 ppm.

¹³C-NMR (126 MHz, CDCl₃): δ = 138.8, 138.5, 138.3, 138.2, 128.7, 128.5, 128.2, 128.1, 127.9, 127.8, 127.7, 127.6, 127.4, 109.6, 109.3, 108.9, 108.5, 104.4 (**C1_b**), 103.9 (**C1_a**), 96.4 (**C1_c**), 96.3 (**C1_c**), 84.8, 84.5, 81.8, 81.5, 75.7, 75.6, 71.3, 70.8, 70.7, 70.6, 70.5, 70.4, 70.3, 68.1, 67.4, 67.3, 66.9, 26.0, 25.9, 24.9, 24.3 ppm.

The spectroscopic data were the same than reported in the literature.¹⁷³

LRMS-ESI⁺ (m/z) C₇₃H₈₂O₁₆: calculated [M + Na⁺] = 1237.5495, found [M + Na⁺] = 1237.5455.

7.5.5. Computational details

The experimental part on the computational calculations was performed by Gonzalo Jiménez-Osés (Departamento de Química, Centro de Investigación en Síntesis Química, Universidad de La Rioja, 26006 Logrono, Spain).

7.5.6. NMR studies

The described activation reaction of thioglycosides **68-71** with MSH **27** were performed directly in the NMR tube. Before the addition of the activating agent MSH **27** and K_2CO_3 , the NMR of the starting material was measured. The reactions were conducted at room temperature while the NMR tubes were gently moved. For the kinetic calculations, the peak of the anomeric proton **H1** of the starting material was used as internal reference with the value 1. The reaction progress was measured, calculating the ratio of the anomeric proton **H1'** of the intermediate.

8. References

1. Ghazarian, H. et al. A glycobiochemistry review: carbohydrates, lectins and implications in cancer therapeutics. *Acta Histochem.* **113**, 236-247 (2011).
2. Varki A., K.S. Historical Background and Overview. in *Essentials of Glycobiochemistry* (Cold Spring Harbor, New York, 2017).
3. Feizi, T. Carbohydrates and glycoconjugates Glycomics: the new era of carbohydrate biology. *Curr. Opin. Struct. Biol.* **13**, 602-604 (2003).
4. Lindhorst, T.K. Structure and biosynthesis of glycoconjugates. in *Essentials of Carbohydrate Chemistry and Biochemistry* (Wiley-VCH GmbH & Co. KGaA, Weinheim, 2007).
5. Solis, D. et al. A guide into glycosciences: How chemistry, biochemistry and biology cooperate to crack the sugar code. *Biochim. Biophys. Acta* **1850**, 186-235 (2015).
6. Stanley P, T.N., Aebi M. N-Glycans. in *Essentials of Glycobiochemistry* (ed. Varki A, C.R., Esko JD) (Cold Spring Harbor, New York, 2017).
7. Brockhausen I, S.P. O-GalNAc Glycans. in *Essentials of Glycobiochemistry* (ed. Varki A, C.R., Esko JD) (Cold Spring Harbor, New York, 2017).
8. Hart, G.W. et al. Cross talk between O-GlcNAcylation and phosphorylation: roles in signaling, transcription, and chronic disease. *Annu. Rev. Biochem.* **80**, 825-858 (2011).
9. Harris, R.J. et al. Tissue plasminogen activator has an O-linked fucose attached to threonine-61 in the epidermal growth factor domain. *Biochemistry* **30**, 2311-2314 (1991).
10. Schegg, B. et al. Core glycosylation of collagen is initiated by two beta(1-O)galactosyltransferases. *Mol. Cell. Biol.* **29**, 943-952 (2009).
11. Dube, D.H. et al. Glycans in cancer and inflammation--potential for therapeutics and diagnostics. *Nat. Rev. Drug. Discov.* **4**, 477-488 (2005).
12. Turner, G.A. N-glycosylation of serum proteins in disease and its investigation using lectins. *Clin. Chim. Acta* **208**, 149-171 (1992).
13. Fu, C. et al. Tumor-associated antigens: Tn antigen, sTn antigen, and T antigen. *HLA* **88**, 275-286 (2016).

14. Paredes, J. et al. Epithelial E- and P-cadherins: Role and clinical significance in cancer. *Biochim. Biophys. Acta* **1826**, 297-311 (2012).
15. de Freitas Junior, J.C. et al. Inhibition of N-linked glycosylation by tunicamycin induces E-cadherin-mediated cell-cell adhesion and inhibits cell proliferation in undifferentiated human colon cancer cells. *Cancer Chemother. Pharmacol.* **68**, 227-238 (2011).
16. Carvalho, S. et al. Preventing E-cadherin aberrant N-glycosylation at Asn-554 improves its critical function in gastric cancer. *Oncogene* **35**, 1619 (2015).
17. Fleuren, E.D.G. et al. The kinome at large in cancer. *Nat. Rev. Cancer* **16**, 83-98 (2016).
18. Lau, K.S. et al. Complex N-Glycan Number and Degree of Branching Cooperate to Regulate Cell Proliferation and Differentiation. *Cell* **129**, 123-134 (2007).
19. Liu, Y.-C. et al. Sialylation and fucosylation of epidermal growth factor receptor suppress its dimerization and activation in lung cancer cells. *Proc. Natl. Acad. Sci.* **108**, 11332-11337 (2011).
20. Tra, V.N. et al. Glycans in pathogenic bacteria - potential for targeted covalent therapeutics and imaging agents. *Chem. Commun.* **50**, 4659-4673 (2014).
21. Bagdonaite, I. et al. Global aspects of viral glycosylation. *Glycobiology* **28**, 443-467 (2018).
22. Dube, D. et al. Chemical tools to discover and target bacterial glycoproteins. *Chem. Commun.* **47**, 87-101 (2010).
23. Nizet V, E.J. Bacterial and Viral Infections. in *Essentials of Glycobiology* (ed. Varki A, C.R., Esko JD) (Cold Spring Harbor, New York, 2017).
24. Szymanski CM, S.R., Aebi M. Bacterial and Viral Infections. in *Essentials of Glycobiology* (ed. Varki A, C.R., Esko JD) (Cold Spring Harbor, New York, 2017).
25. James T. Park, J.L.S. Mode of Action of Penicillin. *Science* **125**, 99-101 (1957).
26. Perkins, H.R. Specificity of Combination between Mucopeptide Precursor and Vancomycin or Restocetin. *Biochem. J.* **111**, 195-205 (1968).
27. Aoki, F.Y. et al. Oseltamivir: a clinical and pharmacological perspective. *Expert Opin. Pharmacother.* **2**, 1671-1683 (2001).
28. Hutter, J. et al. Carbohydrate-Based Vaccines: An Overview. *Methods Mol. Biol.* **1331**, 1-10 (2015).

29. Rappuoli, R. Glycoconjugate vaccines: Principles and mechanisms. *Sci. Transl. Med.* **10**, eaat4615 (2018).
30. Shi, M. et al. STn-PS A1 as an Entirely Carbohydrate Immunogen: Synthesis and Immunological Evaluation. *J. Am. Chem. Soc.* **138**, 14264-14242 (2016).
31. Hakomori, S.-i. Tumor-Associated Carbohydrate Antigens Defining Tumor Malignancy: Basis for Development of Anti-Cancer Vaccines. in *The Molecular Immunology of Complex Carbohydrates —2* (ed. Wu, A.M.) 369-402 (Springer US, Boston, MA, 2001).
32. Varki, A. Biological roles of glycans. *Glycobiology* **27**, 3-49 (2017).
33. Lopez Aguilar, A. et al. Tools for Studying Glycans: Recent Advances in Chemoenzymatic Glycan Labeling. *ACS Chem. Biol.* **12**, 611-621 (2017).
34. Lara K. Mahal, K.J.Y., Carolyn R. Bertozzi. Engineering Chemical Reactivity on Cell Surfaces Through Oligosaccharide Biosynthesis. *Science* **276**, 1125-1128 (1997).
35. Sminia, T.J. et al. Getting a grip on glycans: A current overview of the metabolic oligosaccharide engineering toolbox. *Carbohydr. Res.* **435**, 121-141 (2016).
36. Sminia, T.J. et al. Getting a grip on glycans: A current overview of the metabolic oligosaccharide engineering toolbox. *Carbohydr. Res.* **435**, 121-141 (2016).
37. Cheng, B. et al. Metabolic Remodeling of Cell-Surface Sialic Acids: Principles, Applications, and Recent Advances. *ChemBioChem* **17**, 11-27 (2016).
38. Wang, H. et al. Selective in vivo metabolic cell-labeling-mediated cancer targeting. *Nat. Chem. Biol.* **13**, 415-424 (2017).
39. Chuh, K.N. et al. Changes in metabolic chemical reporter structure yield a selective probe of O-GlcNAc modification. *J. Am. Chem. Soc.* **136**, 12283-12295 (2014).
40. Spiciarich, D.R. et al. Bioorthogonal Labeling of Human Prostate Cancer Tissue Slice Cultures for Glycoproteomics. *Angew. Chem. Int. Ed. Engl.* **56**, 8992-8997 (2017).
41. Dold, J. et al. Dienophile-Modified Mannosamine Derivatives for Metabolic Labeling of Sialic Acids: A Comparative Study. *ChemBioChem* **18**, 1242-1250 (2017).
42. Spate, A.K. et al. Exploring the Potential of Norbornene-Modified Mannosamine Derivatives for Metabolic Glycoengineering. *ChemBioChem* **17**, 1374-1383 (2016).

43. Clark, E.L. et al. Development of Rare Bacterial Monosaccharide Analogs for Metabolic Glycan Labeling in Pathogenic Bacteria. *ACS Chem. Biol.* **11**, 3365-3373 (2016).
44. Dube, D. Metabolic oligosaccharide engineering as a tool for glycobiology. *Curr. Opin. Chem. Biol.* **7**, 616-625 (2003).
45. Gilormini, P.A. et al. A sequential bioorthogonal dual strategy: ManNAI and SiaNAI as distinct tools to unravel sialic acid metabolic pathways. *Chem. Commun. (Camb.)* **52**, 2318-2321 (2016).
46. Schart, V.F. et al. Triple Orthogonal Labeling of Glycans Applying Photoclick Chemistry. *ChemBioChem* **20**, 166-171 (2018).
47. Feng, L. et al. Bifunctional Unnatural Sialic Acids for Dual Metabolic Labeling of Cell-Surface Sialylated Glycans. *J. Am. Chem. Soc.* **135**, 9244-9247 (2013).
48. Oliveira, B.L. et al. Inverse electron demand Diels-Alder reactions in chemical biology. *Chem. Soc. Rev.* **46**, 4895-4950 (2017).
49. Knall, A.C. et al. Inverse electron demand Diels-Alder (IEDDA)-initiated conjugation: a (high) potential click chemistry scheme. *Chem. Soc. Rev.* **42**, 5131-5142 (2013).
50. Jiménez-Moreno, E. et al. Vinyl Ether/Tetrazine Pair for the Traceless Release of Alcohols in Cells. *Angew. Chem. Int. Ed. Engl.* **56**, 243-247 (2017).
51. Davies, S. et al. Tetrazine-triggered release of carboxylic-acid containing molecules for activation of an anti-inflammatory drug. *ChemBioChem* (2019).
52. Liu, F. et al. Theoretical Elucidation of the Origins of Substituent and Strain Effects on the Rates of Diels–Alder Reactions of 1,2,4,5-Tetrazines. *J. Am. Chem. Soc.* **136**, 11483-11493 (2014).
53. Liu, F. et al. Diels–Alder Reactivities of Strained and Unstrained Cycloalkenes with Normal and Inverse-Electron-Demand Dienes: Activation Barriers and Distortion/Interaction Analysis. *J. Am. Chem. Soc.* **135**, 15642-15649 (2013).
54. Versteegen, R.M. et al. Click to Release: Instantaneous Doxorubicin Elimination upon Tetrazine Ligation. *Angew. Chem. Int. Ed.* **52**, 14112-14116 (2013).
55. Vrabel, M. et al. Norbornenes in Inverse Electron-Demand Diels–Alder Reactions. *Chem-Eur. J.* **19**, 13309-13312 (2013).
56. Meijer, A. et al. Effects of the Hydrophobicity of the Reactants on Diels–Alder Reactions in Water. *J. Org. Chem.* **63**, 8989-8994 (1998).

57. Wijnen, J.W. et al. Substituent Effects on an Inverse Electron Demand Hetero Diels–Alder Reaction in Aqueous Solution and Organic Solvents: Cycloaddition of Substituted Styrenes to Di(2-pyridyl)-1,2,4,5-tetrazine. *J. Org. Chem.* **61**, 2001-2005 (1996).
58. Patterson, D.M. et al. Functionalized cyclopropenes as bioorthogonal chemical reporters. *J. Am. Chem. Soc.* **134**, 18638-18643 (2012).
59. Cole, C.M. et al. Fluorescent live-cell imaging of metabolically incorporated unnatural cyclopropene-mannosamine derivatives. *ChemBioChem* **14**, 205-208 (2013).
60. Yilmaz, B. et al. Gut Microbiota Elicits a Protective Immune Response against Malaria Transmission. *Cell* **159**, 1277-1289 (2014).
61. Aguilar, R. et al. Antibody responses to alpha-Gal in African children vary with age and site and are associated with malaria protection. *Sci. Rep.* **8**, 9999 (2018).
62. Cowman, A.F. et al. Malaria: Biology and Disease. *Cell* **167**, 610-624 (2016).
63. World Malaria Report 2018. 210 (World Health Organization, Geneva, 2018).
64. Beeson, J.G. et al. Challenges and strategies for developing efficacious and long-lasting malaria vaccines. *Sci. Transl. Med.* **11**(2019).
65. The RTS, S.C.T.P. First Results of Phase 3 Trial of RTS,S/AS01 Malaria Vaccine in African Children. *New Engl. J. Med.* **365**, 1863-1875 (2011).
66. Efficacy and safety of RTS,S/AS01 malaria vaccine with or without a booster dose in infants and children in Africa: final results of a phase 3, individually randomised, controlled trial. *The Lancet* **386**, 31-45 (2015).
67. Aide, P. et al. Safety, immunogenicity and duration of protection of the RTS,S/AS02(D) malaria vaccine: one year follow-up of a randomized controlled phase I/IIb trial. *PLoS One* **5**, e13838 (2010).
68. Seder, R.A. et al. Protection Against Malaria by Intravenous Immunization with a Nonreplicating Sporozoite Vaccine. *Science* **341**, 1359-1365 (2013).
69. Jongo, S.A. et al. Safety, Immunogenicity, and Protective Efficacy against Controlled Human Malaria Infection of Plasmodium falciparum Sporozoite Vaccine in Tanzanian Adults. *Am. J. Trop. Med. Hyg.* **99**, 338-349 (2018).

70. Sissoko, M.S. et al. Safety and efficacy of PfSPZ Vaccine against Plasmodium falciparum via direct venous inoculation in healthy malaria-exposed adults in Mali: a randomised, double-blind phase 1 trial. *Lancet Infect. Dis.* **17**, 498-509 (2017).
71. Eugene A. Davidson, D.C.G. Glycobiology of Plasmodium Falciparum. *Biochimie* **83**, 601-604 (2001).
72. Guha-Niyogi, A. et al. Glycoconjugate structures of parasitic protozoa. *Glycobiology* **11**, 45R-59R (2001).
73. von Itzstein, M. et al. Hot, sweet and sticky: the glycobiology of Plasmodium falciparum. *Trends Parasitol.* **24**, 210-218 (2008).
74. Cristiana S de Macedo, R.T.S., Lucia Mendonca-Preciato. Overlooked post-translational modifications of proteins in Plasmodium falciparum: N- and O-glycosylation - A Review. *Mem. Inst. Oswaldo Cruz.* **105**, 949-956 (2010).
75. Cova, M. et al. Sugar activation and glycosylation in Plasmodium. *Malar. J.* **14**, 427-437 (2015).
76. Bushkin, G.G. et al. Suggestive Evidence for Darwinian Selection against Asparagine-Linked Glycans of Plasmodium falciparum and Toxoplasma gondii. *Eukaryot. Cell* **9**, 228-241 (2010).
77. Glison, P.R. et al. Identification and Stoichiometry of Glycosylphosphatidylinositol-anchored Membrane Proteins of the Human Malaria Parasite Plasmodium falciparum. *Mol. Cell. Proteomics* **5**, 1286-1299 (2006).
78. Hofsteenge, J. et al. C-mannosylation and O-fucosylation of the thrombospondin type 1 module. *J. Biol. Chem.* **276**, 6485-6498 (2001).
79. Naik, R.S. et al. Glycosylphosphatidylinositol Anchors of Plasmodium falciparum. *J. Exp. Med.* **192**, 1563-1576 (2000).
80. Sanz, S. et al. Biosynthesis of GDP-fucose and other sugar nucleotides in the blood stages of Plasmodium falciparum. *J. Biol. Chem.* **288**, 16506-16517 (2013).
81. Ginsburg, H. Progress in in silico functional genomics: the malaria Metabolic Pathways database. *Trends Parasitol.* **22**, 238-240 (2006).
82. Janczuk, A.J. et al. The synthesis of deoxy- α -Gal epitope derivatives for the evaluation of an anti- α -Gal antibody binding. *Carbohydr. Res.* **337**, 1247-1259 (2002).

83. Huai, G. et al. Characteristics of alpha-Gal epitope, anti-Gal antibody, alpha1,3 galactosyltransferase and its clinical exploitation (Review). *Int. J. Mol. Med.* **37**, 11-20 (2016).
84. Sianturi, J. et al. Development of alpha-Gal-Antibody Conjugates to Increase Immune Response by Recruiting Natural Antibodies. *Angew. Chem. Int. Ed. Engl.* **58**, 4526-4530 (2019).
85. Cabezas-Cruz, A. et al. Immunity to alpha-Gal: Toward a Single-Antigen Pan-Vaccine To Control Major Infectious Diseases. *ACS Cent. Sci.* **3**, 1140-1142 (2017).
86. Moura, A.P.V. et al. Virus-like Particle Display of the α -Gal Carbohydrate for Vaccination against Leishmania Infection. *ACS Cent. Sci.* **3**, 1026-1031 (2017).
87. Almeida, I.C. et al. Complement-mediated lysis of Trypanosoma cruzi trypomastigotes by human anti-alpha-galactosyl antibodies. *J. Immunol.* **146**, 2394 (1991).
88. Avci, F.Y. et al. Carbohydrates and T cells: a sweet twosome. *Semin. Immunol.* **25**, 146-151 (2013).
89. Siegrist, C.-A. Vaccine Immunology. in *Plotkin's Vaccines* (Elsevier).
90. Avci, F.Y. et al. A mechanism for glycoconjugate vaccine activation of the adaptive immune system and its implications for vaccine design. *Nat. Med.* **17**, 1602-1609 (2011).
91. Clem, A.S. Fundamentals of vaccine immunology. *J. Glob. Infect. Dis.* **3**, 73-78 (2011).
92. Greenberg, D.P. et al. Enhanced antibody responses in infants given different sequences of heterogeneous Haemophilus influenzae type b conjugate vaccines. *J. Pediatr.* **126**, 206-211 (1995).
93. Adamo, R. et al. Synthetically defined glycoprotein vaccines: current status and future directions. *Chem. Sci.* **4**, 2995-3008 (2013).
94. Grayson, E.J. et al. A Coordinated Synthesis and Conjugation Strategy for the Preparation of Homogeneous Glycoconjugate Vaccine Candidates. *Angew. Chem. Int. Ed.* **50**, 4127-4132 (2011).
95. Stefanetti, G. et al. Sugar-Protein Connectivity Impacts on the Immunogenicity of Site-Selective Salmonella O-Antigen Glycoconjugate Vaccines. *Angew. Chem. Int. Ed. Engl.* **54**, 13198-13203 (2015).
96. Graaf, A.J.d. et al. Nonnatural Amino Acids for Site-Selective Protein Conjugation. *Bioconjug. Chem.* **20**, 1281-1295 (2009).

97. Hoyt, E.A. et al. Contemporary approaches to site-selective protein modification. *Nat. Rev. Chem.* **3**, 147-171 (2019).
98. Boutureira, O. et al. Advances in chemical protein modification. *Chem. Rev.* **115**, 2174-2195 (2015).
99. Lang, K. et al. Cellular incorporation of unnatural amino acids and bioorthogonal labeling of proteins. *Chem. Rev.* **114**, 4764-4806 (2014).
100. Bruce Albert, K.H., Alexander Johnson, David Morgan, Martin Raff, Keith Roberts, Peter Walter. *Essential Cell Biology*, (W. W. Norton & Company, New York, 2019).
101. Matos, M.J. et al. Chemo- and Regioselective Lysine Modification on Native Proteins. *J. Am. Chem. Soc.* **140**, 4004-4017 (2018).
102. Bernardim, B. et al. Stoichiometric and irreversible cysteine-selective protein modification using carbonylacrylic reagents. *Nat. Commun.* **7**, 13128 (2016).
103. Chin, J.W. Expanding and reprogramming the genetic code. *Nature* **550**, 53 (2017).
104. Lang, K. et al. Genetically encoded norbornene directs site-specific cellular protein labelling via a rapid bioorthogonal reaction. *Nat. Chem.* **4**, 298-304 (2012).
105. Marino, S.M. et al. Cysteine function governs its conservation and degeneration and restricts its utilization on protein surfaces. *J. Mol. Biol.* **404**, 902-916 (2010).
106. Gunnoo, S.B. et al. Chemical Protein Modification through Cysteine. *ChemBioChem* **17**, 529-553 (2016).
107. Bernardes, G.J.L. et al. Facile Conversion of Cysteine and Alkyl Cysteines to Dehydroalanine on Protein Surfaces: Versatile and Switchable Access to Functionalized Proteins. *J. Am. Chem. Soc.* **130**, 5052-5053 (2008).
108. Chalker, J.M. et al. Methods for converting cysteine to dehydroalanine on peptides and proteins. *Chem. Sci.* **2**, 1666 (2011).
109. Morrison, P.M. et al. Chemical generation and modification of peptides containing multiple dehydroalanines. *Chem. Commun. (Camb.)* **51**, 13470-13473 (2015).
110. Agarwal, P. et al. Site-specific antibody-drug conjugates: the nexus of bioorthogonal chemistry, protein engineering, and drug development. *Bioconjug. Chem.* **26**, 176-192 (2015).
111. Bernardes, G.J.L. et al. Combined Approaches to the Synthesis and Study of Glycoproteins. *ACS Chem. Biol.* **4**, 703-713 (2009).

112. Adamo, R. et al. Synthetically defined glycoprotein vaccines: current status and future directions. *Chem. Sci.* **4**, 2995-3008 (2013).
113. Ranade, S.C. et al. Mechanism of Chemical Glycosylation: Focus on the Mode of Activation and Departure of Anomeric Leaving Groups. *J. Carbohydr. Chem.* **32**, 1-43 (2013).
114. Hosoya, T. et al. Theoretical foundation for the presence of oxacarbenium ions in chemical glycoside synthesis. *J. Org. Chem.* **79**, 7889-7894 (2014).
115. Park, J. et al. Stereoselective Glycosylations of 2-Azido-2-deoxy-glucosides Using Intermediate Sulfonium Ions. *Org. Lett.* **9**, 1959-1962 (2007).
116. Chatterjee, S. et al. An Empirical Understanding of the Glycosylation Reaction. *J. Am. Chem. Soc.* **140**, 11942-11953 (2018).
117. Adero, P.O. et al. The Experimental Evidence in Support of Glycosylation Mechanisms at the SN1-SN2 Interface. *Chem. Rev.* **118**, 8242-8284 (2018).
118. Das, R. et al. Chemical O-Glycosylations: An Overview. *ChemistryOpen* **5**, 401-433 (2016).
119. Frihed, T.G. et al. Mechanisms of glycosylation reactions studied by low-temperature nuclear magnetic resonance. *Chem. Rev.* **115**, 4963-5013 (2015).
120. Lindhorst, T.K. O-Glycoside synthesis. in *Essentials of Carbohydrate Chemistry and Biochemistry* (ed. Lindhorst, T.K.) 157-182 (Wiley-VCH 2007).
121. Koenigs, W. et al. Ueber einige Derivate des Traubenzuckers und der Galactose. *Ber. Dtsch. Chem. Ges.* **34**, 957-981 (1901).
122. Schmidt, R.R. et al. Einfache Synthese von α -und β -O-Glykosylimidaten; Herstellung von Glykosiden und Disacchariden. *Angew. Chem.* **92**, 763-764 (1980).
123. Codee, J.D. et al. Thioglycosides in sequential glycosylation strategies. *Chem. Soc. Rev.* **34**, 769-782 (2005).
124. Yang, B. et al. Strategies for one-pot synthesis of oligosaccharides. in *Glycochemical Synthesis* (ed. S. Hung, M.M.Z.) 155-187 (2016).
125. Yu, B. et al. One-Pot Glycosylation (OPG) for the Chemical Synthesis of Oligosaccharides. *Curr. Org. Chem.* **9**, 179-194 (2005).

126. Veeneman, G.H. et al. An efficient thioglycoside-mediated formation of α -glycosidic linkages promoted by iodonium dicollidine perchlorate. *Tetrahedron Lett.* **31**, 275-278 (1990).
127. Pornsuriyasak, P. et al. Glycosyl thioimidates in a highly convergent one-pot strategy for oligosaccharide synthesis. *Tetrahedron-Asymmetr.* **16**, 433-439 (2005).
128. Kaeothip, S. et al. On orthogonal and selective activation of glycosyl thioimidates and thioglycosides: application to oligosaccharide assembly. *J. Org. Chem.* **76**, 7388-7398 (2011).
129. Rodrigues, J.G. et al. Glycosylation in cancer: Selected roles in tumour progression, immune modulation and metastasis. *Cell Immunol.* **333**, 46-57 (2018).
130. Gilormini, P.-A. et al. Asking more from metabolic oligosaccharide engineering. *Chem. Sci.* **9**, 7585-7595 (2018).
131. Jaurigue, J.A. et al. Parasite Carbohydrate Vaccines. *Front Cell. Infect. Microbiol.* **7**, 248 (2017).
132. Soares, M.P. et al. Microbiota Control of Malaria Transmission. *Trends Parasitol.* **32**, 120-130 (2016).
133. Chakravarty, S. et al. CD8⁺ T lymphocytes protective against malaria liver stages are primed in skin-draining lymph nodes. *Nat. Med.* **13**, 1035-1041 (2007).
134. Späte, A.-K. et al. Terminal Alkenes as Versatile Chemical Reporter Groups for Metabolic Oligosaccharide Engineering. *Chem-Eur. J.* **20**, 16411-16411 (2014).
135. Freeze HH, H.G., Schnaar RL. Glycosylation Precursors. in *Essentials of Glycobiology* (ed. Varki, A., Cummings RD, Esko JD et al) (Cold Spring Harbor, New York, 2017).
136. Hsu, T.L. et al. Alkynyl sugar analogs for the labeling and visualization of glycoconjugates in cells. *Proc. Natl. Acad. Sci. USA* **104**, 2614-2619 (2007).
137. Sarkar, A.K. et al. Disaccharide uptake and priming in animal cells: inhibition of sialyl Lewis X by acetylated Gal beta 1->4GlcNAc beta-O-naphthalenemethanol. *Proc. Nat. Aca. Sci.* **92**, 3323-3327 (1995).
138. Qin, W. et al. Artificial Cysteine S-Glycosylation Induced by Per-O-Acetylated Unnatural Monosaccharides during Metabolic Glycan Labeling. *Angew. Chem. Int. Ed. Engl.* **57**, 1817-1820 (2017).

139. Joet, T. et al. Validation of the hexose transporter of *Plasmodium falciparum* as a novel drug target. *Proc. Natl. Acad. Sci. USA* **100**, 7476-7479 (2003).
140. Slavic, K. et al. Plasmodial sugar transporters as anti-malarial drug targets and comparisons with other protozoa. *Malar. J.* **10**, 165-175 (2011).
141. Meireles, P. et al. GLUT1-mediated glucose uptake plays a crucial role during *Plasmodium* hepatic infection. *Cell. Microbiol.* **19**, e12646 (2017).
142. Carruthers, A. et al. Will the original glucose transporter isoform please stand up! *Am. J. Physiol. Endocrinol. Metab.* **297**, E836-848 (2009).
143. Thorens, B. et al. Glucose transporters in the 21st Century. *Am. J. Physiol. Endocrinol. Metabol.* **298**, E141-E145 (2010).
144. Liu, Y. et al. A small-molecule inhibitor of glucose transporter 1 downregulates glycolysis, induces cell-cycle arrest, and inhibits cancer cell growth in vitro and in vivo. *Mol. Cancer. Ther.* **11**, 1672-1682 (2012).
145. Xintaropoulou, C. et al. A comparative analysis of inhibitors of the glycolysis pathway in breast and ovarian cancer cell line models. *Oncotarget* **6**, 25677-25695 (2015).
146. Ramasamy, R. et al. Terminal galactosylation of glycoconjugates in *Plasmodium falciparum* asexual blood stages and *Trypanosoma brucei* bloodstream trypomastigotes. *Exp. Parasitol.* **130**, 314-320 (2012).
147. Ramasamy, R. Evaluation of the importance of antibodies to a-galactosyl epitopes in immunity to malaria. *J. Vector Borne Dis.* **52**, 337-338 (2015).
148. Aly, A.S. et al. Malaria parasite development in the mosquito and infection of the mammalian host. *Annu. Rev. Microbiol.* **63**, 195-221 (2009).
149. Meimetis, L.G. et al. Ultrafluorogenic Coumarin-Tetrazine Probes for Real-Time Biological Imaging(). *Angew. Chem. Int. Ed. Engl.* **53**, 7531-7534 (2014).
150. Tewari, R. et al. Function of Region I and II Adhesive Motifs of *Plasmodium falciparum* Circumsporozoite Protein in Sporozoite Motility and Infectivity. *J. Biol. Chem.* **277**, 47613-47618 (2002).
151. Goddard-Borger, E.D. et al. Implications of *Plasmodium* glycosylation on vaccine efficacy and design. *Future Microbiol.* **13**, 609-612 (2018).

152. Swearingen, K.E. et al. Interrogating the Plasmodium Sporozoite Surface: Identification of Surface-Exposed Proteins and Demonstration of Glycosylation on CSP and TRAP by Mass Spectrometry-Based Proteomics. *PLoS Pathog.* **12**, e1005606 (2016).
153. Doud, M.B. et al. Unexpected fold in the circumsporozoite protein target of malaria vaccines. *Proc. Natl. Acad. Sci. USA* **109**, 7817-7822 (2012).
154. Lopez-Gutierrez, B. et al. Sugar nucleotide quantification by liquid chromatography tandem mass spectrometry reveals a distinct profile in Plasmodium falciparum sexual stage parasites. *Biochem. J.* **474**, 897-905 (2017).
155. Darabedian, N. et al. The Metabolic Chemical Reporter 6-Azido-6-deoxy-glucose Further Reveals the Substrate Promiscuity of O-GlcNAc Transferase and Catalyzes the Discovery of Intracellular Protein Modification by O-Glucose. *J. Am. Chem. Soc.* **140**, 7092-7100 (2018).
156. Gama, Y. et al. A Novel Activation Method for Methyl Thioglucoside Using O-Mesitylsulfonylhydroxylamine. *J. Jpn. Oil Chem. Soc.* **43**, 520-523 (1994).
157. Issa John Paul et al. Reagent controlled beta-specific dehydrative glycosylation reactions with 2-deoxy-sugars. *Org. Lett.* **15**, 4170-4173 (2013).
158. D'Angelo, K.A. et al. Borinic Acid Catalyzed Stereo- and Regioselective Couplings of Glycosyl Methanesulfonates. *J. Am. Chem. Soc.* **138**, 11058-11066 (2016).
159. Mootoo, D.R. et al. Armed and disarmed n-pentenyl glycosides in saccharide couplings leading to oligosaccharides. *J. Am. Chem. Soc.* **110**, 5583-5584 (1988).
160. Salvadó, M. et al. Synthesis of Fluorosugar Reagents for the Construction of Well-Defined Fluoroglycoproteins. *Org. Lett.* **17**, 2836-2839 (2015).
161. Piñero, T. et al. Metabolic oligosaccharide engineering of Plasmodium falciparum intraerythrocytic stages allows direct glycolipid analysis by mass spectrometry. *Mol. Biochem. Parasitol.* **182**, 88-92 (2012).
162. Crich, D. Mechanism of a chemical glycosylation reaction. *Acc. Chem. Res.* **43**, 1144-1153 (2010).
163. Qin, L. et al. General and Efficient Synthesis of O-Sulfonylhydroxylamine Derivatives. *Synth. Commun.* **40**, 642-646 (2010).

164. Mancini, R.S. et al. Organoboron-Promoted Regioselective Glycosylations in the Synthesis of a Saponin-Derived Pentasaccharide from *Spergularia ramosa*. *J. Org. Chem.* **80**, 8501-8510 (2015).
165. Xia, J. et al. Complex Oligosaccharide Investigations: Synthesis of an Octasaccharide Incorporating the Dimeric Lex Structure of PSGL-1. *J. Org. Chem.* **68**, 2752-2759 (2003).
166. Balcerzak, A.K. et al. Structurally diverse disaccharide analogs of antifreeze glycoproteins and their ability to inhibit ice recrystallization. *Bioorg. Med. Chem. Lett.* **22**, 1719-1721 (2012).
167. Bianchini, R. et al. Efficient double glycoconjugation to naturalize high molecular weight disperse dyes. *Carbohydr. Res.* **356**, 104-109 (2012).
168. Pozsgay, V. et al. Synthesis of two glycolipid antigens of the causative agent of Lyme disease. *Tetrahedron* **61**, 10470-10481 (2005).
169. Sugimura, H. et al. Formal Synthesis of Cytosamine—a Component of Nucleoside Antibiotics, the Amicetin Family. *Synth. Commun.* **31**, 2313-2321 (2001).
170. Crich, D. et al. 4,6-O-Benzylidene-Directed β -Mannopyranosylation and α -Glucopyranosylation: The 2-Deoxy-2-fluoro and 3-Deoxy-3-fluoro Series of Donors and the Importance of the O2–C2–C3–O3 Interaction. *J. Org. Chem.* **72**, 1681-1690 (2007).
171. Walvoort, M.T.C. et al. Mannopyranosyl Uronic Acid Donor Reactivity. *Org. Lett.* **13**, 4360-4363 (2011).
172. Agarwal, A. et al. Selective deprotection of terminal isopropylidene acetals and trityl ethers using HClO₄ supported on silica gel. *Carbohydr. Res.* **340**, 1661-1667 (2005).
173. Adinolfi, M. et al. Tunable Activation of Glycosyl Trichloro- and (N-phenyl)trifluoro-acetimidates with Ytterbium(III) Triflate: One-Pot Synthesis of -Trisaccharides under Catalytic Conditions. *Synlett* **2006**, 0583-0586 (2006).